The regulation of 11 β-hydroxysteroid dehydrogenase type 1 by ageing and glucocorticoids in key tissues

By

Dr Mark Sherlock

A thesis submitted to the University of Birmingham for the degree of

Doctor of Philosophy (PhD) in Medicine

School of Clinical and Experimental Medicine

College of Medical and Dental Sciences

University of Birmingham

Submitted August 2011

Abstract

In recent decades, the control of cortisol metabolism within tissues by the 11 beta-hydroxysteroid dehydrogenase (11 β-HSD) enzyme system has been studied in detail, however there is limited data regarding the effect of this enzyme system on skeletal muscle.

The results of this thesis show that 11 β-HSD1 is biologically active in skeletal muscle. 11 β-HSD1 plays a key role in glucocorticoid (GC) mediated myopathy by increasing atrophy pathways, decreasing hypertrophy pathways and inhibiting myoblast proliferation. There are many similarities between glucocorticoid mediated myopathy and the muscle loss associated with ageing (sarcopaenia). We have shown that 11 β-HSD1 is increased with age in murine skeletal muscle and this may have a key role to play in the development of sarcopaenia. Further work is required in this area to examine the impact of modulation of 11 β-HSD1 on muscle with ageing.

We have shown that hypopituitary patients receiving hydrocortisone replacement therapy have significant alterations in cortisol metabolites and an increase in 11 β-HSD1. The alterations in cortisol metabolism are associated with an adverse body composition. New modified release hydrocortisone preparations, which replace cortisol in a more physiological manner, need to be assessed for their impact on cortisol metabolism.

For Niamh and My Family

Acknowledgements

I would like to express my sincerest gratitude to Professor Paul Stewart who supervised this thesis and has been a mentor to me in both my research and clinical career. I would also like to thank Dr Andy Toogood who supervised this thesis for his help and support. I would also like to express my appreciation to Dr Gareth Lavery for teaching me most of the methods used in this thesis, discussions and friendship.

I would like to thank everyone in the 'Stewart Group' for his or her help. In particular, Dr Stuart Morgan and Dr Jeremy Tomlinson for their collaboration with regard to effects of glucocorticoids on muscle. I would also like to thank Beverly Hughes, Pushpa Patel, Phil Guest, Charlie Shaikh, Carol Kenny and Sue Hughes for their expert technical help. I would like to thank Dr Nina Semjonous for her invaluable help with regard to the ageing studies. I would also like to acknowledge the help and great friendship of Dr Laura Gathercole, Dr Jan Idkowiak, Dr Stuart Morgan, Dr Iwona Bujalska, Dr Aurora Aragon Alonso, Professor Wiebke Arlt and Dr Fabian Hammer, which helped make my time in the lab even more enjoyable. I would like to acknowledge the students, who I helped supervise over the last few years (as their questions often made me question what I was doing), including Oliver Wilson, Kamen Tsvetanov and Chris Jones. I would like to thank Dr Chris Shaw in the School of Sports and Exercise Science for his collaboration with regard to muscle histology.

I would like to thank all the nurses on the Wellcome Trust Clinical Research Facility at the Queen Elizabeth Hospital Birmingham and the patients who kindly took part in the clinical study in this thesis. I would like to thank the

Medical Research Council for funding this work and Novo Nordisk for funding the clinical study in this thesis.

I would like to thank my family for all their support. Finally, I would like to thank Niamh for her support and constant encouragement.

Table of contents

Chapter 1

Chapter 2

Materials and Methods **Page**

Chapter 3

Characterising 11 β-HSD1 in skeletal muscle **Page**

Chapter 4

The role of 11 β-HSD1 in glucocorticoid mediated myopathy **Page**

Chapter 5 **Page**

Effect of ageing on 11 β-HSD1 and atrophy markers in skeletal muscle

Chapter 6 **Page**

The modulation of corticosteroid metabolism by hydrocortisone therapy in hypopituitarism

List of Figures

Chapter 1 **Page**

Chapter 2

Chapter 3 **Page**

Chapter 4

Chapter 5

Page

Chapter 6

List of Tables

Chapter 1

Chapter 2

Chapter 3

Abbreviations

4EBP1	Eukaryotic translation initiation factor 4E binding protein 1
11 β-HSD1	11 beta-hydroxysteroid dehydrogenase type 1
11 β-HSD2	11 beta-hydroxysteroid dehydrogenase type 2
11-DHC	11-dehydrocorticosterone
A	
A	Corticosterone
ACTH	Adrenocorticotrophic hormone
ADP	Adenosine diphosphate
Akt	Protein kinase B
AMPK	AMP dependent protein kinase
AU	Arbitrary units
ATP	Adenosine triphosphate
B	
B	11 dehydrocorticosterone
BSA	Bovine serum albumin
C	
cAMP	Cyclic adenosine monophosphate
CREBP	cAMP response element binding protein
cDNA	Complimentary deoxyribonucleic acid
CPM	Counts per minute
CRH	Corticotropin releasing hormone
CO2	Carbon dioxide
CS	Cushing’s Syndrome
Ct	Cycle threshold
D	
DAB	3,3’ diaminobenzidine
DABCO	1,4-diazolbicyclo-[2.2.2]-octane
Dex	Dexamethasone
DHEA	Dehydroepiandrosterone

DMEM	Dilbecco’s modified eagle media
DMSO	Dimethyl Sulfoxide
DNA	Deoxyribonucleic acid
DPX	Dibutyl polystyrene xylene
E	
E	Cortisone
EDTA	Ethylenediaminetetraacetic acid
ER	Endoplasmic reticulum
eIF2B	Eukaryotic initiation factor
F	
F	Cortisol
FCS	Foetal calf serum
FOXO	Forkhead transcription factors
FRET	Fluorescence resonance energy transfer
G	
G6P	Glucose-6-phosphate
G6Pase	Glucose-6-phosphatase
GC	Glucocorticoid
GE	Glycyrrhetinic acid
GH	Growth Hormone
GLUT4	Glucose transporter 4
GR	Glucocorticoid receptor
GRE	Glucocorticoid response element
GTT	Glucose tolerance test
H	
H6PDH	Hexose-6-phosphate dehydrogenase
HPA	Hypothalamic-pituitary-adrenal
HRP	Horse radish peroxidase
HSP	Heat shock protein
I	
IGF-I	Insulin like growth factor

IL	Interleukin
IQR	Inter quartile range
IRS	Insulin receptor substrate
L	
LDL	Low density lipoprotein
LPL	Lipoprotein lipase
M	
MAFbx	Muscle Atrophy F box
MAO	Monoamine oxidase
MR	Mineralocorticoid receptor
MRF	Myogenic regulatory factors
mRNA	Messenger ribonucleic acid
mTOR	Mammalian target of Rapamycin
MURF	Muscle specific ring finger protein
MyHC	Myosin heavy chain
Myf5	Myogenic factor 5
N	
NAD	Nicotinamide adenine dinucleotide
NADP	Nicotinamide adenine dinucleotide phosphate
P	
P70S6K	Ribosomal protein S6 kinase
PBS	Phosphate buffered saline
PCR	Polymerase chain reaction
PI3K	Phosphoinositide 3-kinase
PMS	Phenazine methosulfate
PVDF	Polyvinylidine diflorise
R	
RIPA	Radioimmunoprecipitation
RNA	Ribonucleic acid
RT-PCR	Reverse transcriptase polymerase chain reaction
S	

SD	Standard deviation
SEM	Standard error mean
StAR	Steroidogenic acute regulatory protein

T

Taq	Thermus aquaticus polymerase
THE	Tetrahydrocortisone
THF	Tetrahydrocortisol
TNF	Tumour necrosis factor
Tris	tris(hydroxymethyl)aminomethane

Chapter 1

Introduction

1.1 Introduction

Glucocorticoids are essential for the normal function of most organ systems, however, in excess they can lead to several adverse consequences including insulin resistance, hypertension, osteoporosis, obesity and muscle loss/ weakness (myopathy) (1). In recent decades, the control of cortisol metabolism within tissues by the 11 beta-hydroxysteroid dehydrogenase (11 β-HSD) enzyme system has been studied in detail, however there is limited data regarding the effect of this enzyme system on skeletal muscle (2).

The population of western societies are increasing in age and there are a number of conditions that increase in prevalence in an ageing population which include sarcopaenia (loss of muscle mass and strength), cardiovascular disease, metabolic syndrome (and Type 2 diabetes mellitus) and osteoporosis. Each of these conditions place a considerable burden upon limited health care resources (3). One of the commonest complications of ageing is the loss of muscle mass and strength, known as 'sarcopaenia'. Muscle strength peaks between the 2nd and 3rd decade of life and remains the same until approximately 45-50 years. After this strength decreases at the rate of 12-15% per decade until the 8th decade (4) and up to 24% of people aged <65 years and 50% of people aged >80 years have sarcopaenia. There are several similarities between the muscle changes reported in sarcopaenia and glucocorticoid mediated myopathy.

There is some evidence for alterations in cortisol secretion and tissue specific metabolism (via 11 β-HSD1) with increasing age in certain tissues including bone (5) and skin (6) and 11β-HSD1 KO mice are resistant to hippocampal changes

associated with ageing (7). However, there are no data regarding changes in 11 β-HSD1 within skeletal muscle with ageing.

1.2 Skeletal muscle

1.2.1. Skeletal myocyte differentiation

The regulation of skeletal muscle formation (myogenesis) is essential for normal muscle development as well as in pathological conditions (8). Myogenesis is a dynamic process in which mononucleated undifferentiated myoblasts first proliferate, then withdraw from the cell cycle and finally differentiate and fuse to form the multinucleated mature muscle fibre (8).

Activation of muscle differentiating-specific genes is controlled by the myogenic regulatory factors (MRFs), which belong to the bHLH family of transcription factors. The MRF family consists of four members (Myf5, MyoD, myogenin and MRF4) which bind to the sequence specific DNA elements (E box:…CANNTG…) present in the promoter region of muscle specific genes (8). Selective and productive recognition of E boxes on muscle promoters require heterodimerisation of MyoD with the ubiquitously expressed bHLH E proteins; the formation of this functional heterodimer is the key event in initiating skeletal myogenesis (8-10).

Different muscle genes are expressed at different times during myogenesis, despite all of them having E boxes in their promoter regions. Thus, promoter specific and temporal constraints are likely to be superimposed upon the basic

model of myogenic transcriptional activation by MRFs (8). Full activation of muscle gene expression by MRFs is also dependent on their association with members of the MEF2 family of transcription factors (MEF2A-D). MEF2 cannot activate muscle genes on their own but they can potentiate the activity of the MRFs (8). MAP kinases also have a key role in the control of muscle gene expression at different stages of the myogenic process (8).

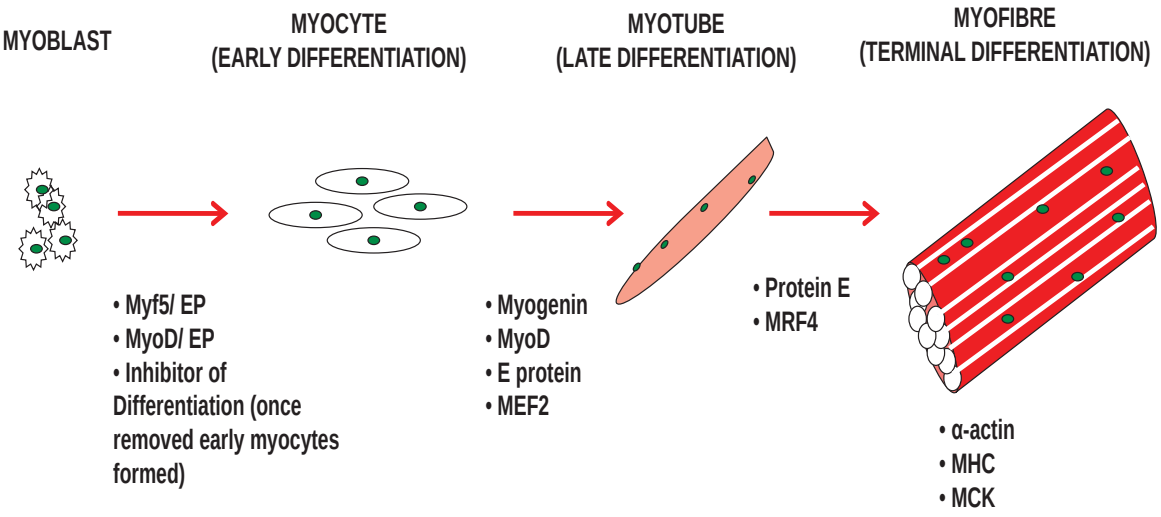

Figure 1.1. *Skeletal myofibre synthesis is controlled at different stages of development by different myogenic regulatory factors. EP = E protein (Based on a figure from Lluis et al.) (8).*

A key feature of terminally differentiated myocytes is the presence of multiple nuclei per cell. Each nucleus originated from separate myoblasts which fused together to form single, elongated, cylindrical cells referred to as myotubules, which no longer have the capacity to proliferate (Figure 1.1). Within the myofibre and between the myotubules (adjacent to the basal lamina) lie myogenic progenitor or satellite cells which are essential for growth and regeneration of myotubules (11). In healthy adult skeletal muscle these cells are mitotically

quiescent but can be activated in response to various stimuli such as exercise or injury, at which point they undergo multiple rounds of cell division generating myoblasts which can fuse to form new myotubules.

1.2.2. Skeletal muscle physiology

Multinucleated myotubule formation from myocytes, leads to tubules of varying diameter and length. Each myofibre contains the contractile proteins myosin and actin, which are incorporated into long filaments, which are organised into units called sarcomeres. Sarcomeres in series are referred to as myofibrils, and give skeletal muscle a striated appearance (Figure 1.2).

Movement in muscle is generated by the myosin cross bridges, which interact cyclically with actin filaments and transport them past the myosin thick filaments, during this process an ATP is hydrolysed (12). The swinging cross-bridge theory for muscle contraction is one in which myosin cross bridges bind to the actin filament in an initial conformation and then undergo a swinging motion that ‘rows’ the actin filament along (12). Myosin is a product-inhibited ATPase, which is strongly stimulated by binding to actin (which is a nucleotide exchange factor for myosin (12). ATP binding to the catalytic domain of the myosin motor head induces a conformational change, leading to the dissociation of myosin from actin. Myosin then hydrolyses ATP and forms a stable myosin-products complex, with which actin recombines. The resultant actin-myosin complex allows the cross bridge to undergo a conformational change allowing the products of hydrolysis to be released, which allows the rowing-like stroke (power-stroke)

causing the myosin filament to slide longitudinally with respect to the actin filament (12).

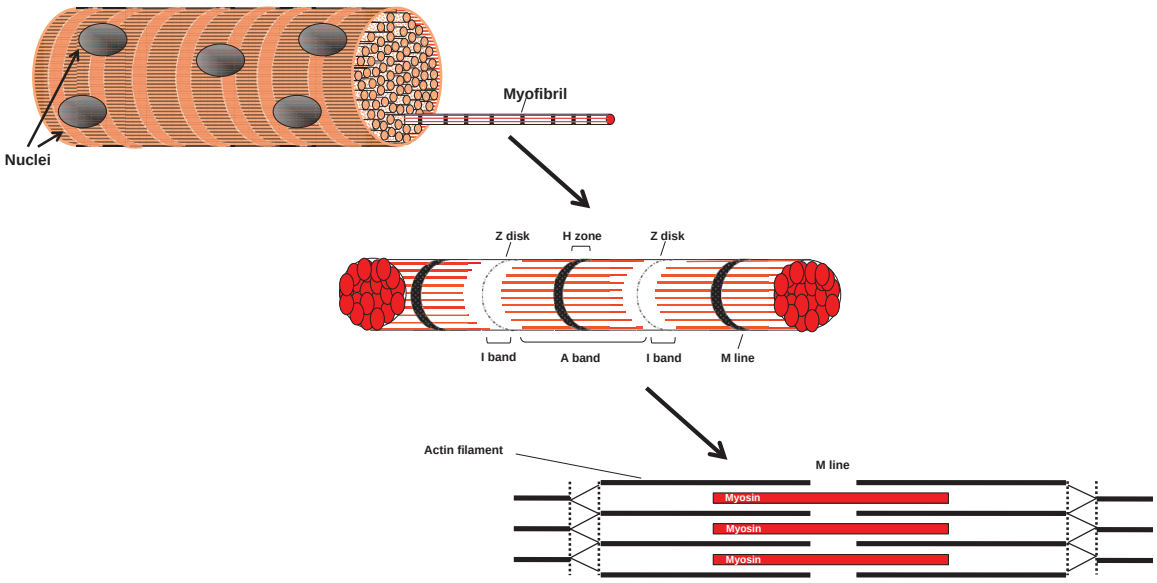

Figure 1.2. *Representation of the structure of skeletal muscle. Sarcomeres represent the contractile mechanism of skeletal muscle. Z disk = forms the borders of sarcomere, H zone = area at centre of sarcomere that contains only myosin, I band = area surrounding Z disk, A band = dark staining zone of the sarcomere which contains actin and myosin, M line = middle of sarcomere which contains cross connective elements of cytoskeleton. Based on a figure from Morgan (13).*

1.2.3. Human and rodent skeletal muscle fibre Types and nomenclature

Human muscle fibres can be divided into a number of subgroups including slow twitch oxidative (Type I fibres), fast twitch oxidative (Type IIa fibres) and fast twitch glycolytic (Type IIx or IIb). Type I fibres contain high levels of slow isoform contractile proteins, high volumes of mitochondria, high levels of myoglobin and capillary densities and a high oxidative enzyme capacity (14). Type IIa fibres are

characterised by fast contraction with high oxidative capacity. Type IIb fibres are characterised by low volumes of mitochondria, high glycolytic enzyme activity, high myosin ATPase activity, increased rate of contraction and low fatigue resistance (14) (Table 1.1).

Fibre Type	Type I Fibres	Type IIa Fibres	Type IIx Fibres	Type IIb Fibres
Contractile Properties				
Predominant MyHC isoform	MYH7	MYH2	MYH1	MYH4
Speed of contraction	Slow	Moderately Fast	Fast	Very Fast
Exercise type	Aerobic	Long-term aerobic	Short-term aerobic	Short-term Anaerobic
Resistance to fatigue	High	High	Intermediate	Low
Force generated	Low	Medium	High	Very High
Metabolic Properties				
Mitochondrial number	High	High	Medium	Low
Fuel store	Triglycerides	Creatine phosphate, glycogen	Creatine phosphate, glycogen	Creatine phosphate, glycogen
Oxidative capacity	High	High	Intermediate	Low
Glycolytic capacity	Low	High	High	High
Capillary number	High	Intermediate	Low	Low

Table 1.1. *Representation of key differences in contractile and metabolic properties between subclasses of muscle fibres. MyHC = myosin heavy chain.*

Along with the 'pure' fibre Types, there are also hybrid fibres composed of both Type I and IIa myosin heavy chains (MyHC) and Type IIA and IIb MyHC (15).

In contrast to humans, adult rodents limb muscle contain 4 'pure' fibre Types, 3 of which are fast twitch (fast Type IIa, IIb and IId) and 1 slow twitch (Type I). There are also several hybrid fibre Types co-expressing different MyHC (Type I/IIa and

Type IIa/I, known as Type Ic and IIc, respectively), Type IIad, IIda, IIdb and IIbd (16).

1.3 Sarcopaenia

1.3.1. Background

The 2001 census showed that for the first time the number of people in England and Wales aged 60 and over was greater than the number aged below 16 years of age. People over the age of 60 currently consume 38% of NHS total expenditure (17). It is estimated that >20% of the UK population will be >65 years by the year 2020 (17). There are a number of conditions that increase in prevalence in an ageing population which include sarcopaenia (age related loss of muscle), cardiovascular disease, metabolic syndrome (and Type 2 diabetes mellitus) and osteoporosis. Each of these conditions place a considerable burden upon limited health care resources (3).

In health, skeletal muscle tissue represents 40%-45% of body mass. For an 80kg male and 60kg female, this equates to 32-36kg and 24-27kg and thus represents a considerable source of protein where the contractile machinery, actin and myosin, can be degraded into amino acids ready for gluconeogenesis, immunological and wound healing processes. The term 'sarcopaenia' was coined to describe the loss of skeletal muscle mass that occurs with increasing age. *Baumgartner et al*. (18) defined sarcopaenia as an appendicular skeletal mass (muscle mass/ height^2) more than 2 standard deviations (SD) below the mean of a young reference group. Sarcopaenia is associated with a significant decrease in muscle strength. Muscle strength peaks between the 2nd and 3rd decade and

remains the same until approximately 45-50 years, after this strength decreases at the rate of 12-15% per decade until the 8th decade (4). Using Baumgartners' definition, up to 24% of people aged <65 years and 50% of people aged >80 years would fulfil the criteria for sarcopaenia as assessed using dual x-ray absorptiometry (DEXA). Sarcopaenia was more prevalent in men aged >75 years (58%) compared with women of the same age (45%). Several other studies have used DEXA to quantify the loss in skeletal muscle mass with age and have reported similar dimorphic patterns. *Melton et al.* (19) and *Iannuzzi-Sucich et al.* (20) demonstrated a greater prevalence of sarcopaenia amongst men (10% to ~27%) than women (8% to ~23%) in their 6th decade. This increased to 40-45% for men and 18-31% in women in their 8th decade (19).

1.3.2. Health consequences of sarcopaenia

This loss of muscle mass and strength has functional consequences and sarcopaenia has been linked to multiple morbid outcomes in older adults including falls, functional decline, osteoporosis, impaired thermoregulation and glucose intolerance (21-24). In the UK, 30% of those over the age of 65 will fall at least once a year, and 40% of those over 75 will fall at least twice per year**.** Falls are the commonest reason cited for institutional care and for 40% of admissions to nursing homes or residential homes (25). Sarcopaenic subjects are also at increased risk of osteoporosis, this combined with increased falls leads to an increase risk of fractures in this group.

1.3.3. Pathological changes in Sarcopaenic muscle

There are many pathological changes which occur within muscle with ageing including a decrease in muscle mass and cross-sectional area (26-28) and a decrease in Type I and II fibre number (predominantly Type II) (29-31). There is an infiltration of fat and connective tissue (32) as shown on both histology and conventional imaging (33-36). Several ultrastructural changes occur including accumulation of internal nuclei, ring and ragged fibres, lipofuscin and nemaline rod structures (37) with a disarrangement of myofilaments and Z-lines (37) and proliferation of the sarcoplasmic reticulum and t-tubular system (37). Mitochondrial function is impaired with ageing (38) leading to a decrease in muscle respiratory capacity and mitochondrial volume (39). All these factors may explain the decrease in aerobic endurance noted with ageing (40). Myosin heavy chain synthesis rate declines with advancing age implying a decreased ability to remodel this important muscle contractile protein therefore contributing to the declining muscle mass and contractile function in the elderly (41).

1.3.4. Factors associated with the development of Sarcopaenia

Many factors have been proposed to explain the development of sarcopaenia including the effects of oxidative stress, cytokines, endocrine changes, diet and exercise. Elevated levels of cytokines (IL-1, IL-6 and TNFα) have been reported with increasing age and TNFα and IL-6 levels have been shown to predict sarcopaenia in an elderly community (42, 43). The effects of oxidative stress (44) diet and exercise in relation to sarcopaenia have been previously described (4), Table 1.2.

Mechanism	Ref
Whole Body	
Reduced physical activity and muscle disuse	(45)
Reduced growth hormone and insulin-like growth factor-I production	(46)
Elevated catabolic cytokine production and activity	(47)
Malnutrition	(48)
Disease	(49)
Muscle Specific	
Reduced availability and recruitment of skeletal muscle satellite cells	(50)
Mitochondrial DNA mutations and apoptosis	(51)
Impaired insulin mediated increase in (micro) vascular blood flow	(52)
Insulin resistance of muscle protein synthesis by amino acids	(53-55)
Muscle fibre denervation	(56)
Impaired translation initiation and protein synthesis	(54)
Increased muscle protein breakdown	(49)

Table 1.2. *Summary of the potential mechanisms underlying sarcopaenia.*

1.3.5. Molecular mechanisms underpinning sarcopaenia

The maintenance of muscle mass depends on the balance between muscle protein synthesis via anabolic stimuli (feeding, muscle contraction, anabolic hormones) and muscle protein breakdown via catabolic stimuli (fasting, glucocorticoids, inflammatory cytokines). Where muscle protein synthesis exceeds protein breakdown, hypertrophy occurs, whereas the reverse is true for muscle atrophy. It is clear, therefore, that sarcopaenia might be associated with a decrease in anabolic stimuli, an increase in catabolic stimuli, or a combination of the two.

1.3.5.1. Satellite cells in sarcopaenia

One possible mechanism underpinning sarcopaenia is the decline in regenerative capacity of skeletal muscle, possibly as a consequence of a decreased number or impaired function of skeletal muscle satellite cells (57). There is conflicting data regarding satellite cell number and function in sarcopaenic muscle with some authors describing a decrease (58-60) some reporting no change and others reporting an increase in satellite cell number with age (61, 62). There is also some evidence to suggest that there is fibre Type specificity to the decrease in satellite cells with Type II fibres having lower satellite cell number than Type I fibres (63). Some studies have reported an increased expression of key regulators of myogenesis (myoD and myogenin) in elderly rat muscle which the authors believed to be a compensatory mechanism to combat sarcopaenia (64-67). However, there are many other genes and co-factors involved in myogenesis which may not be increased with ageing (57).

1.3.5.2. Role of Myostatin in sarcopaenia

Myostatin is a member of the tumour growth factor β family and is a potent inhibitor of muscle growth, regulating satellite cell activation, myoblast proliferation and terminal differentiation. Cell proliferation requires the completion of the G, M and S cell cycle phases and myostatin prevents myoblasts from progressing past the G0/G1 and G2 phase (68) through the cyclin CDK inhibitor protein 21 (CKIp21), a key component of cell cycle arrest during the G and M phase (69). Thus, fewer cells accumulate in the S-phase and proliferation is prevented. Myostatin also down regulates MyoD1 expression (70) preventing myoblast differentiation into multinucleated myotubules (71, 72). Disruption of the myostatin gene in mice increased muscle mass through hypertrophy and hyperplasia (70).

There are conflicting data with regard to the role of myostatin in sarcopaenic muscle. Some rodent studies have shown no change in myostatin expression in young vs. old mice (73), whereas other studies have shown an increased expression (74). Similarly, human studies reveal conflicting results with some studies reporting no increased expression (75) and other an increase in myostatin expression with increasing age (76). Therefore, further work is needed to clarify the role of myostatin in sarcopaenic muscle.

The calpain system has also been reported to be activated in sarcopaenic muscle suggesting an increase in calcium dependent proteolysis (57).

1.3.5.3. Protein synthesis in sarcopaenia

Elderly individuals do not demonstrate a decrease in basal muscle protein synthesis despite a reduction in muscle mass with age (77), but do show impaired muscle protein synthesis in response to amino acids, in the presence of insulin, despite demonstrating normal glucose tolerance and insulin concentrations comparable to the younger cohort (78). As such, healthy ageing muscle appears to be selectively resistant to anabolic stimuli such as insulin-stimulated muscle protein synthesis despite normal insulin-mediated glucose uptake. A gradual, long-term diminution of muscle sensitivity to insulin induced protein synthesis may contribute to sarcopaenia.

1.3.5.4. Role of MURF-1 and MAFbx-1 in sarcopaenia

Proteins scheduled for degradation in the proteasome are labelled by conjugation with ubiquitin. The 26s proteasome enzyme complex can then recognise the ubiquitin and initiate protein degradation using at least three classes of proteins. These include the E1 (ubiquitin activating enzymes), E2 (ubiquitin-conjugating enzymes) and E3 (Ubiquitin ligase). Within skeletal muscle, MAFBX and MURF-1 are two important E3 ubiquitin ligases clearly associated with many models of muscle atrophy such as sepsis (79, 80) and disuse atrophy (81). These genes encode E3 ubiquitin ligase proteins that bind and mediate ubiquitination of specific proteins for degradation (82), such as myosin, actin, troponin and tropomyosin found within skeletal muscle sarcomere (83).

Translocation of the forkhead transcription factor (FOXO-1) into the cell nucleus increases MAFbx and MURF-1 mRNA expression (84). Phosphorylation of FOXO-1 by Akt sequesters FOXO-1 from the cell nucleus to the cytoplasm by 14-3-3 proteins (85) preventing MAFbx and MURF-1 upregulation.

IGF-I inhibits MAFbx-1 and MURF-1 expression (84, 86), and as IGF-I decreases with age (87), one might expect an associated increase in the expression of MAFbx-1 and MURF-1 with age, especially in sarcopaenic individuals. However, there is conflicting evidence surrounding the role of MURF-1 and MAFbx-1 in sarcopaenia. In ageing, MURF-1 and MAFbx-1 mRNA expression in human vastus lateralis muscle is unchanged (88, 89), whilst in rodent muscle MURF-1 and MAFbx-1 mRNA expression is increased 2 to 2.5 fold (90), decreased (91), or MURF-1 expression decreases whilst MAFbx-1 expression remains unchanged (92) compared with younger control groups. The disagreement between studies is likely due to several confounding factors including the species sampled, the strains of animals, gender and the types of muscles biopsied. *Edstrom et al.* (91) suggests the reduction in MURF-1 and MAFbx-1 expression in the rat gastrocnemius muscle was part of a compensatory effect which was also suggested in a human study (93). However, it is clear from the discordance in the above data that further evaluation of the role of these genes is required in sarcopaenia.

1.3.5.5. Fibre specificity of sarcopaenia

A post-mortem assessment of the vastus lateralis muscle recovered from men aged 19-37 and 70-73 years demonstrated a substantial loss in muscle fibre number in the elderly group compared with the younger cohort (~364,000 fibres present in the elderly group vs. ~478,000 in the younger cohort) (94). *Andersen et al.* (95) dissected 2264 single muscle fibres from 12 biopsies of elderly individuals and found just 20% of the fibres contained Type I MyHC which is half of that found in younger muscle (96). The number of fibres co-expressing Type I and Type IIa MyHC (28.5%) increased 5.5 fold compared with younger individuals. However, only 0.3% of the fibres contained MyHC Type IIb which is very low (95), but is in line with specific apoptosis/ atrophy of Type IIb fibres with age. Finally, fibres co-expressing all three MyHC's together were observed which has not been reported in younger individuals (95).

Whole muscle and individual muscle fibre atrophy is heavily implicated in the reduction in cross-sectional area with age, especially Type IIb fibres (29, 39, 56, 94, 97-99), whereas the cross-sectional area of Type I fibres, although undergoing mild atrophy, generally appears well conserved with age (29). Type I fibres atrophy by 20% and Type II fibres by 43% in elderly individuals compared to their younger counterparts (100).

The reason for the sensitivity of ageing Type II fibres to atrophy compared with Type I fibres remains to be elucidated. However, there are many similarities between sarcopaenia and studies reporting muscle fibre atrophy, especially Type II muscle fibres, in individuals with excess endogenous or exogenous glucocorticoid concentrations (101-108).

1.3.6. Endocrinology of ageing and putative role in sarcopaenia

There are a number of hormonal changes, which occur with ageing which have been implicated in the development of sarcopaenia, including a decrease in testosterone, DHEA and GH/IGF-I levels. Testosterone levels decrease with increasing age and this decrease has been shown to be a strongly correlated with muscle mass and strength (109), however the data regarding increased muscle strength following testosterone replacement in this cohort is conflicting (110-113). The mechanism by which testosterone increases muscle strength and mass is not known, however, it may have its effect via IGF-I (114) as, *in vitro*, testosterone increases both IGF-I and IGF-binding proteins in muscle (110, 115). DHEAS levels also decrease with increasing age and studies replacing DHEA in an elderly cohort have not shown an increase in muscle strength (116).

1.3.6.1. The GH/ IGF-I system and ageing

GH secretion declines by approximately 14% per decade (87) with a decrease in GH pulse amplitude, but maintenance of pulse frequency (117). However, the pituitary GH reserve, determined by the response to GH-releasing hormone (GHRH) + GH releasing peptide-6, is not affected by ageing (118). Insulin-like growth factor-I (IGF-I) is produced predominantly in the liver and in tissues such as bone under the direct influence of GH and serum IGF-I levels also fall with increasing age (119).

The GH/IGF-I axis has been implicated in sarcopaenia following a number of studies which have shown a correlation between IGF-I levels and sarcopaenia

(42) and GH treatment has been associated with an increase in lean body and muscle mass (120-123). Over expression of IGF-I exclusively in skeletal muscle prevents age-related decline in number of dihydropyridine receptor which are essential in the basic mechanism for excitation-contraction uncoupling (124) of muscle contraction. However, despite this promising data, the use of GH for treatment of sarcopaenia or the GH decrease in ageing (somatopause) is not recommended due to a significant incidence of adverse events (125).

1.3.6.2. Glucocorticoids and Ageing

There are contradictory data regarding the changes in plasma cortisol which occur with ageing, with a number of groups reporting there are no changes (126) while others reporting that plasma cortisol levels increase with ageing and in a sex specific manner (127). *Van Cauter et al.* have reported that there are a number of changes in cortisol which occur with increasing age including an increase in mean plasma cortisol levels between 20-50% between 20-80 years, an increase in the nocturnal nadir of cortisol and age related dampening of diurnal rhythm with an advancement of the timing of the circadian elevation (127). They hypothesise that these changes could be due to excess exposure of the hippocampal neurons to glucocorticoids with subsequent neuronal degeneration and as the hippocampal neurons normally inhibit ACTH release when these degenerate there is unchecked ACTH secretion (128).

There are a number of ultrastructural changes seen in the muscles of people with myopathy complicating glucocorticoid excess (Cushing's syndrome) (129) (which

will be reviewed in Section 1.5) which are similar to changes seen in sarcopaenic muscles including pronounced mitochondrial damage, with thickening and deep invaginations of the sarcolemmal basement membrane and thickening of the basement membrane of capillaries. Muscle fibres in GC mediated myopathy also show marked disarray and wide interfibrillar spaces containing large vacuoles which represented degenerated mitochondria (129).

1.4 Overview of corticosteroids

Adrenal corticosteroids are essential for life and can be divided into three main types: glucocorticoids (synthesised in the zona fasciculata), mineralocorticoids (synthesised in the zona glomerulosa) and sex steroids (synthesised in the zona reticularis) (130).

Cortisol (the main active glucocorticoid in humans) is secreted by the zona fasciculata of the adrenal cortex under the tight control of the hypothalamic-pituitary-adrenal axis. Corticotrophin releasing hormone (CRH) is synthesized and secreted from the hypothalamus, which leads to ACTH (corticotrophin) synthesis and secretion from the pituitary gland, which acts on the zona fasciculata of the adrenal cortex. Classical endocrine feedback loops are in place to control the secretion of GC through a tightly regulated mechanism in the hypothalamus and pituitary gland (130). (Figure 1.3)

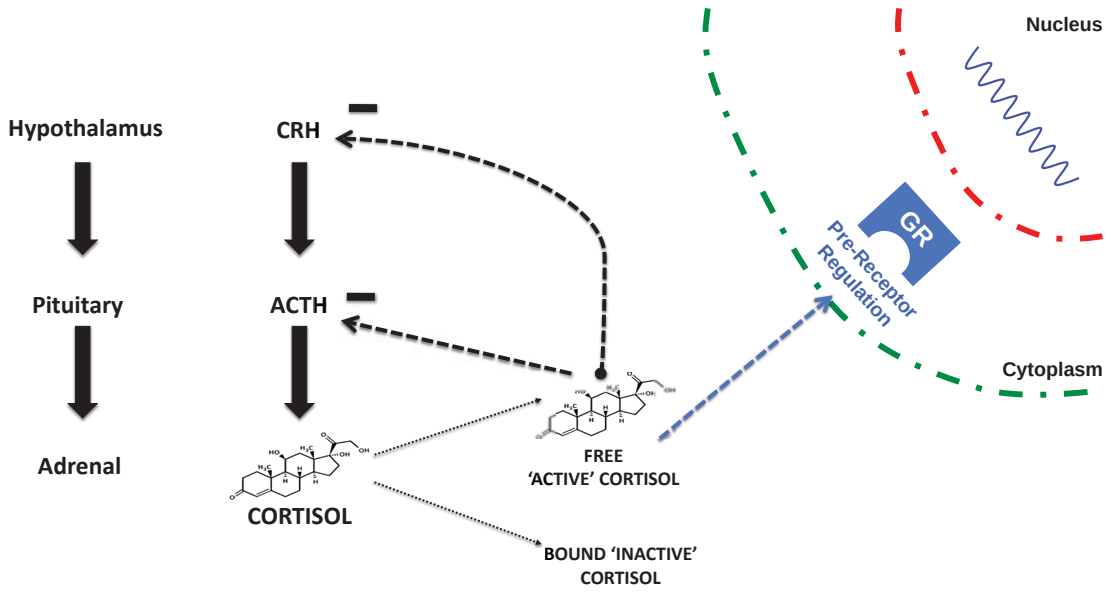

Figure 1.3. *Schema representing the hypothalamic pituitary adrenal axis. GR = glucocorticoid receptor, CRH = corticotrophin releasing hormone, ACTH = adrenocorticotrophic hormone. Bound 'inactive' cortisol is bound to cortisol binding globulin and albumin.*

1.4.1. The glucocorticoid receptor

The glucocorticoid receptor (GR) is a member of the thyroid/ steroid hormone receptor superfamily of transcription factors comprising a C-terminal ligand binding domain, a central DNA binding domain which interacts with specific DNA sequences on target genes and N-terminal hypervariable region (130). The effects of glucocorticoids are mediated by the GC receptor (GR) which is a ligand regulated nuclear receptor that in the absence of its GC ligand remains bound to other proteins within the cytoplasm such as the 90 kDA and 70 kDA heat shock proteins (HSP90, HSP70) (130). GC binding to the GR leads to dissociation of the HSPs and translocation of the GR-ligand complex into the cell nucleus.

Following translocation to the nucleus, gene transcription is altered following binding of the dimerised GR/ ligand complex to the specific DNA sequences known as glucocorticoid response elements (GREs) in the promoter region of the target gene (131); there are several hundred GC responsive genes (130). The GRβ gene may act as a dominant negative regulator of GRα transactivation and the GRγ variant has an additional AA within the DNA binding domain of the receptor protein that may reduce GR transactivation (130, 132). In addition to the GR numerous other factors such as co-activators and co-repressors that may confer tissue specificity in responses are required (130, 133).

The GR is vital in mediating muscle atrophy but a reduction in proteolysis with chronic exposure to GCs may be attributable to the GC induced down regulation of the GR. GCs down regulate the GR in most (134-138) but not all (139) target cells, through the induction of calpains (140) and inhibiting calpains prevents the GC induced GR down regulation (140). A reduction in GR may have important implications for GC myopathy since inhibiting the GR with the antagonist RU38486 (141) or attenuation of GR activation via shRNA (142) prevents upregulation of myostatin (141) and MAFbx and MURF-1 (142) by dexamethasone. This is also supported by *Waddell et al.* (143) where transgenic mice expressing a dimerisation deficient GR prevented dexamethasone induced MURF-1 expression.

1.4.2. Adrenal Steroidogenesis

Cholesterol is the precursor molecule for all adrenal steroidogenesis, it is principally derived from low density lipoprotein cholesterol (LDL) which attaches to specific LDL surface receptors on adrenal cells (144). The resultant vesicles fuse with lysozymes and free cholesterol is produced following hydrolysis. Glucocorticoids are secreted in relatively large amounts (between 5.3 and 9.9mg/m^2/day) (145, 146) from the zona fasciculata through expression of steroidogenic enzymes in a specific zonal manner (Figure 1.4).

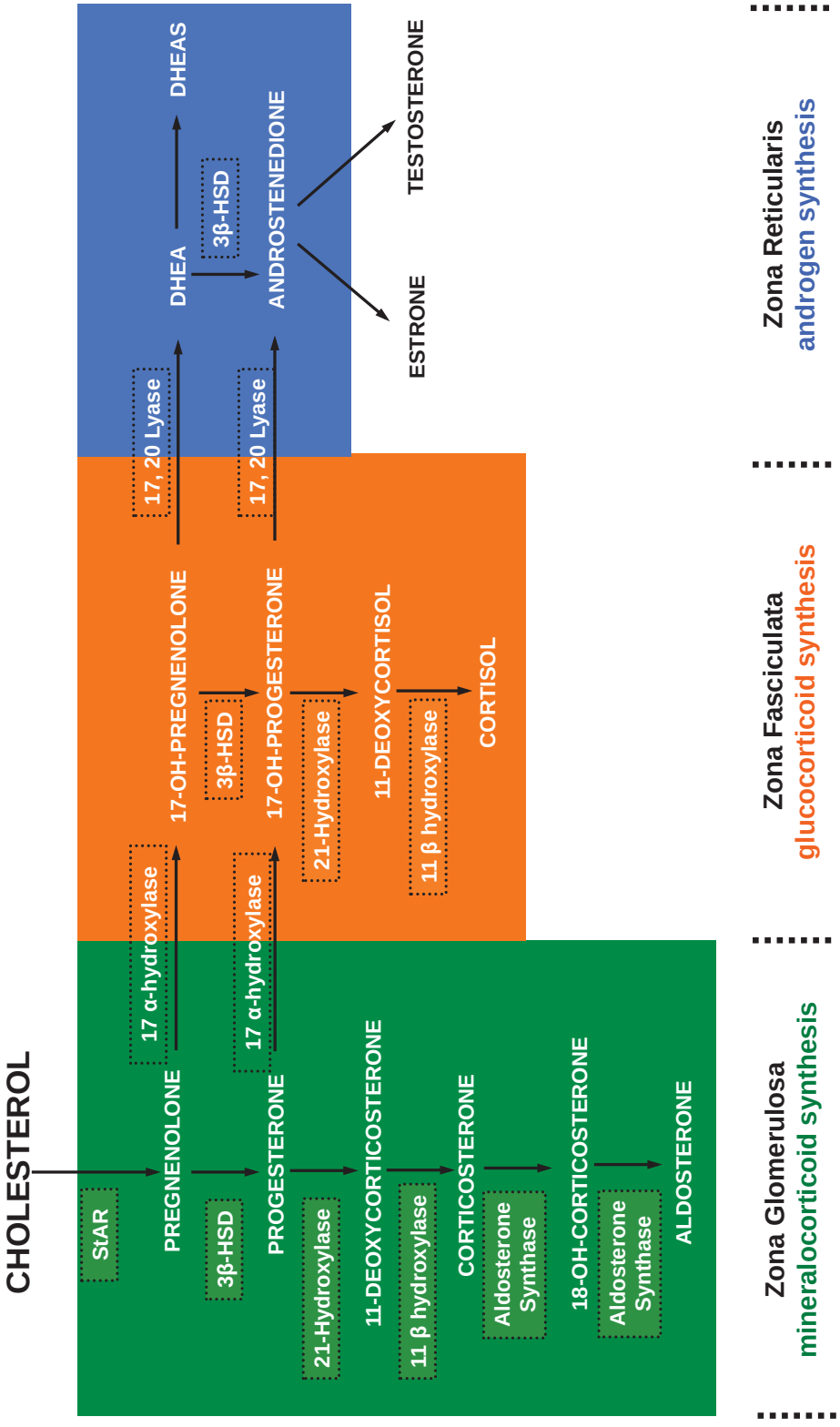

Figure 1.4. *The zonal distribution of corticosteroid synthesis. StAR = steroidogenic acute regulatory protein, 3 β-HSD = 3 beta hydroxysteroid dehydrogenase , DHEA = Dehydroepiandrosterone, DHEAS = Dehydroepiandrosterone sulphate.*

1.4.3. Effects of glucocorticoids

Glucocorticoids affect every organ system with the main physiological and pathophysiological effects being on energy metabolism, the cardiovascular/ blood pressure system, bone, connective tissue (including muscle), the immune system, the central nervous system, the gastrointestinal and the endocrine system (130) (Table 1.3).

METABOLISM	BONE	VASCULAR/ BLOOD PRESSURE	IMMUNE
↑ Serum Glucose	↑ Renal excretion of Ca^{++}	↑Sensitivity to pressor agents	↑ Apoptosis
↑ Liver Glycogen	↑ PTH	↑ GFR	↓ Circulating lymphocytes
↑ Glycogen synthase	↓ Osteoblast activity	↑ Angiotensinogen	↓ Ig synthesis
↑ Gluconeogenesis	↓ Ca^{++} absorption	↑ Proximal Na^{+} epithelium transport	↓ Cytokine production
↑ Circulating chol		↑ Free water clearance	↓ Monocyte differentiation
↑ Circulating TG		↑ MR activity	↓ Phagocytosis
↓ Glycogen phosphorylase		↓ NO mediated vasodilatation	↓ Cytotoxic activity

Table 1.3. *Summary of the physiological and pathophysiological effects of GC on fuel metabolism, bone, vascular system and the immune system. (PTH = parathyroid hormone, GFR = glomerular filtration rate, MR = mineralocorticoid receptor, NO = nitric oxide, TG = triglycerides, Ig = immunoglobulin's, chol = cholesterol).*

GC also have profound effects on the central nervous system, as the GR is abundant in a number of key cortical areas such as the hippocampus, hypothalamus, cerebellum and cortex (147). GC are associated with neuronal

death in the hippocampus which has recently lead to interest in the area of glucocorticoid exposure and memory (130). There are several effects of GC excess on the endocrine system including a suppression in the hypothalamic-pituitary-thyroid and gonadal axis as well as suppressing the GH/ IGF-I axis (130).

1.4.4. Cortisol Binding globulin

Over 90% of circulating cortisol is bound, predominantly to the α2-globulin, cortisol binding globulin (CBG) (148), with 9% bound to albumin. CBG is a 383 AA protein synthesised in the liver, which binds cortisol with high affinity. Levels of CBG are approximately 700nmol/l and levels are increased by oestrogens and in patients with chronic liver disease, renal disease and hyperthyroidism (148).

1.4.5. Corticosteroid hormone metabolism

The metabolism of cortisol has been extensively reviewed by *Tomlinson et al.* (2), below I will briefly summarise the pathways involved (Figure 1.5). The major route comprises the interconversion of cortisol (Kendall's compound F) to cortisone (Kendall's compound E) through the activity of 11 β-HSD isozymes or reduction of the C4-5 bond by either 5α-reductase or 5β-reductase to yield 5α-THF (allo THF) and 5β-THF respectively (2). In normal subjects the 5β metabolites predominate (5β THF:5α, THF 2:1). THF, allo THF and tetrahydrocortisone (THE) are rapidly conjugated with glucuronic acid and excreted in the urine (2). Downstream, cleavage of the THF and THE to the C19

steroids 11 hydro or 11-oxo-androsterone or etiocholanolone occur (2). Alternatively reduction of the 20-oxo group by 20α or 20β hydroxysteroid dehydrogenases yield α and β cortols and cortolones, respectively, with the subsequent oxidation at the C21 position to form the extremely polar metabolites cortolic and cortolonic acids. Hydroxylation at C6 to form 6β-hydroxycortisol is described as is the reduction of the C20 position which may occur without A ring reduction giving rise to 20α and 20β hydroxycortisol (2, 130). Approximately 50% of secreted cortisol appears in the urine as THF, allo THF and THE, 25% appears as cortols/ cortolones, 10% as C19 steroids, 10% cortolic/ cortolonic acids and remaining are free unconjugated steroids (F, E, 6β and 20α/ 20β-metabolites of F and E) (2).

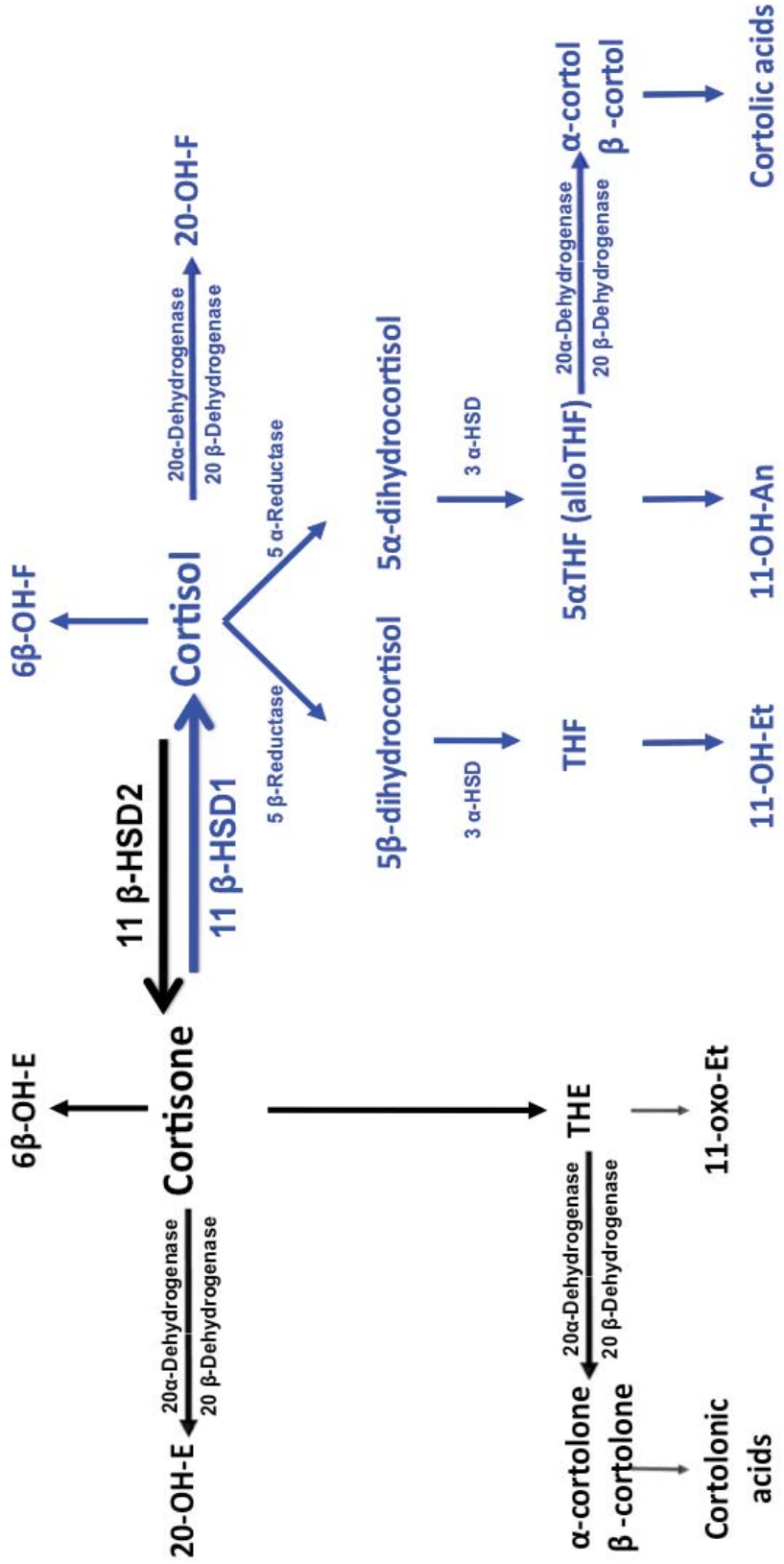

Figure 1.5. *The major pathways involved in cortisol metabolism (E= cortisone, F= cortisol, Et = etiocholanolone, An = androsterone). THE = tetrahydrocortisone, THF = tetrahydrocortisol.*

1.4.5.1. Urinary Gas Chromatography/ Mass spectrometry (GC/MS)

In GC/MS, the sample is initially separated into its components by gas chromatography, following which the individual constituents are ionised and separated to their mass to charge ratio, which allows accurate identification. Analysis of urinary steroid metabolites by GC/MS identifies and quantifies over 55 different metabolites or ratios of metabolites. The technique provides an index of cortisol secretion and global 11 β-HSD activity (149), which is estimated from renal excretion of steroid metabolites. Assessment of 11 β-HSD1 activity is made via the ratio of cortisol to cortisone metabolites i.e. tetrahydrocortisone (THF) + 5αTHF: tetrahydrocortisone (THE) ratio, and 11 β-HSD2 activity is estimated by measuring the urinary free cortisol: urinary free cortisone ratio (Figure 1.5). Measures of 5α-reductase activity can be inferred from 5αTHF, 5αTHF:THE, androsterone, androsterone: etiocholanolone (Figure 1.5) (2).

1.4.6. Tissue specific modulation of Glucocorticoid action: 11 β-hydroxysteroid dehydrogenase (11 β-HSD) isozymes

Within tissues, GC levels are regulated at the pre-receptor level by the isozymes of 11 β-hydroxysteroid dehydrogenase (11 β-HSD), which are located in the endoplasmic reticulum (ER). 11 β-HSD2 is predominantly found in tissues expressing the mineralocorticoid receptor (MR) where it acts as a dehydrogenase, converting the active GC cortisol (corticosterone in rodents) to inactive cortisone (11 dehydrocorticosterone in rodents), thus protecting the MR [which has equal affinity for cortisol (corticosterone) as for aldosterone] from illicit

occupancy by cortisol (150). 11 β-HSD1 is found in many tissues such as adipose tissue, liver, brain and skeletal muscle (2). 11 β-HSD1 *in vivo* acts predominantly as an oxoreductase converting inactive cortisone into active cortisol (2), Figure 1.6. This oxoreductase activity is determined by nicotinamide adenine dinucleotide phosphate (NADPH) co-factor availability produced by the ER specific enzyme hexose-6-phosphate dehydrogenase (H6PDH), Figure 1.6.

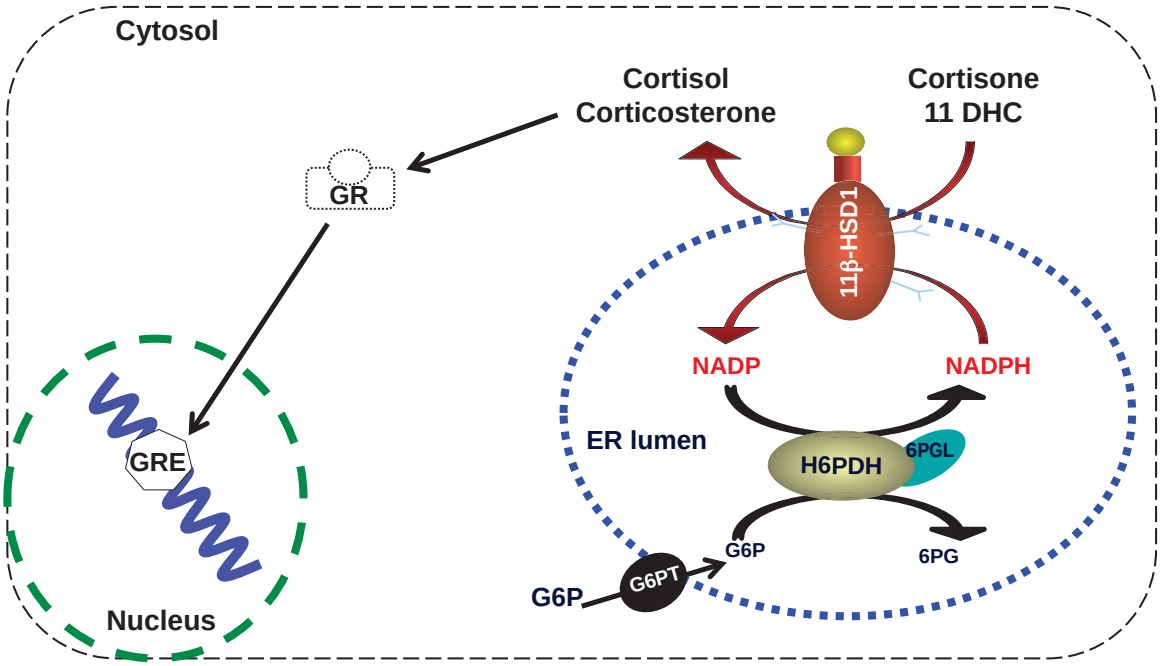

Figure 1.6. *Schema representing the tissue specific regulation of glucocorticoid action. (G6P = glucose-6-phosphate, 6PG = 6 phosphogluconate, NADP = , ER = endoplasmic reticulum, GR = glucocorticoid receptor, GRE = glucocorticoid response elements, G6PT = glucose-6-phosphate transporter).*

Expression of 11 β-HSD1 in skeletal muscle has been reported to be only ~5% that reported in liver (151) with conflicting evidence as to whether 11 β-HSD2 is present in muscle or not (151, 152). In muscle cells extracted from the vastus lateralis of patients with type 2 diabetes, baseline 11 β-HSD1 mRNA was

elevated compared with controls. This was associated with impaired glucose transport in response to acute insulin and cortisone stimulation (152). In myocytes, *Whorwood et al.* (153) demonstrated elevated 11 β-HSD1 activity with increasing GC concentration and 11 β-HSD1 activity decreased with insulin and IGF-I administration, independently. Thus, in GC excess, the activity of 11 β-HSD1 may play a fundamental role in the inhibition of protein synthesis and activation of the atrophy program within skeletal muscle.

1.4.6.1. Hexose 6 Phosphate dehydrogenase (H6PDH) and muscle function

As described in Section 1.4.6, the oxoreductase activity of 11 β-HSD1 is determined by nicotinamide adenine dinucleotide phosphate (NADPH) co-factor availability produced by the ER specific enzyme hexose-6-phosphate dehydrogenase (H6PDH). H6PDH is ubiquitously expressed and utilizes glucose-6-phosphate (G6P), transported into the ER by the G6P transporter (G6PT), to reduce coenzyme $NADP^+$ to NADPH for utilization within an otherwise oxidizing environment. In support of this role of H6PDH in determining directionality of 11 β-HSD1, tissues from H6PDHKO mice have a 'switch' in 11β-HSD1 activity, due to the change in NADPH/$NADP^+$ ratio, and the enzyme acts as a dehydrogenase rather than the native reductase, resulting in local GC inactivation (2). Transgenic mice lacking H6PDH have a severe myopathy with a shift in fibre Type from Type II to Type I (154). This may be due to reduced active GCs, a reduction in NADPH or effects on ER specific metabolism (154, 155). The myopathy is associated with elevated glycogen storage and activation of the unfolded protein response (UPR) suggesting that H6PDH is important in the control of SR metabolic function (154).

The molecular and biochemical basis for UPR activation is unknown and an important aspect to consider within muscle is the activity of 11β-HSD1 in H6PDHKO mice, specifically the gain in dehydrogenase activity and the subsequent inactivation of GCs. Previous reports have documented 11β-HSD1 expression and activity in human and rodent skeletal muscle (151, 156-158). However, 11β-HSD1KO mice have no reported skeletal muscle phenotype (159).

In work performed during my thesis, within Professor Stewart and Dr Lavery's group, but not directly related to the subsequent results chapters we hypothesised that H6PDH is important in muscle, complementary but independent to its role in the regulation of 11β-HSD1 and GC metabolism. To further explore the role of 11β-HSD1 in the pathogenesis of myopathy in H6PDHKO mice, the 11β-HSD1/ H6PDH double KO (DKO) mice was generated, in which 11β-HSD1 dehydrogenase activity is negated. We have shown that the DKO is a phenocopy of the major features of myopathy reported in the H6PDHKO at both the histological and molecular level. Using the DKO we have provided clear evidence for a role of H6PDH in skeletal muscle integrity that is independent of 11β-HSD1 by using the DKO mice. The most striking differences were apparent in the TA of DKO and H6PDHKO mice, a muscle abundant in 'fast-twitch' glycolytic Type IIb muscle fibres, in which atrophy and vacuolation of distinct fibres was severe. In contrast, no gross histological differences were seen in soleus with only the appearance of some atrophied fibres being present. Soleus is a muscle rich in 'slow-twitch' oxidative Type I fibres, again highlighting that this myopathy is Type II fibre specific.

1.4.6.2. 11 β-HSD1 substrate specificity, affinity and kinetics

The main substrate for 11 β-HSD1 in humans is cortisone and in rodents 11-dehydrocorticosterone (2). Many mammalian steroid dehydrogenases including 11 β-HSD1 have been implicated in the detoxification of molecules in addition to roles in steroid metabolism (160-162). 11 β-HSD1 also has roles in biotransformation of several carbonyl group compounds xenobiotics, drugs, insecticides, carcinogens. Prednisolone and prednisone are also substrates for 11 β-HSD1 (163, 164). 9a-fluorinated steroids such as dexamethasone are not metabolised by 11 β-HSD2 (165) but may also be regenerated by 11 β-HSD1 (166).

Homogenous enzyme has a rectilinear Eadie plot and Michaelis Menton (Km) constant of 1.83 +/- 0.06mM for corticosterone and 17.3 +/ - 2.24mM for cortisol (2). First-order rate constants are one order of magnitude higher for corticosterone than cortisol, but maximal velocities are similar (167). There are species and tissue differences in Km values for 11 β-HSD1, for example, in mice the Km for liver is 0.7 for A and 1.7 for B (mM) (168) and 0.09mM for pancreas for A (169). In comparison in humans the Km in liver is 13.9 (E), 41.3 (F), 19.7 (A), 42.8 (B) (170) and in omental preadipocytes 2.8 for F and 0.27 for E (2).

1.4.6.3. Molecular Biology of 11 β-HSD1

The gene for 11 β-HSD1 is on chromosome 1 (1q32.2-41), has 6 exons (182, 130, 111, 185, 143 and 617bp respectively) and 5 introns (776, 767, 120, 25,300 and 1,700 bp, respectively) (2).

Human 11 β-HSD1 transcription initiates 93bp upstream from the start of translation, yielding a 5' untranslated region similar in length to that of the rat 11 β-HSD1 mRNA (2). Recent studies on the rat 11 β-HSD1 promoter showed that it is predominantly regulated by the C/EBP family of transcription factors, mainly C/EBPα. C/EBPα regulates a series of genes concerned with the metabolism of fuels (171). C/EBPα is regulated by GC in a tissue specific manner (172), for example in liver basal C/EBPα levels are high ensuring high levels of 11 β-HSD1 transcription and hence high intra hepatic GC levels (173).

1.4.6.4. Recombinant models of 11 β-HSD1

Tomlinson et al have extensively reviewed transgenic models of 11 β-HSD1 (2), which have shown that elevated 11 β-HSD1 expression and activity, either globally or in a tissue specific manner, is associated with the development of cognitive impairment (174), the metabolic syndrome (175) and insulin resistance (176), which is due to increased intracellular glucocorticoid action.

Conversely, knockout animals or pharmacological inhibition of 11 β-HSD1 reveal improved insulin sensitivity and resistance to diet induced obesity (177). Much less is known about the role of 11 β-HSD1 in skeletal muscle and the consequences of local production of GCs. Transgenic mice with a null HSD11B1 gene have previously been generated by *Kotelevtsev et al.* replacing the genomic region containing exons 3 and 4 with a neomycin-resistant cassette via homologous recombination in mouse 129 embryonic stem cells (159). In homozygous mutant mice, hepatic 11 β-HSD1 activity was less than 5% that of

wild type. When WT and KO mice were adrenalectomised and implanted with pellets of 11-dehydrocorticosterone (A) the WT mice converted 11-dehydrocorticosterone (A) to corticosterone (B) whereas B levels in the KO mice remained undetectable. This demonstrated that 11 β-HSD1 is the only 11 oxo-reductase (in the mouse) able to generate active GC from inert 11 keto-steroids.

11 β-HSD1KO mice have adrenal hyperplasia due to reduced negative feedback on the HPA axis causing increased ACTH-stimulated corticosterone secretion and zona fasciculata hypertrophy. There was no compensatory change in 11 β-HSD2 activity or expression in this model (159).

A global KO a transgenic mouse over-expressing 11 β-HSD1 specifically within adipose tissue has also been developed (178) through fusion of the 5.4kb of the aP2 promoter/ enhancer, which is an adipocyte specific promoter and a 1.6kb fragment of rat 11 β-HSD1 cDNA followed by an SV40 consensus polyadenylation signal. This led to a 7-fold increase in expression of transgene mRNA compared with endogenous mRNA. 11 β-HSD1 enzyme activity was increased almost 3 fold in adipose tissue, a level comparable to ob/ob mice or that seen in obese humans (179), demonstrating that the extent of transgenic amplification of 11 β-HSD1 activity is physiologically relevant (2). Transgenic mice had similar serum concentrations as controls whereas concentrations in adipose tissue were elevated 30% higher compared with WT mice secondary to local increased activation of glucocorticoid via 11 β-HSD1 (2).

1.4.6.5. Putative Role of 11β-HSD1 in ageing

Although the effect of ageing on serum levels of cortisol is controversial there is evidence that 11β-HSD1 is elevated in a number of tissues. There is also evidence from a recent paper by *Weinstein et al.*, which shows an increase in endogenous glucocorticoid concentrations and adrenal weights with increasing age in C57BL/6 mice (180). In bone, 11β-HSD1 regulates the effects of glucocorticoids upon osteoblasts (181), *Cooper et al.,* within our group has shown that enzyme activity in primary cultures of human osteoblasts increases with advancing age (5). *Tiganescu et al.,* from our group, has shown that 11β-HSD1 increases in skin with increasing age (6). From a functional perspective, there is evidence that 11β-HSD1KO mice are resistant to hippocampal changes associated with ageing (7). There is, however, no data to date regarding the effect of ageing on skeletal muscle 11β-HSD1.

1.4.6.6. Growth Hormone /IGF-I system interaction with 11 β-HSD1

GH acting via IGF-I inhibits the autocrine generation of cortisol through inhibition of 11β-HSD1 (182). The phenotype of GHD in the context of hypopituitarism may, in part be mediated through increased 11β-HSD1 activity (182) as in these GHD patients the THF + allo-THF/ THE ratio (indicative of increased 11β-HSD1 activity) is increased by 50% from baseline and reduces after commencing GH therapy (even in elderly patients) without alteration in the UFF/UFE ratio, indicative of a resulting decrease in 11β-HSD1 oxoreductase activity (183, 184) without any change in 11β-HSD2 activity. Conversely, patients with acromegaly

and high IGF-I concentrations have decreased 11β-HSD1 activity; a defect that resolves with appropriate treatment of the GH excess (182). These studies are endorsed by *in vivo* studies, which show a decrease in hepatic 11β-HSD1 expression in rats treated with GH (185-187). Subsequent *in vitro* experiments have shown that GH has no direct effect on 11β-HSD1 but rather acts via IGF-I (i.e. IGF-I inhibits 11β-HSD1 activity) (182, 188).

1.5 Glucocorticoid mediated myopathy

1.5.1. Introduction

Excess circulating cortisol can be due to either exogenous or endogenous sources and if chronic leads to Cushing's syndrome (CS) (130). Endogenous CS is a rare condition with an incidence of 1.5-3.9 million per year, however CS secondary to exogenous glucocorticoid use is far more common (between 0.5-1% of the western population is receiving GC therapy at any point in time) (130). Proximal muscle weakness is one of the key features of CS (observed in 56-90% of cases), along with thin skin, easy bruising and osteoporosis (130). Harvey Cushing noted muscle weakness in his original patients, however, it was Muller and Kugelberg, who in the 1950's first performed systematic studies of myopathy in CS (189). In this study of 6 patients with CS, 5/6 presented with lower limb proximal muscle weakness. On histological examination of the quadriceps muscle in these patients there was replacement of muscle fibres with fat and connective tissue and degenerated muscle fibres clustered in groups or individually among normal fibres. The degenerated muscle fibres appeared

hyalinised with their striations indistinct, and there was no evidence of muscle fibre regeneration (189).

Subsequently, several clinical studies have examined muscle function, histology and metabolism in patients with endogenous and exogenous glucocorticoid (GC) related myopathy (103, 107, 108, 190, 191). The effects of GCs on muscle appear to be related to dose, duration and type of steroid (192). Duration of exposure to GCs and different sensitivities of skeletal muscle fibre types also play an important role in the development of myopathy (193).

1.5.2. Features of Glucocorticoid myopathy

In vitro (194-199) and *in vivo* studies of rodent (84, 141, 143, 200-210) and human skeletal muscle (96, 101-108, 191) clearly demonstrate a causal relationship between GC and muscle atrophy. Type II fibre atrophy is the classically described histological abnormality reported in GC mediated myopathy (104, 107, 189, 191). In the majority of studies Type I fibres generally display little, if any, abnormalities despite Type I fibres containing twice as many GR binding sites in the cytoplasm (211) and a greater GR binding capacity than Type II fibres (212). There are also a number of ultrastructural changes described in the muscle of patients with CS including a marked disarray of muscle fibres with wide interfibrillar spaces containing large vacuoles representing damaged and degenerating mitochondria (129). Muscle fibres also demonstrate thickening and deep invaginations of the sarcolemmal basement membrane and thickening of the basement membrane of capillaries (129). *Khaleeli et al.* reported a

sarcolemmal accumulation of glycogen and mitochondria with small deposits of lipofuscin pigment (103).

1.5.3. Molecular mechanisms underpinning glucocorticoid myopathy

Many molecular pathways have been described as playing an important role in the development of GC mediated myopathy including abnormalities in protein metabolism, myostatin, atrophy related genes, collagen metabolism, mitochondrial function and myosin heavy chain isoform synthesis and degradation.

1.5.3.1. Effect of Glucocorticoids on Protein metabolism

Most studies indicate that GC excess increases the rate of whole body proteolyis, even during short term treatment, by inhibiting protein synthesis (213). In patients with CS, plasma leucine concentration, leucine metabolic clearance rate, leucine transport into muscle, leucine turnover and leucine incorporation into protein are all significantly reduced compared to controls (214). Leucine oxidation rates were similar in both groups and this along with other findings suggest that CS associated muscle wasting is associated with a reduction in protein synthesis (214). This may in part be related to the insulin resistance, which occurs in CS leads to a blunted anabolic response to insulin and amino acids (213).

Age may also have an effect on sensitivities of muscle to GC induced myopathy as compared with younger rats, ageing rats with GC induced muscle wasting

have more rapid wasting and slower recovery of muscle function following cessation of GC treatment (215). The underlying pathogenesis in the older rats was depressed protein synthesis compared to increased protein breakdown in the younger rats and this was associated with the activation of the ubiquitin-proteasome proteolytic pathways (215). This change in protein metabolism may be explained by leucine resistance on muscle protein synthesis in older rats as the time to recovery of leucine responsiveness following dexamethasone withdrawal is significantly slower in older rats (216).

1.5.3.2. Effect of glucocorticoids on myocyte proliferation and differentiation

There is conflicting data with regard to the effect of GC treatment on myoblast proliferation rate. Some studies have reported an increase in myoblast proliferation rate with GC treatment (217, 218) (particularly with low dose), others reporting no effect of treatment with glucocorticoids (219) and others reporting a dose dependent decrease in myoblast proliferation with glucocorticoid therapy (220). *Te Pas et al.* reported that GCs are capable of attenuating proliferation and differentiation of myocytes in a dose response manner by altering mRNA levels of myoD1 and myf-5 and myogenin (220). When C2C12 myoblasts were incubated with dexamethasone or α-methyl-prednisolone for 9 days, the cell proliferation rate was reduced in a dose dependent manner despite increasing the mRNA expression of MyoD1 and myf-5 (220). The differences reported in the above studies may be due to the use of different models, different glucocorticoid doses, different glucocorticoid types (e.g. dexamethasone, corticosterone and

alpha methylprednisolone), duration of myoblast proliferation assessed and method of proliferation assay used.

1.5.3.3. Glucocorticoid regulation of myostatin

As previously described in section 1.3.5.2 myostatin is a member of the tumour growth factor β family and is a potent inhibitor of muscle growth, regulating satellite cell activation, myoblast proliferation and terminal differentiation. Cell proliferation requires the completion of the G, M and S cell cycle phases and myostatin prevents myoblasts from progressing past the G0/G1 and G2 phase (68) through the cyclin CDK inhibitor protein 21 (CKIp21), a key component of cell cycle arrest during the G and M phase (69). Thus, fewer cells accumulate in the S-phase and proliferation is prevented. Myostatin also down regulates MyoD1 expression (70) preventing myoblast differentiation into multinucleated myotubules (71, 72). Disruption of the myostatin gene in mice increased muscle mass through muscle hypertrophy and hyperplasia (70). In rats treated with dexamethasone, the resultant muscle atrophy was associated with significantly elevated myostatin mRNA expression and protein concentrations (141). In contrast, myostatin knockout mice resisted GC induced muscle atrophy, whilst also showing increased muscle IGF-I and II mRNA expression (201), indicating that myostatin may play a key role in GC mediated myopathy.

In rodent studies, Type IIb fibres (which are more sensitive to GC mediated myopathy) contain more myostatin than Type I muscle fibres (71, 221, 222), although this might not be the case in humans (223). Transgenic mice over-

expressing the myostatin gene develop severe atrophy in Type IIb fibres compared to Type I fibres (221) with a 20% decrease in gastrocnemius cross sectional area (224). Conversely, the gain in muscle cross sectional area in the myostatin null mouse is predominantly due to Type IIb fibre hypertrophy. Myostatin null mice are 30% larger than age matched wild type litter mates (225) with a 50% increase in gastrocnemius cross sectional area and also increased size of tibialis anterior (62% increase) and soleus (41% increase).

Inhibition of myostatin using a blocking antibody increases mouse quadriceps and gastrocnemius muscle mass by 30% and 23%, respectively (226). This increase in muscle mass is secondary to muscle fibre hypertrophy (227), or a combination of hyperplasia and hypertrophy depending on the species and methodology employed (225, 228). The first reported human with a mutation in the myostatin gene also had gross muscle hypertrophy (229).

The human myostatin promoter region has several GRE (141) and glucocorticoids increase myostatin transcription in a dose dependent fashion in C2C12 cells (141, 230). In the short term (5 days), GCs increased myostatin mRNA expression and reduced MyHC Type II expression by 43% without a change in MyHC Type I expression (141). In the long term (10 days), myostatin expression returned to control values, suggesting a possible down-regulation to protect from sustained muscle loss (141). *Gilson et al.* (201), reported increased mRNA for markers of muscle atrophy such as muscle atrogin-1/ atrophy factor f-box (MAFbx), muscle ring finger-1 (MURF-1) and cathepsin L, a lysosomal protease, in wild type mice after high dose dexamethasone, but these genes were unaltered in myostatin KO mice (201). After 10 days of treatment with

dexamethasone, wild type mice developed a ~15% reduction in tibialis anterior and gastrocnemius cross sectional area, whereas myostatin KO mice showed no signs of atrophy compared with wild type littermates. In conclusion, GC mediated myopathy and its prediliction for Type II fibres, may be caused, in part, by the upregulation of myostatin which has a negative impact on myocyte proliferation and differentiation.

1.5.3.4. Glucocorticoid regulation of atrophy related genes

Within each muscle cell there is a fine balance between atrophy and hypertrophy, which is regulated by a number of cellular pathways. The atrophy pathways include the lysosomal proteases (eg. Cathepsins), the calcium dependent protease calpain family and the ATP-dependent ubiquitin-proteasome pathway (231). Blockade of any of these atrophy pathways (by IGF-I for example) reduces proteolysis (232-234) and attenuates the loss in muscle mass. The pathway primarily associated with muscle atrophy and the breakdown of myofibrillar protein is the ATP-dependent ubiquitin-protease pathway (235). GC treatment increases (~250%) the activity of this pathway (236, 237) with smaller changes (60-100%) in the maximal capacity of the lysosomal process, but no change in the calcium dependent proteolytic system (236, 237).

1.5.3.5. Effect of Glucocorticoids on FOXO/ MURF-1/ MAFbx

As discussed in detail in Section 1.3.5.4, proteins scheduled for degradation in the proteasome are labelled by conjugation with ubiquitin. The 26s proteasome

enzyme complex can then recognise the ubiquitin and initiate protein degradation using at least three classes of proteins. These include the E1 (ubiquitin activating enzymes), E2 (ubiquitin-conjugating enzymes) and E3 (Ubiquitin ligase). Within skeletal muscle, MAFBX and MURF-1 are two important E3 ubiquitin ligases clearly associated with many models of muscle atrophy such as sepsis (79, 80) and disuse atrophy (81) . These genes encode E3 ubiquitin ligase proteins that bind and mediate ubiquitination of specific proteins for degradation (82), such as myosin, actin, troponin and tropomyosin found within skeletal muscle sarcomere (83).

Increased MAFbx and MURF-1 mRNA expression are both associated with translocation of the forkhead transcription factor (FOXO-1) into the cell nucleus (84). Phosphorylation of FOXO-1 by Akt sequesters FOXO-1 from the cell nucleus to the cytoplasm by 14-3-3 proteins (85) preventing MAFbx and MURF-1 upregulation. However, GCs dephosphorylate FOXO-1 allowing subsequent translocation to the cell nucleus. GCs do not activate MAFbx transcription directly, since MAFbx does not contain GREs (238). Instead, GCs target MAFbx via changes in phosphorylation status of FOXO-1 and FOXO-3, leading to increased MAFbx expression (84, 239).

GCs upregulate MURF-1 expression *in vivo* and *in vitro* (84, 86, 239, 240) through the co-binding of the GR and FOXO-1 with the GRE and Fbox response element (FBE) found on MURF-1's promoter region. This combination results in a substantial synergistic upregulation of MURF-1 (143).

When phosphorylated, FOXO-1 is also capable of disrupting mTOR signalling. *In vivo* , mice over-expressing FOXO-1 demonstrated reduced mTOR

phosphorylation and protein abundance with a concomitant reduction in p70S6K threonine^{389} phosphorylation (239). Reduced p70S6K phosphorylation was similarly observed in C2C12 myotubes with a corresponding reduction in [^{14}C] phenylalanine incorporation into muscle protein (239). The authors also demonstrated that FOXO-1 increased 4EBP1 mRNA expression, cellular abundance, hypophosphorylation status, and binding of 4EBP1 to eIF4E by interacting with the 4EBP1 DNA binding domain. These effects were in spite of unchanged total or phosphorylated Akt. Taken together, the GC induced increase in FOXO-1 expression inhibits protein synthesis by targeting mTOR, 4eBP1 and p70S6K, whilst increased FOXO-1 nuclear abundance targets MAFbx and MURF-1 (alone or in combintion with the GR) to initiate proteolysis (239).

In addition to the above activities the activation of FOXO-1 and FOXO-3a in response to GCs can also promote a shift in utilisation from carbohydrate to fat metabolism (241, 242), sparing glucose and its precursors (alanine, glycerol) for glucose dependent cells during periods of starvation, disease or exercise. *Constantin et al.* (243) showed simultaneous increases in fat metabolism and MAFbx and MURF-1 expression after stimulation of FOXO-1, but, crucially, there was no evidence of muscle protein breakdown since the 20s proteasome transcription was unchanged.

1.5.3.6. Effect of Glucocorticoids on hypertrophy related genes

Four major signalling pathways regulate protein synthesis and cell growth including the energy status of the cell (244); the amino acid sensing pathway

(245); mechanotransduction (246, 247) and the insulin/ IGF-I-AI3K-Akt-mTOR signalling system (245).

1.5.3.6.1 Effect of Glucocorticoids on insulin/ IGF-I-AI3K-Akt-mTOR signalling

The insulin/ IGF-I-AI3K-Akt-mTOR signalling pathway increases protein synthesis in the short term (minutes to hours) (240, 248) by activating translational machinery such as eukaryotic initiation factors (eIFs) and eukaryotic elongation factors (eEFs) (249). Over the long term (hours to days), increased protein synthesis stems from elevated ribosome biogenesis, ribosomal cellular content and protein synthesis capacity (249).

Binding of insulin to its cell surface receptor leads to a conformational change and tyrosine autophosphorylation. Consequently, the insulin receptor substrate (IRS) family of adaptor proteins are recruited to the intracellular domain of the receptor and are phosphorylated at multiple tyrosine residues by the receptor tyrosine kinase to permit the docking of phosphatidylinositol-3-kinase (PI3K) and subsequent generation of $PI(3,4,5)P_3$. Generation of this second messenger acts to recruit the Akt/PKB family of serine/threonine kinases to the plasma membrane where they are then activated (250). Further downstream, activated Akt1/protein kinase B (PKB) phosphorylates a rab-GAP (GTPase) protein, AS160, which is a crucial regulator of the translocation of GLUT4 GLUT storage vesicles to the plasma membrane (251). It is this mechanism that permits insulin-stimulated glucose entry into target tissues including skeletal muscle (252). The molecular mechanisms underpinning insulin resistance are complex and variable. Serine/threonine phosphorylation of IRS1 (in particular Ser307 phosphorylation) has been shown to negatively regulate insulin signalling through multiple

mechanisms including decreased affinity for the insulin receptor and increased degradation (253, 254). The interaction of glucocorticoids and the insulin signaling cascade has only been examined in a small number of studies that have offered variable explanations for the induction of insulin resistance (255-258). Importantly, the role of serine phosphorylation and the impact of prereceptor glucocorticoid metabolism have not been explored.

The insulin/ IGF-I-AI3K-Akt-mTOR signalling cascade can also inhibit several regulators of muscle atrophy (196). In rats, 5 days of treatment with cortisone increased the insulin receptor (IR) protein by 36%, but reduced skeletal muscle total IR tyrosine kinase phosphorylation by 69%, which was attributed to a loss in the pool of IR undergoing tyrosine phosphorylation. Although muscle IRS-1 tyrosine phosphorylation was unaffected by GC treatment, GCs were associated with a 50% reduction in total IRS-1 protein content (255).

GC mediated alterations in the expression and cellular abundance of the two PI3K regulatory subunits, p85α and p85β may also induce insulin resistance (259, 260) and impair protein synthesis. GCs act on p85α via the GR (261), leading to a 3-fold increase in p85α mRNA expression and total cellular abundance, whereas p85β remains unchanged. The increased ratio of p85α:p85β can enable more p85α (unbound to its catalytic p110 subunit) to competitively associate with IRS-1, reducing p110 activity and suppressing PI3K activity by 50% (260). Thus, GC myopathy may stem, in part from a GC mediated decrease in the anabolic IR-IRS-1-PI3K-Akt signalling pathway.

1.5.3.7. Effect of glucocorticoids on muscle ribosome function

The reduction in overall rates of translation initiation in GC treated muscle is associated with a reduction in mRNA translational rates, ribosome biogenesis and total cellular RNA abundance (262). Six days of GC treatment reduced rat Type I and Type II muscle fibre RNA synthesis rates by ~29% and 51%, respectively, and resulted in a ~19% and 48% reduction in Type I and Type IIb muscle RNA, respectively. The reduced muscle RNA may be due to to impaired ribosomal capacity (RNA:protein) for protein synthesis (262) and a reduced number of muscle ribosomes (263).

1.5.3.8. Effect of glucocorticoids on muscle collagen

Basement membranes form the extracellular matrix surrounding tissues and this matrix provides the enclosed cells with information, acts as a scaffold and maintains cellular integrity through mechanical strength and stress tolerance (264). The extracellular matrix is composed of a number of proteins such as laminin, glycoproteins, proteoglycans and collagen (in particular Type IV). Slow twitch muscle fibres contain approximately 50% more collagen than fast twitch muscle fibres (265) and GC treatment has been shown to reduce rat Type IV collagen expression in slow twitch soleus, and fast twitch muscles of the extensor digitorum longus (EDL) and tibialis anterior (TA). However, the overall amount of Type IV collagen remained unchanged suggesting either a reduced turnover of Type IV collagen with GC treatment or that the duration of treatment (10 days) was insufficient (266). Another study also showed a GC induced reduction in

Type I, II and IV collagen mRNA that was similar between slow and fast twitch rat muscle fibres (266).

1.5.3.9. Effect of glucocorticoids on muscle mitochondria

Mitochondrial function is also altered by GC therapy. In a micro-array study of 501 human mitochondrial related genes, a number of genes were altered by GC treatment, the most significantly upregulated being monoamine oxidase A (MAO-A) (267). MAO-A's main function is to metabolise cathecholamines and dietary amines, and this up regulation in GC treated cells leads to an increase in MAO-A mediated hydrogen peroxide production which in turn may lead to muscle cell damage (267).

1.5.3.10. Effect of glucocorticoids myosin heavy Chains (MyHCs)

Myosin is a key structural protein in skeletal muscle that is essential for contraction and force generation. Each myosin protein contains 2 myosin heavy chains (MyHC) and 2 myosin light chains (MyLC), the type of MyHC expressed is closely associated with the contractile and metabolic characteristics of a particular muscle fibre (268). The human soleus is a Type I, slow oxidative muscle fibre and expresses 99% Type I MyHC, whereas the gastrocnemius contains a mixture of Type I and IIa isoforms. The quadriceps has a mixture of all 3 fibre Types (95).

GCs have been shown to have a potent effect on MyHC levels. Rats treated with GC displayed increased degradation of muscle contractile proteins and a

decrease in MyHCIIb isoforms and MyHC Type IIa, IIb and IId synthesis rates (269). The resistance of Type I compared to Type II muscle fibres to GC may be attributable to the different MyHC isoforms present in each muscle fibre. *Seene et al.* assessed the effect of dexamethasone treatment on rodent MyHC content and synthesis rates (269). Dexamethasone treatment had no effect on MyHC Type I isoform synthesis rates in the soleus and plantaris muscles whereas significant reductions in plantaris MyHC Type IIa, Type IId and Type IIb synthesis rates were observed. In the EDL muscle, MyHC IIa, IIb synthesis rates were also reduced, but there was no effect of GC on MyHC IId (269).

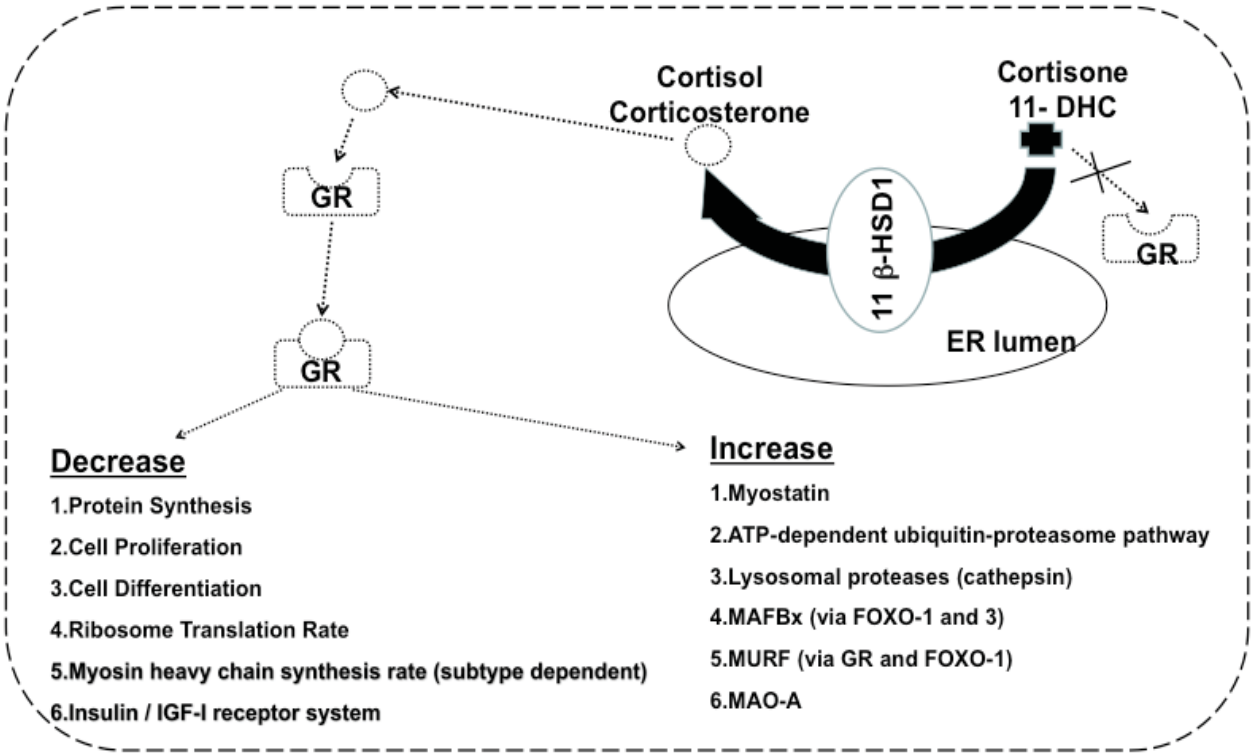

Figure 1.7. *Schema summarising the effect of GCs on regulators of muscle atrophy and hypertrophy.*

1.5.3.11. Role of glutamine synthase in resistance of Type I fibres to glucocorticoids

The precise mechanisms underpinning the increased sensitivity of fast twitch fibres to GC mediated myopathy compared with slow twitch fibres is yet to be fully elucidated. However, the fibre type differences in glutamine synthetase concentrations, an enzyme which catalyses the formation of amino acid glutamine, may partially be responsible. Glutamine synthetase is targeted by the GR (270) and regulates the export of glutamine from muscle. During GC mediated atrophy, glutamine efflux accounts for between 25-30% of the total protein exported from muscle (271). Basal glutamine synthetase activity and expression is lowest in GC resistant rat soleus, intermediate in fast twitch red quadriceps and highest in fast twitch white quadriceps (272). GC treatment increased glutamine synthetase activity and mRNA by 2-4 fold in all muscles; however, the low levels present in the soleus muscle were not related to atrophy (272). Taken together, the fibre type differences in basal glutamine activity and expression are consistent with the sensitivity of fibres to GCs.

1.5.3.12. Potential treatments of glucocorticoid mediated myopathy

Normalisation of GC concentrations in patients treated for CS with pituitary surgery (which normalised of GC concentrations), lead to an increase in overall muscle and Type II mean fibre area (103). The findings suggest that the increase in muscle mass which may follow cure of CS is due to an increase in individual cell size (103).

1.5.3.12.1 GH/IGF-I in the treatment of GC mediated myopathy

Chronic GC excess is associated with a number of changes to growth hormone (GH) secretion. These include a decrease in mean 24hr serum GH concentration, peak GH heights and peak GH areas, but normal GH pulse frequency (273). Despite this, patients with CS often have a normal IGF-I concentration (which may be explained by changes to other sex steroids or increased tissue sensitivity to GH or by a decrease in GH binding protein) (274). When administered during a short time period, the deleterious effects of pharmacological doses of GC on protein metabolism can be prevented with the concomitant administration of GH in normal volunteers (assessed by nitrogen balance and isotope dilution techniques) (275). IGF-I gene transfer into GC treated rats also prevented GC induced muscle atrophy (276). IGF-I has been shown to inhibit many proteolytic pathways including lysosomal, protease dependent and calpain dependent proteolysis (277) and regulate the ubiquitin system (278).

1.5.3.12.2 Exercise in the treatment of GC mediated myopathy

Endurance training is not typically associated with skeletal muscle hypertrophy, but aerobic training can reduce GC induced muscle atrophy in rodents (212, 272, 279-284), but human data is lacking. Endurance training (running 28.7m/minute for 90 minutes/ day for 11 consecutive days) in GC treated rats decreased atrophy by 60% (plantaris) and 25% (gastrocnemius), compared to a control group treated with GC but no exercise. Using the same exercise protocol *Falduto et al.*, (280) showed that the endurance training treatment with GC prevented

100% and 50% of the atrophy in the deep and superficial regions, respectively, of Type IIa muscle fibres and a 67% and 40% reduction in atrophy of Type IIb deep and superficial regions, respectively.

These findings may be explained by the protective effect of exercise on MyHCs. Rats treated with GC who underwent endurance training had a GC induced decrease in MyHC synthesis rates but endurance training did reduce the rate of MyHC breakdown to ~80% of those receiving GCs (285).

A further explanation might involve reduction in glutamine synthetase in skeletal muscle. When rats completed a 12 to 16 week endurance training program, glutamine synthetase expression was reduced to 60% of the sedentary control values with similar findings observed in GC treated, endurance trained rats (286). Moreover, endurance training reduced glutamine synthetase activity and expression in rat fast twitch red fibres to between 35-70% of sedentary control values (287) . Endurance training also reduced glutamine synthetase activity in soleus, but did not alter basal or GC mediated expression in fast twitch white muscle fibres.

Resistance training has also been shown to increase muscle mass and strength in patients receiving GC treatment after heart transplantation. Following transplantation, 6 months of resistance exercise increased fat free mass by 3.9% above pre-transplant levels. Knee extension, chest press and lumbar extension strength improved between 4-6 fold after resistance training compared with controls (288). In a more recent study, transplant recipients presenting with GC mediated myopathy underwent 6 months of resistance training following transplantation (289). Type I MyHC increased 73% in the training group

compared with a 28% reduction in the control group. A 17% increase in MyHC IIb and 33% decrease was observed in the training and control groups. Taken together, these studies demonstrate an inhibitory effect of endurance and resistance exercise on GC mediated atrophy, although the underlying molecular mechanisms remain unclear.

1.6 Conclusions

As the population ages, conditions such as sarcopaenia are becoming more prevalent. Sarcopaenia has many similarities with GC mediated myopathy and there is evidence from other tissue that glucocorticoids exposure may increase with age as a result of upregulation of 11 β-HSD1. GCs impact on atrophy and hypertrophy pathways within muscle. Type I fibres are more resistant to the effects of GC compared to Type II fibres, yet the mechanisms underpinning the disparity are not fully understood. Our knowledge of the role of 11 β-HSD1 in skeletal muscle is starting to emerge, but further research is required in this area. Pharmacological inhibition of 11 β-HSD1 may possibly provide a therapeutic target to reduce muscle atrophy in ageing and those with GC excess.

1.7 Hypothesis

a. 11β-HSD1 is abundant and biologically important in skeletal muscle.

b. 11β-HSD1 activity and expression is increased with glucocorticoid treatment, therefore leading to higher tissue glucocorticoid levels. 11β-HSD1 may be a key regulator of glucocorticoid mediated myopathy.

c. 11β-HSD1 increases in muscle with age and may be associated with muscle atrophy.

d. In patients with hypopituitarism and cortisol deficiency, hydrocortisone replacement therapy may increase tissue glucococorticoid exposure, which may explain some of the adverse phenotype in these patients.

1.8 Aims

a. Characterise the expression and activity of 11β-HSD1 in skeletal muscle.

b. Determine the role of 11β-HSD1 in glucocorticoid-mediated myopathy.

c. Determine the role of ageing on 11β-HSD1 expression and activity in skeletal muscle and the impact of changes in 11β-HSD1 during ageing.

d. Determine the effect of exogenous glucocorticoid replacement therapy on 11β-HSD1 in patients with hypopituitarism.

Chapter 2

Materials and Methods

The procedures described in this chapter were commonly used in this thesis. Methods specific to individual chapters are found in the methods section of those particular chapters. Unless otherwise stated, all reagents were purchased from Sigma Aldrich, Dorset, UK.

2.1 C2C12 cell culture

The C2C12 cell line is a well-established model of both skeletal muscle proliferation and differentiation. The C2C12 cell line was originally generated by serial passage of myoblasts cultured from the thigh muscles of C2H mice 70 hours following a crush injury (290). A subclone of these myoblasts was selected for its ability to differentiate rapidly and express characteristic muscle proteins (291). The C2C12 cell line has been widely used in research with regard to muscle atrophy and glucocorticoid induced myopathy (84, 86, 195, 197).

2.2 Proliferation and Differentiation

2.2.1 Proliferation

Cryofrozen C2C12 myoblasts (passage 17) were purchased from ECACC (Salisbury, UK), and maintained in 75cm^3 TC flasks (Corning, Surrey, UK) in 15mL of DMEM with high glucose and L-glutamine (PAA, Somerset, UK) supplemented with 10% FCS, in incubators at 37°C under a 5% CO_2 atmosphere. At 60-70% confluence cells were trypsinised and re-seeded into fresh flasks. Prior to experiments being performed, cells were trypsinised and subcultured into 24 well TC plates (Corning, Surrey, UK) and cultured until 60-70% confluent. Proliferation media was replaced every 48 hours. Cells were not proliferated beyond passage 25 in order to ensure they retained adequate myoblast/ myotubule characteristics.

2.2.2 Differentiation

Once myoblasts had reached 60-70% confluence, differentiation was initiated by replacing proliferation media with DMEM with high glucose and L-glutamine (PAA, Somerset, UK) supplemented with 5% horse serum. Differentiation media was replaced every 48 hours. After 8 days, myoblasts had fused to form multinucleated myotubes (Figure 2.1).

Figure 2.1. *C2C12 myoblast cells were differentiated in chemically defined media for 8 days forming multinucleated myotubes*.

2.2.3. Freezing down cells

Cells to be frozen were grown in 25cm^2 flasks until 70% confluent at which point cells were trypsinised and resuspended in 10mls of proliferation media before being centrifuged at 1000g for 10 minutes. Media was aspirated to leave the remaining pellet which was resuspended in 3mls of foetal calf serum (FCS) supplemented with 10% DMSO. The cell mixture was then aliquoted into 1.5ml cryovials. Cryovials were frozen at 1^{o}C per minute in a Cryo freezing container (Nalgene, Hereford, UK) containing isopropanol. They were kept at -80^{o}C

overnight following which the cells were transferred to a liquid nitrogen storage container for long-term storage.

2.3. RNA extraction

2.3.1. Principle

Total RNA was extracted from monolayer cells using TRIreagent (Sigma-Aldrich, Dorset, UK). The procedure was carried out according to protocol provided with the reagent (Sigma-Aldrich, Dorset, UK).

RNA was extracted from cultured cell monolayers or tissue explants using a single step procedure developed by Chomczynski (292). This was achieved by homogenizing tissue or lysis of cultured cells in TRI reagent. This solution contains phenol and guanidine thiocyanate and immediately and effectively inhibits RNase activity. The addition of chloroform, followed by centrifugation results in the formation of three phases. RNA is present exclusively in the aqueous phase following centrifugation at 10,000G for 15 minutes, and is subsequently precipitated with isopropanol.

2.3.2. Methods

Monolayer cells were washed on ice with PBS. 1.0ml of TRIreagent (Sigma-Aldrich, Dorset, UK) was added per well and cells were incubated at room temperature for 5 minutes and then the cell lysates were transferred into eppendorfs. For tissue explants approximately 20mg of tissue was homogenized in 1.0mL of TRIreagent, then incubated at room temperature for 5 min. 200ml of

chloroform was added to the eppendorf for every 1ml of TRIreagent initially added, and the tubes were shaken for 30 seconds at room temperature, following which they were allowed to stand at room temperature for 15 minutes. The eppendorf was then transferred to a refrigerated centrifuge and centrifuged at 10,000g for 15 minutes at 4^{o}C. After this there were 3 layers an upper aqueous, middle protein layer and lower organic layer containing DNA. The upper aqueous phase containing RNA was then transferred to a fresh eppendorf and 0.5mls of isopropanol was then added. Tubes were mixed by inverting and placed at -20^{o}C overnight, following which they were centrifuged at 10,000g at 4^{o}C for 15 minutes. This resulted in a visible pellet and the supernatant was carefully removed. The pellet was then washed with 75% ethanol, following which the eppendorf was vortexed and subsequently centrifuged at 5000g for 10 minutes at 4^{o}C. Again a pellet was found at the bottom of the eppendorf and the ethanol supernatant was removed by aspiration. The RNA pellet was allowed to air dry for 5 minutes and then re-suspended in 50ml of RNAase/ Nuclease free H_20 and put on a heating block at 55^{o}C to aid dissolving of the pellet. Finally, the RNA was stored in a -80^{o}C freezer until further use.

2.3.3. RNA quality and quantification

The quality of the RNA was assessed by gel electrophoresis on a 1% agarose gel with 0.15µg/ml ethidium bromide. The gel was visualised under a UV light in a G:Box gel documentation system (Syngene, Cambridge, UK). The RNA separates down the gel according to its molecular mass and the resultant bands werw visualized under UV light. Intact RNA shows two sharp bands corresponding to the highly abundant 28S and 18S rRNA.

The quantity of RNA was measured using NanoDrop ND-1000 UV-Vis Spectrophotometer (Thermofisher, Surrey, UK). The absorbance of 2µl of RNA at 260nm and 280nm was determined where 1 OD_{260} = 40µg/mL of RNA and the OD_{260}/OD_{280} ratio indicates the RNA purity. Only OD_{260}/OD_{280} ratios in the range of 1.8-2 were used. All measurements were made with respect to a blank consisting of the nuclease free water in which the RNA was suspended.

2.4. Reverse transcription and polymerase chain reaction of RNA

2.4.1. Principles

Reverse transcription polymerase chain reaction (RT-PCR) is the process of converting single strand mRNA into complimentary DNA (cDNA) using RNA-dependent DNA polymerase. Initially the extracted RNA is heated to allow annealing of random hexamers to the RNA template.

The reverse transcription process is initiated by increasing the temperature further allowing the RNA-bound primers to be extended generating a complementary DNA copy of the RNA template. Lastly, the reaction is heated to a high temperature to inactivate the enzyme and terminate the reaction.

2.4.2. Method

All RT reactions were carried out using Applied Biosystems High-Capacity Reverse Transcription Kit (Applied Biosystems, Warrington, UK). The reagents listed in Table 2.1 were combined in an eppendorf tube to generate a 2x RT master mix.

Component	Volume (µl) per sample
10X RT Buffer	2
25X dNTP mix (100mM)	0.8
10X Random Hexomers	2
MultiScribe Reverse Transcriptase	1
RNase inhibitor	1
Nuclease-free H_2O	3.2
TOTAL VOLUME	**10**

Table 2.1. *Constituents of reverse transcriptase reactions*

1µg of RNA was diluted with nuclease free water to a volume of 10µl before 10µl of 2x RT master mix was added giving a final volume of 20µl. Samples were loaded onto a thermal cycler (Applied Biosystems, Warrington, UK) and incubated at 25°C for 10 minutes followed by 48°C for 30 minutes and finally 95°C for 5 minutes to terminate the reaction.

2.5. Conventional PCR

2.5.1. Principles

Regions of DNA or cDNA can be amplified using oligonucleotide primers that are complimentary to the 3' and 5' ends of a region of interest DNA or cDNA fragments by PCR. High temperature is used to denature double stranded DNA which is then cooled to allow the oligonucleotides primers to anneal. When the temperature is increased to the optimal catalytic temperature for taq polymerase, these oligonucleotides are extended to generate complementary DNA strands. Taq DNA polymerase is then used to extend the oligonucleotide and produce a complementary strand. Both strands act as templates for subsequent cycles. Therefore the amount of product increases exponentially until production plateaus due to limiting nucleotides and Taq concentrations. Conventional PCR, was used to check the integrity of cDNA prior to RT-PCR and to assess presence of a gene sequence in cDNA.

2.5.2. PCR Methods

All conventional PCR reactions were carried out using Promega reagents (Promega, Southampton, UK). In a 20ml reaction the following components were added: reaction buffer (final conc 1x), $MgCl_2$ (1-2.5nM), deoxy-NTPs (0.5mM), Taq polymerase (0.05U/mL), forward and reverse primers (0.6mM) and 100mg cDNA taken from RT-PCR reaction). In a thermal cycler, samples were incubated at 95°C for 5 minutes and then cycled 30 times at 95°C for 30 seconds, 60°C,

30°C and 72°C for 1 minute. Samples were then incubated for 7 minutes at 72°C. Samples were then stored in a -80°C freezer.

2.6. Relative quantitative (Real Time) PCR reaction

2.6.1. Principles

Real-time PCR or relative quantitative PCR is a technique used to monitor the progress of a PCR reaction in real-time. Taqman Real-Time PCR technology uses fluorogenic probe to allow detection of a specific PCR product as it accumulates during the PCR reaction. An oligonucleotide probe is synthesized containing a fluorescent reported dye on its 5' end and a quencher dye on its 3' end. The proximity of the quencher dye reduces the fluorescence emitted by the reporter dye by fluorescence resonance energy transfer (FRET). The probe anneals downstream from one of the primer sites and during the primer extension is cleaved by the 5' nuclease activity of Taq polymerase. The removal of the probe allows primer extension to continue and does not inhibit the PCR process. The cleavage of the probe separates the reporter and the quencher dye, increasing the reporter dye signal (Figure 2.2). During each cycle additional reporter dye molecules are cleaved, resulting in an increase in fluorescence intensity proportional to the amount of PCR product produced.

Real time PCR allows collection of data through the PCR process and thus allowing detection during the amplification cycling. The method insures one can measure when the target is first detected rather than the amount of target produced after a fixed number of cycles. The value at which the product is

detected is the Ct value. The higher the target copy number in a sample the lower the cycle number where the fluorescence is first observed (lower Ct value). This technique was used for relative quantification, whereby the Ct value for the target gene is compared to the Ct value of a housekeeping gene, with a constant expression level (such as 18s or GAPDH). This comparison (Ct of the gene of interest – Ct of the house keeping gene) allows calculation of the changes in expression due to treatment relative to the housekeeping gene, this is known as the delta Ct (ΔCt). For ease of data interpretation and graphical representation the ΔCt was converted to arbitrary units (AU = $1000x2^{-\Delta Ct}$) (Figure 2.3).

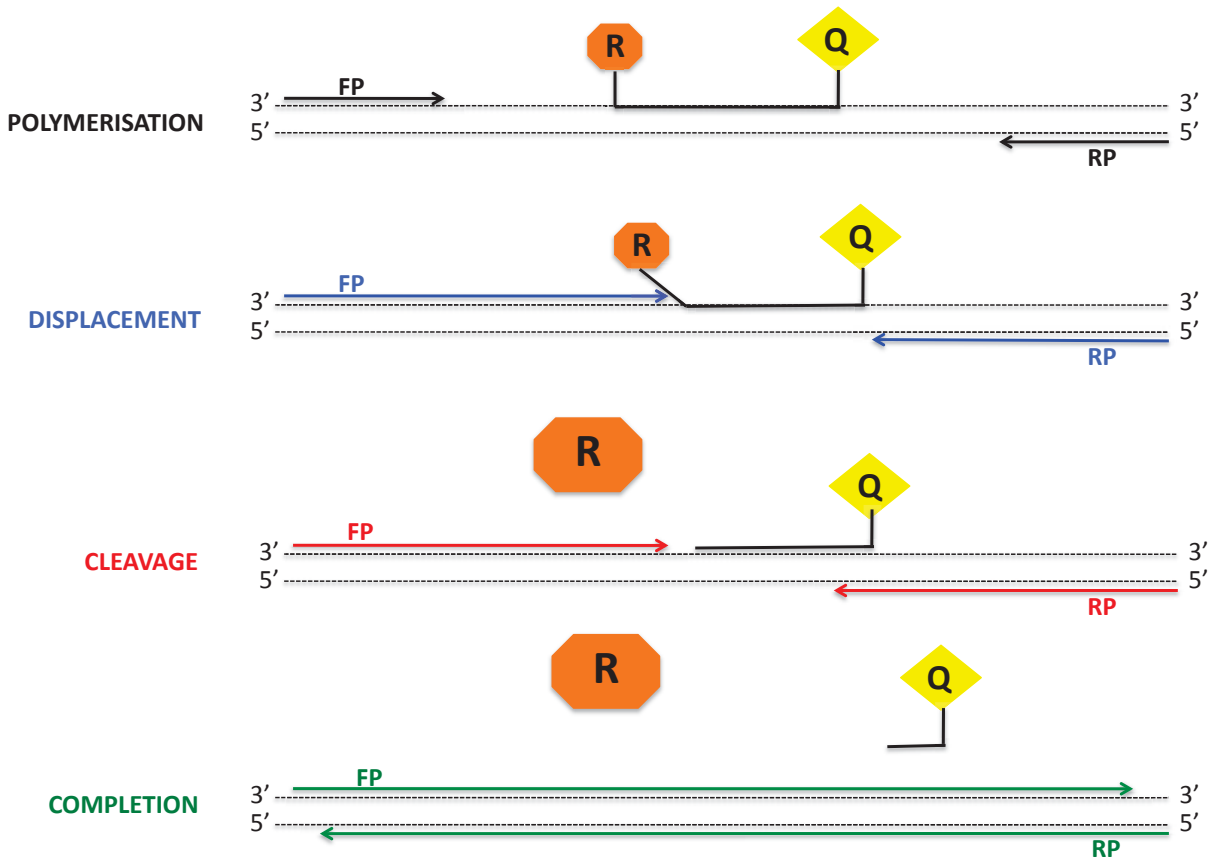

Figure 2.2. *Schematic representation of real-time PCR. Separation of reporter dye from the quencher allows detection of fluorescence. Fluorescence is proportional to the amount of PCR product produced (FP = forward primer, RP = reverse primer, R = reporter and Q = Quencher).*

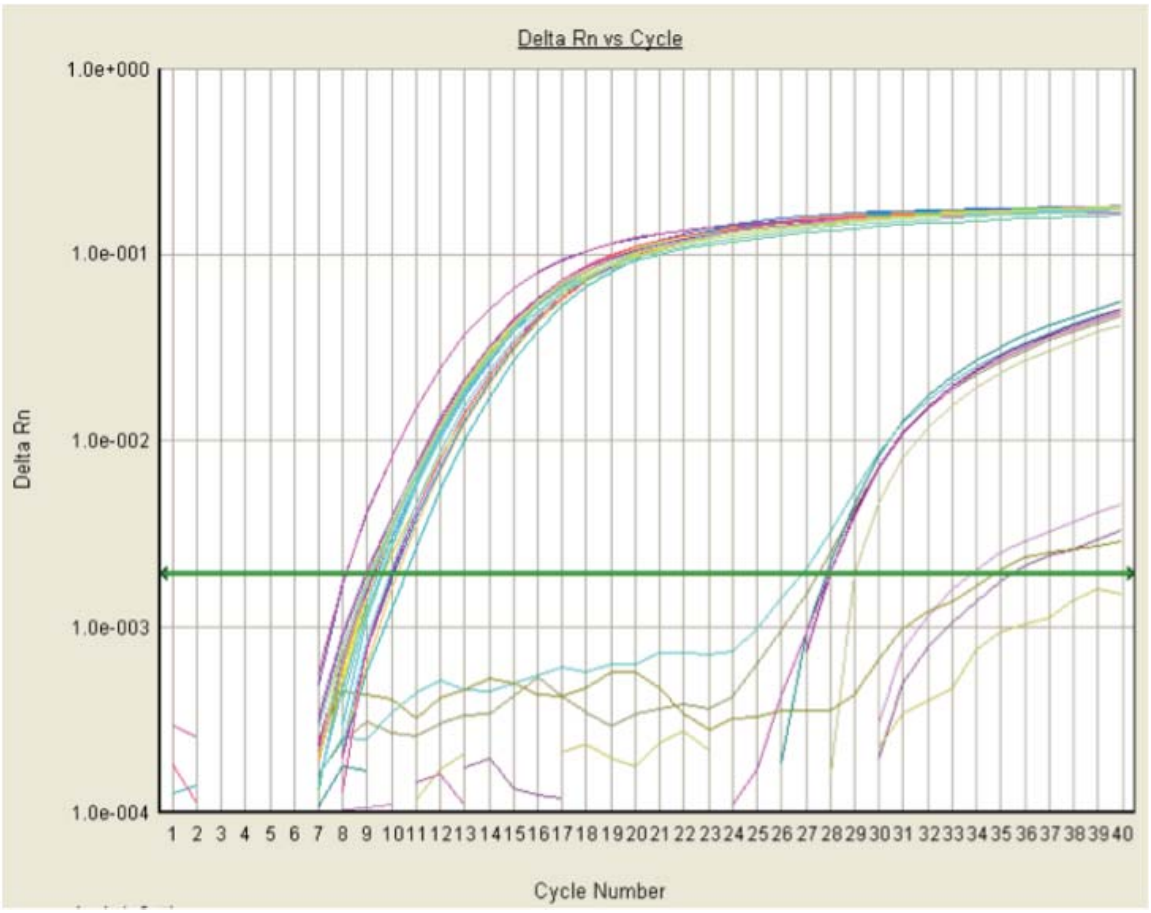

Figure 2.3. *Representative real time PCR graph showing differences in expression between target and housekeeping genes.*

2.6.2. Real-Time PCR Method

Unless otherwise stated, quantitative PCR was carried out using Applied Biosystems Reagents and gene expression assays (AssayonDemand) (Applied Biosystems, Warrington, UK). PCRs for genes of interest and for 18s/ GAPDH housekeeping genes were carried out in singleplex. For the 18s house keeping gene, the following components were combined per well: 10µl of 2x MasterMix, 18s forward and reverse primers and vic labelled probe (final concentration 25nM

each), 100ng of cDNA and nuclease free water to a final volume of 20µl. For the gene of interest, the following components were combined per well: 10µl of 2x MasterMix, 1µl of 20x expression assay, 100ng of cDNA and nuclease free water to a total volume of 20µl. Plates were sealed with clear adhesive film (Applied Biosystems, Warrington, UK) and run on a 7500 real-time PCR system (Applied Biosystems, Warrington, UK). Target gene expression was normalised against the 18s RNA house keeping gene Ct value and these measurements were carried out in separate wells from target gene expression measurements (singleplex). All reactions were carried out in duplicate in 96-well plates (Applied Biosystems, Warrington, UK). Data were expressed as Ct values (Ct=cycle number at which logarithmic PCR plots cross a calculated threshold line). And used to determine ΔCt values (ΔCt = (Ct of the target gene) – (Ct of the housekeeping gene), lower ΔCt values reflecting higher mRNA expression. Data are expressed as arbitrary units using the following transformation [expression in arbitrary units = $1000*(2^{-\Delta Ct})$] or fold changes were calculated using the transformation [fold increase = 2-difference in ΔCt].

2.7. Protein Extraction on monolayer cells

2.7.1. Principles

Monolayer cells were lysed in Radio-Immunoprecipitation (RIPA) buffer containing detergent which enables efficient cell lysis and protein solubilisation while avoiding protein degradation and interference with protein immunoreactivity and biological activity. The lysate was freeze thawed to further break open cell membranes and the insoluble components removed by centrifugation.

2.7.2. Methods

Monolayer cells were washed on ice with cold phosphate buffered saline (PBS). For cells grown in 24-well plates 70µl of RIPA buffer was added to each well. The constituents of RIPA buffer included (1mM EDTA, 150mM NaCl, 0.25% SDS, 1% NP40, 50mM Tris pH 7.4, supplemented with protease inhibitor cocktail (Roche, Sussex, UK) and phosphatase inhibitor (Thermofisher, Surrey, UK)). After the addition of RIPA buffer the cells were scraped using a 1mL syringe plunger. The resultant cell lysate was transferred into an eppendorf and incubated at -80^{o}C for 20 minutes and thawed on ice. The lysate was then centrifuged at 14000g for 15 minutes at 4°C to spin down the insoluble cellular components. The supernatant, containing soluble proteins was measured and samples were stored at -80^{o}C.

2.7.3. Protein extraction from mouse tissue explants

Mouse tissue was quickly harvested and snap frozen using liquid nitrogen. Samples were then transferred to a -80°C freezer until required. Proteins were extracted by homogenising approximately 20mg of tissue in 1.5mL of RIPA buffer using a mechanical homogeniser. Cell lysates were then incubated at -80°C for 20 mins, thawed out on ice, then centrifuged at 14,000 g for 15 mins at 4°C. The supernatants containing soluble proteins was transferred to fresh eppendorfs tubes and stored at -80°C prior to assessment of protein concentrations (see below).

2.7.4. Measuring protein concentration

2.7.4.1. Principles of measuring protein concentration

Total soluble protein concentrations of cell extracts and tissue explants were measured using BioRad RC DC protein assay (BioRad, Herts, UK). This is a colourmetric assay for protein concentration following detergent solubilisation, the RC means the assay is reducing agent compatible and the DC means it is detergent compatible. The assay is based on the Lowry method, that is the reaction of protein with an alkaline copper tartrate solution and then reduction of Folin reagent. Folin reagent is reduced by the loss of 1,2 or 3 oxygen atoms, primarily due to amino acids tyrosine, tryptophan and to a lesser extent, cystine, cysteine and histidine.

The protein to be quantified initially reacts with the copper in an alkaline copper tartrate solution. Folin then reacts with the copper treated protein subsequently leading to the generation of various reduced folin species all of which have a characteristic blue colour and absorb maximally at 750nM and minimally at 405nM.

2.7.4.2. Methods of protein measurement

Protein assays were carried out according to the protocol provided by manufacturer (BioRad, Herts, UK) in a 96 well plate. 5µl of protein sample or standard were added per well in duplicate. The range of standards were 0, 0.25, 0.5, 1, 2, 4, 8 and 10mg/ mL of Bovine Serum Albumin (BSA) in RIPA buffer. 25ml of solution A (alkaline copper tartrate) (with 20µl of solution S per ml of

solution A) was initially added followed by 200µl of solution B (Folin reagent). Once the solutions were added the plate was incubated at room temperature for 10 minutes and the absorbance read at 690nm on a Victor3 1420 multilabel counter (PerkinElmer, Beaconsfield, Bucks, UK). Protein concentration in the sample was then calculated according to the slope of the standards line.

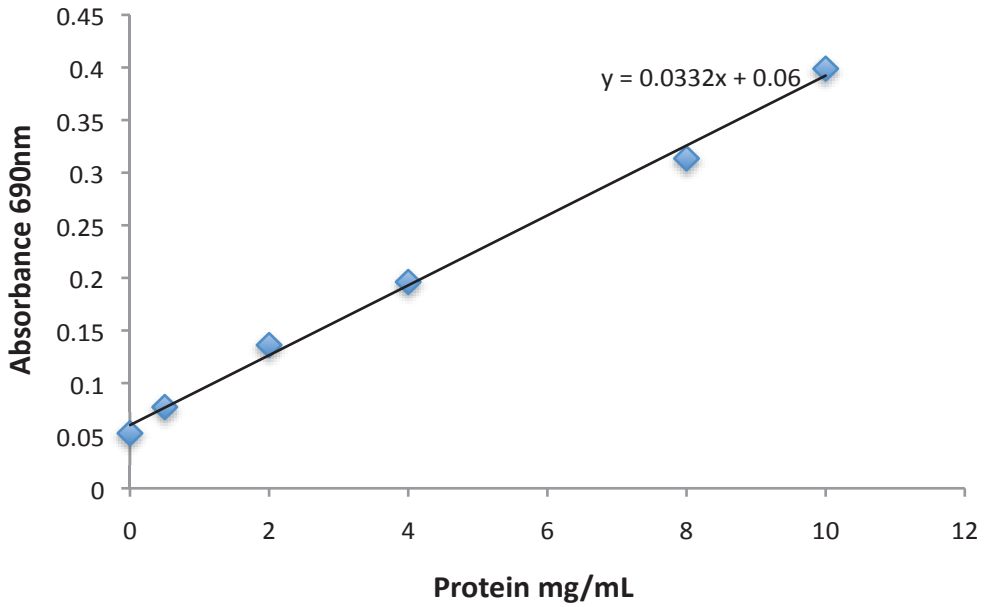

Figure 2.4. *Representative BSA protein standard curve for the BioRad RC DC protein assay. Protein concentrations can be determined from the equation y=mx+c once the absorbance at 690nm is known.*

2.8. 11 β-hydroxysteroid dehydrogenase type 1 and 2 enzyme activity assay

2.8.1. Principles

This technique allows for the measurement of the inter-conversion between the inactive glucocorticoid cortisone (E) in humans [11-dehydrocorticosterone (A) in rodents] and active cortisol (F) in humans [corticosterone (B) in rodents] by

isozymes of 11β-HSD. This protocol was carried out on both monolayers of intact cells and whole tissue explants. Prior to the assay monolayer cells were left in serum free media for 1-2 hours. Media was then removed from cells and the cells were then washed in PBS.

2.8.2. Method of 11β-HSD assay on monolayers

Confluent cell monolayers (C2C12 murine skeletal muscle cells) were incubated with serum free DMEM media for 2 hours following which they were washed once with PBS then and then 1ml of serum free DMEM media containing 100nM of either 11-DHC enriched with 20000cpm/reaction ^{3}H-11DHC (for synthesis see below) or corticosterone enriched by 20000cpm/reaction of ^{3}H-corticosterone (GE Healthcare, Bucks, UK). Incubations were carried out at 37°C under a 5% CO_2 atmosphere for 20minutes to 2 hours depending on the cell or tissue type. Media was then transferred to a glass test tube and 6mL of dichloromethane was added. The cells were retained in 100µL of PBS (or 70µl RIPA) and stored at -80°C for protein quantification (see Section 2.5). Steroids were extracted from media by vortexing the tubes for 20 seconds. Aqueous and organic phases were separated by centrifugation at 1000 g for 10 minutes. The aqueous phase was aspirated off and the organic phase containing the steroids was evaporated at 55°C using an air blowing sample concentrator (Techne, New Jersey, US). Steroids were resuspended in 70µl of dichloromethane and spotted onto a silica coated thin layer chromatography plate (Thermofisher, Surrey, UK) using a glass Pasteur pipette followed by spotting of 2µl of non-radiolabelled 11-DHC/corticosterone or cortisone/cortisol (10mM in ethanol) as a cold standard.

Each spot was separated by at least 1.5cm from adjacent samples and 2cm from the bottom of the plate. Steroids were then separated by thin layer chromatography using 200mL of cholorform:ethanol (92:8) as the mobile phase for 2.5 h. Radioactivity of the separated ^{3}H-11-DHC/^{3}H-corticosterone or ^{3}H-cortisone/^{3}H-cortisol was measured using a Bioscan 200 Imaging Scanner (LabLogic, Sheffield, UK) for 10 minutes per lane. Finally, to assign the radioactivity peaks with the correct steroids the plates were placed under UV light to visualise the position of the cold standards.

Percentage conversion was calculated using region counts for the individual peaks. Enzyme activity was expressed in pmoles of steroid converted per mg of protein per hour (pmol/mg/h). Calculation for steroid conversion (V):

Steroid conversion = % conversion/100 x S x (1000/P)/T

S = substrate concentration in reaction volume; e.g. if 100nM of substrate used in 0.1ml volume, S=100pmol/reaction, P= protein concentration in well in mg, T = time in hours

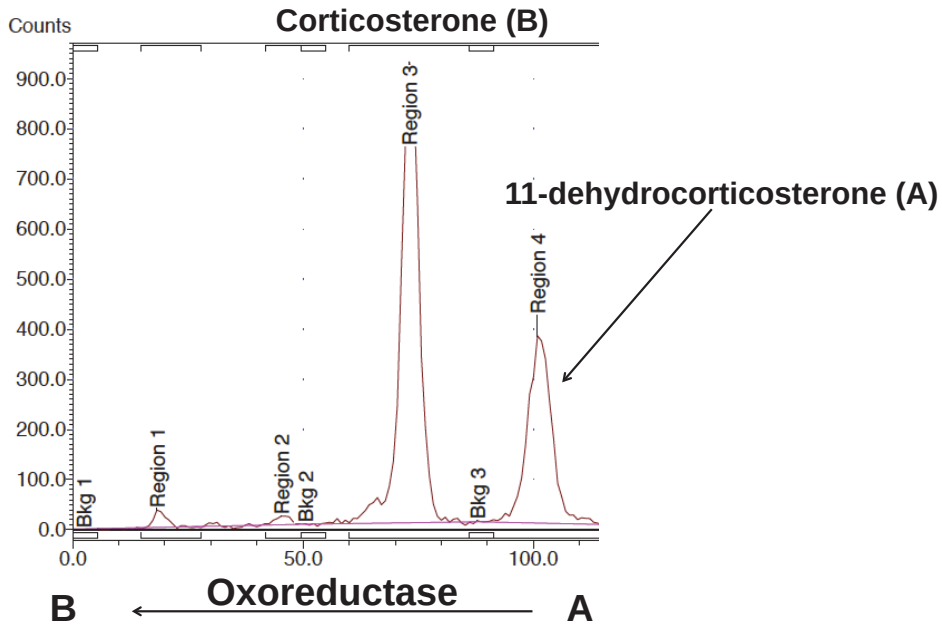

Figure 2.5. *Representative Bioscan traces for 11β-HSD1 oxo-reductase activity in C2C12 myotubes.*

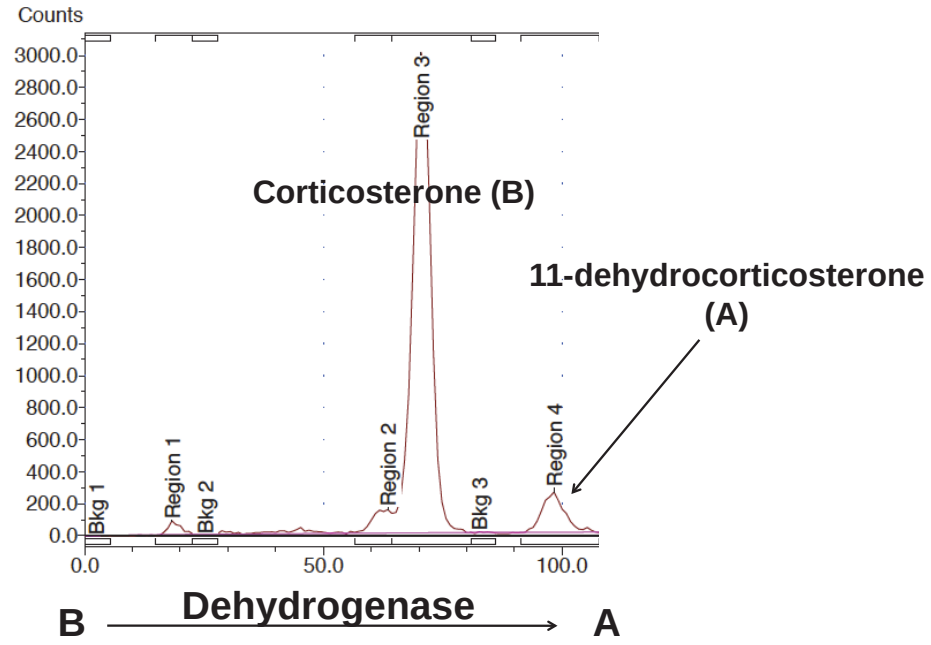

Figure 2.6. *Representative Bioscan traces for 11β-HSD1 dehydrogenase activity in mouse C2C12 myotubes.*

2.8.3. Method of 11β-HSD assay on Mouse tissue explants

Fresh tissue explants were chopped to ~20mg/well and the above protocol was followed. Activity expressed as pmoles of steroid converted per mg of tissue per hour (pmol/mg/h). Incubations were carried out at 37°C under a 5% CO_2 atmosphere for 20 minutes (liver) to 2 hours (muscle and adipose tissue) depending on the tissue type.

2.8.4. Production of tritiated 11-dehydrocorticosterone (3H-11DHC)

Unlike tritiated cortisone (^{3}H-cortisone), cortisol (^{3}H-cortisol) and corticosterone (^{3}H-corticosterone), tritiated 11-dehydrocorticosterone (^{3}H-11DHC) is not commercially available; consequently tritiated corticosterone [^{3}H-corticosterone (GE Healthcare, Bucks, UK] was used to generate ^{3}H-11DHC by a dehydrogenase reaction employing 11β-HSD2 dehydrogenase activity in placenta. Initially, mouse placenta was homogenised with a few strokes of homogeniser in 2ml of 0.154 M KCl. This tissue homogenate was then centrifuged at 1500rpm for 10 min at 4^{o}C and supernatant was aliquoted into eppendorfs and stored at -80^{o}C until required (at this stage protein concentration was measured using BioRad method, Section 2.5).

In glass test tubes, 20µl of ^{3}H-corticosterone (1mCi/mL) was incubated with 250µg of homogenised mouse placenta in 500µl of 0.1M phosphate buffer (pH7.4), with 500µM NAD^+. Conversion was carried out overnight in a shaking water bath at 37°C. Steroids were extracted by addition of 6mL of dichloromethane and vortexing the tubes for 20 seconds. Aqueous and organic

phases were separated by centrifugation at 1000 g for 10 minutes. The aqueous phase was aspirated off and the organic phase containing the steroids was evaporated at 55°C using an air blowing sample concentrator (Techne, New Jersey, US). Steroids were resuspended in 5µl of dichloromethane and spotted onto a singly point of a silica coated thin layer chromatography plate (Thermofisher, Surrey, UK) using a Pasteur pipette. Cold standards of corticosterone and 11-dehydrocorticosterone were spotted onto the plate but at least 4cm distant to the spotted hot steroids, to avoid contamination. Steroids were then separated by thin layer chromatography using 200mL of cholorform:ethanol (92:8) as the mobile phase for 2.5 hour. To establish the position of ^{3}H-11DHC, the silica plates were read using a Bioscan 200 Imaging Scanner (LabLogic, Sheffield, UK). The silica at the corresponding position to ^{3}H-11DHC was scraped into a glass test tube and eluted in 500mL of ethanol overnight at 4°C. The eluted ^{3}H-11DHC and silica were separated by centrifugation at 1000 g for 5 minutes. Radioactivity of ^{3}H-11DHC was determined by spotting 5µL of stock by thin layer chromatography and number of counts determined using the Bioscan 200 Imaging Scanner. Stock was then diluted in ethanol to give ~1000 counts/µL.

2.9. Immunohistochemistry of 11β-HSD1

2.9.1. Principles of Immunohistochemistry

Immunohistochemistry is based on the binding of antibodies (usually IgG) to a specific antigen in tissue sections (293). Fixation of tissues is necessary as it adequately preserves the cellular components and proteins, prevents autolysis and displacement of cell constituents, stabilizes cellular materials and facilitates immunostaining (293). Fixation modifies the tertiary structure of antigens which may make it more difficult for antibodies to detect them (85% of antigens fixed in formalin require some type of antigen retrieval to optimize immunoreaction). Antigen retrieval reverses some of these changes (293). Another factor is the antibody type as polyclonal antibodies are more likely to detect antigens than monoclonal antibodies without antigen retrieval (293). Methods of antigen retrieval include protease induced epitope retrieval, heat induced epitope retrieval and pretreatment with formic acid (293).

The antigen-antibody reaction cannot be seen with the light microscope unless it is labelled, therefore labels are attached to the primary, secondary or tertiary antibodies of a detection system to allow visualisation of the immune reaction (293). Detection systems are either direct or indirect, the direct method is a one step process with a primary antibody conjugated with a reporter molecule. Indirect methods (two steps) are needed for more sensitive antigen detection. In this method the first antibody added is unlabelled but the second layer, raised against the primary antibody is labelled. This is superior and more sensitive to the direct method as the primary antibody is not labelled therefore retaining its activity and resulting in a strong signal and the number of labels per molecule of primary

antibody is higher, therefore increasing the intensity of the reaction. Indirect methods include the Avidin-Biotin, Peroxidase-antiperoxidase, polymeric labelling two step method, tyramine amplification and immuno-rolling method (293).

2.9.2. Method of Immunohistochemistry

Immunohistochemistry was performed on paraffin embedded sections of tissue that were collected in 10% formalin. Slides were dewaxed and rehydrated by initially placing in an oven at 60^{o}C for 20 minutes followed by immersion in xylene for 2 minutes (x2), then 100% ethanol for 5 minutes (x2) and finally 95% ethanol for 5 minutes (x2).

Following this an antigen retrieval step was performed by placing slides in a beaker containing 0.01M citrate buffer (pH 6) which was microwaved on high power (2x2mins with 5 minute rest in between) or 8 minutes until boiling. This was then allowed to cool to room temperature and washed thoroughly with tap water. Slides were then incubated for 15 minutes in methanol hydrogen peroxide 30% (62.5:1 v/v) for 5 minutes followed by a rinse in copious tap water and finally a wash in PBS.

Three different primary antibodies for 11β-HSD1 were used and primary and secondary antibody concentrations were as shown in Table 2.2.

Antibody	Primary antibody stock	Primary antibody dilution and final concentration	Secondary antibody dilution
Binding Site (polyclonal) (294)	1mg/ml	1:33 30µg/ml	anti-sheep/goat peroxidase (1:100)
Abcam (polyclonal) Ab39364	0.6mg/ml	1:20 30µg/ml	goat/ anti-rabbit peroxidase (1:100)
Cayman (polyclonal) Cayman No: 10004303	0.6mg/ml	1:20 30µg/ml	goat/ anti-rabbit peroxidase (1:100)

Table 2.2. *Summary of the three different primary antibodies for 11β-HSD1 used and primary and secondary antibody concentrations.*

Blocking was then performed with 10% normal donkey serum in PBS v/v for 30 minutes at room temperature to reduce background staining (goat serum for Caymen and Abcam), importantly, the blocking agent was not washed off prior to placing the primary antibody on the slide. Sections were incubated with 100µl primary antibody (final concentration 30µg/ml) in 10% NDS/PBS (NB for Cayman/

Abcam 10% NGS/ PBS) for 1.5 hours at room temperature. Following the incubation of primary antibody the slides were washed once in PBS and then incubated with 100µl secondary antibody (goat anti-sheep IgG peroxidase conjugate for binding site and goat anti-rabbit for Abcam and Cayman) at a dilution of 1:100 (in PBS for 30 minutes at room temperature). The slides were then rinsed in PBS prior to visualisation of the secondary antibody. To visualise staining one DAB (3,3'-Diaminobenzidine) tablet, Sigma Aldrich, Dorset, UK with the H2O2 tablet was dissolved in 15mls of H2O and the solution mixed and filtered through Whatman filter paper. Sufficient DAB solution was added to each slide to completely cover the section and left to develop for 5 minutes or until brown stain appears. Following this the slide was submerged in tap water to stop the chromagen reaction and washed with copious tap water. The slide was then counterstained by immersing in Meyers haematoxylin for 30 seconds, following which it was washed in copious tap water. The slide was then placed in 100% ethanol for 5 minutes (x2), then Xylene for 5 minutes (x2) and mounted using dibutyl polystyrene xylene (DPX).

Negative controls were carried out using anti-11β-HSD1 immunising peptide 1:100-1:500 (pre-adsorbed), blank or isotype control.

2.9.3. Methods for Immunoflourescence

Immunoflourescence was performed in collaboration with Dr Chris Shaw, School of Sports and Exercise Science, University of Birmingham. Muscles to be processed for immunoflourescence were handled differently than those for standard immunohistochemistry. Briefly, muscle samples were embedded in

Tissue-Tek OCT Compound (Sakura Finetek Europe, The Netherlands) and immediately frozen in liquid nitrogen-cooled isopentane. Serial 5 μm sections were cut at -30°C and collected onto room temperature, uncoated glass slides. Cross-sections were cut and used to stain 11 β-HSD1, and myosin heavy chain I and IIa protein.

Slides were left to air dry for a minimum of 1 h before treatment. Briefly slides were fixed in acetone at -20C for 20 minutes, followed by 30 second washes (x3) in deionised water. The slides were then permeabilised in 0.5% Triton-X for 5 minutes followed by 5 minute washes (x3) in PBS. The muscle samples were then blocked for 30 minutes with 5% normal donkey serum. Following which they were incubated in appropriate primary antibodies for 60 minutes, followed by 5 minutes washes (x3) in PBS. The 11 β-HSD1 binding site antibody concentration was 1:100, whereas the myosin heavy chain I (Developmental Studies Hybridoma Bank, University of Iowa, Dr Blau, A4.840) and IIa (Developmental Studies Hybridoma Bank, University of Iowa, Dr Blau, N2.261) antibody concentration were both 1:25. The samples were further incubated in appropriately targeted secondary fluorescent conjugated antibodies for 30 min [11 β-HSD1, donkey anti-sheep IgG 568 (red)] and followed by treatment with Alexa Fluor GAMIgM 350 MyHCI (blue) and Alexa Fluor GAMIgM 488 MyHCIIa (green) (Invitrogen, Paisley, UK).

This was followed by 5 minute washes (x3) in PBS. Coverslips were mounted in a glycerol and mowiol 4–88 solution in 0.2 M Tris-buVer (pH 8.5) with the addition of 0.1% 1,4-diazobicyclo-[2.2.2]-octane (DABCO) antifade medium. Muscle cross-sections were illuminated with a mercury lamp and viewed with a Nikon E600

microscope with a 40 x 0.75 NA objective. A SPOT RT KE colour 3 shot CCD camera (Diagnostic Instruments Inc, MI, USA) was coupled to the microscope for digital image capture. In order to visualise the Alexa fluor 350 (blue) and 488 (green) fluorophores the DAPI UV (340–380 nm) and FITC (465–495) excitation filters were used respectively. Sections stained Alexa fluor 568 (red) were examined using a Texas red (540–580 nm) excitation filter. Images were processed using Image-Pro Plus 5.1 software (Media Cybernetics, MD, USA) (295).

2.10. Immunoblotting

2.10.1. Principles of immunoblotting

Immunoblotting allows the measurement of relative amounts of a specific protein in a mixed protein sample (296). Proteins are boiled in a strong reducing agent which removes all secondary and tertiary structures and gives them a uniform negative charge. SDS-PAGE electrophoresis is then employed to separate the proteins according to molecular mass. Since the proteins are negatively charged they are pulled through the gel towards the anode at a speed that is dependent on their size (small proteins migrate fast and large proteins migrate slowly). The separated proteins are then transferred to a membrane, usually polyvinylidene diflorise (PVDF) or nitrocellulose using electrical current. Since these membranes strongly bind proteins they will also bind to any antibodies that it is exposed to. To prevent this non-specific binding the membrane is incubated in a blocking solution containing a generic protein such as milk or BSA. The next step involves probing

the membrane with a primary antibody that specifically recognises the protein of interest, followed by incubation with a secondary antibody that is directed against the primary antibody. The secondary antibody is conjugated to horseradish peroxidase (HRP), which, in the presence of hydrogen peroxide, catalyses a reaction involving the oxidation of luminol. Upon oxidation of luminol, an iridescent blue light is produced which is proportional to the amount of protein on the membrane. The reaction is captured on photographic film.

2.10.2. Method of Immunoblotting

20µg of protein was mixed with an appropriate amount to 5 x loading buffer and boiled for 5 minutes. Samples were loaded into a 4-20% gradient SDS-PAGE gel (BioRad, Herts, UK) and run at 200V for 1 h - 1 h 30 minutes. Transfer of proteins to nitrocellulose membrane (GE Healthcare, Bucks, UK) was conducted at 140mA for 1-2 h depending on the size of the protein of interest. Efficient transfer was assessed by incubating the membrane in ponceau stain with agitation for 60 seconds, and then rinsed with water to allow visualisation of the protein bands. Electrophoresis and protein transfer was carried out in BioRad mini protein 3 apparatus (BioRad, Herts, UK). Membranes were blocked in 10mL of blocking buffer for 1 hour at room temperature with constant agitation, then incubated with primary antibody overnight at 4°C on an orbital shaker. Membranes were washed with 100mL of washing buffer 3 times for 15 minutes. Secondary antibody incubation was conducted at room temperature with constant agitation. The membrane was then washed with 100mL of washing buffer 3 times for 15 minutes. Bound antibody was detected using Enhanced Chemiluminescence

(ECL, GE Healthcare, Bucks, UK). The reaction mixture was set up by combining substrate A with substrate B at a 50:50 ratio (final volume: 1mL per membrane). Following equilibration for 5 minutes, 1mL was added per membrane and left to incubate for 2 minutes before the membrane was placed between two plastic sheets in a photo cassette. Photographic film (PerkinElmer, Surrey, UK) was placed over the membrane in the dark and exposed for 30 seconds to 3 h, then developed on Compact X4 automatic film processor (Xograph Imaging Systems, Gloustershire, UK). Membranes were routinely stripped to remove bound primary/secondary antibodies by incubating the membrane in stripping buffer (2% SDS, 100mM β-mercaptoethanol, 50mM Tris, pH 6.8) at 50°C for 1 h with gentle agitation. Membranes were then washed with 100mL of washing buffer 3 times for 15 minutes before being re-probed with a different primary antibody. Immunoblots were evaluated by integrating densitometry using GeneSnap and GeneTool (Chemigenius Gel Documenting System, Syngene, Cambridge, UK). Equal loading was confirmed by reprobing membrane with anti-β-actin antibody conjugated to HRP and visualized as described above.

2.11. Proliferation assays

2.11.1. Principles of Proliferation assay using Promega Cell Titre 96 ® Aqueous Non-Radioactive Cell Proliferation Assay (MTS)

The Cell Titre 96 ® AQ_{ueous} Non-Radioactive Cell proliferation assay is a homogenous, colorimetric method for determining the number of viable cells in proliferation, cytotoxicity or chemosensitive assays. The Cell Titre 96 ® AQ_{ueous}

assay is composed of solutions of a novel tetrazolium compound [3-(4,5-dimethylthiazol-2-yl)-5-(3-carboxymethoxyphenyl)-2-(4-sulfophenyl)-“H-tetrazolium, inner salt; MTS] and an electron coupling reagent (phenazine methosulfate) PMS. MTS is bioreduced by cells into a formazan product that is soluble in tissue culture medium. The absorbance of the formazan product at 490nm can be measured directly from 96-well assay plates without additional processing. The conversion of MTS into the aqueous soluble formazan product is accomplished by dehydrogenase enzymes found in metabolically active cells. The quantity of formazan product is measured by the amount of 490nm absorbance is directly proportional to the number of living cells in culture. Data from proliferation bioassays comparing the Cell Titre 96 ® AQ_{ueous} Non-Radioactive Cell proliferation assay and the [^{3}H]-thymidine incorporation show similar results, however the Promega assay was more flexible and reproducible.

2.11.2. Procedure of MTS assay

The assay was performed according to the manufacturers protocol. C2C12 cells were trypsinised and counted, they were then seeded at a concentration of approximately 1000 per well on 96 well plate (in a volume of 100 µl) and left for 24 hrs. After 24 hours treatments were added to cells (e.g. glucocorticoids, IGF-I) and the cells were incubated in treatment for another 24 hours at 37°C.

The CellTiter 96® AQ_{ueous} One Solution Reagent was thawed and 20µl of CellTiter 96® AQ_{ueous} One Solution Reagent (a mix of 2mls of reagent MTS and100 µl of reagent PMS) was pipetted into each well of the 96-well assay plate containing the samples in 100µl of culture medium. The plate was then incubated for 1 hour

at 37°C in a humidified, 5% CO_2 atmosphere. The absorbance at 490nm was recorded using a 96-well spectrophotometer Victor3 1420 multilabel counter (PerkinElmer, Beaconsfield, Bucks, UK). The plate can was returned to the incubator for another 24 hours and the procedure repeated on cells which have not been previously assayed (results shown are from 24 and 48 hour proliferation studies). IGF-I was used as a positive control in all experiments as it is well described as leading to myoblast proliferation in C2C12 cells (297).

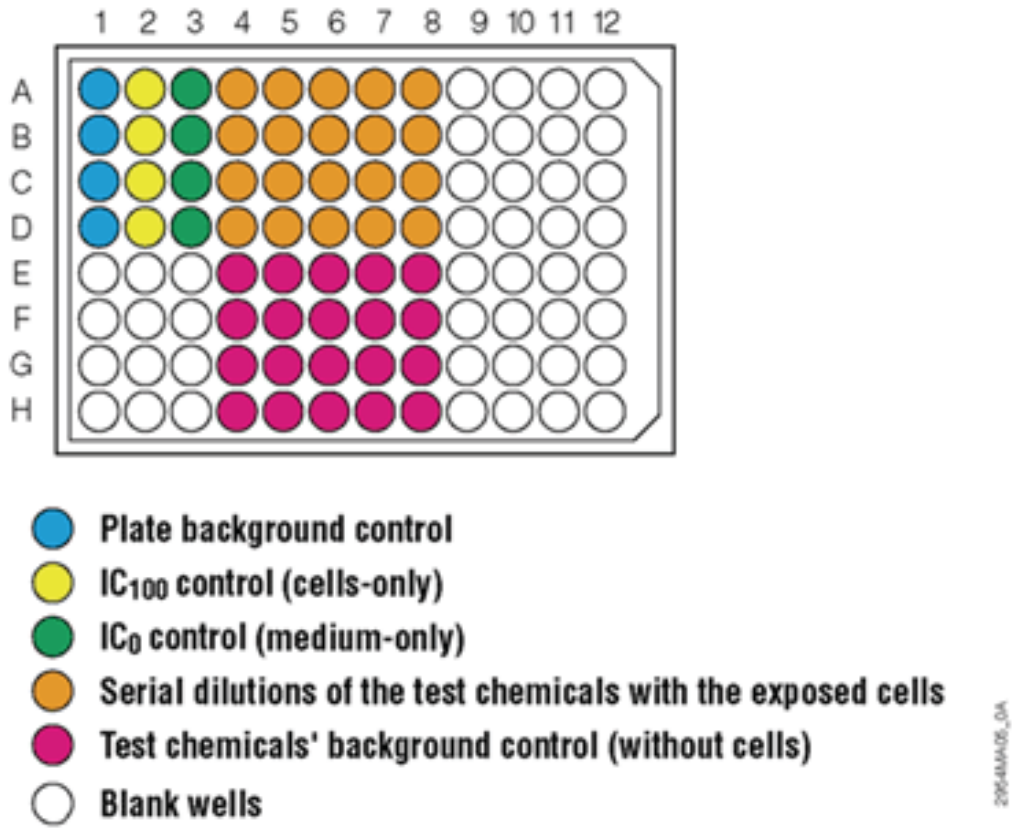

Figure 2.7. Plate set up for The CellTiter 96® AQueous plate as per manufacturers guidance. (http://www.promega.com/resources/protocols/technical-bulletins/0/celltiter-96-aqueous-nonradioactive-cell-proliferation-assay-protocol).

2.12. 11 β-HSD1 inhibitors and Glucocorticoid receptor anatagonists used in this thesis

2.12.1. LJ2 (PF-877423)

LJ2 (PF-877423, Pfizer Global R&D, La Jolla, CA, USA) is a selective 11 β-HSD1 inhibitor. The potency of this inhibitor is strongly affected by the presence of substrate in the assay buffer, K_i^{app} values increased at high concentrations of cortisone suggesting that the inhibitor behaved as a reversible and competitive inhibitor against cortisone, inhibition constant K_i 0.2 ± 0.04 and Michaelis Menten constant K_m 333.4 ± 109.2 nM (298).

2.12.1.1. Specificity of LJ2 (PF-877423)

LJ2 (PF-877423, Pfizer Global R&D, La Jolla, CA, USA) is a selective 11 β-HSD1 inhibitor. This group have previously published the efficacy of LJ2 in assays on HEK293T1 and HEK293T2 cells showing total abolition of oxoreductase activity (34.7 ± 0.6 vs. 0.4 ± 0.1, % cortisone to cortisol conversion, mean ± SD) activities of 11 β-HSD1 following incubation with 100nM PF-877423 for 24 hours but no effect on 11 β-HSD2 activity. No toxic effects of PF-877423 were observed up to 10μM concentrations using a commercially available assay kit (CellTitre 96 Aqueous, Promega) (298). The dose of LJ2 used in all experiments was 100nM.

2.12.2. Glycyrrhetinic Acid

Glycyrrhizic acid, a glycosylated saponin and a major constituent of licorice and glycyrrhetinic acid (its aglycone) (299) are non-specific inhibitors of 11 β-HSD isozymes. In addition to its established role as a competitive inhibitor of 11 β-HSD isozymes, liquorice results in pretranslational inhibition of 11 β-HSD both *in vitro* and *in vivo* (300). In addition glycyrrhetinic acid inhibits 11 β-HSD2 with an inhibition constant (Ki) of 5-10nM (301, 302).

2.12.3. Glucocorticoid receptor blockade – RU486

The bulky dimethyl-aminophenyl residue in RU486 fits snugly into the hydrophobic pocket of the glucocorticoid receptor (GR) and the progesterone receptor and explains its bifunctional antagonism at the level of these receptors (303). RU486 has a prolonged metabolic half-life of about 20 hours, thus it effectively excludes cortisol from receptor binding by binding to the receptor itself (304). After RU486 binds to the cytosolic GR, the interaction of the GR with HSP 90 and 59 is strengthened, therefore, not allowing it to enter the nucleus and bind to GREs (304).

2.13. Rodent Models used in this thesis

All mice were group housed under controlled temperature (21-23^{o}C) and light (12:12 light-dark cycle; lights on at 0700h) with ad libitum access to standard rodent chow and water. Body weights were monitored weekly. Animal

procedures were approved under the British Home Office Animals (Scientific Procedures) Act 1986.

In the ageing mouse experiments, the colony of aged mice were between 22 and 26 months, this time frame was determined from published data regarding age related myopathy which describes 'old mice' as being aged from 19 to 28 months (305-308). In the initial ageing mouse experiments the colony of young mice were approximately 12 weeks old and aged mice were between 22 and 26 months (all mice C57Bl\6). In our 11β-HSD1 KO model the mice strain was of mixed background C57Bl6/129SVJ.

2.13.1. Generation of targeted 11β-HSD1 knock out mouse

The 11β-HSD1 knock out mouse was developed within our group by Dr Gareth Lavery. The murine HSD11B1 gene contains 6 exons and a targeted vector to flank exon 5 (containing the catalytic domain of the enzyme) with LoxP sites. Genomic DNA from 129SvJ embryonic stem cells was used to amplify 6kb 5' and 2kb 3' homology arms, which were subsequently cloned into pBluescript SK(+) containing a thymidine kinase cassette. A loxP flanked Neomycin cassette was subcloned into a *XhoI* site 5' of exon 5 and an additional loxP site subcloned into a *PmlI* site 3' of exon 5. Following verification by DNA sequencing, the construct was linearized with BamHI and electroporated into E14TG2a mouse embryonic stem cells. Southern hybridization of Spe1 and NcoI digested genomic DNA probed with 500-bp H6PD fragments located at the 5' and 3' ends of the targeting vector respectively identified cells positive for a recombined HSD11B1 tri-loxed allele after selection in G418 and gancyclovir (see Figure 2.8). Three targeted

embryonic stem cell clones were expanded, screened, and karyotyped to ensure correct recombination and chromosomal integrity. Two clones were injected into C57BL/6 blastocysts and chimeric mice derived from embryonic stem cell clone were mated with C57BL/6 females to achieve germ line transmission of the recombined allele. Mice heterozygous for a tri-loxed allele were crossed with the ZP3-Cre expressing strain (309) which is a powerful deleter expressing early in development and will recombine between the most distant LoxP sites with high efficiency, thus rendering the allele null which can be passed into the next generation. Germline transmission of a disrupted allele was detected by PCR (depicted schematically in Figure 2.8). For genotyping HSD11B1 alleles the following primers were multiplexed in a standard PCR reaction: P1 5'-GGGAGCTTGCTTACAGCATC-3'; P2 5'-CATTCTCAAGGTAGATTGAACTCTG-3'; P3 5'-TCCATGCAATCAACTTCTCG-3'. PCR genotyping confirmed germline transmission of the disrupted allele, which was subsequently bred to homozygosity generating a 11β-HSD1KO. The validity of the model was assessed by demonstrating no 11β-HSD1 gene expression or enzyme activity in a number of tissues.

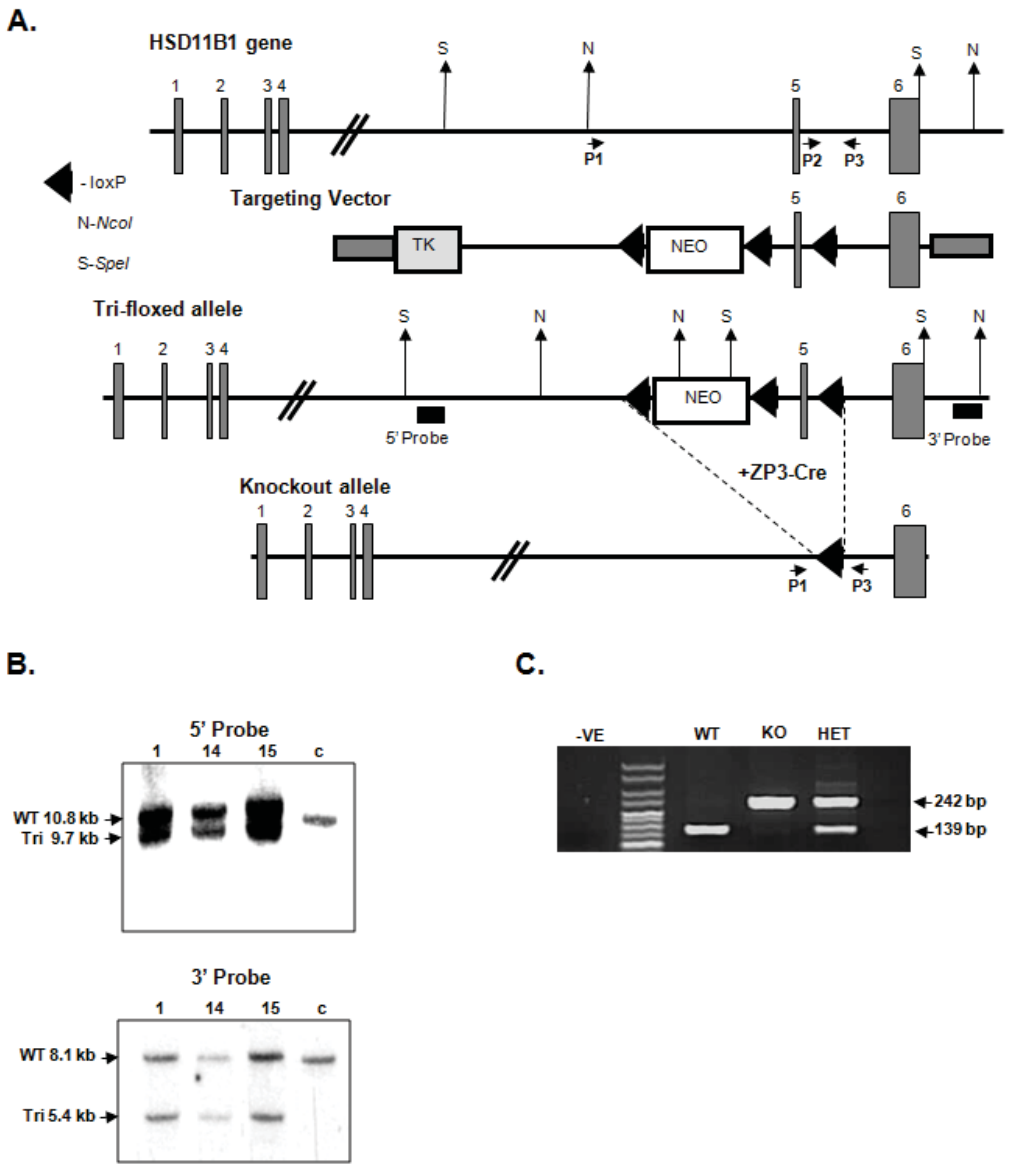

Figure 2.8. *Targeted disruption of murine HSD11B1 using the Cre-LoxP system. A. schematic representation of the 6 exons of the HSD11B1 gene, the targeting vector, tri-floxed recombined allele and the KO allele upon ZP3-Cre mediated recombination. The location of the 5' and 3' external probes used for Southern hybridization and PCR primers P1, P2, and P3 used for genotyping are indicated. NEO, neomycin resistance cassette; TK, thymidine kinase cassette. B. Successful targeting of HSD11B1 in 3 independent lines (1, 14 and 15. c-control non targeted cells) of embryonic stem cells confirmed by Southern hybridization of SpeI and NcoI digested genomic DNA. SpeI digests produced a WT fragment of 10.8kb which in the presence of the tri-floxed recombined allele produced a fragment to 9.7kb. For the NcoI digest the WT fragment is 8.1Kb and the recombined allele is5.4kb. C. PCR detection of knockout alleles (see material and methods for primer details). Primers P2 and P3 produce a band of 139bp representing the presence of a WT allele. Amplicons representing amplification between P1 and P3 are not detected due to the distance between these primers. In the KO allele a P2 binding site is removed and P1 and P3 are brought in to*

proximity generating a product of 242bp allowing us to detect WT, heterozygote and homozygote animals (310).

2.14. Mouse Muscle Strength Testing

2.14.1. Procedure

In experimental animals, the Linton Grip-Strength meter (Linton Instrumentation, Norfolk, UK) was used to assess muscle performance (4). The Linton Grip-Strength meter reproducibly measures peak grip strength (4;5). This is a non-invasive method whereby the peak grip strength is routinely measured by holding the animal by the base of the tail and gently and gradually assessing grip strength following the animal holding onto a grasp grid which assesses force via sensors in the machine while the animal is being gently pulled in the opposite direction.

Mice will naturally reach and grasp an object if an object is brought in front of their forepaws. On each assessment, the mouse will be removed from their housing and lowered into the apparatus so that it grasps the grip grid, one with each paw, with its back legs standing on the smooth floor of the apparatus. The mouse will then be held by the base of the tail and pulled gently in a rearward direction. The applied force at which the mouse releases the cage with each paw was measured by the strain gauges.

2.15. Gas Chromatography/ Mass spectrometry for corticosteroid metabolites in human and mouse urine

2.15.1. Principles

GC/MS urinary steroid analysis was carried out by Beverley Hughes at the Institute for Biomedical Research, Centre for Endocrinology, Diabetes and Metabolism (CEDAM), University of Birmingham. The GC/MS was based on the method described by *Palermo et al.* (311). The methods of sample work-up for GC/MS analysis (conjugate hydrolysis, extraction and derivatization) and their methodologies have been published in detail in several manuscripts (149, 312) and in depth description is beyond the scope of this thesis.

GC/MS was used to analyse the metabolites of steroid hormones and their precursors. In the CEDAM at the University of Birmingham, approximately 40 steroids are targeted for selected-ion-monitoring analysis, which cover all disorders of steroid synthesis and metabolism. A recent review by *Krone et al.* from this Department has highlighted several key features of urinary steroid metabolite analysis including the major shortcoming of data presentation in clinical GC/MS urine steroid profiling (313). Tabulating only the quantified amounts of steroid metabolites can be confusing and difficult to interpret, therefore improvement in the visual presentation of data has been made within the department (313).

The pathway to steroid hormone production is commonly divided into the synthesis of mineralocorticoid, glucocorticoids and sex steroids (Figure 2.9). We have added two groups to this classification; ‘androgen precursors’ includes the Δ5-steroids pregnenolone, 17OHpregenenolone, DHEA and the Δ4-steroids

androstenedione and their metabolites as this represents the main pathway to active androgens. The second additional group is 'glucocorticoid precursors', which consists of the Δ4-steroids progesterone, 17OHprogesterone and 21-deoxycortisol and their metabolites (313). Within CEDAM, normal ranges have been developed from a large number of healthy controls. The GC/MS profile of an individual patient is plotted for each determined parameter against the normal reference population (Figure 2.10). Such profiles allow for an immediate overview of the complete set of metabolites (313). In this thesis ratios of glucocorticoid metabolites are used to determine the relative activity of 11 β-HSD1.

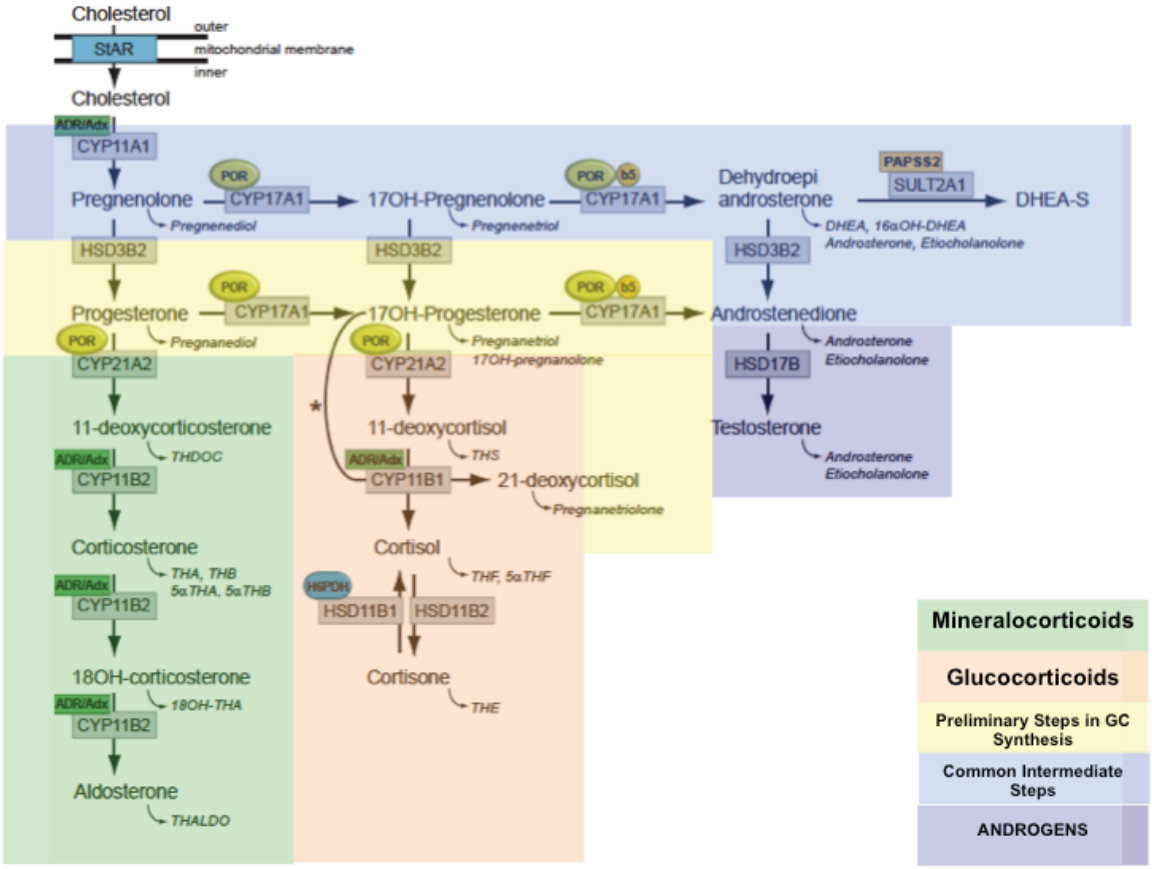

Figure 2.9 - *Synthesis and metabolism of hormonal steroids. This figure illustrates the formation of the major hormone classes from cholesterol. Steroid names in conventional script are steroid hormones and precursors; those in italics are urinary metabolites of the aforementioned. The major transformative enzymes are in rectangular boxes, the cofactor ("facilitator") enzymes in ovals. Mitochondrial CYP type I enzymes requiring electron transfer via adrenodoxin reductase (ADR) and adrenodoxin (Adx) CYP11A1, CYP11B1, CYP11B2, are marked with a labelled box ADR/Adx. Microsomal CYP type II enzymes receive electrons from P450 oxidoreductase (POR), CYP17A1, CYP21A2, CYP19A1, are marked by circled POR. The 17,20-lyase reaction catalyzed by CYP17A1 requires in addition to POR also cytochrome b5 indicated by a circled b5. Similarly, hexose-6-phosphate dehydrogenase (H6PDH) is the cofactor-generating enzyme for 11β-HSD1. The asterisk (*) indicates the 11 hydroxylation of 17OHP to 21-deoxycortisol in 21-hydroxylase deficiency. The conversion of androstenedione to testosterone is catalyzed by HSD17B3 in the gonad and AKR1C3 (HSD17B5) in the adrenal. StAR, steroidogenic acute regulatory protein; CYP11A1, P450 side-chain cleavage enzyme; HSD3B2, 3β-hydroxysteroid dehydrogenase type 2; CYP17A1,17α-hydroxylase; CYP21A2, 21-hydroxylase; CYP11B1, 11β-hydroxylase; CYP11B2, aldosterone synthase; HSD17B, 17β-hydroxysteroid dehydrogenase; CYP19A1, P450 aromatase; SRD5A2, 5α-reductase type 2; SULT2A1 from Krone et al (313). Figure based on a diagram courtesy of Dr Nils Krone.*

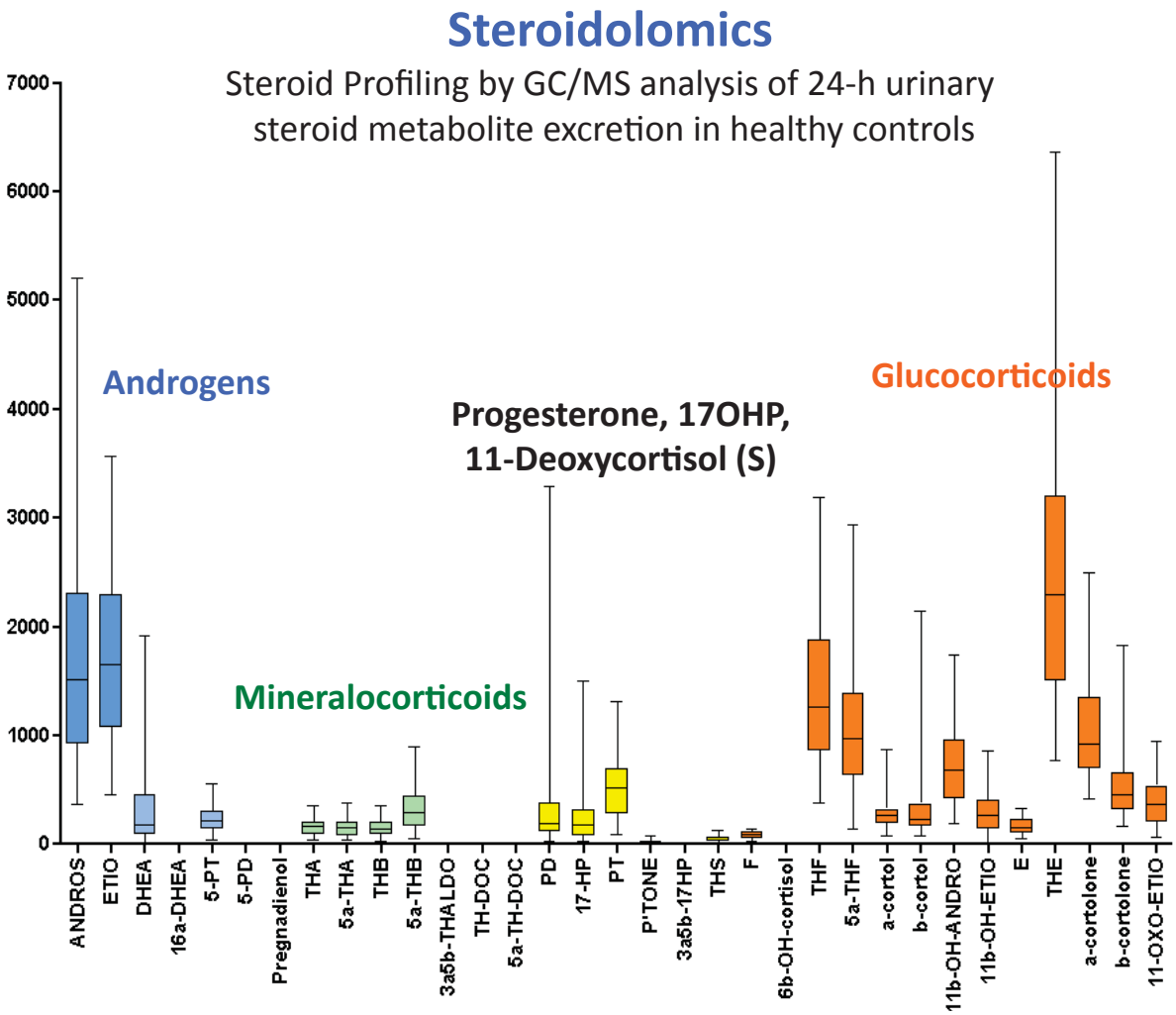

Figure 2.10. *Graphical representation of the normal range of urinary steroid metabolites (quantity reported in µg/24 h). The groups are the same as described in* ***Figure 2.9****. Box and whisker plots represent mean values, 5th and 95th percentile and given (courtesy of Professor Wiebke Arlt).*

2.15.2. Gas Chromatography/ Mass Spectrometry Methods

Quantitative data on excretion of individual steroids requires accurate 24 hour sampling and 1ml of a 24-hour collection for analysis. For murine studies individual mouse urine was collected on filter paper and processed.

The following isotope labelled internal standards were used; (9,11,12,12-^{2}H) cortisol and (9,12,12-^{2}H) cortisone. The standards were calibrated by high performance liquid chromatography (HPLC) analysis of solubilised, non-labelled standard on known weight. Free steroid was extracted using Sep-pak C18 cartridges (314). Labelled steroid d_4-cortisol (0.18μg), and d_3-cortisone (0.12μg), as well as internal standards (stigmasterol and cholesteryl butyrate), 200μg were then added. The samples were then derived using 100μl of 2% methoxyamine hydrochloride in pyridine and 50μl of trimethylsilylimidzole. Lipidex chromatography was then used to purify the steroid derivative.

GC/MS was carried out using a Hewlett Packard 5970 mass spectometer and 15m fused-silica capillary column, 0.25mmID, 0.25μm film thickness (J&B Scientific, Folsom CA, USA) using 2μl of sample. Steroids were quantified by comparing individual peak area to the peak area of the internal standards, for cortisol fragment 605m/z compared to 609 m/z and for cortisone fragment 531 m/z compared to 534 m/z. The relative peak area was calculated and the metabolite concentration expressed as μg/24hr. A quality control (QC) was analysed with each batch. The intra and inter-assay co-efficient of variance was <10%.

2.16. Assays and DEXA scan methods for clinical study

These will be discussed in detail in Chapter 6.

2.17. Statistical methods

Statistical analysis was performed using Prism for Windows version 5.0 (GraphPad Software Inc, San Diego, CA, USA) software packages. Continuous data were summarised using means and standard deviations (or standard error of mean) if parametrically distributed or medians and inter-quartile ranges if non-parametrically distributed. Parametric data was compared using a paired t-test and non-parametric data was analysed using a Mann-Whitney test. Multiple comparisons were assessed using one-way analysis of variance (ANOVA), with Kruskal-Wallis for non-parametric data. Associations between variables were analysed using Pearson correlation for parametric data and Spearman rank correlation for non-parametric data. The level for statistical significance throughout the thesis is $p<0.05$.

Chapter 3

Characterising 11 β-HSD1 in skeletal muscle

3.1. Introduction

Within tissues, GC levels are regulated at the pre-receptor level by the isozymes of 11 β-hydroxysteroid dehydrogenase (11 β-HSD), which are located in the endoplasmic reticulum (ER). 11 β-HSD2 acts as a dehydrogenase converting active cortisol (corticosterone in rodents) to inactive cortisone (11-dehydrocorticosterone in rodents) to protect the mineralocorticoid receptor from illicit occupancy by cortisol (150). In contrast, 11 β-HSD1 *in vivo* acts predominantly as an oxoreductase converting inactive cortisone (11-dehydrocorticosterone in rodents) into active cortisol (corticosterone in rodents) (2). This oxoreductase activity is determined by nicotinamide adenine dinucleotide phosphate (NADPH) co-factor availability produced by the ER specific enzyme hexose-6-phosphate dehydrogenase (H6PDH).

The biological activity of glucocorticoids is dependent on their binding to the glucocorticoid receptor (GR) which is a ligand regulated nuclear receptor that in the absence of its GC ligand remains bound to other proteins within the cytoplasm such as the 90 kDA and 70 kDA heat shock proteins (HSP90, HSP70). GC binding to the GR leads to dissociation of the HSPs and translocation of the GR-ligand complex into the cell nucleus where it binds to specific DNA sequences known as glucocorticoid response elements (GREs) in the promoter region of the target gene (131).

The role of 11 β-HSD1 in adipose tissue, liver and brain has been extensively studied (2), however the role of 11 β-HSD1 in skeletal muscle is less well-defined. Expression of 11 β-HSD1 in human skeletal muscle has been reported to be only ~5% that reported in liver (151) with conflicting evidence as to whether 11 β-

HSD2 is present in muscle or not (151, 152). In muscle cells extracted from the vastus lateralis of patients with type 2 diabetes, baseline 11 β-HSD1 mRNA expression was elevated compared to controls. This increase in 11 β-HSD1 mRNA expression was associated with impaired glucose transport in response to acute insulin and cortisone stimulation (152). In human myocytes, *Whorwood et al.* (153) demonstrated elevated 11 β-HSD1 activity with increasing GC concentration and 11 β-HSD1 activity decreased with insulin and IGF-I administration, independently.

Glucocorticoids are known to have profound effects on skeletal muscle biology and in excess can lead to myopathy as clearly demonstrated through *in vitro* (194-199) and *in vivo* studies of rodent (84, 141, 143, 200-210) and human skeletal muscle (96, 101-108, 191). The effect of glucocorticoids on muscle, liver and fat are also associated with a number of metabolic derangements including hyperglycaemia, insulin resistance and hyperlipidaemia (130). Thus, both in health and disease 11 β-HSD1 may play a fundamental role in skeletal muscle biology by altering intracellular glucocorticoid concentrations.

3.2. Aims

The aim of this chapter is to characterise 11 β-HSD1 in murine skeletal muscle and the murine skeletal muscle cell line (C2C12), which will be the models used for the remainder of the thesis.

3.3 Strategy of Research

Using cultured C2C12 myocytes as a skeletal muscle model and skeletal muscle tissue from C57BL\6 mice we assessed 11 β-HSD1 activity, mRNA expression and protein content (with immunohistochemistry).

3.4. Methods

3.4.1. C2C12 cell culture

The C2C12 cell line is a well-established model of both skeletal muscle proliferation and differentiation which has been widely used in research with regard to muscle atrophy and glucocorticoid induced myopathy (84, 86, 195, 197). This cell line was derived as a subclone of a myoblast line established from normal adult C3H mouse leg muscle. They differentiate rapidly; produces extensive contracting myotubes and express characteristic muscle proteins. They provide an excellent model to study in vitro myogenesis and muscle cell differentiation, which until recently have been difficult to primary culture. The use of C2C12 in muscle molecular biology research has been reported in many high impact citations. Cryofrozen C2C12 myoblasts (passage 17) were purchased

from ECACC (Salisbury, UK), Once myoblasts had reached 60-70% confluence, differentiation was initiated by replacing proliferation media with DMEM with high glucose and L-glutamine (PAA, Somerset, UK) supplemented with 5% horse serum. Differentiation media was replaced every 48 hours. After 8 days, myoblasts had fused to form multinucleated myotubes (Figure 3.1).

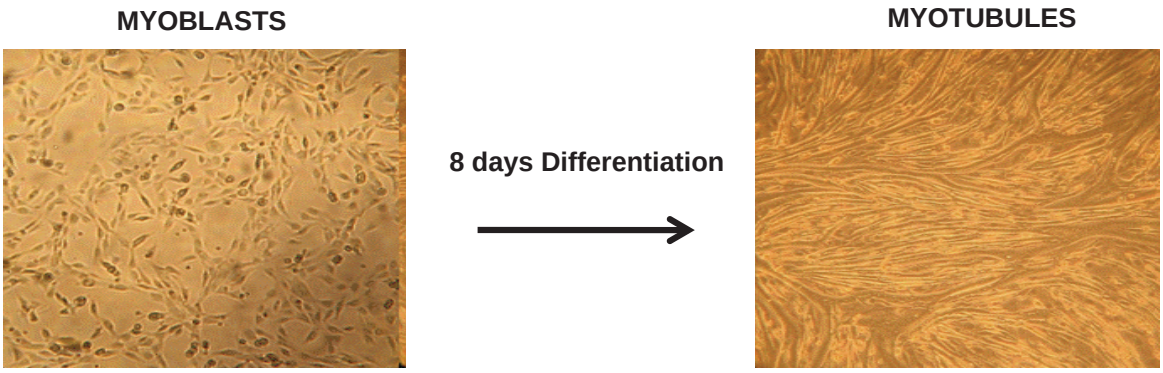

Figure 3.1. *C2C12 myoblast cells were differentiated in chemically defined media for 8 days to form multinucleated myotubes*.

3.4.2. RNA extraction and cDNA synthesis

Total RNA was extracted from monolayer cells using TRIreagent (Sigma-Aldrich, Dorset, UK). The procedure was carried out according to protocol provided with the reagent (Sigma-Aldrich, Dorset, UK). The quantity of RNA was measured using NanoDrop ND-1000 UV-Vis Spectrophotometer (Thermofisher, Surrey, UK). The reverse transcription process was carried out using Applied Biosystems High-Capacity Reverse Transcription Kit (Applied Biosystems, Warrington, UK) For a full description of methods used see Section 2.4.

3.4.3. Quantitative or Real Time PCR

Quantitative PCR was carried out using Applied Biosystems Reagents and gene mRNA expression assays (AssayonDemand) (Applied Biosystems, Warrington, UK). PCRs for genes of interest and for 18s housekeeping genes were carried out in singleplex. Data were expressed as Ct values (Ct=cycle number at which logarithmic PCR plots cross a calculated threshold line). And used to determine ΔCt values (ΔCt = (Ct of the target gene) – (Ct of the housekeeping gene), lower ΔCt values reflecting higher mRNA mRNA expression. Data are expressed as arbitrary units using the following transformation [mRNA expression in arbitrary units = $1000*(2^{-\Delta Ct})$]. For a full description of methods used see Section 2.6.

3.4.4. Protein Extraction and concentration measurement on monolayer cells

Monolayer cells were lysed in Radio-Immunoprecipitation (RIPA) buffer containing detergent. The lysate was freeze-thawed to further break open cell membranes and the insoluble components removed by centrifugation. The supernatant, containing soluble proteins was measured using BioRad RC DC protein assay (BioRad, Herts, UK). 5µl of protein sample or standard were added per well in duplicate. The ranges of protein standards were 0, 0.25, 0.5, 1, 2, 4, 8 and 10mg/mL of Bovine Serum Albumin (BSA) in RIPA buffer. 25ml of solution A (alkaline copper tartrate) (with 20µl of solution S per ml of solution A) was initially added followed by 200ml of solution B (Folin reagent). Once the solutions were added the plate was incubated at room temperature for 10 minutes and the absorbance read at 690nm on a Victor3 1420 multilabel counter (PerkinElmer,

Beaconsfield, Bucks, UK). Protein concentration in the sample was then calculated according to the slope of the standards line. For a full description of methods used see Section 2.7.

3.4.5. 11 β-hydroxysteroid dehydrogenase type 1 and 2 enzyme activity assay on monolayer and tissue explants

11 β-hydroxysteroid dehydrogenase type 1 and 2 enzyme activity assay was carried out on both monolayers and whole tissue explants. Incubations were carried out at 37°C under a 5% CO_2 atmosphere for 20 minutes to 2 hours depending on the cell/tissue type. Enzyme activity was expressed in pmols of steroid converted per mg of protein per hour (pmol/mg/h) for monolayers or steroid converted per mg tissue per hour (explants). For a full description of methods used see Section 2.8.

3.4.6. Inhibition of 11 β-HSD1 and glucocorticoid receptor antagonism

The most commonly used inhibitors of 11 β-HSD1 for *in vitro* studies are the liquorice derivatives glycyrrhizic acid, its hydrolytic product glycyrrhetinic acid and its hemisuccinate derivative carbenoxolone (CBX). Glycyrrhetinic acid (GE) is a potent inhibitor of 11 β-HSD1 (both competitive and inhibiting 11 β-HSD1 mRNA levels) (300, 315). The dose of GE used in all experiments was 2μM.

LJ2 (PF-877423, Pfizer Global R&D, La Jolla, CA, USA) is a selective 11 β-HSD1 inhibitor. This group has previously published the efficacy of LJ2 in assays on HEK293T1 and HEK293T2 cells showing total abolition of oxoreductase activity (34.7 ± 0.6 vs. 0.4 ± 0.1, % cortisone to cortisol conversion, mean ± SD) activities of 11 β-HSD1 following incubation with 100nM PF-877423 for 24 hours but no effect on 11 β-HSD2 activity (298). The dose of LJ2 used in all experiments was 100nM.

RU486 is a potent glucocorticoid receptor (GR) antagonist receptors (303). After RU486 binds to the cytosolic GR, the interaction of the GR with HSP 90 and 59 is strengthened thus not allowing it to enter the nucleus and bind to GREs (304). The dose of RU486 used in all experiments was 10μM.

3.4.7. Immunohistochemistry of 11β-HSD1

Immunohistochemistry was performed on paraffin embedded sections of tissue that were collected in 10% formalin. An antigen retrieval step was performed following which three different primary antibodies for 11β-HSD1 were used and primary and secondary antibody concentrations were as shown in Table 3.1.

Blocking was then performed with 10% normal donkey serum in PBS v/v for 30 minutes at room temperature to reduce background staining (goat serum for Caymen and Abcam antibodies). Importantly, the blocking agent was not washed off prior to placing the primary antibody on the slide.

Sections were incubated with 100μl primary antibody (final concentration 30μg/ml) in 10% NDS/PBS (NB for Cayman/ Abcam 10% NGS/ PBS) for 1.5

hours at room temperature. Following the incubation of primary antibody the slides were washed once in PBS and then incubated with 100μl secondary antibody (goat anti-sheep IgG peroxidase conjugate for binding site and goat anti-rabbit for Abcam and Cayman) at a dilution of 1:100 (in PBS for 30 minutes at room temperature). To visualise staining one DAB (3,3'-Diaminobenzidine) tablet, Sigma Aldrich, Dorset, UK with the H_2O_2 tablet was dissolved in 15mls of H_2O and applied to completely cover the section and left to develop for 5 minutes The slide was then counterstained by immersing in Meyers haematoxylin for 30 seconds, following which it was washed in copious tap water.

Negative controls were carried out using anti-11β-HSD1 immunising peptide 1:100-1:500 (pre-adsorbed), blank or isotype control. For a full description of methods used see Section 2.9.

Binding Site **(polyclonal)** **(294)**	1mg/ml	1:33 30µg/ml	anti-sheep/goat peroxidase (1:100)
Abcam **(polyclonal)** **Ab39364**	0.6mg/ml	1:20 30µg/ml	goat/ anti-rabbit peroxidase (1:100)
Cayman **(polyclonal)** **Cayman No: 10004303**	0.6mg/ml	1:20 30µg/ml	goat/ anti-rabbit peroxidase (1:100)

Table 3.1. *Summary of the three different primary antibodies for 11β-HSD1 used and primary and secondary antibody concentrations.*

3.4.8. Methods for Immunoflourescence

Immunoflourescence was performed in collaboration with Dr Chris Shaw, School of Sports and Exercise Science, University of Birmingham. Muscles to be processed for immunoflourescence were handled differently than those for standard immunohistochemistry. Briefly, muscle samples were embedded in Tissue-Tek OCT Compound (Sakura Finetek Europe, The Netherlands) and immediately frozen in liquid nitrogen-cooled isopentane. Serial 5 μm sections were cut at -30°C and collected onto room temperature, uncoated glass slides.

Cross-sections were cut and used to stain 11 β-HSD1, and myosin heavy chain I and IIa.

Slides were left to air dry for a minimum of 1 h before treatment. Briefly slides were fixed in acetone at -20C for 20 minutes, followed by 3 x 30 s washes in deionised water. The slides were then permeabilised in 0.5% Triton-X for 5 min followed by three 5 min washes in PBS. The muscle samples were then blocked for 30 minutes with 5% normal donkey serum. Following which they were incubated in appropriate primary antibodies for 60 min, followed by three 5 min washes in PBS. The 11 β-HSD1 binding site antibody concentration was 1:100, whereas the myosin heavy chain I (Developmental Studies Hybridoma Bank, University of Iowa, Dr Blau, A4.840) and IIa (Developmental Studies Hybridoma Bank, University of Iowa, Dr Blau, N2.261) antibody concentration were both 1:25. The samples were further incubated in appropriately targeted secondary fluorescent conjugated antibodies for 30 min [11 β-HSD1, donkey anti-sheep IgG 568 (red)] and followed by treatment with Alexa Fluor GAMIgM 350 MyHCI (blue) and Alexa Fluor GAMIgM 488 MyHCIIa (green) (Invitrogen, Paisley, UK).

This was followed by three 5 min washes in PBS. Coverslips were mounted in a glycerol and mowiol 4–88 solution in 0.2 M Tris-buVer (pH 8.5) with the addition of 0.1% 1,4-diazobicyclo-[2.2.2]-octane (DABCO) antifade medium. Muscle cross-sections were illuminated with a mercury lamp and viewed with a Nikon E600 microscope with a 40 x 0.75 NA objective. A SPOT RT KE colour 3 shot CCD camera (Diagnostic Instruments Inc, MI, USA) was coupled to the microscope for digital image capture. In order to visualise the Alexa fluor 350 (blue) and 488 (green) fluorophores the DAPI UV (340–380 nm) and FITC (465–495) excitation

filters were used respectively. Sections stained Alexa fluor 568 (red) were examined using a Texas red (540–580 nm) excitation filter. Images were processed using Image-Pro Plus 5.1 software (Media Cybernetics, MD, USA) (295).

3.4.9. Rodent Models used in this chapter

C57BL\6 mice were group housed under controlled temperature (21-23^{o}C) and light (12:12 light-dark cycle; lights on at 0700h) with ad libitum access to standard rodent chow and water. Body weights were monitored weekly. Animal procedures were approved under the British Home Office Animals (Scientific Procedures) Act 1986.

3.5. Statistical methods

Statistical analysis was performed using Prism for Windows version 5.0 (GraphPad Software Inc, San Diego, CA, USA) software packages. Continuous data were summarised using means and standard deviations (or standard error of mean) if parametrically distributed or medians and inter-quartile ranges if non-parametrically distributed. Parametric data was compared using a paired t-test and non-parametric data was analysed using a Mann-Whitney test. Multiple comparisons were assessed using one-way analysis of variance (ANOVA), with Kruskal-Wallis for non-parametric data. The level for statistical significance was $p<0.05$.

3.6. Results

3.6.1. 11 β-HSD1 activity and mRNA expression in C2C12 myocytes

Both oxoreductase and dehydrogenase activity of 11 β-HSD1/2 was assessed in C2C12 myoblasts and compared to myotubules. There was minimal dehydrogenase activity, indicating that 11 β-HSD2 was not biologically relevant in C2C12 myoblasts or myotubules (not shown). There was a significant increase in 11 β-HSD1 oxoreductase activity and mRNA expression during myocyte differentiation (Figure 3.2). To ensure myocyte differentiation at a molecular level, actin and myogenin mRNA expression was measured which increased 10-fold and 3-fold, respectively, between myoblast and day 8 myotubules. These changes in the molecular markers of differentiation characterised day 8 myotubules as having undergone terminal differentiation (see Section 1.2). The mRNA expression of other key genes in glucocorticoid regulation in day 8 C2C12 myotubules was assessed GRα [0.259 $\pm$ 0.02 arbitrary units (AU)] and H6PDH (2.49 $\pm$ 0.4 AU).

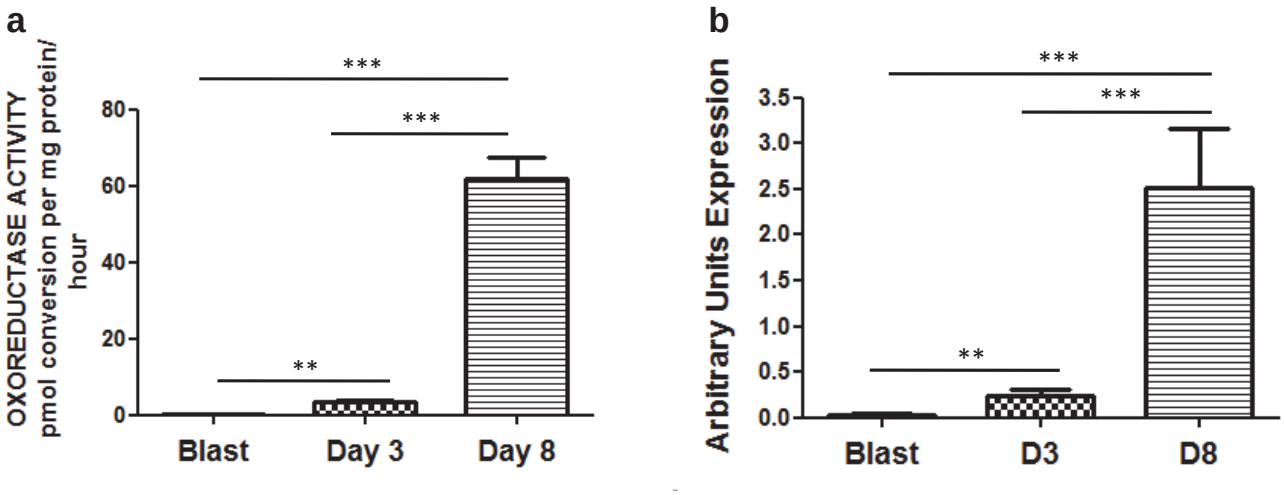

Figure 3.2. *11 β-HSD1 activity (a) and mRNA expression (b) increases during differentiation from C2C12 myoblasts to Day 8 myotubules C2C12 (Data shown are the mean+SE, n = 5, p** <0.001, p*** = <0.0001).*

3.6.1.1. The inhibition of oxoreductase activity in C2C12 myotubules

To ensure the oxoreductase activity documented in Figure 3.2 was secondary to 11 β-HSD1, Day 8 C2C12 cells were treated with the specific (LJ2) and non-specific (GE) 11 β-HSD1 inhibitors. 11 β-HSD1 oxoreductase activity in Day 8 C2C12 myotubules was inhibited by 24 hour treatment with non-specific (GE) and specific (LJ2) inhibition of 11 β-HSD1. Additionally, it was noted that the GRα antagonist RU486 had no effect on oxoreductase activity (Figure 3.3).

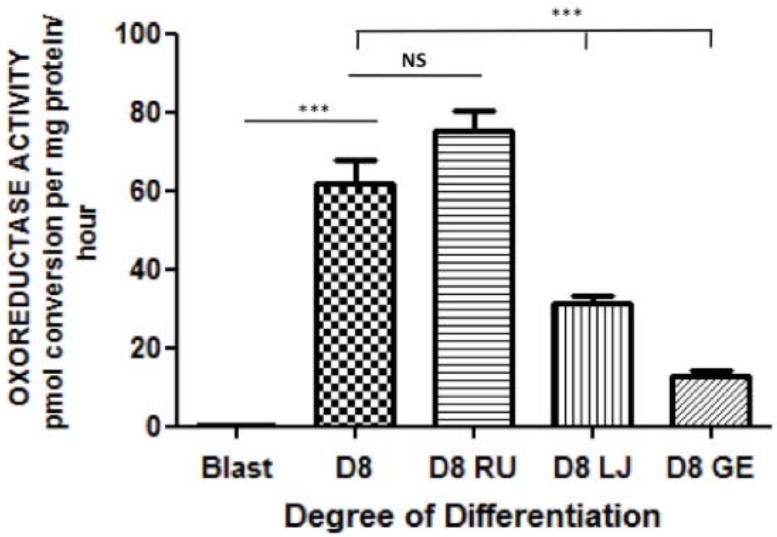

Figure 3.3. *11 β-HSD1 activity in C2C12 myoblast compared to day 8 myotubules and the effect of treatment with a non-specific11 β-HSD1 inhibitor (GE) and specific 11 β-HSD1 inhibitor (LJ2) and the GRα antagonist RU486 (Data shown are the mean+SE, n = 4, p NS = non statistically significant, p*** = <0.0001).*

In the initial phases of the PhD preliminary data assessed the effect of GR antagonism and inhibition of 11 β-HSD1 following 8 day continuous treatment (i.e. treatments from time of commencement of differentiation to Day 8 differentiation). The cell photographs below show that 8 days treatment with RU486 and LJ2 an 11 β-HSD1 inhibitor lead to significant abnormalities in myotubule formation (from myoblast to myotubule).

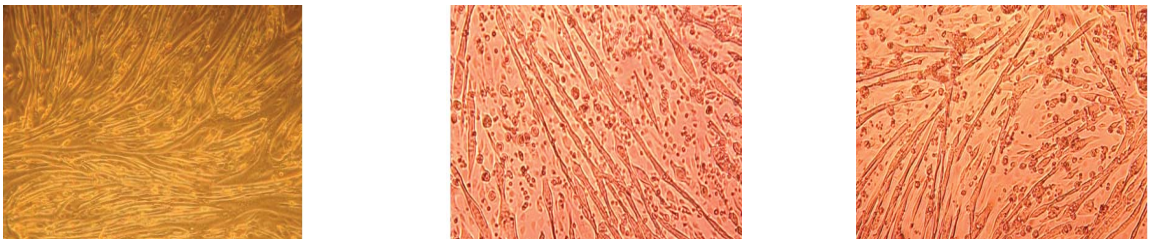

Figure 3.4. *The effect of 8 days treatment (initiated at change of media from proliferation to differentiation) with the glucocorticoid receptor antagonist RU486 and the specific 11 β-HSD1 inhibitor LJ2.*

Rather than assessing the effect of these treatments over 8 days which had significant alterations in myotubule formation in Chapter 4 we decided to focus on the short term modulation of 11 β-HSD1 and the GR on myoblasts proliferation rate and the effect of short term treatment (24 hours) on fully differentiated Day 8 myotubules on atrophy/ hypertrophy markers rather than prolonged treatment.

3.6.2. 11 β-HSD1 activity and mRNA expression in murine tissues

The activity and mRNA expression of 11 β-HSD1 and other key genes for tissue specific regulation of glucocorticoid action (GRα and H6PDH) were assessed in different muscle groups and compared to that of murine liver and omental fat. Liver had the highest 11 β-HSD1 oxoreductase activity when compared to quadriceps and tibialis anterior. However, there was no difference in activity between liver and gonadal fat and soleus (Figure 3.5.a). The high level of 11 β-HSD1 oxoreductase activity in the soleus may either be due to increased 11 β-

HSD1 activity or due to the small weight of tissue which would impact on the calculation of activity per mg/tissue (Section 2.8). 11 β-HSD1 mRNA expression was higher in liver than in all other tissues (including gonadal fat and soleus), Figure 3.5.b.

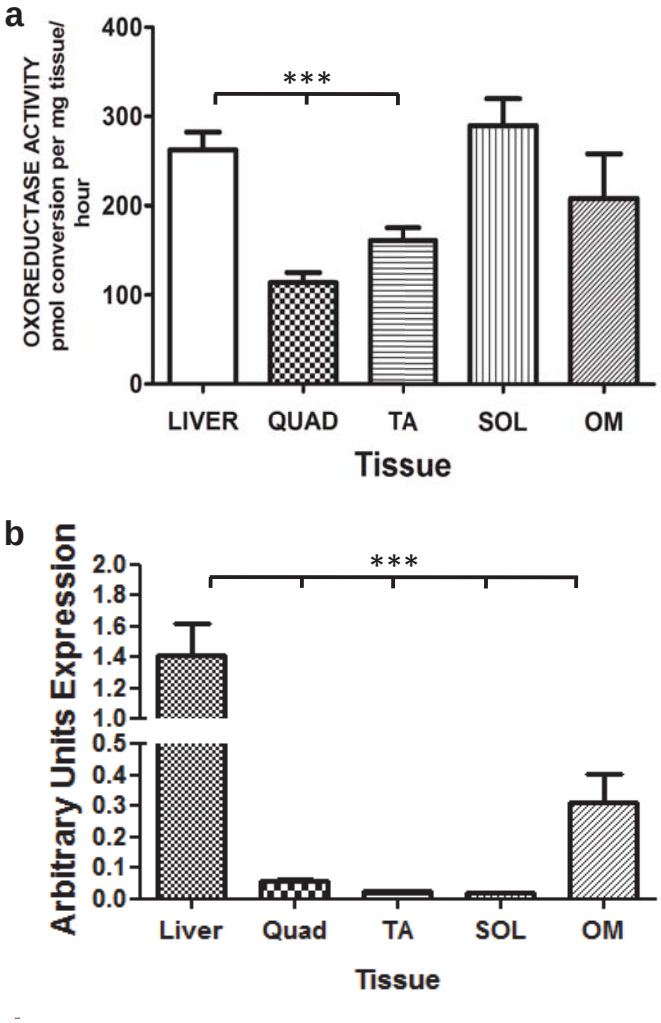

Figure 3.5. *11 β-HSD1 activity (a) and mRNA expression (b) in murine liver, quadriceps (Quad), tibialis anterior (TA), soleus (SOL) and omental/ gonadal fat (OM) (Data shown are the mean±SE, n = 6).*

To ensure that the oxoreductase activity measured in tissue was secondary to 11 β-HSD1, tissues were incubated with GE during the course of the 11 β-HSD1

activity assay. This led to a significant decrease in oxoreductase activity in both liver and quadriceps.

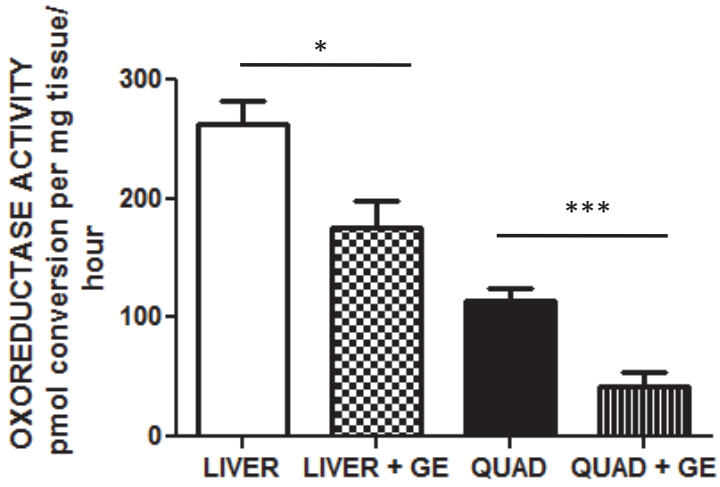

Figure 3.6. *11 β-HSD1 oxoreductase activity is reduced in liver and quadriceps (Quad) when co-incubated with the non-specific 11 β-HSD1 inhibitor glycyrrhetinic acid (GE) during activity assay. n=3, * p<0.05, *** p<0.0001.*

3.6.3. mRNA expression of hexose 6 phosphate dehydrogenase and the glucocorticoid receptor alpha in murine tissue

The expression of H6PDH and GRα were assessed in liver, quadriceps, tibialis anterior, soleus and gonadal fat. There were no differences in mRNA expression of GRα between tissues. There was a lower level of mRNA expression of H6PDH in quadriceps and soleus when compared with liver (Table 3.2).

Expression AU	Liver	Quadriceps	Tibialis Anterior	Soleus	Gonadal Fat
GRα	0.322 ± 0.120	0.471 ±0.05	0.286 ± 0.03	0.3338 ± 0.06	0.2365 ± 0.06
H6PDH	0.4246 ± 0.07	0.1573 ± 0.02 **	0.0323 ± 0.08	0.09 ± 0.02***	0.342 ± 0.08

Table 3.2. GRα and H6PDH mRNA expression in murine liver, quadriceps, tibialis anterior, soleus and gonadal fat (Data shown are the mean±SE, n = 5). ** p<0.001. *** p<0.0001 compared to liver. AU = arbitrary units.

3.6.4. 11 β-HSD1 immunohistochemistry

In order to assess the localisation of 11 β-HSD1 within skeletal muscle immunohistochemistry was performed on young (12 weeks) murine liver (positive control) and quadriceps muscle. Initially the in-house designed binding site antibody (294) was used and a fibre specific pattern of staining was observed (Figure 3.6.d). To further evaluate this finding and clarify whether fibre specificity, immunohistochemistry was performed using two further 11 β-HSD1 polyclonal antibodies [Abcam (Ab39364) and Cayman (10004303)], Figures 3.8 and 3.9, respectively. The fibre specific staining was also present in the quadriceps muscle using the Abcam and Cayman polyclonal antibodies. The staining of 11 β-HSD1 appeared to be predominantly in the smaller diameter fibres which would be characteristic of Type I fibres (slow twitch fibres). Type I fibres are the most resistant to glucocorticoid induced myopathy. In contrast to other muscle fibres (Type II a/b) whose main fuel is glycogen, Type I fibres use fatty acids and triglycerides as their major source of fuel (the increase in tissue specific cortisol concentrations could play a key role in the activity of hormone sensitive lipase which converts diacylglycerol to a fatty acid and diacylglycerol).

a

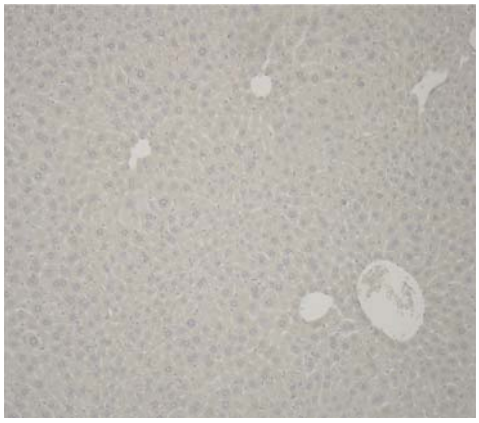

Binding site isotype control and 2° liver

b

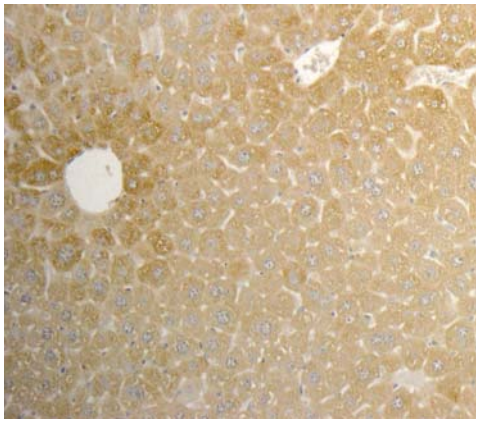

Binding Site 1° and 2° liver

c

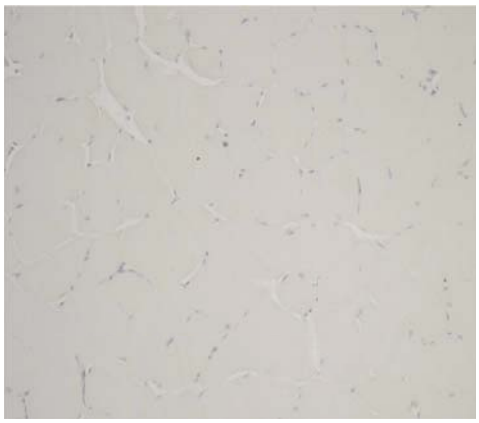

Binding Site isotype control and 2° quadriceps

d

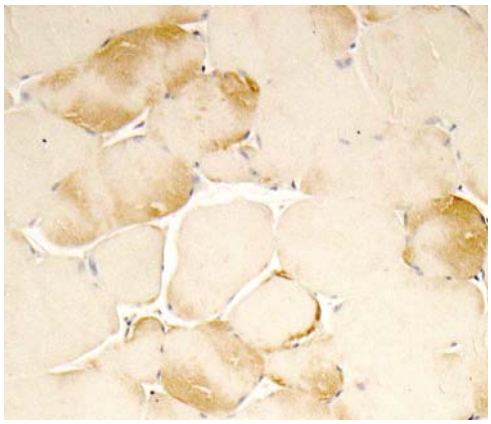

Binding Site 1° and 2° Quadriceps

Figure 3.7. *Immunohistochemistry of 11 β-HSD1 using the binding site 11 β-HSD1 primary antibody (294) (a = negative control liver with isotype control and secondary antibody, b = positive control liver with primary 11 β-HSD1 and secondary binding site antibody, c = negative control quadriceps with isotype control and secondary antibody and d = quadriceps with primary 11 β-HSD1 and secondary binding site antibody).*

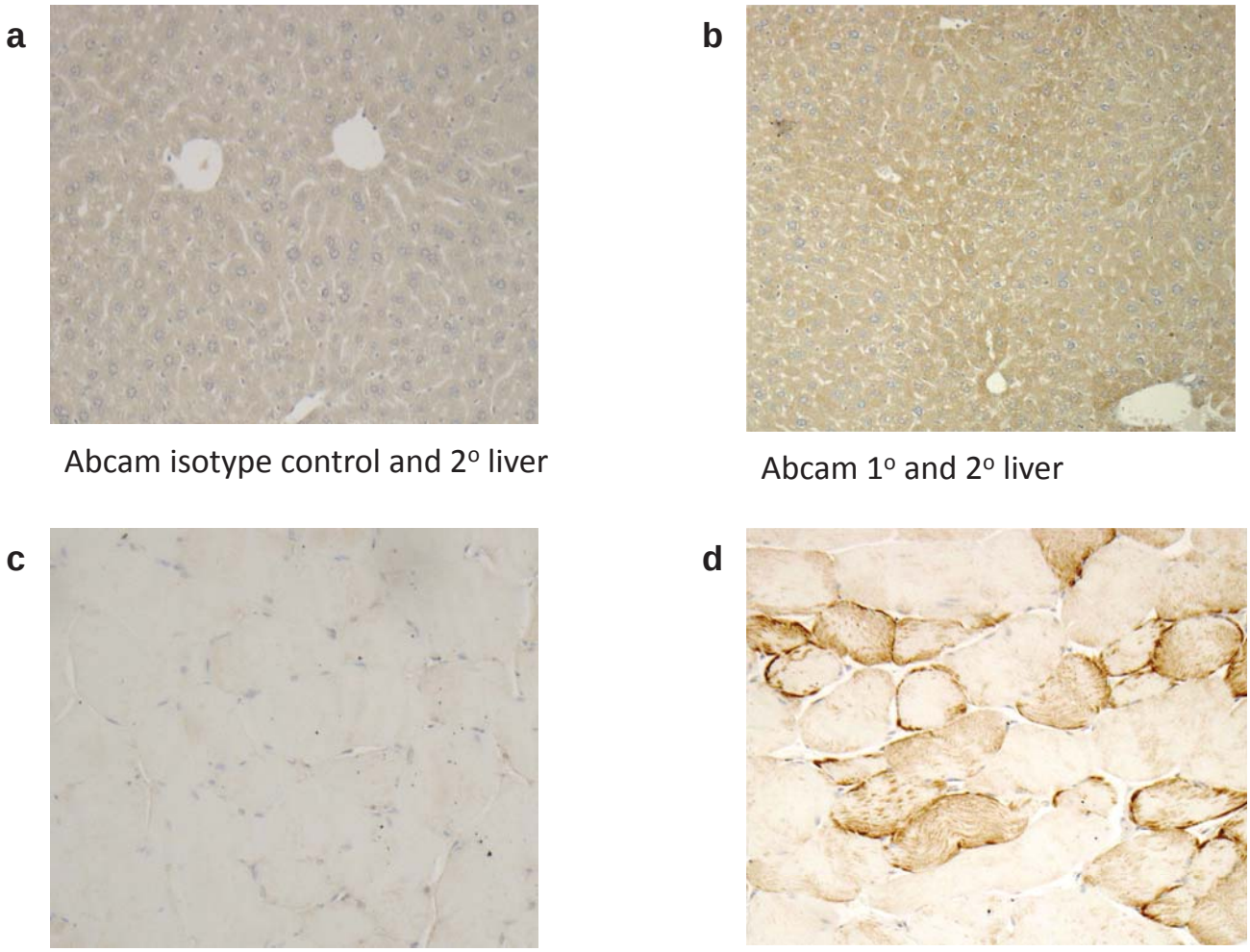

Figure 3.8. *Immunohistochemistry of 11 β-HSD1 using the Abcam (Ab39364) 11 β-HSD1 primary antibody (a = negative control liver with isotype control and secondary antibody, b = positive control liver with primary 11 β-HSD1 and secondary Abcam antibody, c = negative control quadriceps with isotype control and secondary Abcam antibody and d = quadriceps with primary 11 β-HSD1 and secondary Abcam antibody).*

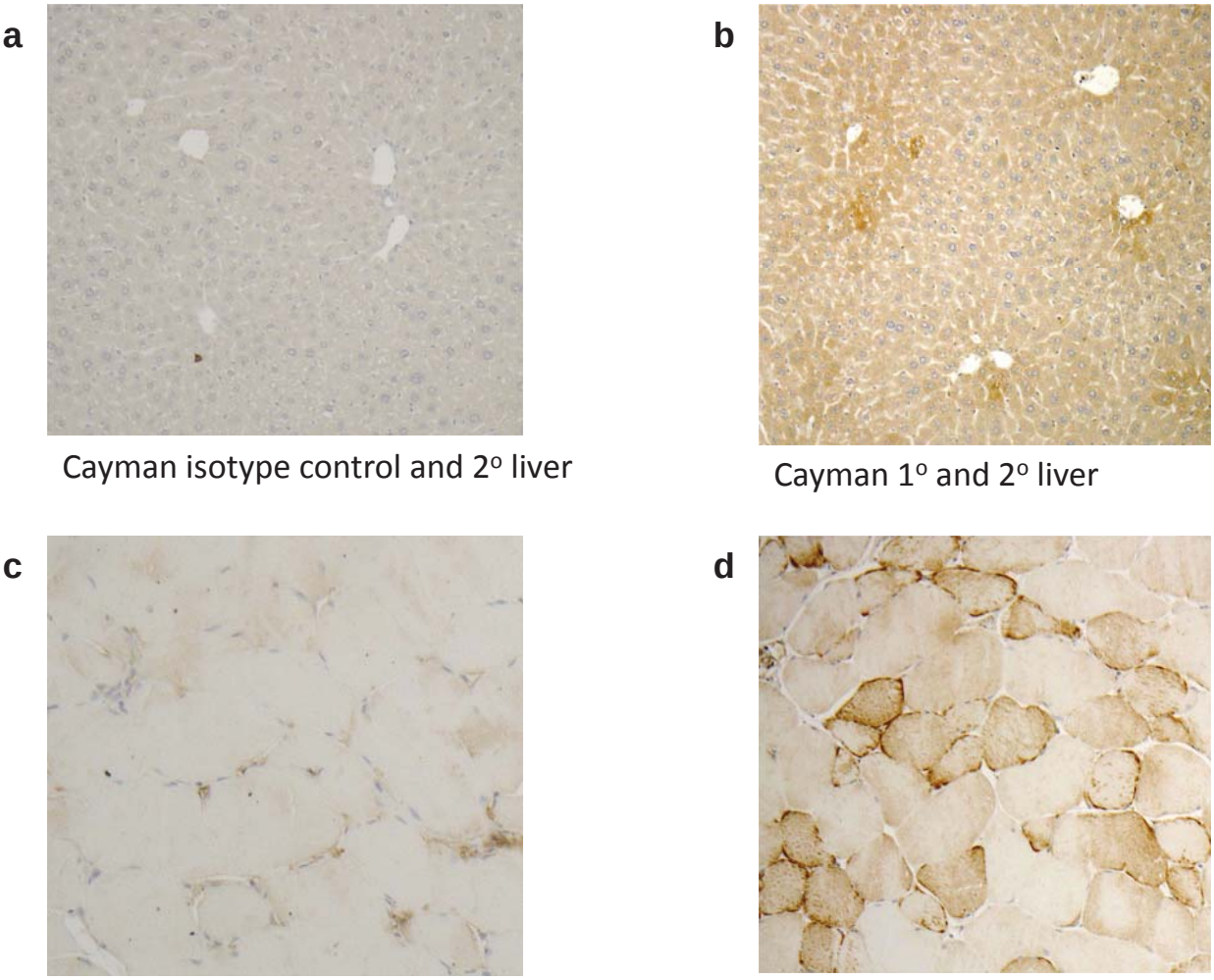

Figure 3.9. *Immunohistochemistry of 11 β-HSD1 using the Cayman (10004303) 11 β-HSD1 primary antibody (a = negative control liver with isotype control and secondary antibody, b = positive control liver with primary 11 β-HSD1 and secondary Cayman antibody, c = negative control quadriceps with isotype control and secondary Cayman antibody and d = quadriceps with primary 11 β-HSD1 and secondary Cayman antibody).*

3.6.5. Immunoflourescence of 11 β-HSD1 and fibre type specificity in skeletal muscle.

To further assess the apparent fibre specificity seen with immunohistochemistry, immunoflourescence was performed on serial sections of isopentane frozen skeletal muscle (soleus). Serial sections were stained for 11 β-HSD1 (Figure 3.10.a) and fibre type (Figure 3.10.b). There was no obvious fibre type specificity on immunoflourescence and in particular no evidence of specific co-localisation with Type I fibres.

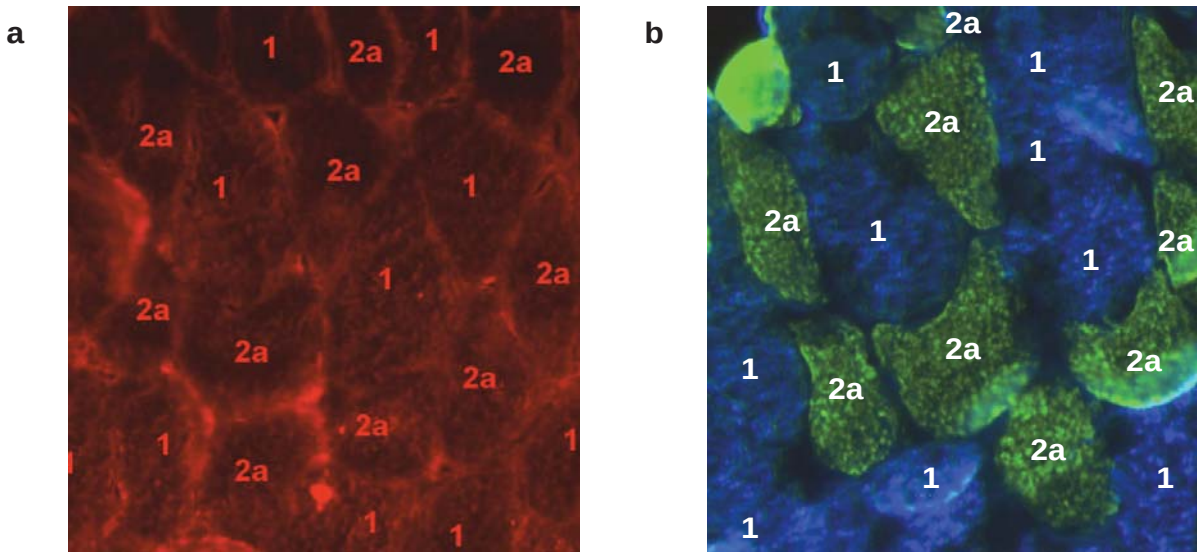

Figure 3.10. *Immunofluorescence of 11 β-HSD1 (red, Figure a) and fibre type specificity with antibody for Type I MyHC (Blue, 1) and Type IIa MyHC (green, 2a) in soleus muscle (Figure b). Images are matched and there is no fibre type specific localisation of 11 β-HSD1.*

3.7. Discussion

11 β-HSD1 is expressed and is biologically active in murine skeletal muscle and the C2C12 murine muscle cell line in significant amounts as evident by the 11 β-HSD1 oxoreductase in all muscle groups tested. Importantly, the oxoreductase activity of 11 β-HSD1 in muscle groups ranged from 40% to 100% that of liver, whereas mRNA expression in liver was orders of magnitude greater than that seen in muscles. This highlights the fact that murine 11 β-HSD1 is a very efficient enzyme (2) and low levels of mRNA expression may be sufficient to deliver significant oxoreductase activity. To ensure that this oxoreductase activity was secondary to 11 β-HSD1 in both C2C12 cells and murine tissue, both specific (LJ2) and non-specific (GE) inhibitors of 11 β-HSD1 were used, which lead to significant decreases in conversion of inactive 11-dehydrocorticosterone to biologically active corticosterone.

We observed significant increases in the activity and mRNA expression of 11 β-HSD1 during differentiation in the C2C12 murine skeletal muscle cell line, as observed previously (157). There is conflicting evidence for the role of glucocorticoids in muscle differentiation. *Nishimura et al.* treated C2C12 cells with the synthetic glucocorticoid, dexamethasone for 24 hours, which significantly increased mRNA expression of several key myogenic differentiation genes including myogenin, MyoD1, Myf5 and MRF4 (316). *Aubrey et al.* did not, however, report any changes on C2C12 differentiation despite retinoic acid leading to a downregulation of 11 β-HSD1 (157).

This tissue specific regulation of glucocorticoid action in skeletal muscle may have important implications for the biological effects of glucocorticoids in skeletal

muscle. Within skeletal muscle glucocorticoid excess is associated with significant changes in atrophy (upregulation) and hypertrophy (downregulation) pathways which lead to glucocorticoid mediated myopathy.

The effect of exposure of skeletal muscle to supraphysiological active glucocorticoid concentration in serum (in endogenous and exogenous Cushing's syndrome) may be further affected by 11 β-HSD1 activity within muscles. Muscle specific activation of the inactive glucocortoid cortisone (11-dehydrocorticosterone in rodents) which is produced from cortisol (corticosterone) by the dehydrogenase activity of 11 β-HSD2 in the kidney (which is known to be significantly elevated in Cushing's syndrome) (317) may lead to a more significant phenotype.

Levels of 11 β-HSD1 oxoreductase activity were particularly elevated in soleus muscle which is a Type I fibre rich muscle. This could either be due to elevated levels of 11 β-HSD1 in type I fibres or a product of the method of calculation of oxoreductase activity which may exaggerate the oxoreductase activity of small amounts of tissue due to increased surface area to weight ratios (Section 2.8).

Immunohistochemistry revealed evidence of a specific subset of fibres staining greater for 11 β-HSD1 than others and following review with our Sports and Exercise physiology colleagues, we attempted to co-stain 11 β-HSD1 and Myosin heavy chains to further assess this. Muscle fibres can be divided into a number of subgroups including slow twitch oxidative (Type I fibres), fast twitch oxidative (Type IIa fibres) and fast twitch glycolytic (Type IIx or IIb) (Table 1.1). Type I fibres contain high levels of slow isoform contractile proteins, high volumes of mitochondria, high levels of myoglobin and capillary densities and a high

oxidative enzyme capacity (14). Type IIa fibres are characterised by fast contraction with high oxidative capacity. Type IIb fibres are characterised by low volumes of mitochondria, high glycolytic enzyme activity, high myosin ATPase activity, increased rate of contraction and low fatigue resistance (14) (Table 1.1). To assess if the fibres which stained preferentially for 11β-HSD1 were indeed Type I fibres, we performed immunoflourescence and co-localisation using Type I MyHC (i.e. Type I fibres). There was no obvious pattern of co-staining in these studies, however, it should be highlighted that we had difficulties with auto-flourescence using the Binding site 11 β-HSD1 antibody and future studies are going to further examine this fibre specificity using alternative 11 β-HSD1 antibodies.

Chapters 4 and 5 of this thesis will examine the role of 11 β-HSD1 in skeletal muscle related to glucocorticoid mediated myopathy and age related sarcopaenia.

Chapter 4

The role of 11 β-HSD1 in glucocorticoid mediated myopathy

4.1. Introduction

Glucocorticoids affect every organ system with the main physiological and pathophysiological effects being on energy metabolism, bone, connective tissue (including muscle) and cardiovascular, immune, central nervous, gastrointestinal and endocrine systems (130).

Excess circulating cortisol either secondary to exogenous or endogenous sources [Cushing's syndrome (CS)] is associated with proximal muscle weakness (130). Several clinical studies have examined muscle function, histology and metabolism in patients with endogenous and exogenous glucocorticoid (GC) related myopathy (103, 107, 108, 190, 191). The effects of GCs on muscle appear to be related to dose, duration and type of steroid (192). Different sensitivities of skeletal muscle fibre types also play an important role in the development of myopathy (193). Muscle atrophy has been widely associated with glucocorticoids treatment in multiple experimental models, *in vitro* (194-199) and *in vivo* studies of rodent (84, 141, 143, 200-210) and human skeletal muscle (96, 101-108, 191). Type II fibre atrophy is the classically described histological abnormality reported in GC mediated myopathy (104, 107, 189, 191). In the majority of studies Type I fibres generally display little, if any, abnormalities.

4.1.1. Molecular pathways associated with glucocorticoid myopathy

Many molecular pathways have been described as playing an important role in the development of GC mediated myopathy including abnormalities in protein

metabolism, myostatin, atrophy related genes, collagen metabolism, mitochondrial function and myosin heavy chain isoform synthesis and degradation which are covered in detail in Section 1.5. Areas of glucocorticoid mediated myopathy which will be assessed further in this chapter, and summarised below, include atrophy related genes (particularly the ATP-ubiquitin-protease pathway), hypertrophy pathways (insulin/ IGF-I-AI3K-Akt-mTOR, particularly the role of IRS-1 and its phosphorylation) and the effects of GC on myocyte proliferation rates.

4.1.1.1. Atrophy pathways in glucocorticoid mediated myopathy

The atrophy pathways include the lysosomal proteases (eg. Cathepsins), the calcium dependent protease calpain family and the ATP-dependent ubiquitin-proteasome pathway (231) (described in detail in Section 1.5.3.4). The pathway primarily associated with muscle atrophy and the breakdown of myofibrillar protein is the ATP-dependent ubiquitin-protease pathway (235) which include the E1 (ubiquitin activating enzymes), E2 (ubiquitin-conjugating enzymes) and E3 (Ubiquitin ligase). Within skeletal muscle, MAFBX and MURF-1 are two important E3 ubiquitin ligases clearly associated with many models of muscle atrophy such as sepsis (79, 80) and disuse atrophy (81). Translocation of the forkhead transcription factor (FOXO-1) into the cell nucleus increases MAFbx and MURF-1 mRNA expression (84). Phosphorylation of FOXO-1 by Akt sequesters FOXO-1 from the cell nucleus to the cytoplasm by 14-3-3 proteins (85) preventing MAFbx and MURF-1 upregulation. However, GCs dephosphorylate FOXO-1 allowing subsequent translocation to the cell nucleus.

4.1.1.2. Apoptotic pathways in glucocorticoid mediated myopathy

Caspase-3 is an important regulator of glucocorticoid regulated myocyte apoptosis, *Orzechowski et al.* have shown a relationship between caspase-3 and apoptosis in skeletal muscle following longer periods of glucocorticoid exposure (for example 8 days rather than 24 hours) (318). There is no evidence of GC regulating the effect of short term treatment on caspase-3 mRNA expression but this may not be surprising as Caspase-3 is an effector caspase (319). An effector caspase depends on upstream initiator caspases (caspase 8, 9, 12) to be cleaved and activated which then carries out the proteolytic events that result in cellular breakdown and demise (319) which may take a number of days of GC exposure to modify expression (caspase 8 was increased after 8 days GC treatment in rats) (320).

4.1.1.3. Hypertrophy pathways in glucocorticoid mediated myopathy

Four major signalling pathways regulate protein synthesis and cell growth including the energy status of the cell (244); the amino acid sensing pathway (245); mechanotransduction (246, 247) and the insulin/ insulin-like growth factor I (IGF-I) system (245).

The insulin/ IGF-I-AI3K-Akt-mTOR signalling pathway has been described in detail in Section 1.5.3.6.1. Briefly, binding of insulin to its cell surface receptor leads to a conformational change and tyrosine autophosphorylation. Consequently, the insulin receptor substrate (IRS) family of adaptor proteins are recruited to the intracellular domain of the receptor and are phosphorylated at

multiple tyrosine residues by the receptor tyrosine kinase to permit the docking of phosphatidylinositol-3-kinase (PI3K) and subsequent generation of $PI(3,4,5)P_3$. Generation of this second messenger acts to recruit the Akt/PKB family of serine/threonine kinases to the plasma membrane where they are then activated (250). The molecular mechanisms underpinning insulin resistance are complex and variable. Serine/threonine phosphorylation of IRS1 (in particular Ser307 phosphorylation) has been shown to negatively regulate insulin signalling through multiple mechanisms including decreased affinity for the insulin receptor and increased degradation (253, 254). The interaction of glucocorticoids and the insulin signalling cascade has only been examined in a small number of studies that have offered variable explanations for the induction of insulin resistance (255-258). The role of serine phosphorylation and the impact of prereceptor glucocorticoid metabolism have not been explored.

The insulin/ IGF-I-AI3K-Akt-mTOR signalling cascade can also inhibit several regulators of muscle atrophy (196). In rats, 5 days of treatment with cortisone increased the insulin receptor (IR) protein by 36%, but reduced skeletal muscle total IR tyrosine kinase phosphorylation by 69%, which was attributed to a loss in the pool of IR undergoing tyrosine phosphorylation. Although muscle IRS-1 tyrosine phosphorylation was unaffected by GC treatment, GCs were associated with a 50% reduction in total IRS-1 protein content (255). Thus, GC myopathy may stem, in part from a GC mediated decrease in the anabolic IR-IRS-1-PI3K-Akt signalling pathway.

4.1.1.4. Myocyte proliferation in glucocorticoid mediated myopathy

There are conflicting data with regard to the effect of GC treatment on myoblast proliferation rate. Some studies have reported an increase in myoblast proliferation rate with GC treatment (217, 218) (particularly with low dose GC treatment), others reporting no effect of treatment with glucocorticoids (219) or a dose dependent decrease in myoblast proliferation (220). *Te Pas et al.* reported that GCs are capable of attenuating proliferation and differentiation of myocytes in a dose response manner by altering mRNA levels of myoD1, myf-5 and myogenin (220). When C2C12 myoblasts were incubated with dexamethasone or α-methyl-prednisolone for 9 days, the cell proliferation rate was reduced in a dose dependent manner despite increasing the mRNA expression of MyoD1 and myf-5 (220). Evidence suggests that GCs have an impact on myoblast proliferation; however data are conflicting and precise mechanisms underpinning the GC manipulation of myogenic growth factors remain to be determined. The reported differences may be due to a number of factors including the use of different experimental models, variable glucocorticoid doses and ligands (e.g. dexamethasone, corticosterone and alpha methylprednisolone), duration of myoblast proliferation assessed and proliferation assay used.

4.1.2. 11 β-HSD1 within muscle

Within tissues, GC levels are regulated at the pre-receptor level by the isozymes of 11 β-hydroxysteroid dehydrogenase (11 β-HSD), which are located in the endoplasmic reticulum (ER). 11 β-HSD1 *in vivo* acts predominantly as an oxoreductase converting inactive cortisone into active cortisol (2). The role of 11

β-HSD1 in skeletal muscle is less well-defined and has only been investigated in a small number of studies over recent years, which are discussed in Section 1.4.6.

4.2. Hypothesis

In myocytes, 11 β-HSD1 is increased with glucocorticoid exposure and this is associated with alterations of genes associated with glucocorticoid mediated myopathy. Glucocorticoids have effects on myoblast proliferation and modulation of 11 β-HSD1 may alter this.

4.3. Strategy of Research and Aims

C2C12 myoblasts and Day 8 myotubules were used to assess the role of 11 β-HSD1 in glucocorticoid mediated myopathy, which included:

a. Assessment of 11 β-HSD1 activity and mRNA expression following treatment with the active glucocorticoid [corticosterone, (B)] and the inactive glucocorticoid [11-dehydrocorticosterone (A)], which requires 11 β-HSD1 activation for biological activity.

b. Assessment of the mRNA expression of key glucocorticoid regulated markers of atrophy following treatment with the active glucocorticoid (corticosterone, B) and the inactive glucocorticoid (11-dehydrocorticosterone, A).

c. Assessment of the effect of glucocorticoid treatment and modulation of 11 β-HSD1 on the insulin/ IGF-I-AI3K-Akt-mTOR signalling pathway (in particular IRS1 and Ser307 phosphorylation of IRS1).

d. The effect of glucocorticoids and the modulation of 11 β-HSD1 on C2C12 myoblast proliferation.

4.4. Methods

4.4.1. C2C12 cell culture

The C2C12 cell line is a well-established model of both skeletal muscle proliferation and differentiation which has been widely used in research with regard to muscle atrophy and glucocorticoid induced myopathy (84, 86, 195, 197). Cryofrozen C2C12 myoblasts (passage 17) were purchased from ECACC (Salisbury, UK), Once myoblasts had reached 60-70% confluence, differentiation was initiated by replacing proliferation media with DMEM with high glucose and L-glutamine (PAA, Somerset, UK) supplemented with 5% horse serum. Differentiation media was replaced every 48 hours. After 8 days, myoblasts had fused to form multinucleated myotubes.

4.4.1. RNA extraction and cDNA synthesis

Total RNA was extracted from monolayer cells using TRIreagent (Sigma-Aldrich, Dorset, UK). The procedure was carried out according to protocol provided with the reagent (Sigma-Aldrich, Dorset, UK). The quantity of RNA was measured using NanoDrop ND-1000 UV-Vis Spectrophotometer (Thermofisher, Surrey,

UK). The reverse transcription process was carried out using Applied Biosystems High-Capacity Reverse Transcription Kit (Applied Biosystems, Warrington, UK) For a full description of methods used see Section 2.2 and 2.3.

4.4.2. Quantitative or Real Time PCR

Quantitative PCR was carried out using Applied Biosystems Reagents and gene mRNA expression assays (AssayonDemand) (Applied Biosystems, Warrington, UK). PCRs for genes of interest and for 18s housekeeping genes were carried out in singleplex. Data were expressed as Ct values (Ct=cycle number at which logarithmic PCR plots cross a calculated threshold line). And used to determine ΔCt values (ΔCt = (Ct of the target gene) – (Ct of the housekeeping gene), lower ΔCt values reflecting higher mRNA mRNA expression. Data are expressed as arbitrary units using the following transformation [mRNA expression in arbitrary units = $1000*(2^{-\Delta Ct})$]. For a full description of methods used see Section 2.6.

4.4.3. Protein Extraction and concentration measurement on monolayer cells and explants

Monolayer cells were lysed in Radio-Immunoprecipitation (RIPA) buffer containing detergent. The lysate was freeze-thawed to further break open cell membranes and the insoluble components removed by centrifugation.

Mouse tissue was quickly harvested and snap frozen using liquid nitrogen. Samples were then transferred to a -80°C freezer until required. Proteins were extracted by homogenising approximately 20mg of tissue in 1.5mL of RIPA buffer

using a mechanical homogeniser. Cell lysates were then incubated at -80°C for 20 mins, thawed out on ice, then centrifuged at 14,000 g for 15 mins at 4°C.

The supernatant, from both monolayers and tissue explants, containing soluble proteins was measured using BioRad RC DC protein assay (BioRad, Herts, UK). 5µl of protein sample or standard were added per well in duplicate. The ranges of protein standards were 0, 0.25, 0.5, 1, 2, 4, 8 and 10mg/mL of Bovine Serum Albumin (BSA) in RIPA buffer. 25ml of solution A (alkaline copper tartrate) (with 20µl of solution S per ml of solution A) was initially added followed by 200ml of solution B (Folin reagent). Once the solutions were added the plate was incubated at room temperature for 10 minutes and the absorbance read at 690nm on a Victor3 1420 multilabel counter (PerkinElmer, Beaconsfield, Bucks, UK). Protein concentration in the sample was then calculated according to the slope of the standards line. For a full description of methods used see Section 2.7.

4.4.4. 11 β-hydroxysteroid dehydrogenase type 1 and 2 enzyme activity assay

11 β-hydroxysteroid dehydrogenase type 1 and 2 enzyme activity assay was carried out on both monolayers and whole tissue explants. Incubations were carried out at 37°C under a 5% CO_2 atmosphere for 20 minutes to 2 hours depending on the cell/tissue type. Enzyme activity was expressed in pmols of steroid converted per mg of protein per hour (pmol/mg/h) for monolayers or steroid converted per mg tissue per hour (explants). For a full description of methods used see Section 2.8.

4.4.5. Proliferation assays

The Cell Titre 96 ® AQ_{ueous} Non-Radioactive Cell proliferation assay is a homogenous, colorimetric method for determining the number of viable cells in proliferation, cytotoxicity or chemosensitive assays. The Cell Titre 96 ® AQ_{ueous} Assay is composed of solutions of a tetrazolium compound [3-(4,5-dimethylthiazol-2-yl)-5-(3-carboxymethoxyphenyl)-2-(4-sulfophenyl)-“H-tetrazolium, inner salt; MTS] and an electron coupling reagent (phenazine methosulfate) PMS. The assay was performed according to the manufacturers protocol. C2C12 cells were trypsinised and counted, they were then seeded at a concentration of approximately 1000 per well on 96 well plate (in a volume of 100 µl) and left for 24 hrs. After 24 hours treatments were added to cells (e.g. glucocorticoids, IGF-I) and the cells were incubated in treatment for another 24 hours at 37°C. For a full description of methods used see Section 2.11. IGF-I was used as a positive control in all experiments as it is well described as leading to myoblast proliferation in C2C12 cells (297).

4.4.6 Immunoblotting

Immunoblotting allows the measurement of relative amounts of a specific protein in a mixed protein sample (296). The theory and procedure is covered in detail in Section 2.10. Briefly, 20µg of protein was mixed with an appropriate amount to 5 x loading buffer and boiled for 5 minutes. Samples were loaded into a 4-20% gradient SDS-PAGE gel (BioRad, Herts, UK) and run at 200V for 1 h - 1 h 30 minutes. Transfer of proteins to nitrocellulose membrane (GE Healthcare, Bucks,

UK) was conducted at 140mA for 1-2 h depending on the size of the protein of interest. Efficient transfer was assessed by incubating the membrane in ponceau stain with agitation for 60 seconds, and then rinsed with water to allow visualisation of the protein bands. Electrophoresis and protein transfer was carried out in BioRad mini protein 3 apparatus (BioRad, UK). Membranes were blocked in 10mL of blocking buffer for 1 hour at room temperature with constant agitation, then incubated with primary antibody overnight at 4°C on an orbital shaker. Membranes were washed with 100mL of washing buffer 3 times for 15 minutes. Secondary antibody incubation was conducted at room temperature with constant agitation. The membrane was then washed with 100mL of washing buffer 3 times for 15 minutes. Bound antibody was detected using Enhanced Chemiluminescence (ECL, GE Healthcare, Bucks, UK). The reaction mixture was set up by combining substrate A with substrate B at a 50:50 ratio (final volume: 1mL per membrane). Following equilibration for 5 minutes, 1mL was added per membrane and left to incubate for 2 minutes before the membrane was placed between two plastic sheets in a photo cassette. Photographic film (was placed over the membrane in the dark and exposed for 30 seconds to 3 h, then developed on Compact X4 automatic film processor (Xograph Imaging Systems, Gloustershire, UK). Membranes were routinely stripped to remove bound primary/secondary antibodies by incubating the membrane in stripping buffer (2% SDS, 100mM β-mercaptoethanol, 50mM Tris, pH 6.8) at 50°C for 1 h with gentle agitation. Membranes were then washed with 100mL of washing buffer 3 times for 15 minutes before being re-probed with a different primary antibody. Immunoblots were evaluated by integrating densitometry using GeneSnap and GeneTool (Chemigenius Gel Documenting System, Syngene, Cambridge, UK).

Equal loading was confirmed by reprobing membrane with anti-β-actin antibody conjugated to HRP and visualized as described above.

Antibodies used included Primary antiIRS1, anti-p-ser^{307}IRS1 antibodies (Upstate, Dundee, UK), secondary Ab (Dako, Glostrop, UK) used at a dilution of 1/5,000. Membranes were reprobed for β-Actin primary and secondary Ab (Abcam plc, Cambridge, UK) at a dilution of 1/5,000.

4.4.7. Statistical Methods

Statistical analysis was performed using Prism for Windows version 5.0 (GraphPad Software Inc, San Diego, CA, USA) software packages. Continuous data were summarised using means and standard deviations (or standard error of mean) if parametrically distributed or medians and inter-quartile ranges if non-parametrically distributed. Parametric data was compared using a paired t-test and non-parametric data was analysed using a Mann-Whitney test. Multiple comparisons were assessed using one-way analysis of variance (ANOVA), with Kruskal-Wallis for non-parametric data and Dunn's multiple comparison test. The level for statistical significance was $p<0.05$.

4.5. Results

4.5.1. 11 β-HSD1 activity and mRNA expression following treatment with the active glucocorticoid [corticosterone, (B)]

Day 8 C2C12 myotubules were treated for 24 hours with increasing doses of corticosterone (B). Following this 11 β-HSD1 mRNA expression was determined and a 20 minute 11 β-HSD1 oxoreductase activity assay was performed. There was a dose dependent increase in both 11 β-HSD1 oxoreductase activity (Figure 4.1.a) and mRNA expression (Figure 4.1.b) with increasing doses of B. Therefore, treatment with B leads to increased generation of intracellular active glucocorticoid via increased activity of 11 β-HSD1 in myotubules.

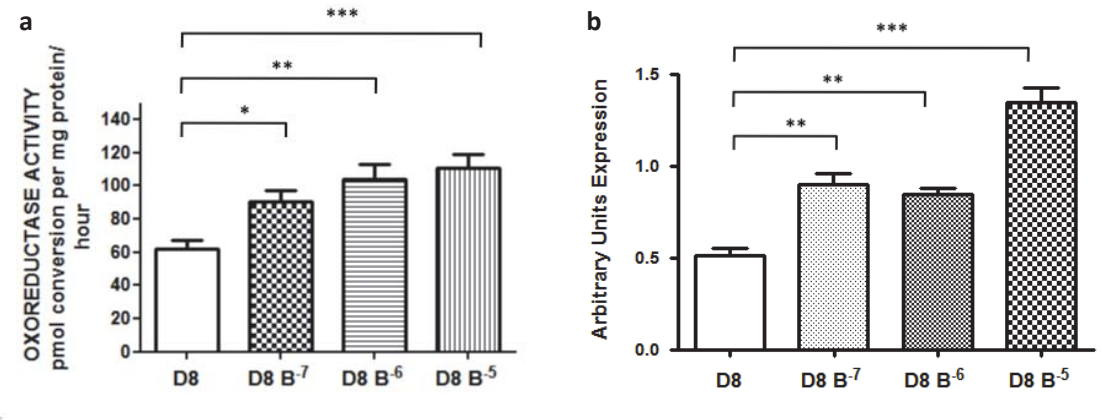

Figure 4.1. *11 β-HSD1 activity (a) and mRNA expression (b) with increasing doses of corticosterone (B). * p<0.05, ** p<0.001, *** P<0.0001, n=4 experiments. Data shown are the mean±SE. p trend for increasing dose of B effect on activity and* mRNA expression = *p<0.001.*

4.5.2. The effect of increasing doses of the active glucocorticoid (corticosterone) on atrophy related genes

To show that the increased GC exposure with increased 11 β-HSD1 expression was associated with upregulation of classic markers of glucocorticoid mediated myopathy, the mRNA expression of MAFbx and MURF-1 (GC regulated atrophy genes) and Caspase 3 (a key regulator of GC mediated apoptosis which is upregulated with chronic treatment, but may not be changed with short-term treatment), was analysed.

Day 8 C2C12 myotubules were treated for 24 hours with increasing doses of corticosterone (B). Following this 11 β-HSD1 (Figure 4.2.a), MAFbx (Figure 4.2.b) and MURF-1 (Figure 4.2.c) and Caspase 3 (Figure 4.2.d) mRNA expression were assessed. There was an upregulation in both MAFbx and MURF-1 with GC treatment but no change in Caspase 3.

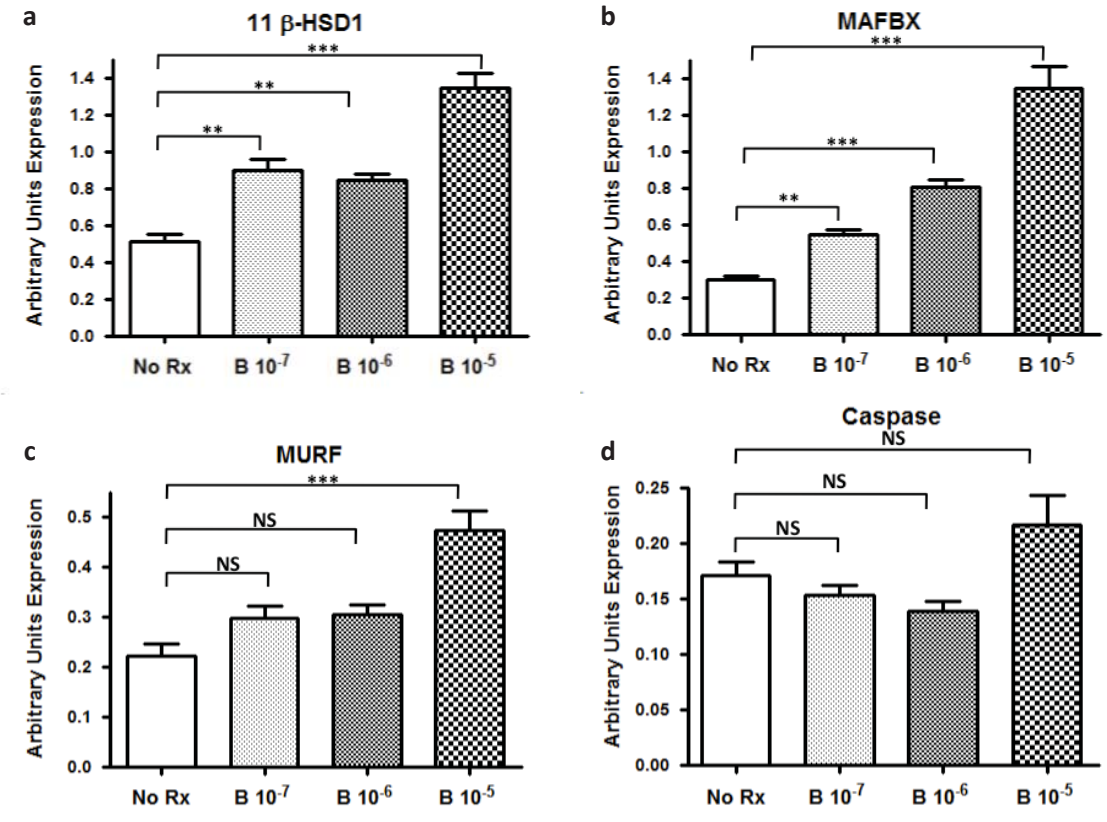

Figure 4.2. *The effect of increasing doses of corticosterone (B) on mRNA expression of 11 β-HSD1 (a), MAFbx (b) and MURF-1 (c) (both of which are key glucocorticoid response atrophy genes). Figure (d) shows the response of Caspase 3 (a key regulator of GC mediated apoptosis in chronic treatment). NS non significant, ** p<0.001, *** P<0.0001, n=3-4 experiments. Data shown are the mean±SE.*

4.5.3. 11 β-HSD1 activity and mRNA expression following treatment with the inactive glucocorticoid 11-dehydrocorticosterone (A).

However, as the previous results could be interpreted solely as the effect of the active GC (B) treatment rather than the effect of tissue specific regulation by 11 β-HSD1 of GC exposure we repeated the previous experiments with 11-dehydrocorticosterone (A) instead of B. 11-dehydrocorticosterone (A) requires 11 β-HSD1 oxoreductase activity to produce active corticosterone (B) in order to exert its biological effects as a glucocorticoid at the level of GRα. Day 8 C2C12 myotubules were treated for 24 hours with increasing doses of 11-dehydrocorticoserone (A). Following this 11 β-HSD1 mRNA expression was determined and a 20 minute 11 β-HSD1 oxoreductase activity assay was performed. There was an increase in both 11 β-HSD1 oxoreductase activity (Figure 4.3.a) and mRNA expression (Figure 4.3.a) with higher concentrations of A. Therefore, following treatment with A 10^{-6} and 10^{-5} there is a significant increase in the generation of B, which in turn leads to increased generation of intracellular active glucocorticoid via 11 β-HSD1.

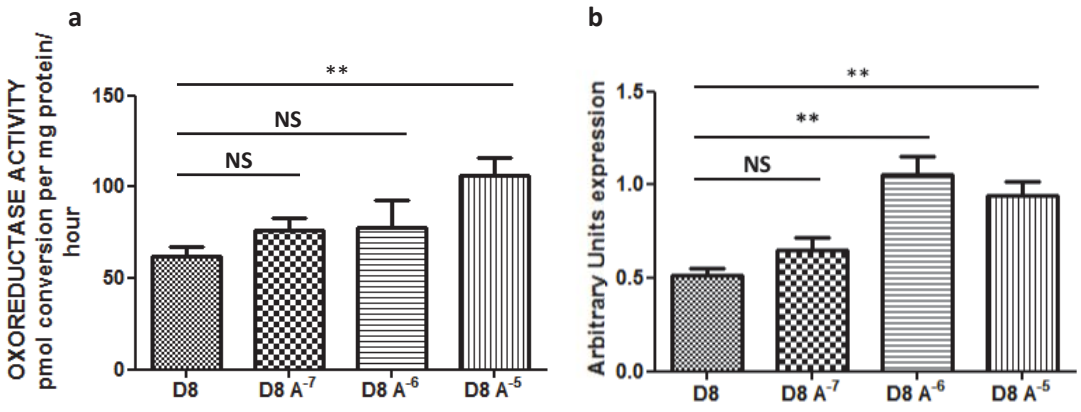

Figure 4.3. *11 β-HSD1 activity (a) and mRNA expression (b) increases with increasing doses of the inactive glucocorticoid A. NS non significant, ** p<0.001, n=3 experiments. Data shown are the mean±SE. p trend for increasing dose of A effect on activity (p<0.0001)and mRNA expression (p<0.001).*

4.5.4. The effect of increasing doses of the inactive glucocorticoid [11-dehydrocorticosterone (A)] on atrophy related genes.

To show that the increased GC via the oxoreductase activity of 11 β-HSD1 was associated with upregulation of classic markers of glucocorticoid mediated myopathy, MAFbx, MURF-1 and Caspase 3 mRNA expression were analysed.

Day 8 C2C12 myotubules were treated for 24 hours with increasing doses of A. Following this the mRNA expression of 11 β-HSD1 (Figure 4.4.a), MAFbx (Figure 4.4.b) and MURF-1 (Figure 4.4.c) and Caspase 3 (Figure 4.4.d) were assessed. At doses of A 10^{-6} and 10^{-5} there was an increase in glucocorticoid mediated atrophy genes. This can be interpreted as the treatment with 11-dehydrocorticosterone (A) leading to generation of corticosterone (B) via 11 β-HSD1, which leads to activation of GC mediated atrophy genes. Therefore, 11 β-HSD1 may play an important role in glucocorticoid mediated myopathy.

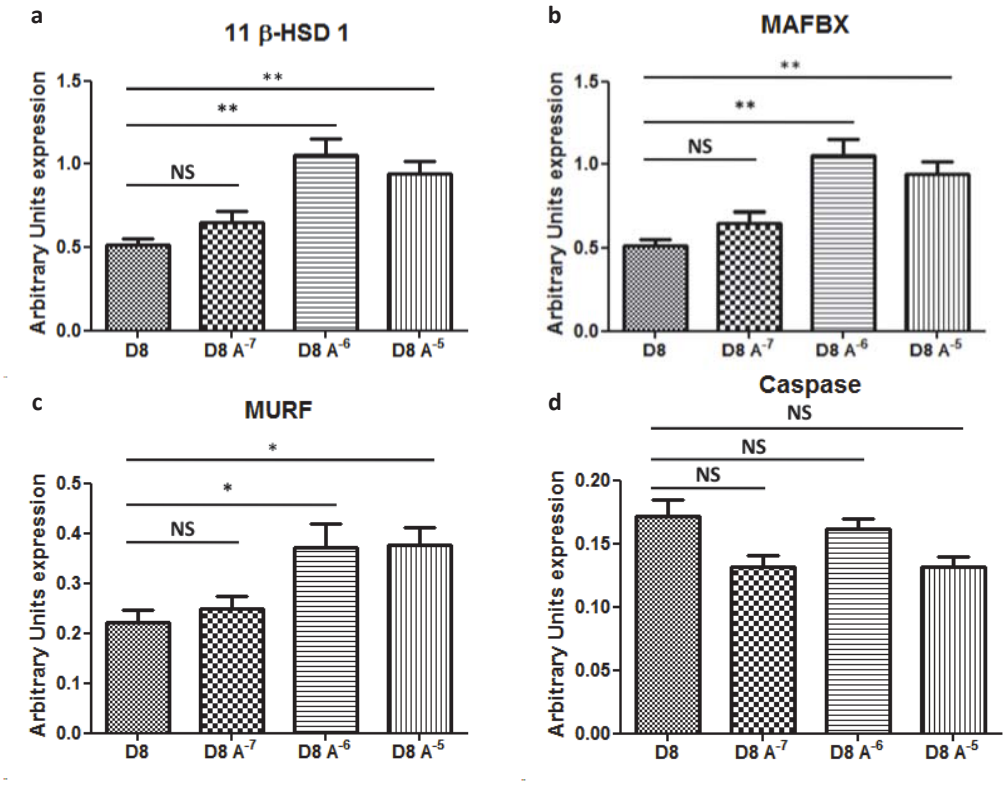

Figure 4.4. *The effect of increasing doses of 11-dehydrocorticosterone on mRNA expression of 11 β-HSD1 (a), MAFbx (b) and MURF-1 (c) (both of which are key glucocorticoid response atrophy genes). Figure (d) shows the response of Caspase 3 (a key regulator of GC mediated apoptosis in chronic treatment). NS non significant, * p<0.05, ** p<0.001, *** P<0.0001, n=3-4 experiments. Data shown are the mean±SE.*

4.5.5. Effect of treatment with glucocorticoids and modulation of 11 β-HSD1 on total IRS1 and pSer307IRS1

The insulin/ IGF-I-AI3K-Akt-mTOR signalling pathway increases protein synthesis (240, 248, 249) and is the key regulator of muscle insulin sensitivity. The insulin/ IGF-I-AI3K-Akt-mTOR signalling pathway can also inhibit several regulators of muscle atrophy (196). In collaboration with members of our group (Dr Stuart Morgan and Dr Jeremy Tomlinson) who were assessing the role of glucocorticoids and 11 β-HSD1 in insulin resistance in skeletal muscle (in particular the effect on IRS1 and its phosphorylation status), the effect of glucocorticoids and modulation of 11 β-HSD1 on the insulin/ IGF-I-AI3K-Akt-mTOR signalling hypertrophy pathway was assessed. Using Day 8 C2C12 myotubules, treated with increasing doses of corticosterone (B) for 24 hours, total IRS1 and pser^{307} IRS1 protein content was assessed.

The role of the insulin/ IGF-I-AI3K-Akt-mTOR signalling pathway in insulin sensitivity has been discussed in detail in Section 1.5.3.6.1. Importantly, Serine/threonine phosphorylation of IRS1 (in particular Ser307 phosphorylation) has been shown to negatively regulate insulin signalling through multiple mechanisms including decreased affinity for the insulin receptor and increased degradation (253, 254). There was a dose dependent decrease in total IRS1 and a dose dependent increase in pser^{307} IRS1 content (which is a known to negatively regulate insulin signalling, therefore decreasing downstream hypertrophy signals) (Figure 4.5).

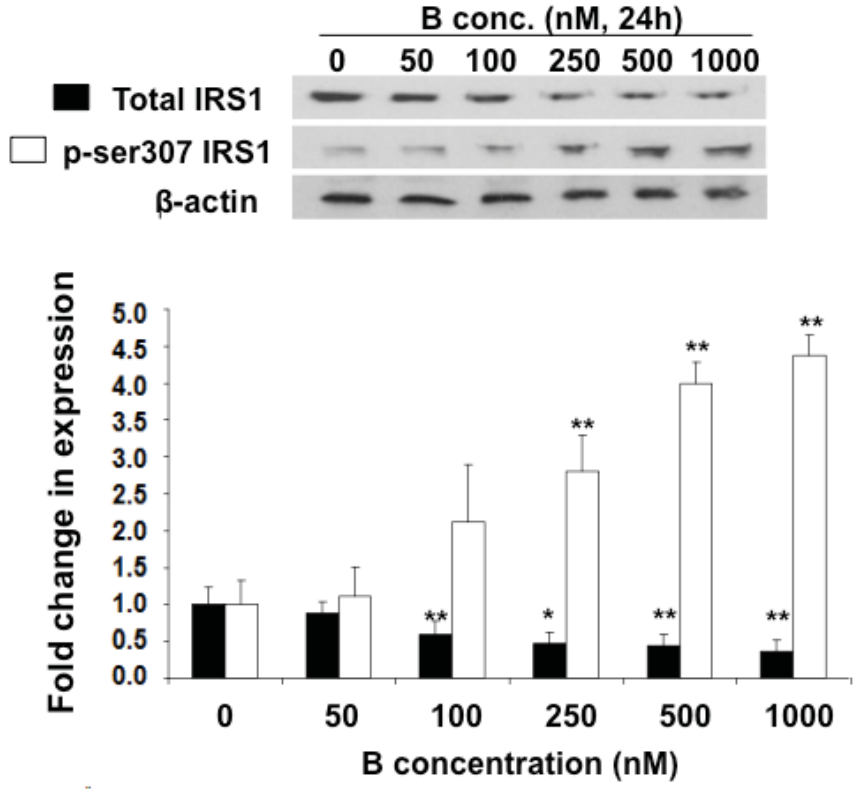

Figure 4.5. The effect of increasing doses of corticosterone (B) on total IRS1 and p-ser307 IRS1 protein content on Day 8 C2C12 myotubules. * p<0.05, ** p<0.00, B = corticosterone, nM = nanomolar. N=4-6 experiments

To further assess the role of tissue specific regulation of glucocorticoid activity by 11 β-HSD1 on the insulin signalling cascade Day 8 C2C12 cells were treated with corticosterone (B), 11–dehydrocorticosterone (A) (an inactive GC unless converted to B via 11 β-HSD1) and A co-incubated with a non-specific 11 β-HSD1 inhibitor (glycyrrhetinic acid, GE). Total IRS1 and p-ser307 IRS1 protein content was then assessed. There was a decrease in total IRS1 and increase in pser^{307} IRS1 content (which is a known to negatively regulate insulin signalling, therefore

decreasing downstream hypertrophy signals) in cells treated with A and B, which was reversed on treatment with the 11 β-HSD1 inhibitor GE (Figure 4.6).

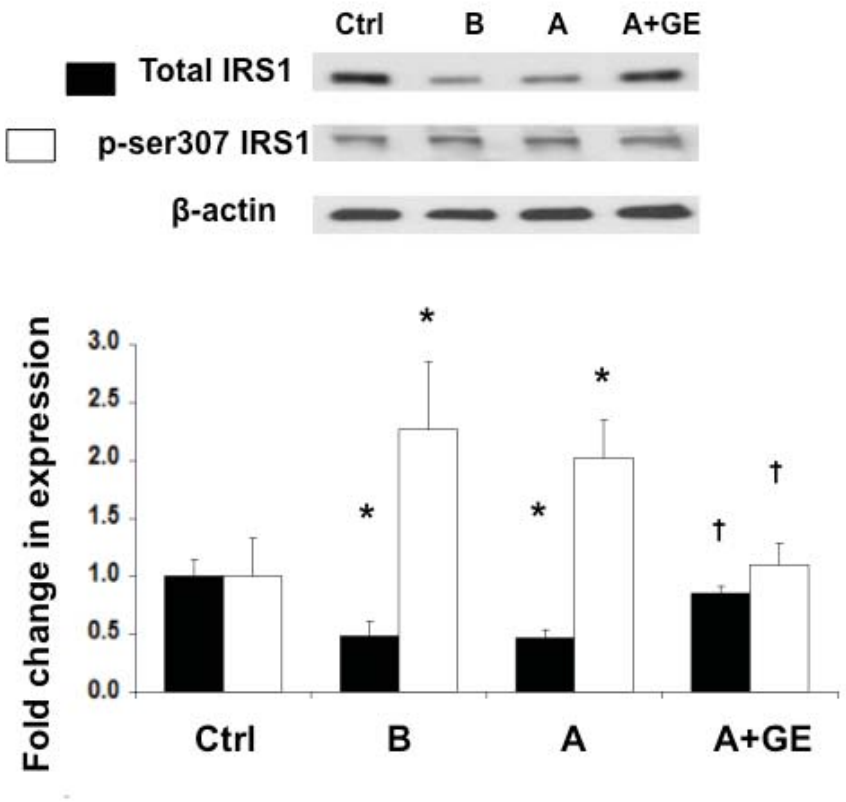

Figure 4.6. The effect of corticosterone (B, 250nM), 11 dehydrocorticosterone (A,250nM) and co-incubation of A and the non-specific 11 β-HSD1 inhibitor (GE, 2.5μM) on total IRS1 and p-ser307 IRS1 protein content on Day 8 C2C12 myotubules. * $p<0.01$ compared to control, † $p<0.01$ compared to A/ and B treatment, N=4-6 experiments.

4.5.6. The effect of treatment with the active glucocorticoid (corticosterone) on myoblast proliferation rate.

To assess the impact of glucocorticoids on myoblast proliferation C2C12 myoblasts were treated with increasing doses of B and IGF-1 100ng/ml (as a positive control) for 48 hours to assess the impact on myoblast proliferation rates (assessed using the Cell Titre 96 ® AQ_{ueous} Non-Radioactive Cell proliferation assay). $B10^{-5}$ lead to decreased proliferation rates. Treatment with IGF-I 100ng/ml was associated with increased proliferation rates (positive control). Co-incubation of cells with IGF-I 100ng/ml (IGF100) and $B10^{-5}$ leads to a significant decrease in the proliferation rate of C2C12 myoblasts compared with IGF-I treatment. Therefore, B can inhibit the proliferative effect of IGF-I.

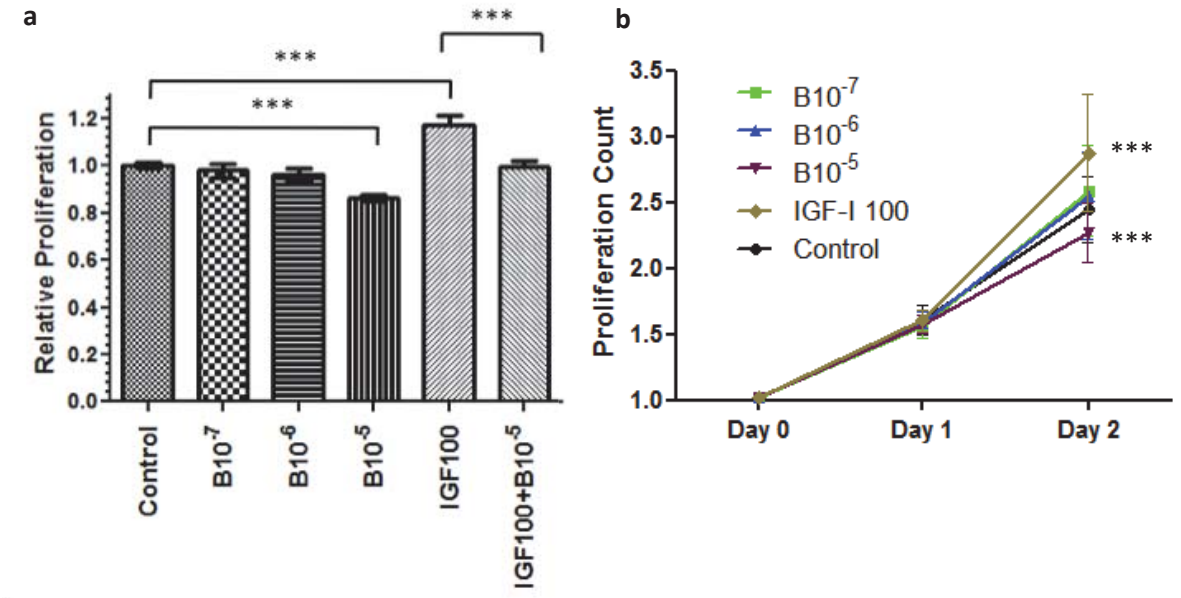

Figure 4.7. *Effect of 48-hour treatment with increasing doses of corticosterone (B) on C2C12 myoblast proliferation rate. Relative proliferation rate compared to controls at 48 hours (a) and trend in raw proliferation counts over 2 days (b) are represented. *** p<0.0001, n=5 experiments. Data shown are the mean±SE.*

4.5.7. Effect of treatment with the inactive glucocorticoid 11-dehydrocorticosterone (A) on C2C12 myoblast proliferation rate.

The effect of 48-hour co-treatment with the inactive glucocorticoid 11-dehydrocorticosterone (A) (which requires 11 β-HSD1 to activate to corticosterone) on C2C12 myoblast proliferation rate was assessed. There was no effect of treatment with A on proliferation rates which may be explained by the low levels of 11 β-HSD1 mRNA expression and oxoreductase activity in C2C12 myoblasts, therefore not generating significant levels of active intracellular glucocorticoid (see Figure 3.2, Section 3.5.1).

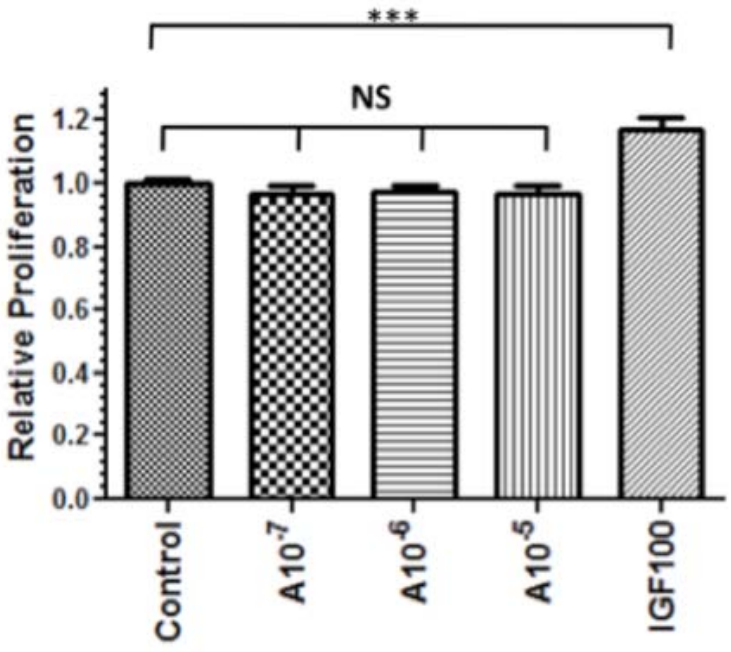

Figure 4.8. *Effect of 48-hour treatment with the inactive glucocorticoid 11-dehydrocorticosterone (A) (which requires 11 β-HSD1 to activate to corticosterone) on C2C12 myoblast proliferation rate. Relative proliferation rate compared to controls at 48 hours. There was no effect of treatment with A on proliferation rates. NS = p non significant compared to controls, *** p<0.0001 (n=5 experiments). Data shown are the mean±SE. IGF100 = IGF-I 100ng/ml, positive control.*

4.5.8. The effect of modulation of 11 β-HSD1 and glucocorticoid receptor antagonism on myoblast proliferation rate.

C2C12 myoblasts were treated with the glucocorticoid receptor antagonist RU486, selective and non-selective 11 β-HSD1 inhibitors (LJ2 and glycyrrhetinic acid, respectively) and IGF-I 100ng/ml (as a positive control) for 48 hours to assess the impact on myoblast proliferation rates.

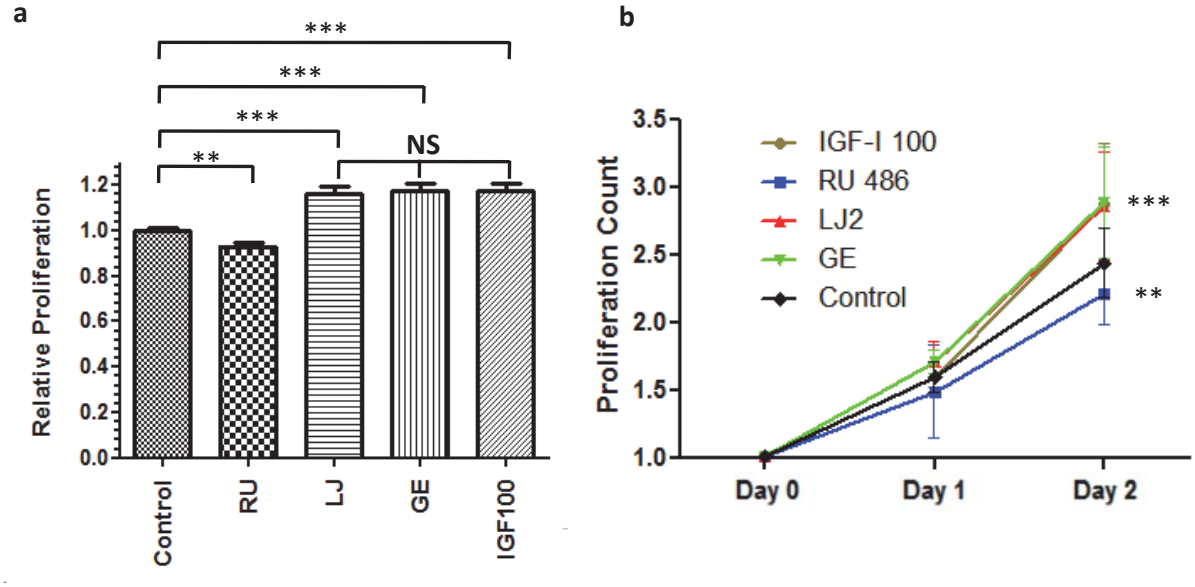

Figure 4.9. *Effect of 48-hour treatment with the glucocorticoid receptor antagonist RU486 and specific and non-specific 11 β-HSD1 inhibitors (LJ2 and glycerrhetinic acid, respectively) on C2C12 myoblast proliferation rate. Relative proliferation rate compared to controls at 48 hours (a) and trend in raw proliferation counts (b) over 2 days are represented. Glucocorticoid receptor antagonism leads to decreased proliferation rates and specific and non-specific 11 β-HSD1 inhibition leads to an increase in the proliferation rates of C2C12 myoblasts similar to that seen in the positive control group (IGF-I 100ng/ml, IGF100). p NS = non significant, ** p<0.001, *** p<0.0001, n=5 experiments. Data shown are the mean±SE.*

4.5.9. Effect of 48-hour co-treatment with corticosterone (B) and glucocorticoid receptor antagonist and 11 β-HSD1 inhibition on C2C12 myoblast proliferation rate.

The effect of co-incubation of corticosterone with 11 β-HSD1 inhibitors (GE and LJ2) and GRα antagonism (RU486) on myoblast proliferation was assessed. As treatment with $B10^{-5}$ was associated with a decrease in proliferation rate we assessed the effect of $B10^{-5}$ co-incubation with GE, LJ2 and RU486.

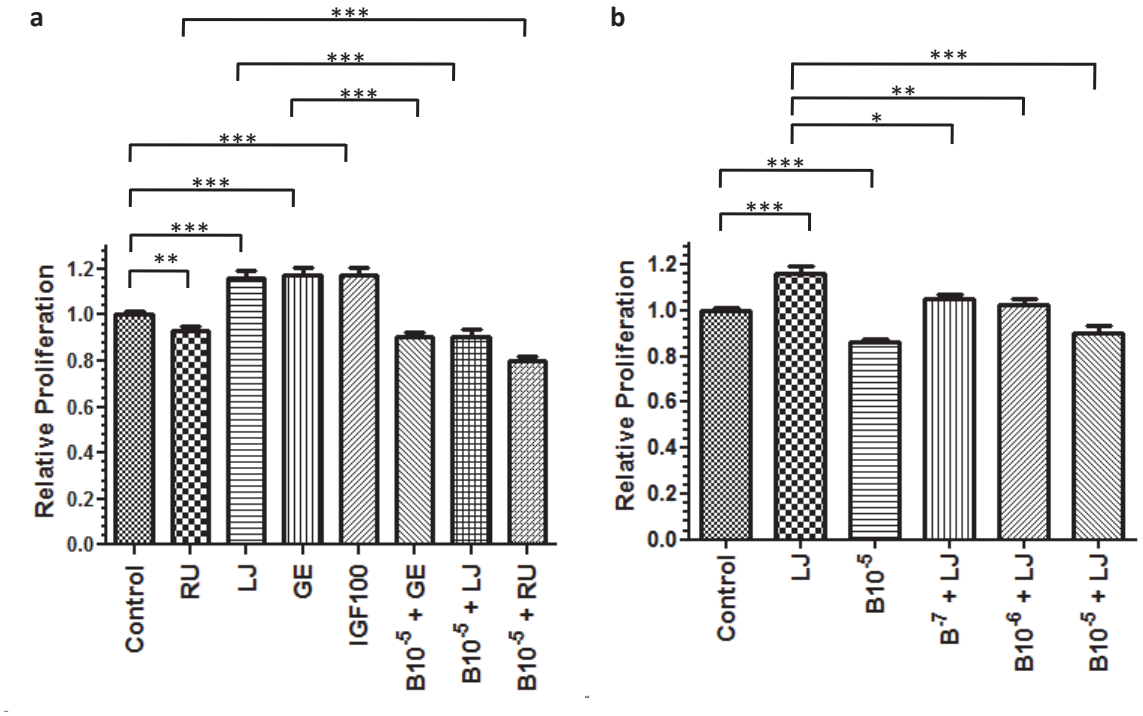

Figure 4.10. *Effect of 48-hour co-incubation with corticosterone (B) and glucocorticoid receptor antagonist RU486, and specific and non-specific 11 β-HSD1 inhibitors (LJ2 and glycerrhetinic acid, respectively) on C2C12 myoblast proliferation rate (a). Relative proliferation rate compared to controls at 48 hours. High dose corticosterone ($B10^{-5}$) treatment leads to decreased proliferation rates when combined with glucocorticoid receptor antagonism and specific and non-specific 11 β-HSD1 inhibition (a). Figure (b) represents the effect of 48-hour co-treatment with increasing doses of corticosterone ($B10^{-7/-6/-5}$) and specific 11 β-HSD1 inhibitor (LJ2) on C2C12 myoblast proliferation rate. There is a dose dependent decrease in proliferation rates with increasing doses of corticosterone (B) treatment (b), indicating that treatment with B can reverse the positive effects*

*on proliferation of 11 β-HSD1 inhibition. *p<0.05, ** p<0.001, *** p<0.0001, n= 5 experiments. Data shown are the mean±SE.*

4.6. Discussion

Our data show that 11 β-HSD1 activity and mRNA expression is increased with glucocorticoid exposure in C2C12 cells and that this increase in 11 β-HSD1 is associated with upregulation of classical GC related atrophy genes (MAFbx and MURF-1). Importantly, to highlight that these changes were not solely related to treatment with the active GC corticosterone and that 11 β-HSD1 had an important role to play in GC mediated myopathy C2C12 cells were also treated with the inactive GC 11-dehydrocorticosterone (A) which is dependent on conversion by 11 β-HSD1 to corticosterone for its biological activity. Treatment with A was also associated with increased 11 β-HSD1 mRNA expression and activity and also the upregulation of genes associated with glucocorticoid mediated atrophy (which one can assume were upregulated via the intracellular conversion of A to B by 11 β-HSD1). This upregulation of 11 β-HSD1 in muscle following exposure to GCs may be important as in clinical practice the effect of exposure of skeletal muscle to supraphysiological glucocorticoid concentrations in serum (in endogenous and exogenous Cushing's syndrome) may be further affected by 11 β-HSD1 activity within muscles. Muscle specific activation of the inactive glucocorticoid cortisone (11-dehydrocorticosterone in rodents) which is produced from cortisol (corticosterone) by the dehydrogenase activity of 11 β-HSD2 in the kidney (which is known to be significantly elevated in Cushing's syndrome) (317) may lead to a more severe muscle phenotype.

MAFBX and MURF-1 are increased in the C2C12 murine skeletal muscle cell line by treatment with A and B. As discussed in Section 1.5.3.4, MAFbx and MURF-1 are two important E3 ubiquitin ligases clearly associated with many models of muscle atrophy such as sepsis (79, 80) and disuse atrophy (81) . Translocation of the forkhead transcription factor (FOXO-1) into the cell nucleus increases MAFbx and MURF-1 mRNA expression (84). Phosphorylation of FOXO-1 by Akt sequesters FOXO-1 from the cell nucleus to the cytoplasm by 14-3-3 proteins (85) preventing MAFbx and MURF-1 upregulation. However, GCs dephosphorylate FOXO-1 allowing subsequent translocation to the cell nucleus. GCs target MAFbx via FOXO-1 and FOXO-3, leading to increased MAFbx expression (84, 239). GCs upregulate MURF-1 expression *in vivo* and *in vitro* (84, 86, 239, 240) through the co-binding of the GR and FOXO-1 with the GRE and Fbox response element (FBE) found on MURF-1's promoter region. The results of the above molecular pathways are to increase the atrophy process within myocytes.

The caspase system is an important regulator of apoptosis. In contrast to the rapid effects of GC on the atrophy related genes MAFbx and MURF-1, 24 hour treatment with A or B was not associated with changes in mRNA expression of Caspase-3 which is an important regulator of glucocorticoid regulated myocyte apoptosis. Studies which have shown a relationship between caspase-3 and apoptosis in skeletal muscle have involved longer periods of glucocorticoid exposure (for example 8 days rather than 24 hours) (318). As discussed in the introduction, this lack of effect of short term GC treatment on caspase-3 mRNA expression may be secondary to Caspase-3's role as an effector caspase (319)

rather than an upstream initiator caspase (caspase 8, 9, 12). Following activation and cleavage effector caspases then carry out the proteolytic events that result in cellular breakdown and demise (319), which may take a number of days of GC exposure to modify expression (caspase 8 was has been described as being increased after 8 days GC treatment in rats) (320). Further work is required to explore the role and timing of changes of initiator and effector caspases in GC mediated myopathy (321).

The insulin/ IGF-I-AI3K-Akt-mTOR signalling pathway increases protein synthesis (Section 1.5.3.6.1). Binding of insulin to its cell surface receptor leads to a conformational change and tyrosine autophosphorylation. Consequently, the insulin receptor substrate (IRS) family of adaptor proteins are recruited. Serine/threonine phosphorylation of IRS1 (in particular Ser307 phosphorylation) has been shown to negatively regulate insulin signalling through multiple mechanisms including decreased affinity for the insulin receptor and increased degradation (253, 254). The interaction of glucocorticoids and the insulin-signalling cascade has only been examined in a small number of studies that have offered variable explanations for the induction of insulin resistance (255-258). We have shown that total IRS1 protein content decreases in a dose dependent manner with increasing doses of active glucocorticoid. Furthermore, pser^{307}IRS1 was increased by corticosterone in a dose dependent manner. The combination of a decrease in IRS1 (which is known to increase muscle hypertrophy pathways and inhibit muscle atrophy pathways) and the increase in pser^{307}IRS1 (which is known to decrease insulin signalling) as well as having effects on insulin sensitivity (322) would lead to a net decrease in muscle

hypertrophy and increase in atrophy pathways. To assess the role of pre-receptor metabolism of GC by 11 β-HSD1 on the insulin/ IGF-I-AI3K-Akt-mTOR signalling pathway, day 8 C2C12 cells were treated with A, B and a combination of A and GE (a non-specific 11 β-HSD1 inhibitor). Results showed that inhibition of 11 β-HSD1 by GE lead to normalisation of IRS1 and pser^{307}IRS1 to that seen in control experiments. This shows that 11 β-HSD1 is a crucial regulator of the insulin signalling cascade which as well as controlling insulin sensitivity in skeletal muscle is a regulator of skeletal muscle hypertrophy. The alterations in the insulin signalling cascade with GC treatment and 11 β-HSD1 inhibition, in combination with the upregulation of 11 β-HSD1 in C2C12 cells with GC therapy highlight 11 β-HSD1 as a key regulator of both atrophy and hypertrophy pathways in skeletal muscle.

There are conflicting data with regard to the effect of GC treatment on myoblast proliferation rate. Some studies have reported an increase in myoblast proliferation rate with GC treatment (217, 218) (particularly with low dose GC treatment), others reporting no effect of treatment with glucocorticoids (219) and others reporting a dose dependent decrease in myoblast proliferation with glucocorticoid therapy (220). We have shown that both high dose glucocorticoid treatment ($B10^{-5}$ but not $B10^{-6/7}$) and antagonism of GRα is associated with a decrease in C2C12 proliferation rates. Therefore there seems to be a threshold effect whereby too much or too little glucocorticoid exposure is associated with decreased proliferation rates. To strengthen this argument, treatment with the inactive glucocorticoid (11-dehydrocorticosterone), did not lead to any changes in proliferation rates.

Te Pas et al. reported that GCs are capable of attenuating proliferation and differentiation of myocytes in a dose response manner by altering mRNA levels of myoD1, myf-5 and myogenin (220). When C2C12 myoblasts were incubated with dexamethasone or α-methyl-prednisolone for 9 days, the cell proliferation rate was reduced in a dose dependent manner despite increasing the mRNA expression of MyoD1 and myf-5 (220). There are some differences in the methodology of this study and our study, as in our experiments the proliferation rate of C2C12 cells was so rapid that cells need to be split every 2nd and proliferation rates were assessed only for 48 hours in order to ensure that proliferation was in the linear range [Figure 4.7(b) and 4.9 (b)].

A surprising finding was the increase proliferation rate in cells treated with the 11 β-HSD1 selective (LJ2) and non-selective (GE) inhibitors. 11 β-HSD1 is active and expressed in myoblasts, however, at significantly lower levels when compared to day 8 myotubules. The activity assays which show low levels of 11 β-HSD1 oxoreductase activity performed in Figure 3.2, Section 3.5.1 were only 20 minutes long. However, when myoblasts were incubated with radiolabelled A for 24 hours there was approximately 5% conversion to B (data not shown). Therefore, although levels are lower than in myotubules there is still some biologically activity present during prolonged incubations. H6PDH is the main regulator of NADPH levels in the endoplasmic reticulum, although there are other sources of NADPH within the ER (323). H6PDH is expressed in C2C12 myoblasts and therefore there is significant NADPH generation in the endoplasmic reticulum (ER) or sarcoplasmic reticulum (SR) in muscle. Inhibition of 11 β-HSD1 by LJ2 or GE leads to an increase of NADPH within the

endoplasmic reticulum by decreasing the use of NADPH as co-factor for 11 β-HSD1 enzyme oxoreductase activity.

Dr Gareth Lavery, from Professor Stewarts group, has previously shown that a decrease in H6PDH and NADPH generation within the sarcoplasmic reticulum in the H6PDHKO mouse is associated with a severe vacuolating myopathy and an upregulation of unfolded protein response pathway (154). Further studies, which I was involved in during my thesis, have further characterised the role of H6PDH and NADPH in the SR independent of the effects of 11 β-HSD1. The H6PDH/11 β-HSD1 double KO mouse is a phenocopy of the H6PDHKO, therefore the myopathy reported in H6PDHKO is independent of 11 β-HSD1 and glucocorticoids and is rather related to alterations in H6PDH and NADPH levels within the SR.

The potential increase in NADPH availability following inhibition of 11 β-HSD1 during proliferation may be used for other key intracellular and intra ER/SR processes. The ER has many functions including the synthesis of proteins, lipids and phospholipids that are required for the synthesis of cell membranes and a key regulator of protein folding and the unfolded protein response, all of which require a normal Redox environment. We do not have a mechanism to explain the increased proliferation with inhibition of 11 β-HSD1; one speculation is that the NADPH which is in normal circumstances used for the oxoreductase activity of 11 β-HSD1 is used in other ER/SR specific metabolism which increases proliferation rate.

In conclusion, the data presented demonstrate that increased activity and expression of 11 β-HSD1 may be involved in glucocorticoid mediated myopathy. However, this impact on atrophy markers with increasing doses of corticosterone is not due solely to the effect of corticosterone increasing 11 β-HSD1 activity and expression but also the direct effect of corticosterone itself on the GR. To clarify the potential importance of 11 β-HSD1 in glucocorticoid mediated myopathy we have also shown that when C2C12 cells are treated with the inactive steroid 11 dehydrocorticosterone (which is solely dependent on 11 β-HSD1 to activate it to corticosterone and thus have its effect on the GR) there is also a dose dependent increase in atrophy markers. 11 β-HSD1 is a crucial regulator of the insulin-signalling cascade which as well as controlling insulin sensitivity in skeletal muscle is a regulator of skeletal muscle hypertrophy. Both high dose glucocorticoid treatment and antagonism of GRα is associated with a decrease in C2C12 proliferation rates and surprisingly 11 β-HSD1 inhibition increased proliferation rate.

The above results are interesting as selective 11 β-HSD1 inhibitors are currently in development. In rodents and primates they limit local glucocorticoid availability and improve glucose tolerance, lipid profiles and insulin sensitivity (324, 325). It is interesting to speculate that 11 β-HSD1 inhibitors, particularly if they can be targeted to muscle, may also limit the severity of glucocorticoid induced myopathy, however these studies have not yet been performed.

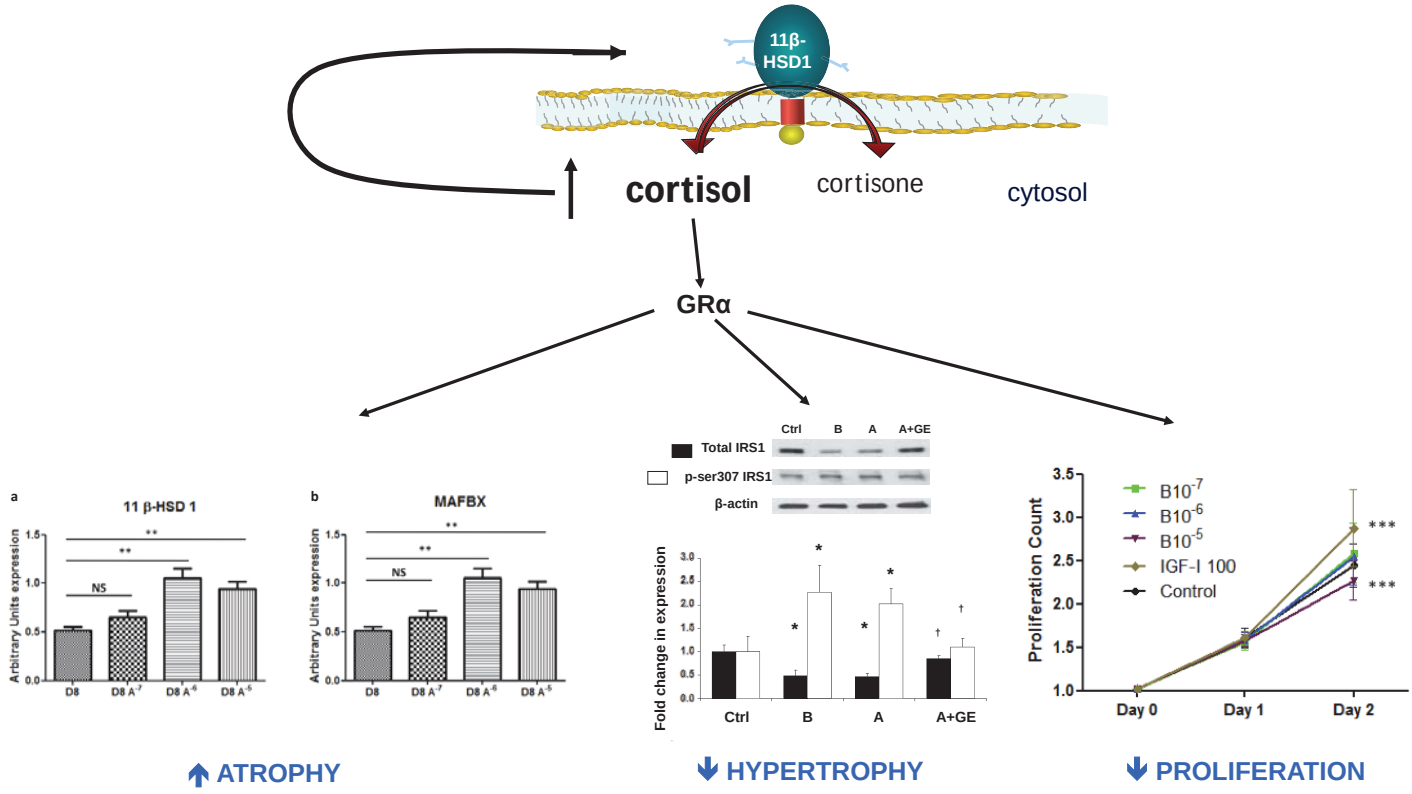

Figure 4.11. *Summary of mechanisms of GC mediated myopathy studied in this chapter and role of 11 β-HSD1 in glucocorticoid mediated myopathy via effects on atrophy, hypertrophy and proliferation. The upregulation of 11 β-HSD1 by glucocorticoids within muscle may lead to a vicious cycle whereby tissue specific increases in GC lead to further muscle atrophy.*

Chapter 5

Effect of Ageing on 11 β-HSD1 and atrophy markers in skeletal muscle

5.1. Introduction

5.1.1. Sarcopaenia

The population of the UK is increasing in age and currently people over the age of 60 consume 38% of NHS total expenditure (326). There are a number of conditions that increase in prevalence in an ageing population including cardiovascular disease, metabolic syndrome (and Type 2 diabetes mellitus), osteoporosis and sarcopaenia. Sarcopaenia is the loss of skeletal muscle mass that occurs with increasing and is associated age with a significant decrease in muscle strength. Muscle strength peaks between the 2nd and 3rd decade of life and remains the same until approximately 45-50 years. After this, strength decreases at the rate of 12-15% per decade until the 8th decade (4). Up to 24% of people aged <65 years and 50% of people aged >80 years would fulfil the criteria for sarcopaenia [an appendicular skeletal mass (muscle mass/ height^2) more than 2 standard deviations (SD) below the mean of a young reference group (18)] The functional consequences of sarcopaenia include falls, functional decline, osteoporosis, impaired thermoregulation and glucose intolerance (21-24). Falls increase with increasing age and often lead to institutional and nursing home care (327).

There are many physiological changes which occur within muscle with ageing including a decrease in muscle mass and cross-sectional area (26-28) and a decrease in Type I and II fibre number (particularly in Type II fibres) (29-31). There is also an infiltration of fat and connective tissue (32-36).

Whole muscle and individual muscle fibre atrophy is heavily implicated in the reduction in cross-sectional area with age, especially Type IIb fibres (29, 39, 56,

94, 97-99) whereas the cross-sectional area of Type I fibres, although undergoing mild atrophy, generally appears well conserved with age (29). Ageing Type I fibres are 25% smaller than that of younger individuals, but Type II fibres are typically 43% smaller than their younger counterparts (100). The reason for the sensitivity of ageing Type II fibres to atrophy compared with Type I fibres remains to be elucidated. However, there are similarities with studies reporting muscle fibre atrophy, especially Type II muscle fibres, in individuals with excess endogenous or exogenous glucocorticoid exposure (101-108).

5.1.2. Molecular mechanisms underpinning sarcopaenia

The maintenance of muscle mass depends on the balance between muscle protein synthesis via anabolic stimuli (feeding, muscle contraction, anabolic hormones) and muscle protein breakdown via catabolic stimuli (fasting, glucocorticoids, inflammatory cytokines). Where muscle protein synthesis exceeds protein breakdown, hypertrophy occurs, whereas the reverse is true for muscle atrophy. It is clear; therefore, that sarcopaenia might be associated with a decrease in anabolic stimuli, an increase in catabolic stimuli, or a combination of the two. These pathways have been discussed in detail in Section 1.3.5 and will be briefly summarised below.

One possible mechanism underpinning sarcopaenia is the decline in regenerative capacity, possibly as a consequence of a decreased number or impaired function of skeletal muscle satellite cells (57). There are conflicting data regarding satellite cell number and function in sarcopaenic muscle with some authors describing a decrease (58-60), some reporting no change, and others reporting an increase in

satellite cell number with age (61, 62). There is also some evidence to suggest that there is fibre Type specificity to the decrease in satellite cells with Type II fibres having lower satellite cell number than Type I fibres (63).

Myostatin is a member of the tumour growth factor β family and is a potent inhibitor of muscle growth, regulating satellite cell activation, myoblast proliferation and terminal differentiation. Data are conflicting data with regard to the role of myostatin in sarcopaenic muscle. Some rodent studies have shown no change in myostatin expression in young vs. old mice (73), whereas other studies have shown increased expression (74). Therefore, further work is needed to clarify the role of myostatin in sarcopaenic muscle. The calpain system has also been reported to be activated in sarcopaenic muscle suggesting an increase in calcium dependent proteolysis (57).

Elderly individuals do not demonstrate a decrease in basal muscle protein synthesis despite a reduction in muscle mass with age (77), but do show impaired muscle protein synthesis in response to amino acids, in the presence of insulin, despite demonstrating normal glucose tolerance and insulin concentrations comparable to the younger cohort (78).

Proteins scheduled for degradation in the proteasome are labelled by conjugation with ubiquitin. The 26s proteasome enzyme complex can then recognise the ubiquitin and initiate protein degradation using at least three classes of proteins. These include the E1 (ubiquitin activating enzymes), E2 (ubiquitin-conjugating enzymes) and E3 (Ubiquitin ligase). Within skeletal muscle, MAFBX and MURF-1 are two important E3 ubiquitin ligases clearly associated with many models of muscle atrophy such as sepsis (79, 80) and disuse atrophy (81). Increased

Translocation of the forkhead transcription factor (FOXO-1) into the cell nucleus increases MAFbx and MURF-1 mRNA expression (84). In ageing, MURF-1 and MAFbx-1 mRNA and protein expression in human vastus lateralis muscle is unchanged (88, 89), whilst in rodent muscle MURF-1 and MAFbx-1 mRNA expression is reported to be increased 2 to 2.5 fold (90), decreased (91), or MURF-1 expression decreases whilst MAFbx-1 expression remains unchanged (92) compared with younger control groups. The disagreement between studies is likely due to several confounding factors including the species sampled, the strains of animals, the genders and the types of muscles biopsied. Further work is required to elucidate the exact role of these above processes in muscle atrophy. The role of ubiquitin ligases in sarcopaenia have been discussed in detail in Section 1.3.5.4.

5.1.3. Endocrinology of ageing and putative role in sarcopaenia

There are a number of hormonal changes, which occur with ageing which have been implicated (by association and correlation) in the development of sarcopaenia, including a decrease in testosterone, DHEA and GH/IGF-I levels (discussed in detail in Section 1.3.6). The data regarding increased muscle strength following testosterone replacement in this cohort is conflicting (110-113). DHEAS levels also decrease with increasing age and studies replacing DHEA in an elderly cohort have not shown an increase in muscle strength (116). GH secretion declines by approximately 14% per decade (87), IGF-I is produced predominantly in the liver and in tissues such as bone under the direct influence of GH and serum IGF-I levels also fall with increasing age (119). The GH/IGF-I

axis has been implicated in sarcopaenia following a number of studies which have shown a correlation between IGF-I levels and sarcopaenia (42) and GH replacement has been associated with an increase in lean body and muscle mass (120-123). However, GH treatment in the elderly is associated with a significant side effect profile and potential morbidity; currently it is recommended not to treat or replace the GH decline of ageing (somatopause) (125).

There are contradictory data regarding the changes in plasma cortisol which occur with ageing, with a number of groups believing there are no changes (126) while others believing that plasma cortisol levels increase with ageing and in a sex specific manner (127). *Van Cauter et al.* have reported an increase in mean plasma cortisol levels of 20-50% between 20-80 years, an increase in the nocturnal nadir of cortisol and age related dampening of diurnal rhythm with an advancement of the timing of the circadian elevation (127).

5.1.4. 11β-HSD1 in muscle and ageing

Within tissues, GC levels are regulated at the pre-receptor level by isozymes of 11 β-hydroxysteroid dehydrogenase (11 β-HSD), which are located in the endoplasmic reticulum (ER). 11 β-HSD1 *in vivo* acts predominantly as an oxoreductase converting inactive cortisone (11-dehydrocorticosterone in rodents) into active cortisol (corticosterone in rodents) (2). The biological activity of glucocorticoids is dependent on their binding to the glucocorticoid receptor (GR) which is a ligand regulated nuclear receptor which binds to specific DNA sequences known as glucocorticoid response elements (GREs) in the promoter region of the target gene (131).

The role of 11 β-HSD1 in adipose tissue, liver and brain has been extensively studied (2), however the role of 11 β-HSD1 in skeletal muscle is less well-defined.

Although the effect of ageing on serum levels of cortisol is controversial there is evidence that 11β-HSD1 is elevated in a number of tissues. There is also evidence from a recent paper by *Weinstein et al*. which shows an increase in endogenous glucocorticoid concentrations and adrenal weights with increasing age in C57BL/6 mice (180). In bone, 11β-HSD1 regulates the effects of glucocorticoids upon osteoblasts (181), *Cooper et al*., within our group has shown that enzyme expression in primary cultures of human osteoblasts increases with advancing age (5). *Tiganescu et al*., from our group, has shown that 11β-HSD1 increases in skin with increasing age (6). From a functional perspective, there is evidence that 11β-HSD1KO mice are resistant to hippocampal changes associated with ageing (7). There is, however, no data to date regarding the effect of ageing on skeletal muscle 11β-HSD1.

5.2. Hypothesis

11 β-HSD1 is increased in skeletal muscle with increasing age and this is associated with sarcopaenia due elevated expression of glucocorticoid regulated atrophy genes.

5.3. Strategy of Research and Aims

3 month (young) versus 22-25 month (old) C57BL/6 mice were investigated to assess the following factors in ageing:

a. The effect on muscle strength and muscle mass.

b. The expression and activity of 11β-HSD1 in liver fat and muscle

c. Global glucocorticoid metabolism, using urinary corticosteroid GC/MS assessments.

d. Further clarification of the expression of atrophy related genes in different muscle groups (quadriceps, tibialis anterior and soleus).

Following the generation of a global 11β-HSD1 knockout (KO) mouse. 3 month (young) versus 22-25 month (old) WT and KO mice were investigated to assess the following factors:

e. The effect of 11β-HSD1 KO on muscle strength and muscle mass

f. Changes in global glucocorticoid metabolism between 11β-HSD1 KO and WT mice with increasing age using GC/MS.

g. The expression of atrophy related genes in different muscle groups (quadriceps, tibialis anterior and soleus) in the 11β-HSD1 KO compared to WT littermates.

5.4. Methods

5.4.1. RNA extraction and cDNA synthesis

Total RNA was extracted from murine tissue explants following homogenisation using TRIreagent (Sigma-Aldrich, Dorset, UK). The procedure was carried out according to protocol provided with the reagent (Sigma-Aldrich, Dorset, UK). The quantity of RNA was measured using NanoDrop ND-1000 UV-Vis Spectrophotometer (Thermofisher, Surrey, UK). The reverse transcription process was carried out using Applied Biosystems High-Capacity Reverse Transcription Kit (Applied Biosystems, Warrington, UK) For a full description of methods used see Section 2.3 and 2.4.

5.4.2. Quantitative or Real Time PCR

Quantitative PCR was carried out using Applied Biosystems Reagents and gene expression assays (AssayonDemand) (Applied Biosystems, Warrington, UK). PCRs for genes of interest and for 18s housekeeping genes were carried out in singleplex. Data are expressed as Ct values (Ct=cycle number at which logarithmic PCR plots cross a calculated threshold line) and used to determine ΔCt values (ΔCt = (Ct of the target gene) – (Ct of the housekeeping gene), lower ΔCt values reflecting higher mRNA expression. Data are expressed as arbitrary units using the following transformation [expression in arbitrary units = $1000*(2^{-\Delta Ct})$]. For a full description of methods used see Section 2.6.

5.4.3. 11 β-hydroxysteroid dehydrogenase type 1 and 2 enzyme activity assay

11 β-hydroxysteroid dehydrogenase type 1 and 2 enzyme activity assay was carried out on whole tissue explants. Fresh tissue explants were chopped to ~20mg/well and the above protocol was followed. Activity expressed as pmols of steroid converted per mg of tissue per hour (pmol/mg/h). Incubations were carried out at 37°C under a 5% CO_2 atmosphere for 20 minutes (liver) to 2 hours (muscle and adipose tissue) depending on the tissue type. For a full description of methods used see Section 2.8.

5.4.4. Rodent Models used in this chapter

All mice were group housed under controlled temperature (21-23 ^{o}C) and light (12:12 light-dark cycle; lights on at 0700h) with ad libitum access to standard rodent chow and water. Body weights were monitored weekly. Animal procedures were approved under the British Home Office Animals (Scientific Procedures) Act 1986.

5.4.4.1. Ageing mouse model

In the initial ageing mouse experiments the colony of young mice were approximately 12 weeks old and aged mice were between 22 and 26 months (all mice C57Bl\6). The time frame for old mice was determined from published data regarding age related myopathy which describes ‘old mice’ as being aged from 19 to 28 months (305-308). In our 11β-HSD1 KO model the mice strain was of mixed

background C57Bl6/129SVJ. Dr Nina Semjonous was key in the management of this colony.

5.4.4.2. Generation of targeted 11β-HSD1 knock out mouse

The 11β-HSD1 knock out mouse was developed within our group by Dr Gareth Lavery. The murine HSD11B1 gene contains 6 exons and a targeted vector to flank exon 5 (containing the catalytic domain of the enzyme) with LoxP sites. Genomic DNA from 129SvJ embryonic stem cells was used to amplify 6kb 5' and 2kb 3' homology arms, which were subsequently cloned into pBluescript SK(+) containing a thymidine kinase cassette. A loxP flanked Neomycin cassette was subcloned into a *XhoI* site 5' of exon 5 and an additional loxP site subcloned into a *PmlI* site 3' of exon 5. Following verification by DNA sequencing, the construct was linearized with BamHI and electroporated into E14TG2a mouse embryonic stem cells. Southern hybridization of Spe1 and NcoI digested genomic DNA probed with 500-bp H6PD fragments located at the 5' and 3' ends of the targeting vector respectively identified cells positive for a recombined HSD11B1 tri-loxed allele after selection in G418 and gancyclovir (see Figure 5.1.A). Three targeted embryonic stem cell clones were expanded, screened, and karyotyped to ensure correct recombination and chromosomal integrity. Two clones were injected into C57BL/6 blastocysts and chimeric mice derived from embryonic stem cell clone were mated with C57BL/6 females to achieve germ line transmission of the recombined allele. Mice heterozygous for a tri-loxed allele were crossed with the ZP3-Cre expressing strain (309) which is a powerful deleter expressing early in development and will recombine between the most distant LoxP sites with high

efficiency, thus rendering the allele null which can be passed into the next generation. Germline transmission of a disrupted allele was detected by PCR (depicted schematically in Figure 5.1). For genotyping HSD11B1 alleles the following primers were multiplexed in a standard PCR reaction: P1 5'-GGGAGCTTGCTTACAGCATC-3'; P2 5'-CATTCTCAAGGTAGATTGAACTCTG-3'; P3 5'-TCCATGCAATCAACTTCTCG-3'. PCR genotyping confirmed germline transmission of the disrupted allele, which was subsequently bred to homozygosity generating a 11β-HSD1KO. The validity of the model was assessed by demonstrating no 11β-HSD1 gene expression or enzyme activity in a number of tissues.

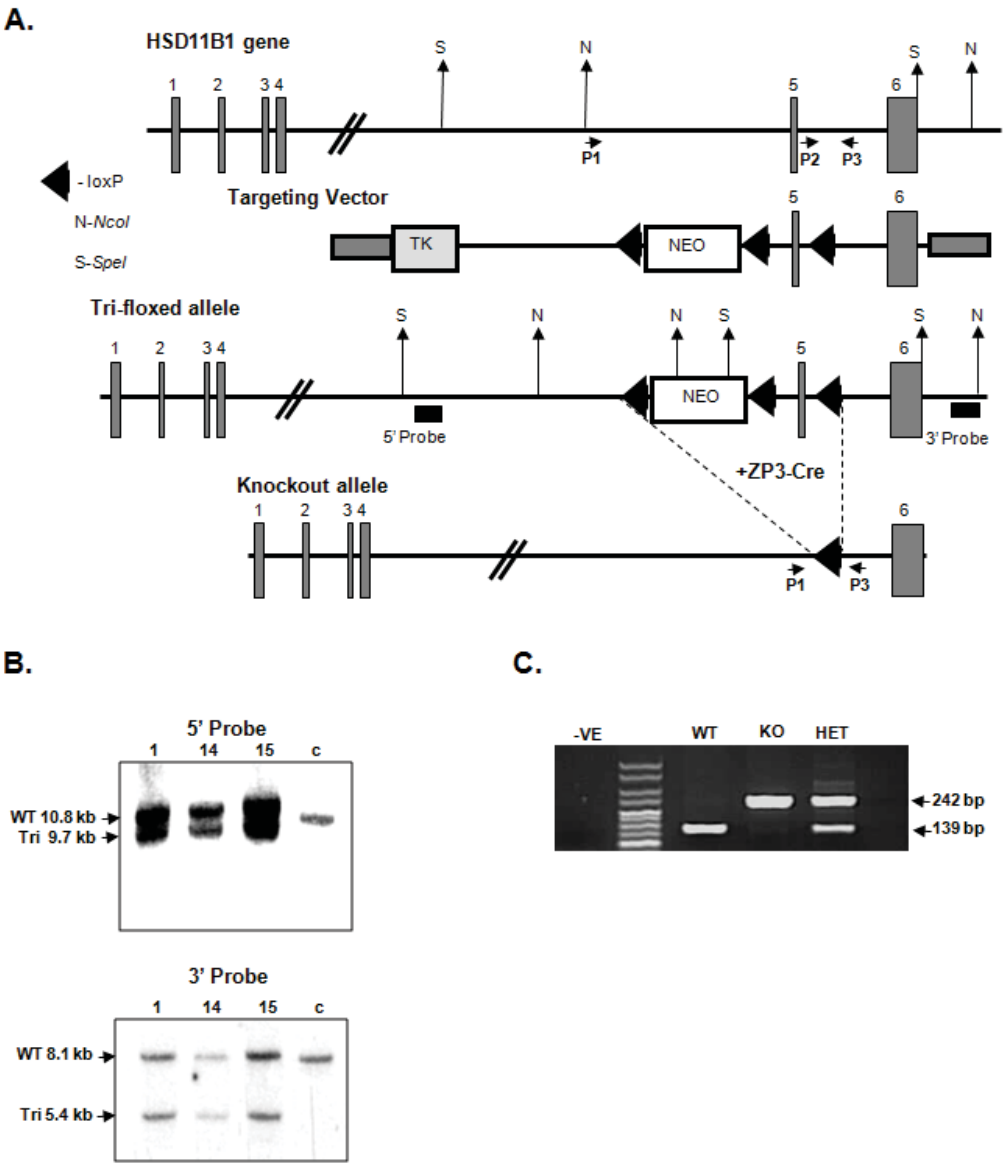

Figure 5.1. *Targeted disruption of murine HSD11B1 using the Cre-LoxP system.* ***A.*** *schematic representation of the 6 exons of the HSD11B1 gene, the targeting vector, tri-floxed recombined allele and the KO allele upon ZP3-Cre mediated recombination. The location of the 5' and 3' external probes used for Southern hybridization and PCR primers P1, P2, and P3 used for genotyping are indicated. NEO, neomycin resistance cassette; TK, thymidine kinase cassette.* ***B.*** *Successful targeting of HSD11B1 in 3 independent lines (1, 14 and 15. c-control non targeted cells) of embryonic stem cells confirmed by Southern hybridization of SpeI and NcoI digested genomic DNA. SpeI digests produced a WT fragment of 10.8kb which in the presence of the tri-floxed recombined allele produced a fragment to 9.7kb. For the NcoI digest the WT fragment is 8.1Kb and the recombined allele is5.4kb.* ***C.*** *PCR detection of knockout alleles (see material and methods for primer details). Primers P2 and P3 produce a band of 139bp representing the presence of a WT allele. Amplicons representing amplification between P1 and P3 are not detected due to the distance between these primers.*

In the KO allele a P2 binding site is removed and P1 and P3 are brought in to proximity generating a product of 242bp allowing us to detect WT, heterozygote and homozygote animals (310).

5.4.5. Mouse Muscle Strength Testing

In collaboration with Dr Nina Semjonous the Linton Grip-Strength meter (Linton Instrumentation, Norfolk, UK) was used to assess muscle performance in experimental animals (4). The Linton Grip-Strength meter reproducibly measures peak grip strength (4;5). This is a non-invasive method whereby the peak grip strength is routinely measured by holding the animal by the base of the tail and gently and gradually assessing grip strength following the animal holding onto a grasp grid which assesses force via sensors in the machine while the animal is being gently pulled in the opposite direction.

Mice will naturally reach and grasp an object if an object is brought in front of their forepaws. On each assessment, the mouse will be removed from their housing and lowered into the apparatus so that it grasps the grip grid, one with each paw, with its back legs standing on the smooth floor of the apparatus. The mouse will then be held by the base of the tail and pulled gently in a rearward direction. The applied force at which the mouse releases the cage with each paw was measured by the strain gauges. To measure combined strength in all four limbs, the mouse was allowed to grasp the grid with fore and hind limbs and then held by the base of the tail and pulled gently in a rearward direction.

5.4.6. Gas Chromatography/ Mass spectrometry for corticosteroid metabolites in mouse urine

GC/MS urinary steroid analysis was carried out by Beverley Hughes at the Institute for Biomedical Research, Centre for Endocrinology, Diabetes and Metabolism (CEDAM), University of Birmingham. The GC/MS was based on the method described by *Palermo et al.* (311) and *Shackleton et al.* (328). Quantitative data on excretion of individual steroids for murine studies individual mouse urine was collected on filter paper and processed.

GC/MS was carried out using a Hewlett Packard 5970 mass spectometer and 15m fused-silica capillary column, 0.25mmID, 0.25μm film thickness (J&B Scientific, Folsom CA, USA) using 2μl of sample. Steroids were quantified by comparing individual peak area to the peak area of the internal standards, for cortisol fragment 605m/z compared to 609 m/z and for cortisone fragment 531 m/z compared to 534 m/z. The relative peak area was calculated and the metabolite concentration expressed as μg/24hr. A quality control (QC) was analysed with each batch. The intra and inter-assay co-efficient of variance was <10%. For full description of principles of GC/MS and methods see Section 2.15.

5.4.7. Statistical methods

Statistical analysis was performed using Prism for Windows version 5.0 (GraphPad Software Inc, San Diego, CA, USA) software packages. Continuous data were summarised using means and standard deviations (or standard error of mean) if parametrically distributed or medians and inter-quartile ranges if non-parametrically distributed. Parametric data was compared using a paired t-test

and non-parametric data was analysed using a Mann-Whitney test. Multiple comparisons were assessed using one-way analysis of variance (ANOVA), with Kruskal-Wallis for non-parametric data and Dunn's multiple comparison test. The level for statistical significance was $p<0.05$.

5.5. Results

5.5.1. Body weight increases with age in wild type C57Bl\6 mice

The total body weight of WT mice was measured on a weekly basis while on normal chow diet. There was a gradual increase in weight during ageing.

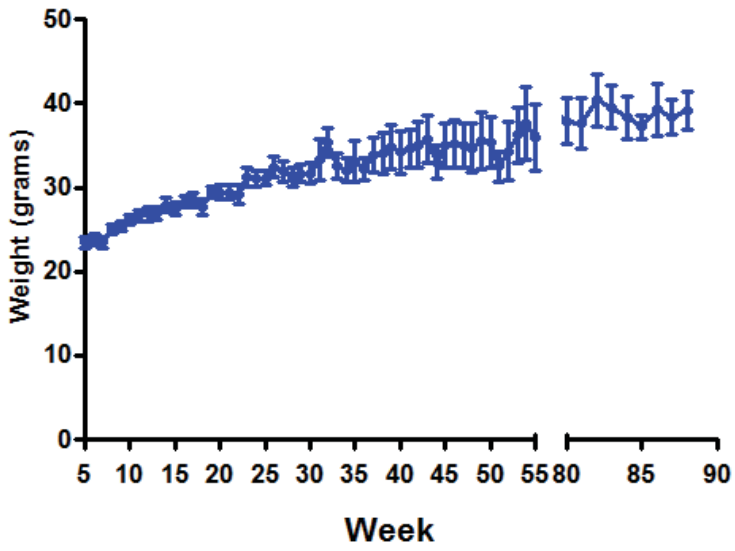

Figure 5.2. *The total body weight of WT mice was measured on a weekly basis while on normal chow diet (n=8-10).*

5.5.2. Muscle strength in young vs. old (wild type) C57BL6 muscle

Muscle strength was assessed in young and old C5&BL/6 mice using a Linton Grip-Strength meter (Linton Instrumentation, Norfolk, UK). Young mice had significantly greater strength (gram grip/ gram body weight) than older mice indicating that the model used did induce functional muscle weakness (Figure 5.3).

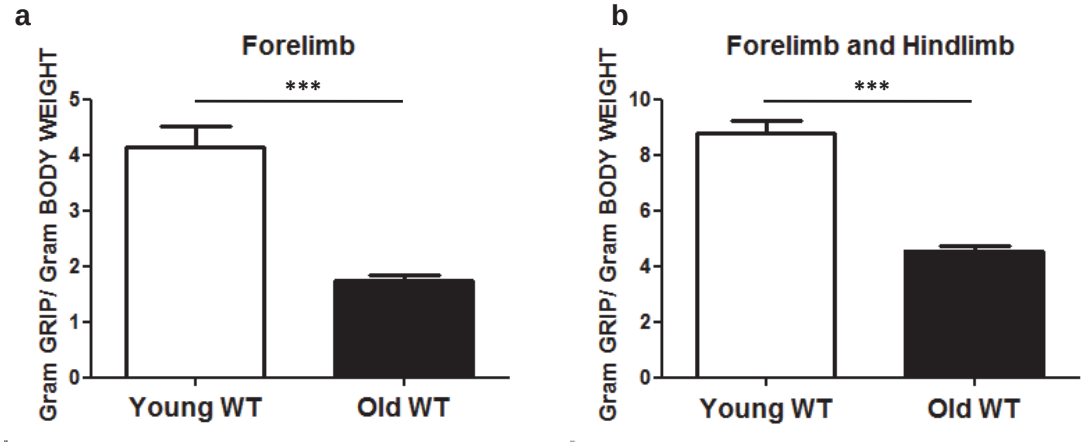

Figure 5.3. *Measurement of mouse forelimb (a) and combined forelimb and hindlimb (b) muscle strength using Linton Grip-Strength meter (Linton Instrumentation, Norfolk, UK). p ***<0.0001, n = 8-10 in each group. WT = wild type. Data shown are the mean±SE. Old mice had significantly lower muscle strength indicating a functional muscle decline with ageing.*

5.5.3. Tissue weights in young versus old wild type mice

The weight of individual muscle groups was assessed to examine differences in tissue weights with increasing age. Despite this significant decrease in strength with increasing age there was no decrease in total muscle mass with age (Figure 5.4 a+b). This may be due to the increased accumulation and infiltration of intramuscular adipose or connective tissue reported previously (32-36). There was increased liver and adipose tissue weight with increasing age. However,

when tissue weights were adjusted for individual animal total body weight, there was a decrease in quadriceps, tibialis anterior, soleus and adrenal gland, an increase in weight of gonadal adipose tissue but no change in adjusted liver weight. Therefore the increase in total body weight with age (Figure 5.4 c) is predominantly secondary to increased adipose tissue depot weight.

a

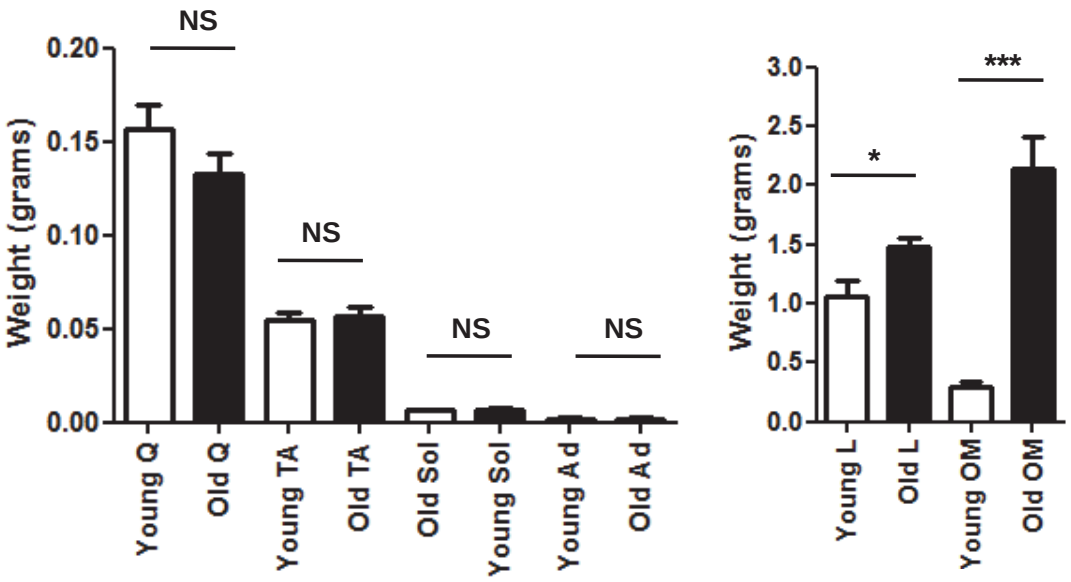

b

	Quad	TA	Soleus	Adrenal		Liver	Omental Fat
Young	0.156 ± 0.01	0.055 ± 0.004	0.0066 ± 0.0005	0.0022 ± 0.0001		1.06 ± 0.13	0.298 ± 0.04
Old	0.133 ± 0.01	0.057 ± 0.004	0.0069 ± 0.0002	0.0021 ± 0.00024		1.49 ± 0.07 *	2.147 ± 0.26 ***

c

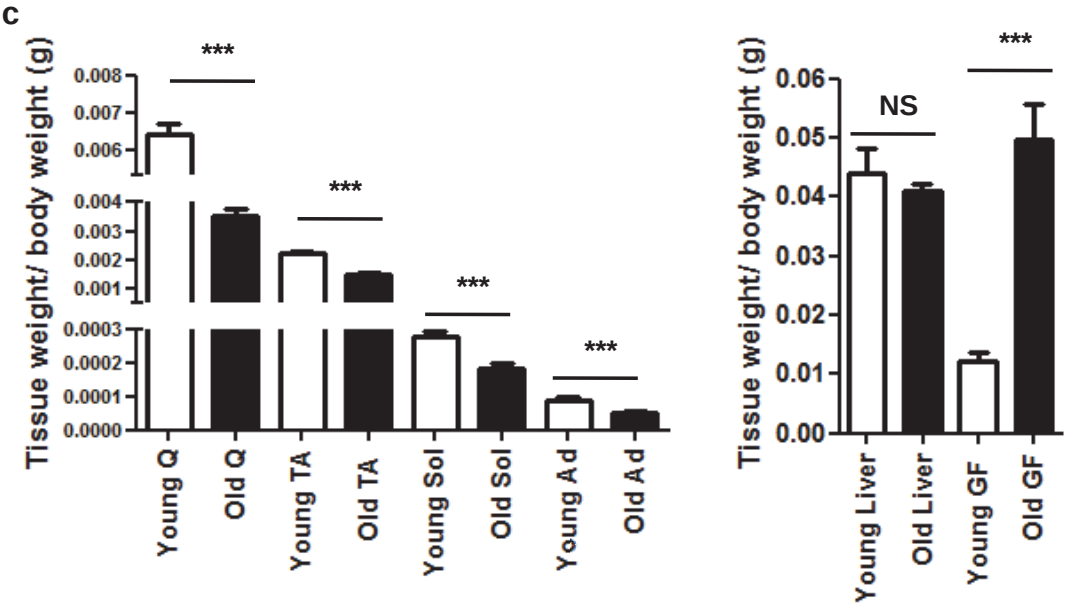

Figure 5.4. *The weight (grams) of key tissues in young versus old mice (and b) (n= 8-10 in each group). Tissues included quadriceps (Q), tibialis anterior (TA), soleus (Sol), adrenal (Ad), liver and gonadal fat (OM). Tissue weights were then normalised to individual total body weights (c). p *<0.05, p ** <0.001, p ** <0.0001, p NS = non significant. Data shown are the mean±SE.*

5.5.4. Urinary GC/MS of corticosteroid metabolites in young vs. old C57BL6 wild type

The overall glucocorticoid exposure in mice was assessed via measurement of GC/MS of urinary corticosteroid metabolites. There was no difference between the % A (11-dehydrocorticosterone) metabolites in mouse urine with ageing. As corticosterone (B) is metabolised by 11 β-HSD2 to 11-dehydrocorticosterone (A) in the kidney, % A metabolites were used as a surrogate for overall circulating B concentrations. The reason for using % A metabolites rather than serum corticosterone is due to the large variation in ELISA based measurements of corticosterone and the relatively low numbers of animals available for analysis due to our breeding scheme.

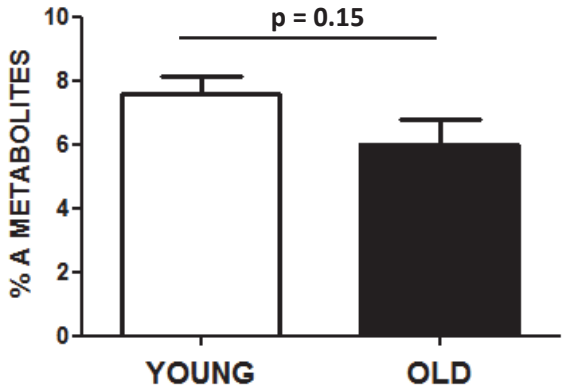

Figure 5.5. *Urinary steroid metabolite assessment with % A metabolites revealed no difference between young and old mice), (n=8). Data shown are the mean±SE.*

5.5.5. 11 β-HSD 1 mRNA expression in young vs. old C57BL6 WT muscle

11 β-HSD 1 mRNA expression was assessed in explants of young (12 weeks) and old (90-112 weeks) C57BL/6 mice quadriceps, tibialis anterior and soleus, liver and gonadal fat. Increased 11 β-HSD 1 expression was seen in quadriceps, tibialis anterior, soleus and adipose tissue but not liver (Figure 5.6).

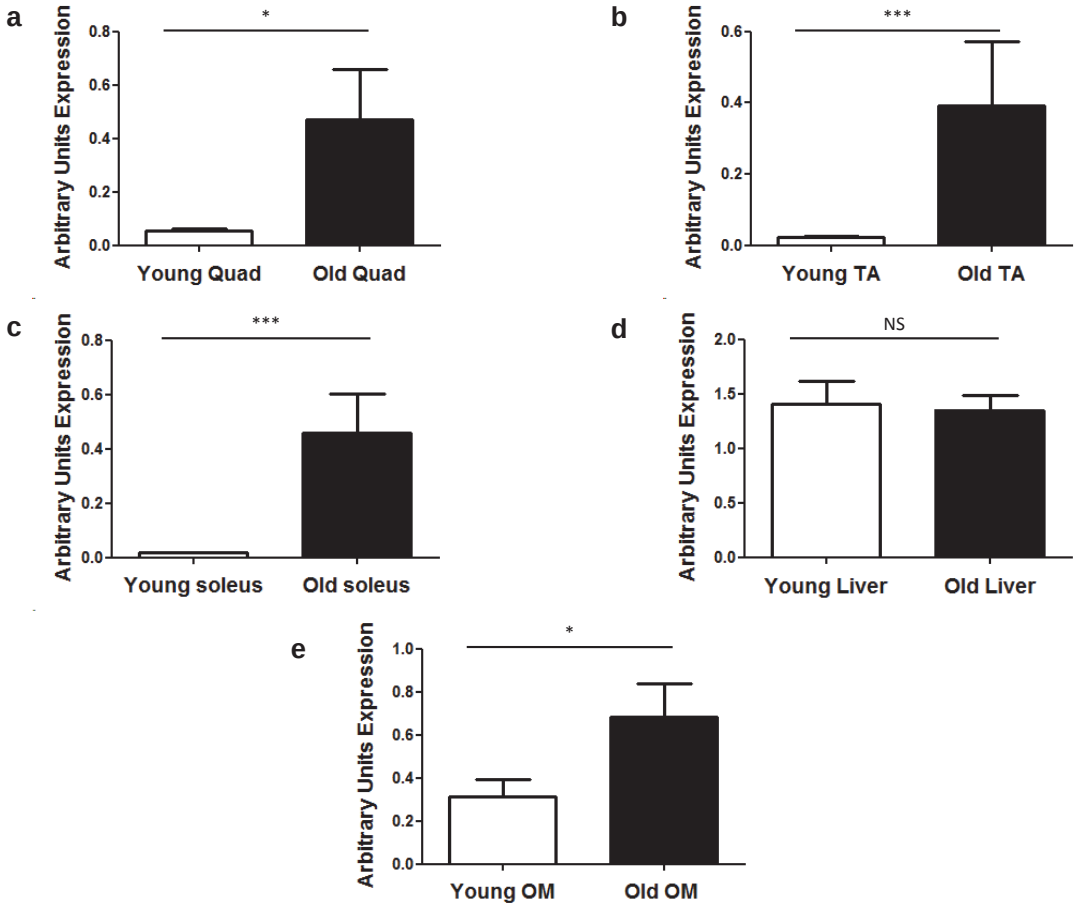

Figure 5.6. *Measurement of 11 β-HSD1 mRNA expression in explants of young compared to old tissue (n=4-5, young 12 weeks, old 90-112 weeks). Tissues included quadriceps (quad) (a), tibialis anterior (TA) (b), soleus (Sol) (c), liver (d) and gonadal fat (OM) (e). p *<0.05, p ***<0.0001, p NS = non significant. Data shown are the mean±SE.*

5.5.6. 11 β-HSD 1 oxoreductase activity in young vs. old C57BL6 WT muscle

11 β-HSD 1 oxoreductase activity assays were performed on explants of young (12 weeks) and old (90-112 weeks) C57BL/6 mice quadriceps, tibialis anterior, soleus, liver and gonadal fat. Results revealed increased 11 β-HSD 1 activity in quadriceps, soleus, liver and gonadal fat but not tibialis anterior (Figure 5.7). This would suggest that there is increased tissue specific activation of glucocorticoids [11-dehydrocorticosterone (A) to corticosterone (B)] within certain tissues with ageing.

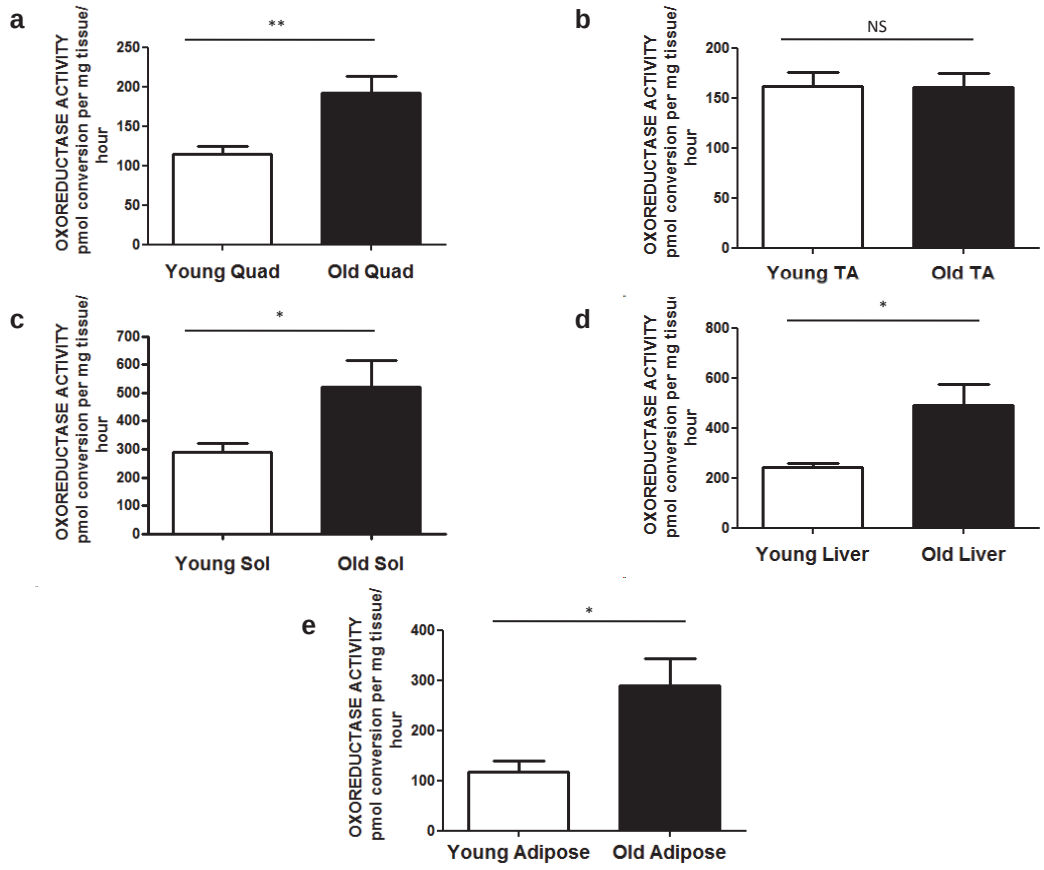

Figure 5.7. *Measurement of 11 β-HSD1 oxoreductase activity in explants of young compared to old tissue (n=4-5, young 12 weeks, old 90-112 weeks). Tissues included quadriceps (quad)(a), tibialis anterior (TA)(b), soleus (Sol)(c), liver (d) and gonadal fat (adipose)(e). p *<0.05, p ** <0.001, p NS = non significant. Data shown are the mean±SE.*

5.5.7. mRNA expression of atrophy genes in young vs. old C57BL6 wild type muscle

The mRNA expression of key glucocorticoid regulated atrophy genes were determined in young compared to old WT mice. Three different muscle groups (quadriceps, tibialis anterior and soleus) were used to assess the mRNA expression of atrophy genes in mixed fibre muscle, type II fibre rich muscle and type I fibre rich, respectively.

5.5.7.1. mRNA expression of MURF-1 and MAFbx in 3 different skeletal muscle depots in young compared to old animals

There was an increase in MURF-1 and MAFbx mRNA expression (key glucocorticoid regulated genes) in quadriceps and tibialis anterior but no change in the Type I fibre rich soleus (the most glucocorticoid resistant muscle type) (Figure 5.8). These results highlight the importance of assessing different muscle groups when assessing the role of specific genes associated with sarcopaenia and glucocorticoid mediated myopathy.

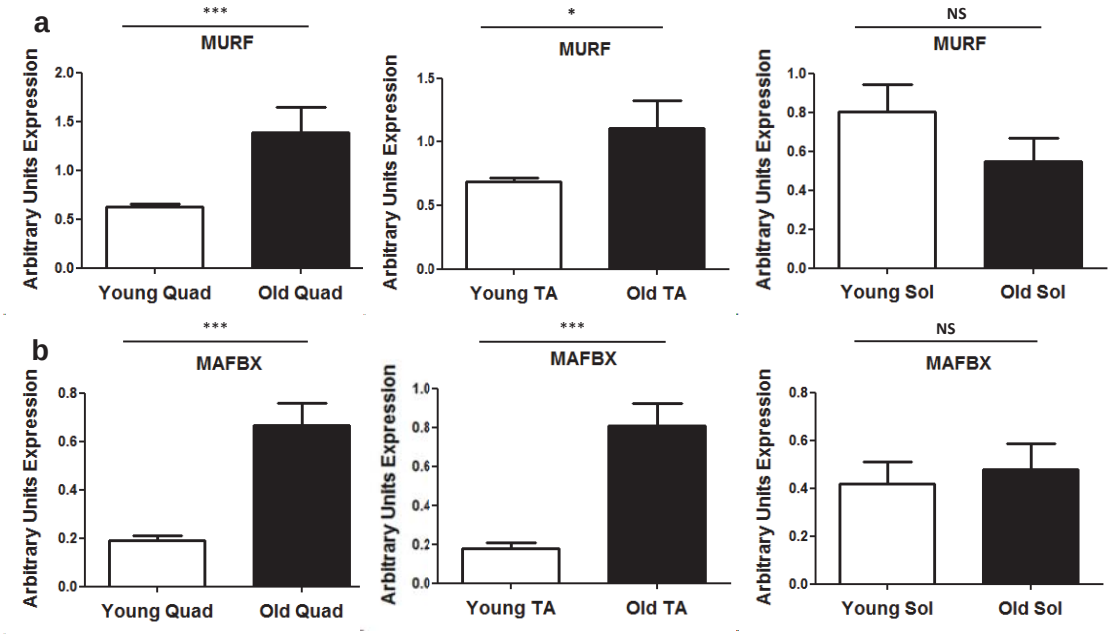

Figure 5.8. *mRNA expression of MURF-1 (a) and MAFbx (b) in 3 different skeletal muscle depots [quadriceps (Quad) representing a mixture of fibre types, tibialis anterior (TA) representing Type II fibres and soleus (Sol) representing Type I fibres]. p *<0.05, p ** <0.001, p ***<0.0001, p NS = non significant, n=4-5. Data shown are the mean±SE.*

5.5.7.2. mRNA expression of FOXO1 and FOXO3 in 3 different skeletal muscle depots in young compared to old animals

There was no change in mRNA expression of FOXO1 (a) and FOXO3 (b) in 3 different skeletal muscle depots with increasing age (Figure 5.9). This is not surprising as both FOXO 1 and 3 are heavily dependent on changes in phosphorylation for activity. Increased MAFbx and MURF-1 mRNA expression are both associated with translocation of the forkhead transcription factor (FOXO-1) into the cell nucleus (84). Phosphorylation of FOXO-1 by Akt sequesters FOXO-1 from the cell nucleus to the cytoplasm by 14-3-3 proteins (85) preventing MAFbx and MURF-1 upregulation. However, GCs dephosphorylate FOXO-1 allowing subsequent translocation to the cell nucleus.

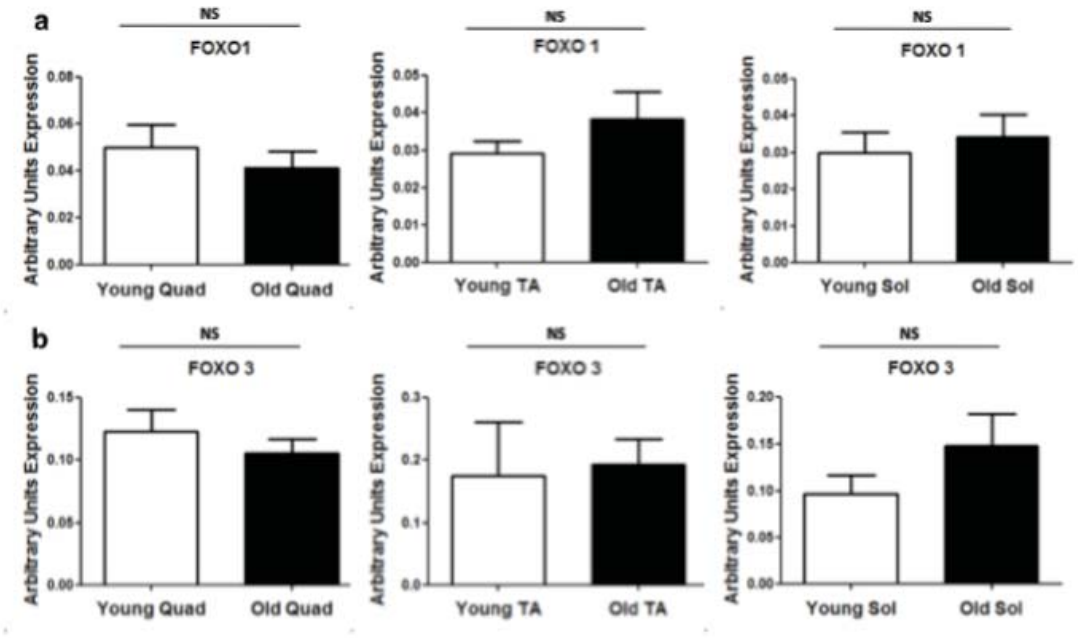

Figure 5.9. *mRNA expression of FOXO1 (a) and FOXO 3 (b) in 3 different skeletal muscle depots [quadriceps (Quad) representing a mixture of fibre types, tibialis anterior (TA) representing Type II fibres and soleus (Sol) representing Type I fibres]. p NS = non significant, n=4-5. Data shown are the mean±SE.*

5.5.7.3. mRNA expression of myogenic factor V and myostatin in 3 different skeletal muscle depots in young compared to old animals

Myogenic factor V (myf5) is a key regulator of myocyte differentiation (Section 1.2.1) and myostatin is a potent inhibitor of muscle myocyte proliferation and differentiation (Section 1.3.5.2). There was an age related decrease in myogenic factor V mRNA expression in all 3 muscle groups (Figure 5.10). There was an age related decrease in myostatin mRNA expression in tibialis anterior and soleus but no significant decrease in quadriceps (Figure 5.10). This decrease in myostatin may be a compensatory mechanism in ageing muscle.

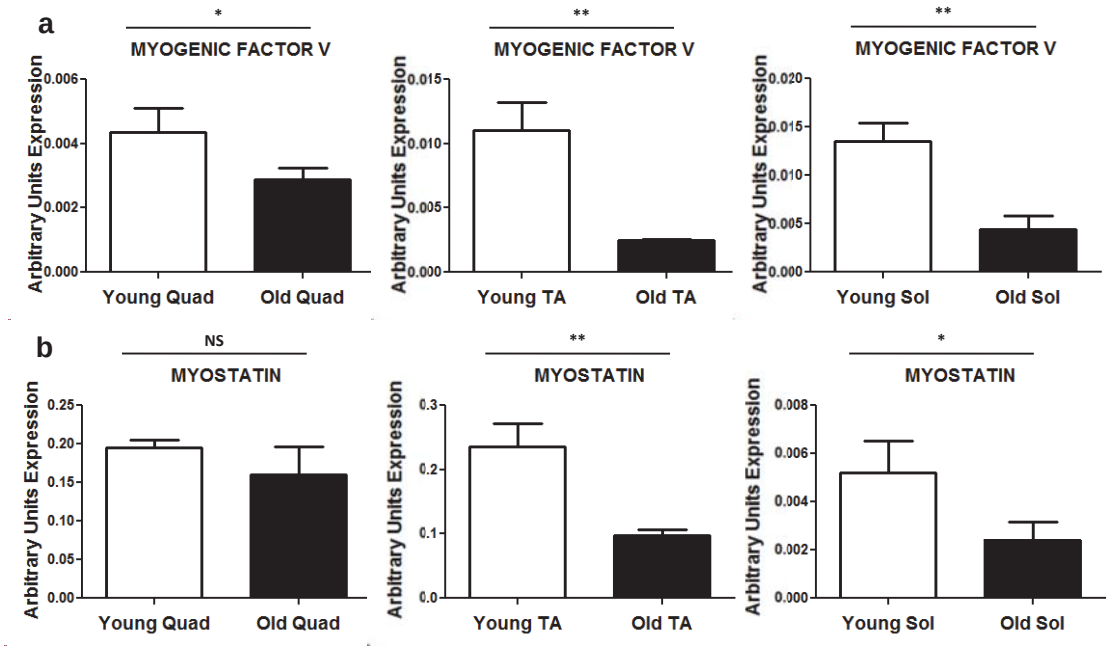

Figure 5.10. *mRNA expression of myogenic factor V (a) and myostatin (a) in 3 different skeletal muscle depots [quadriceps (Quad) representing a mixture of fibre types, tibialis anterior (TA) representing Type II fibres and soleus (Sol) representing Type I fibres]. p *<0.05, p ** <0.001, p ***<0.0001, p NS = non significant, n=4-5. Data shown are the mean±SE.*

5.5.7.4. mRNA expression of PPAR δ and MAO in 3 different skeletal muscle depots in young compared to old animals

Activation of PPARδ has been previously shown to induce a switch to increased formation of Type I fibres (329). Monoamine oxidase is a key mitochondrial enzyme which metabolises catecholamines and has been reported to be elevated in GC mediated myopathy (Section 1.5.3.9). There was a decrease in PPARδ mRNA expression in quadriceps muscle but not in tibialis anterior or soleus (Figure 5.11). There was an age related increase in monoamine oxidase mRNA expression in all 3 muscle groups (Figure 5.11).

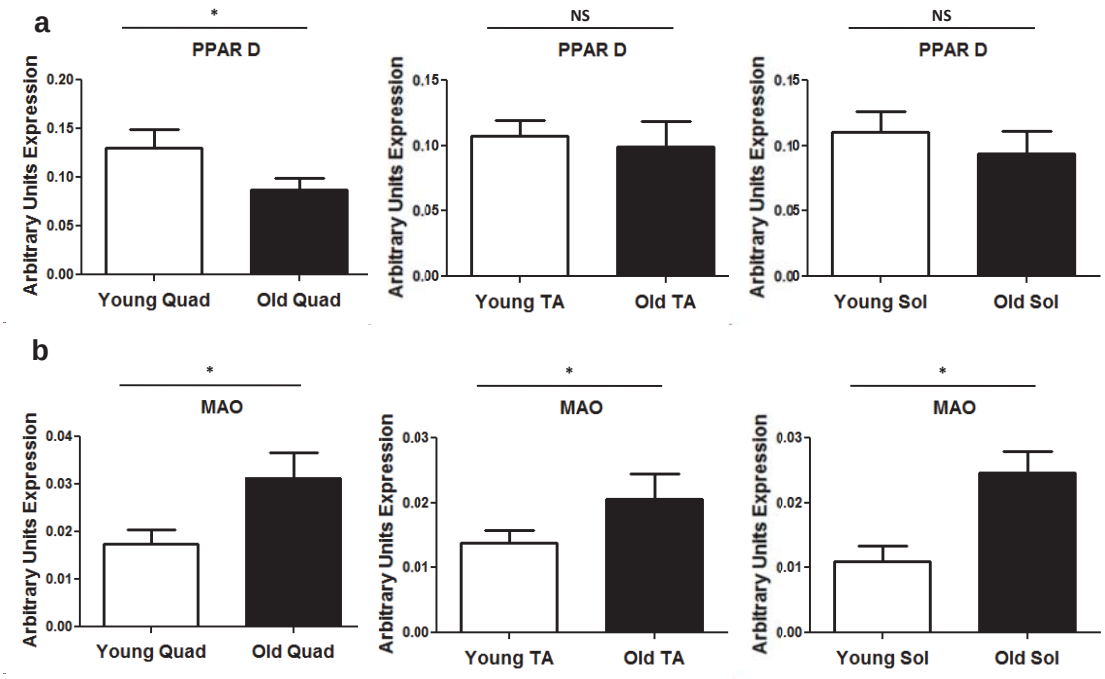

Figure 5.11. *mRNA expression of PPAR δ (a) and MAO (b) in 3 different skeletal muscle depots [quadriceps (Quad) representing a mixture of fibre types, tibialis anterior (TA) representing Type II fibres and soleus (Sol) representing Type I fibres]. p *<0.05, p ** <0.001, p ***<0.0001, p NS = non significant, n=4-5. Data shown are the mean±SE.*

5.5.7.5. mRNA expression of calpain, cathepsin 1 and D in 3 different skeletal muscle depots in young compared to old animals

The atrophy pathways include the lysosomal proteases (eg. Cathepsins), the calcium dependent proteases (Calpain family). There was an age related decrease in calpain mRNA expression in the quadriceps muscle and increase in the soleus muscle, but no change in the tibialis anterior (Figure 5.12). There was an age related increase in cathepsin 1 mRNA expression in the quadriceps and soleus muscles, but no change in the tibialis anterior (Figure 5.12). There was no change in mRNA expression of cathepsin D in any muscle groups with increasing age (Figure 5.12).

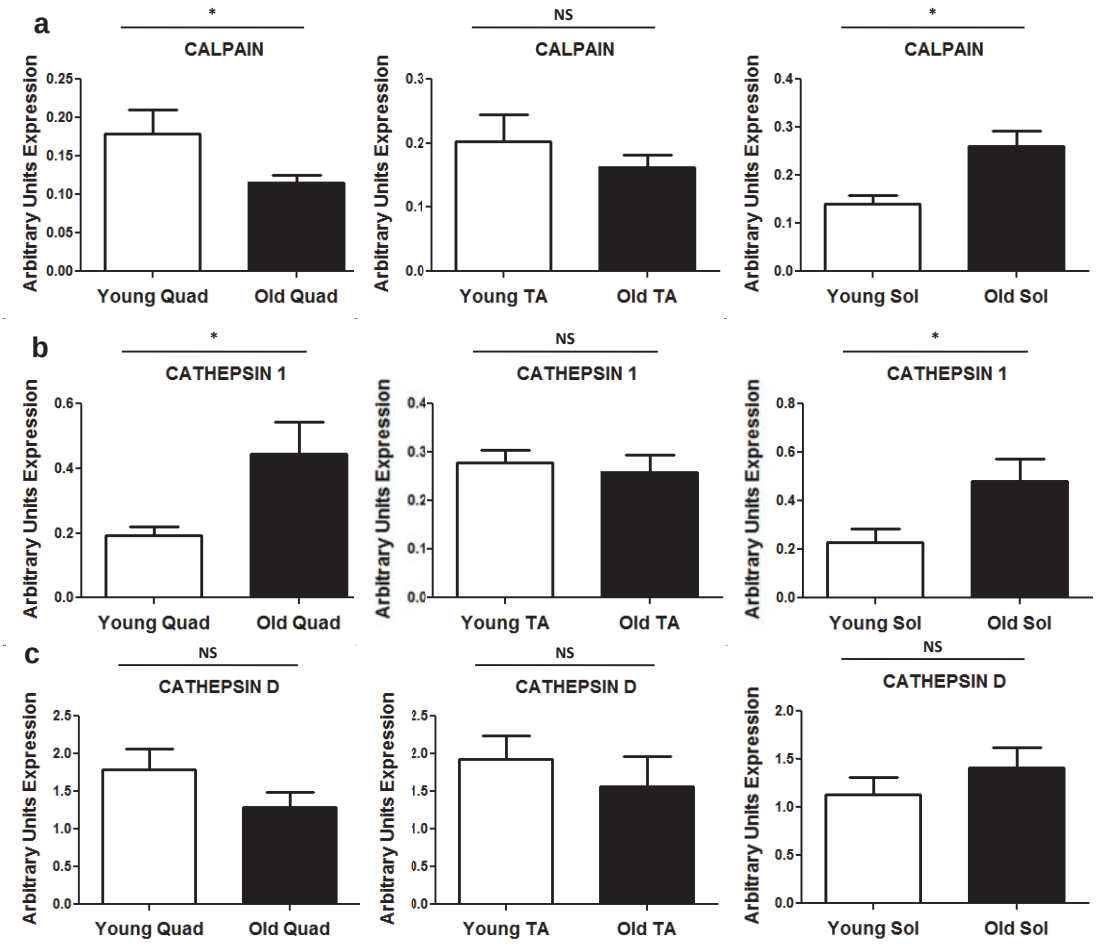

Figure 5.12. *mRNA expression of calpain (a) and cathepsin I (b) and D (c) in 3 different skeletal muscle depots [quadriceps (Quad) representing a mixture of fibre types, tibialis anterior (TA) representing Type II fibres and soleus (Sol) representing Type I fibres]. p *<0.05, p ** <0.001, p ***<0.0001, p NS = non significant, n=4-5. Data shown are the mean±SE.*

Effect of increasing age on mRNA expression	Quadriceps	Tibialis Anterior	Soleus
↑	MURF MAFBx Cathepsin 1 MAO	MURF MAFBx MAO	Calpain Cathepsin 1 MAO
↓	Calpain Myogenic factor V	Myogenic factor V Myostatin	Myogenic factor V Myostatin
↔	FOXO1 FOXO3 Myostatin Cathepsin D PPARD	FOXO1 FOXO3 Cathepsin 1 Cathepsin D PPARD	MURF MAFBx FOXO1 FOXO3 Cathepsin D PPARD

Table 5.1. *Summary of changes in expression of atrophy and hypertrophy related genes in different muscle groups of young compared with old muscle revealing different patterns of mRNA expression changes depending on fibre type preponderance.*

5.6. Studies on the global 11 β-HSD1 KO mouse

Through the use of transgenic rodent models it has been shown that elevated 11 β-HSD1 expression and activity, either globally or in a tissue specific manner, is associated with the development of cognitive impairment (174), the metabolic syndrome (175) and insulin resistance (176), which is due to increased intracellular glucocorticoid action.

Conversely, knockout animals or pharmacological inhibition of 11 β-HSD1 reveal improved insulin sensitivity and resistance to diet induced obesity (177). Much less is known about the role of 11 β-HSD1 in skeletal muscle and the consequences of local production of GCs. Transgenic mice with a null HSD11B1 gene have previously been generated by *Kotelevtsev et al.* (159). In homozygous mutant mice, hepatic 11 β-HSD1 activity was less than 5% that of wild type. When WT and KO mice were adrenalectomised and implanted with pellets of 11 dehydrocorticosterone (A) the WT mice converted A to B whereas B levels in the KO mice remained undetectable. This demonstrated that 11 β-HSD1 is the only 11 oxo-reductase (in the mouse) able to generate active GC from inert 11 keto-steroids. 11 β-HSD1KO mice have adrenal hyperplasia due to reduced negative feedback on the HPA axis causing increased ACTH-stimulated corticosterone secretion and zona fasciculata hypertrophy (159). There was no reported change in 11 β-HSD2 activity or expression in this model (159).

There have not been any studies to date assessing the effect of 11 β-HSD1KO on muscle function or ageing. Of particularly interest, is whether a lifetime of decreased intra-muscular glucocorticoid generation in 11 β-HSD1 KO mice would

impact on the muscle function in a cohort of old C57BL6/129CVJ 11 β-HSD1KO mice when compared to WT littermates.

5.6.1. 11 β-HSD 1 activity in C57BL6 Wild type vs 11 β-HSD 1 KO muscle

11 β-HSD1 oxoreductase activity was assessed in a number of tissues and was abolished in 11 β-HSDKO mice (Figure 5.13).

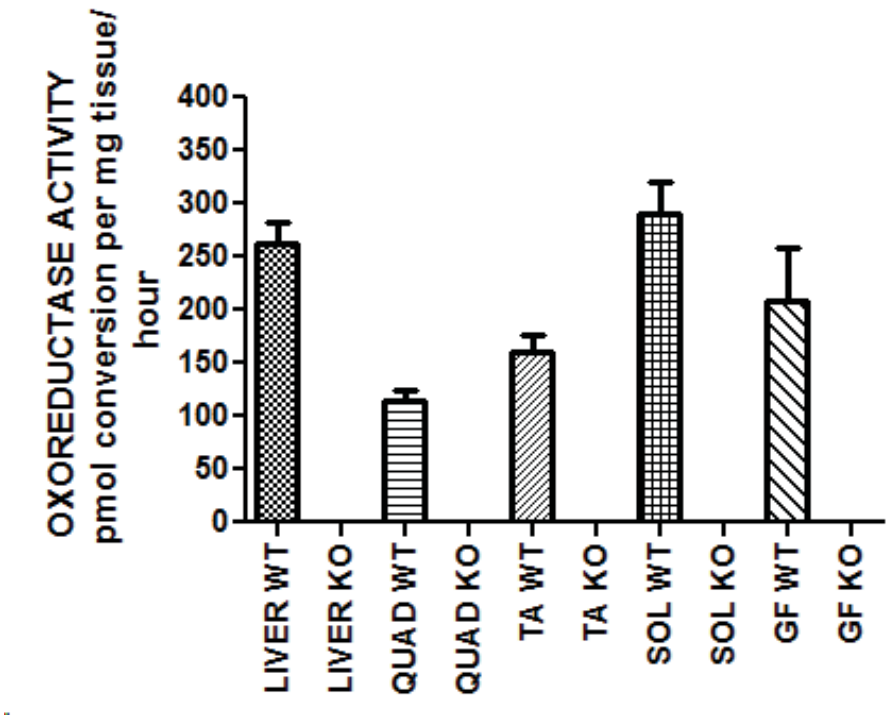

Figure 5.13. *11 β-HSD1 oxoreductase activity was assessed in liver, quadriceps (QUAD), tibialis anterior (TA), soleus (Sol) and gonadal fat (GF) and was abolished in 11 β-HSDKO mice, compared to WT. (WT = wild type, KO = knock out). Data shown are the mean±SE.*

5.6.2. Effect of global 11 β-HSD1 knockout on total body weight with increasing age on normal chow diet.

The total body weight of WT and 11 β-HSD1 KO mice was measured on a weekly basis while on normal chow diet. There was no difference in body weight between WT and 11 β-HSD1 KO mice (Figure 5.14).

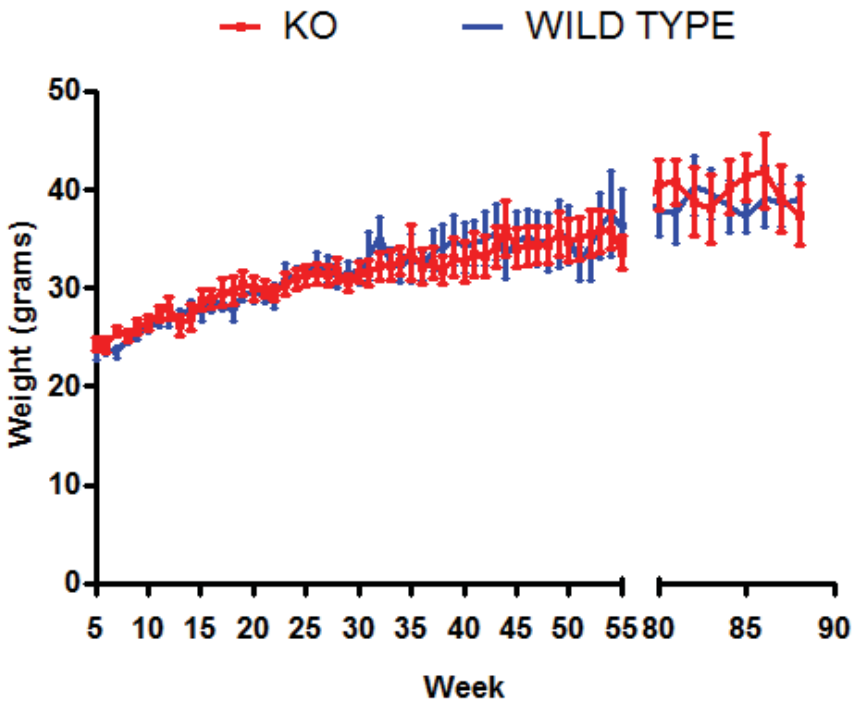

Figure 5.14. *Total body weights during ageing of WT compared to 11 β-HSD1 KO mice (n = 8-10 in each group). There was no difference in body weight between WT and 11 β-HSD1 KO mice with increasing age, fed with ad libitum normal chow diet. Data shown are the mean±SE.*

5.6.3. Effect of global 11 β-HSD1KO on tissue weights with increasing age.

The weight of individual muscle groups and liver, fat and adrenals were assessed to examine differences in tissue weights between young and old WT and 11 β-HSD1KO. There was an increase in quadriceps and adrenal weight (in grams) in the old 11 β-HSD1KO compared to WT(Figure 5.15.a). However, when this was adjusted for body weight there was only an increase in the adrenal weight in the old 11 β-HSD1KO which would be in keeping with the hypothalamic-pituitary-adrenal axis activation previously reported in 11 β-HSD1KO mice (159, 330) (Figure 5.15.b). There was a 45.5% increase in adrenal size between young KO and WT and 52.4% between old KO and WT.

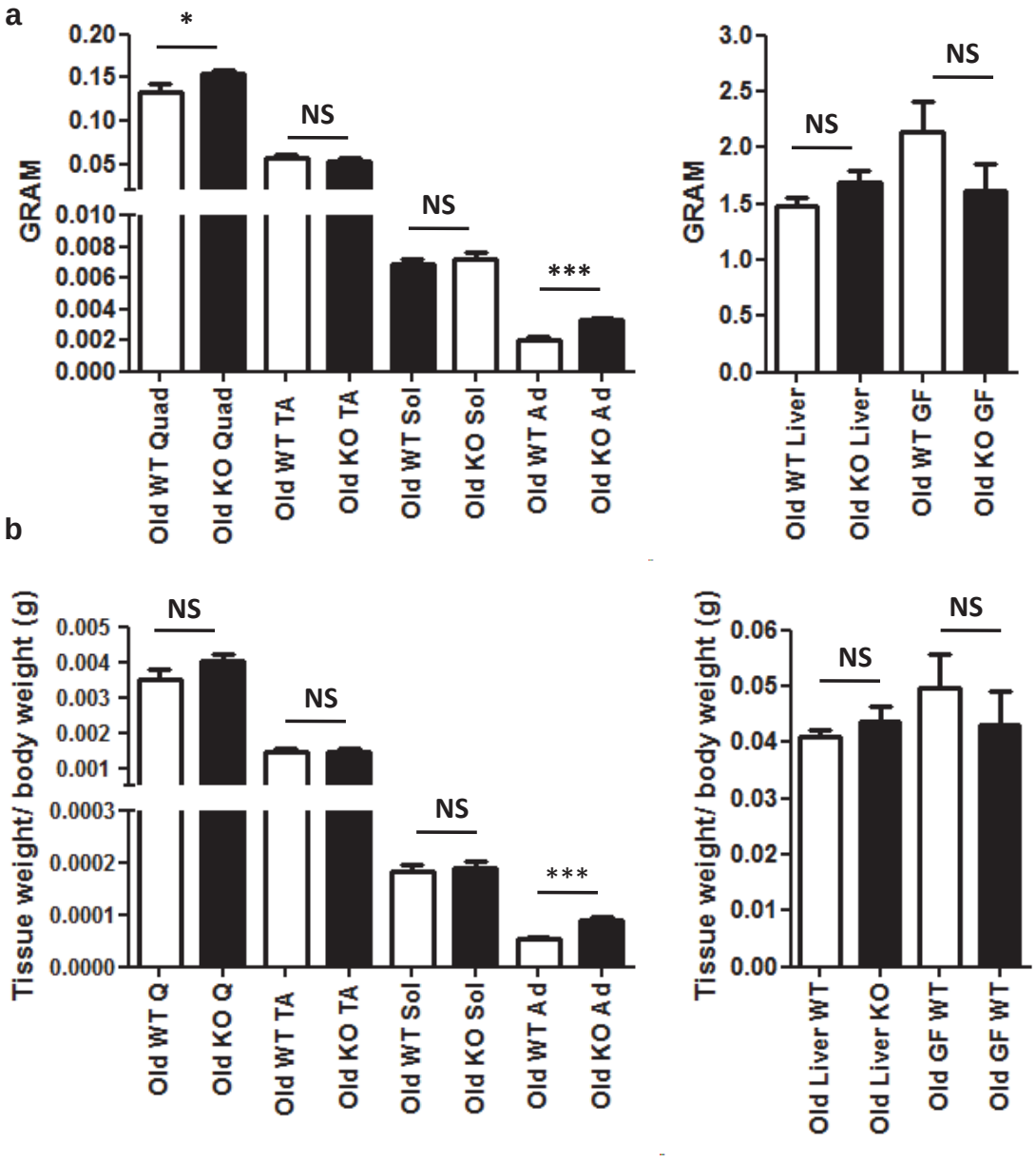

Figure 5.15. *The weight of key tissues in WT compared to* 11 β-HSD1KO *littermates and the effect of increasing age (n-8-10 in each group). Tissues included quadriceps (Quad), tibialis anterior (TA), soleus (Sol), adrenal (Ad), liver and gonadal fat (GF). p *<0.05, p ** <0.001, p ***<0.0001, p NS = non significant, n=8-9 per group. Data shown are the mean±SE. There was an increase in quadriceps and adrenal weight in the 11 β-HSD1KO mice with increasing age compared to wild type but no difference in TA or soleus (Figure 5.16.a). However, when tissue weights were adjusted for total body weight, only the adrenal weight was heavier (Figyre 5.15.b). This significant increase in adrenal size in keeping with adrenal hypertrophy/ hyperplasia secondary to stimulation of the hypothalamic pituitary axis in the* 11 β-HSD1KO *mice.*

5.6.4. Muscle strength in young vs. old C57BL6 wild type muscle WT compared to 11 β-HSD1KO

Muscle strength in young compared to old mice in both the WT and 11 β-HSD1KO mice was assessed using a Linton Grip-Strength meter (Linton Instrumentation, Norfolk, UK). Young mice had significantly greater strength (gram grip/ gram body weight) than older mice in both WT and 11 β-HSD1KO mice indicating that the ageing model used did induce functional muscle weakness but there was no difference between WT and 11 β-HSD1KO mice (Figure 5.16).

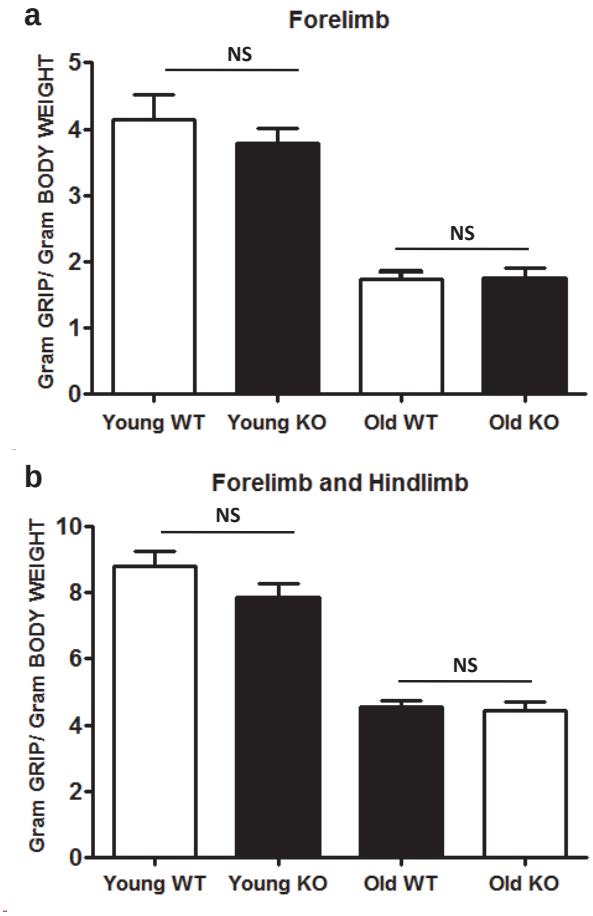

Figure 5.16. *Measurement of mouse forelimb (a) and combined forelimb and hindlimb (b) muscle strength using Linton Grip-Strength meter (Linton Instrumentation, Norfolk, UK). p ***<0.0001, n = 8-10 in each group. WT = wild type. Data shown are the mean±SE. Old mice had significantly lower muscle strength than younger mice indicating a functional muscle decline with ageing. However, there was no difference in muscle strength in old WT vs 11 β-HSD1KO.*

5.6.5. Urinary GC/MS of corticosteroid metabolites in young vs. old C57BL6 wild type compared to 11 β-HSD1KO

The overall glucocorticoid exposure in mice was assessed via measurement of GC/MS of urinary corticosteroid metabolites. There was no difference between the % A (11-dehydrocorticosterone) metabolites in WT mouse urine with ageing. There was, however, a significant increase in % A metabolites in young 11 β-HSD1KO compared to WT (Figure 5.17). This increase was also present in old 11 β-HSD1KO compared to WT, and the % A metabolites increased significantly in young compared to old 11 β-HSD1KO which could be explained by increased 11 β-HSD2 conversion of B to A from increased levels of B produced by activation of the HPA axis (in keeping with increased adrenal size in 11 β-HSD1KO).

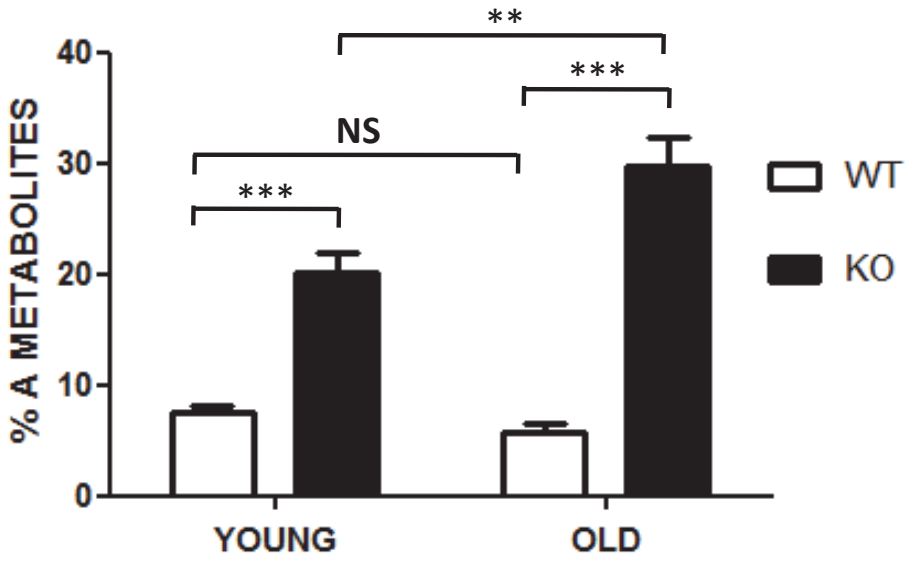

Figure 5.17. *Urinary steroid metabolite assessment with % A metabolites. Data shown are the mean±SE.*

5.6.6. Markers of glucocorticoid mediated myopathy in the muscle of old 11 β-HSD1KO compared to WT littermates.

In order to assess the effect of 11 β-HSD1KO on key regulators of glucocorticoid mediated myopathy, we compared the tibialis anterior (Type IIb fibre rich) and soleus (Type I fibre rich) muscles in old 11 β-HSD1KO compared to WT littermates. These muscles groups were chosen as we have shown in Table 5.1 that different muscle groups have different patterns of gene response to ageing, in particular we wanted to see if there was a difference in the markers of atrophy in tibialis anterior, which is predominantly a Type IIb fibre rich muscle which are known to be sensitive to glucocorticoid mediated myopathy and soleus, which is a Type I fibre rich muscle which is resistant to GC mediated myopathy.

The reduction in 11 β-HSD1 within tissues lead to a different pattern of response in TA compared to soleus for MAFbx, myogenic factor V (Myf5) and monoamine oxidase (Figure 5.18), however no difference was found in calpain-2 and caspase 3 (Figure 5.19).

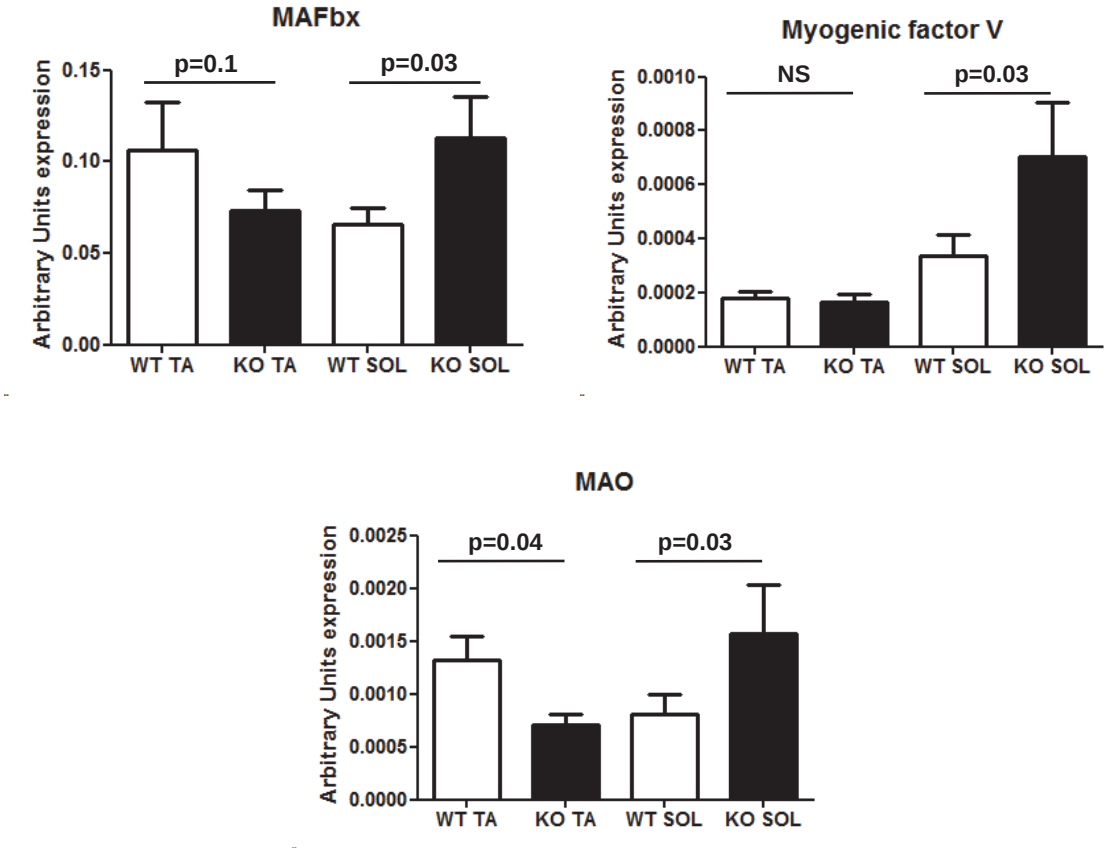

Figure 5.18. *mRNA expression of MAFbx, myogenic factor V and monoamine oxidase in old WT compared to 11 β-HSD1KO, tibialis anterior (TA) representing Type IIb fibres and soleus (Sol) representing Type I fibres. (n=5) Data shown are the mean±SE.*

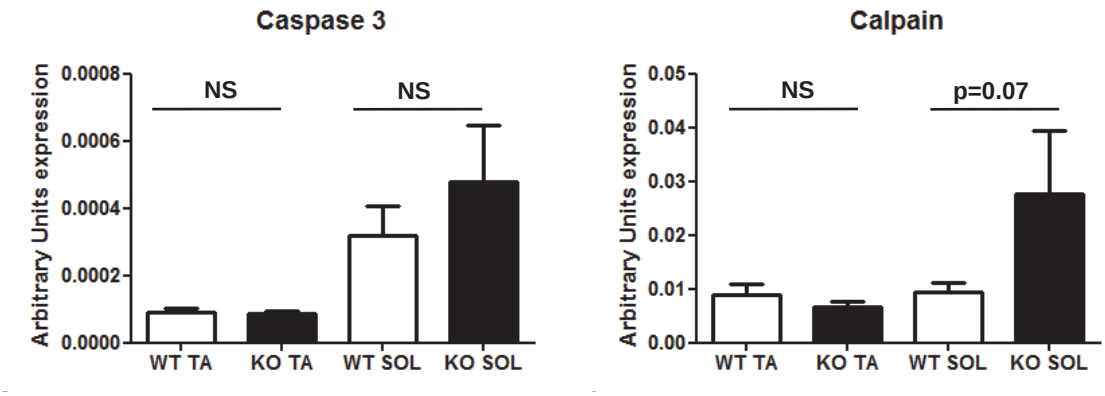

Figure 5.19. *mRNA expression of caspase 3 and calpain in old WT compared to 11 β-HSD1KO, tibialis anterior (TA) representing Type IIb fibres and soleus (Sol) representing Type I fibres. (n=5) Data shown are the mean±SE.*

There is evidence in the 11 β-HSD1KO mouse of improvement in atrophy related markers in the tibialis anterior with decreased levels of expression of MAO and a trend to decrease in MAFbx. There is evidence in the soleus muscle of the 11 β-HSD1KO of increased atrophy related genes including MAFbx, MAO and a trend to an increase in calpain. There is also some evidence of increased markers of myogenesis with increased expression of myogenic factor V.

5.7. Discussion

We have shown in a murine model of sarcopaenia (characterised by decreased muscle strength and individual muscle weight) that 11 β-HSD1 activity and mRNA expression increases in some, but not all, tissues with ageing. This increase in 11 β-HSD1 oxoreductase activity is associated with an increase in active glucocorticoid at a cellular level. In ageing muscle there are several structural, histological and molecular changes that are similar to those reported in GC mediated myopathy and the increased intracellular GC availability secondary to 11 β-HSD1 may play a role in the phenotype of ageing muscle.

In all rodent models of ageing and in particular those related to sarcopaenia there are a number of confounders. The mice were fed normal chow diet and weight increased equally between WT and KO animals with ageing thus allowing us to see any effects specifically of 11 β-HSD1 KO. To ensure weight was not a factor when measuring strength and tissue weights the values were reported as a factor of total body weight. We had not considered subnormal chow diets and due to technical constraints with regard to feeding this may not have been possible. The ideal study to ensure that weight was not a factor in changes reported in atrophy genes with ageing would be to ensure that there was no weight gain during aging however this was not possible in our studies due to technical constraints such as lack of ability to regulate food intake and measurement of energy homeostasis.

There are several variables, which could not be controlled in our cohort due to technical limitations [particularly at a metabolic level, for example activity levels (key in sarcopaenia as inactivity increases the severity of sarcopaenia), dietary

intake, differing insulin sensitivity within individual animals with increasing age]. Therefore, these results must be interpreted with full appreciation of these limitations.

The results in this chapter show that sarcopaenic changes in a murine model of ageing are associated with the upregulation of key glucocorticoid mediated atrophy genes, but importantly, the changes reported depend on the muscle group sampled (Table 5.1). Muscle fibres can be divided into a number of subgroups including slow twitch oxidative (Type I fibres), fast twitch oxidative (Type IIa fibres) and fast twitch glycolytic (Type IIx or IIb) (Table 1.1). In sarcopaenia, muscle fibre atrophy is heavily implicated in the reduction in cross-sectional area with age. Type IIb fibres are particularly susceptible (29, 39, 56, 94, 97-99) whereas the cross-sectional area of Type I fibres, although undergoing mild atrophy, generally appears well conserved with age (29). The reason for the sensitivity of ageing Type II fibres to atrophy and the resistance of Type I fibres remains to be elucidated. We have shown muscle group specific changes in atrophy markers with increasing age. Of particular interest are the changes in mRNA expression of atrophy related genes in the soleus muscle (a Type I fibre rich muscle, which is resistant to both sarcopaenia and GC mediated myopathy). Genes that were not upregulated in soleus muscle (but which were elevated in other muscle groups) during ageing included MURF-1 and MAFbx.

As discussed in detail in Section 1.3.5.4, within skeletal muscle, MAFbx and MURF-1 are two important E3 ubiquitin ligases clearly associated with many models of muscle atrophy such as sepsis (79, 80) and disuse atrophy (81). Increased MAFbx and MURF-1 mRNA expression are both associated with

translocation of the forkhead transcription factor (FOXO-1) into the cell nucleus (84). Phosphorylation of FOXO-1 by Akt sequesters FOXO-1 from the cell nucleus to the cytoplasm by 14-3-3 proteins (85) preventing MAFbx and MURF-1 upregulation. A recent study which assessed atrogin-1 (MAFbx) and MURF-1 in the soleus and extensor digitorum longus of middle aged (11-13 months) and old age mice (25-27 months old) has reported that there is no change in MAFbx and MURF-1 mRNA expression, with increasing age (331). This is in agreement with our data with regard to soleus but the lack of changes in MAFbx and MURF-1 in the EDL (predominantly a Type II fibre muscle), would not be in agreement with our data which revealed an upregulation of both MAFbx and MURF-1 in quadriceps and tibialis anterior. One possible explanation for this is that *Gaugler et al.* compared middle aged mice (11-13 months) to older mice, whereas we assessed younger mice (12 weeks) which may have lead to a greater distinction between young and old quadriceps and tibialis anterior muscle. Importantly, in the FOXO1 transgenic mouse the upregulation of FOXO1 (and as a result MURF-1 and MAFbx) within muscle is associated with downregulation of expression of several genes associated with structural proteins of Type I muscle, a marked reduction in size of both Type I and II fibres and a significant decrease in the number of Type I fibres in the skeletal muscle of FOXO1 transgenic mice. Therefore, in our results the failure of soleus muscle MURF-1 and MAFbx to increase with increasing age may explain why the Type I fibre rich soleus muscle is more resistant to sarcopaenia. There may also be a possible link to FOXO, with regard to why soleus muscle is more resistant to GC mediated myopathy as Type I fibres have the ability to shift fuel utilisation. In both slow and fast twitch skeletal muscles, GCs activate FOXO-1 and FOXO-3a, but the targets of these

transcription factors may change in a fibre specific manner. In Type I (243) and Type II fibres, activation of FOXO-1 and FOXO-3a leads to the transcription of the atrophy genes.

There was no difference in total body weight in the 11 β-HSD1KO mouse compared to young or old WT littermates, however this was on a normal chow diet and previous models have shown a resistance to weight gain (particularly visceral) in 11 β-HSD1KO mice on high fat diets compared to WT littermates (332). There was no difference in muscle weights or muscle strength in the 11 β-HSD1KO mouse compared to young or old WT littermates. However, there was an increase in adrenal weight and % A metabolites in the 11 β-HSD1KO mouse compared to WT littermates (both in young and old), which would be indicative of an activation of the HPA axis, which is in keeping with previously published 11 β-HSD1KO mouse data (159, 330).

There is evidence in the 11 β-HSD1KO mouse of improvement in atrophy related markers in the tibialis anterior with decreased levels of expression of MAO and a trend to decrease expression of MAFbx. This may be interpreted as the decrease in locally generated cortisol leading to decreased GC mediated myopathy in these usually GC sensitive muscle fibres. There is also evidence in the soleus muscle of the 11 β-HSD1KO of increased atrophy related genes including MAFbx, MAO and a trend to an increase in caplain. Type I fibres are GC resistant and the decrease in locally generated GC in the 11 β-HSD1KO appears to have a detrimental effect. Therefore, the local generation of active glucocorticoids by 11 β-HSD1, rather than causing atrophy as in Type IIb fibres may be required for the health of Type I fibres. One possible mechanism is the activity of hormone

sensitive lipase (333) which metabolises triglycerides, the main source of fuel in Type I fibres, is dependent on glucocorticoids, however further work is required to examine this relationship. Within the soleus of 11 β-HSD1KO mice, there is also some evidence of increased markers of myogenesis with increased expression of myogenic factor V that may be interpreted as a compensatory mechanism for increased atrophy.

Importantly, the local decrease in GC may be offset by increases in circulating GC. 11 β-HSD1KO have been previously reported to have elevated corticosterone levels, an exaggerated corticosterone response to restraint stress, with a delayed fall after stress and a decrease sensitivity to exogenous cortisol suppression of the HPA axis, suggesting diminished glucocorticoid feedback (330). In humans with mutations in the 11 β-HSD1 or H6PDH gene [cortisone reductase deficiency (334) and apparent cortisone reductase deficiency (335)] there is also evidence of HPA axis activation, patients have hyperandrogenism due to the effect of increased ACTH drive on adrenal androgens.

It should be noted that previous studies of 11 β-HSD1KO have only assessed the effect of this decrease in intracellular GC exposure in young animals and have not assessed this in older animals that have had longer exposure to elevated circulating corticosterone levels and HPA activation. Another factor, which must be taken into account when interpreting our data and that of previous 11 β-HSD1KO is the effect of the mouse strain on HPA axis activation in 11 β-HSD1KO models. Mice bred on a MF1/129 background had an increase in plasma corticosterone nadir and extended corticosterone peak, leading to increased corticosterone secretion over 24 hours in 11 β-HSD1KO compared to

WT (159, 330, 336). There have been conflicting results in mice developed on a C57BL/6 background, with studies showing no change in plasma corticosterone nadir or diurnal rhythm values between WT and 11 β-HSD1KO (337). Whereas another 11 β-HSD1KO developed on a C57Bl6/ CBA/C3H background reported an increased nadir plasma corticosterone and an altered diurnal rhythm of corticosterone (338). It should be pointed out that all 11 β-HSD1KO models have an increase in adrenal gland weight, but again there is a difference in magnitude of weight increase depending on strain with MF1/129 increasing by 70% (159), C57Bl6 increasing by 20% (337) and C57Bl6/ CBA/C3H increasing by 36% (338). It is not clear if these changes are related to adrenal gland hyperplasia (159) or hypertrophy (338) or a combination as both have been described. In our model (using C57Bl6/129SVJ) we found a 45.5% increase in adrenal size between young KO and WT and 52.4% between old KO and WT.

Therefore, although there was a tissue specific decrease in GC exposure due to absent 11 β-HSD1 oxoreductase activity in the KO mouse there was an increase in circulating GC concentrations as a compensatory mechanism. This increase in circulating GC, but decrease in tissue specific generation of GC, may have resulted in similar GC tissue exposure as WT mice and thus may explain the lack of muscle phenotype in ageing mice. Therefore, to further assess the role of 11 β-HSD1 in skeletal muscle the optimum approach may be a muscle specific 11 β-HSD1KO, which may not lead to activation of the HPA and therefore allow us to elucidate the role of decreased tissue specific glucocorticoid exposure with ageing.

Chapter 6

The modulation of corticosteroid metabolism by hydrocortisone therapy in hypopituitarism

6.1. Introduction

Patients with pituitary hormone deficiency (hypopituitarism) have increased morbidity and mortality (339), however, the exact mechanisms underpinning this have not been fully elucidated. There are a number of possible factors, including metabolic and body composition changes in patients who have GH and ACTH deficiency and the relative impact of pharmacological therapies of these deficiencies.

The studies of cardiovascular risk in hypopituitarism have either been cross-sectional studies comparing patients on conventional replacement (but not GH) to control subjects or interventional studies primarily examining the impact of GH replacement therapy. Patients on conventional replacement therapy for hypopituitarism exhibit abnormalities of protein, fat and carbohydrate metabolism, which contributes to the abnormal body composition observed (reduced lean mass and increased fat mass). There is a propensity to central obesity and intra-abdominal or visceral fat deposition is significantly increased compared to control subjects with similar BMI (340, 341). Visceral adiposity is associated, in the general population, with the metabolic syndrome: insulin resistance or diabetes mellitus, hypercholesterolaemia and hypertension (342, 343).

6.1.1. Abnormalities associated with increased morbidity in patients with hypopituitarism.

There are a number of abnormalities associated with increased morbidity in patients with hypopituitarism including insulin resistance, lipid abnormalities, endothelial dysfunction and alterations in fibrinolysis. Although blood glucose and

plasma insulin levels are similar to those seen in controls, patients treated for pituitary disease have been shown to be insulin resistant (344). In some hypopituitary cohorts, patients have adverse fasting lipid profiles and body composition including low HDL cholesterol, increased triglycerides and decreased LDL particle size, increased BMI (up to 32% being clinical obese BMI>30kg/m^2) and waist circumference (345-349). Importantly, in the large cohort studies characterizing metabolic phenotype, interpretation of the data is hampered by lack of age, sex and demographically matched controls. The serum lipid profile is abnormal in patients on conventional pituitary hormone replacement, with elevated total and low density lipoprotein (LDL) cholesterol and triglyceride levels (345, 350-355), HDL levels are either unchanged (352, 355) or decreased (351, 353, 354) in hypopituitarism. The data regarding the prevalence of hypertension in patients with hypopituitarism compared to the general population is conflicting but it is unlikely to play a major role in vascular morbidity in hypopituitarism (353, 356-362).

Carotid intima media thickness (IMT) which is a predictor of myocardial infarction and cerebrovascular accident in adults aged over 65 years (363) is significantly increased in adults with hypopituitarism compared with age matched controls (348, 364, 365). Impaired endothelial function promotes adhesion of leukocytes to the endothelium which migrate through it and produce an inflammatory response (366). Serum levels of C-reactive protein (CRP), interleukin-6 (IL-6) and tumour necrosis factor-α (TNF-α) are increased in patients with hypopituitarism (367-369).

Fibrinolytic activity is an important contributor to cardiovascular risk; reduced activity is associated with venous thromboembolic disease, stroke and ischaemic heart disease. One of the major regulators of the fibrinolytic system is plasminogen activator inhibitor-1 (PAI-1) which regulates, through inhibition, tissue plasminogen activator (tPA) (370). In the fibrinolytic system PAI-1 levels (which inhibits tissue plasminogen activator) are elevated in patients with hypopituitarism (371-374). *Devin et al.* demonstrated that the 24-hour fibrinolytic profile was abnormal in hypopituitarism reporting a 62% increase in PAI-1 antigen levels ($p<0.05$) and a 24% reduction in tPA levels ($p=0.003$). In addition the normal circadian rhythm of PAI-1 was lost (371). Thus hypopituitarism treated with conventional replacement therapy (but not GH) is a pro-thrombotic state, which may contribute to the increased cardiovascular mortality observed, and this has been shown to be improved by GH replacement therapy in some studies (372, 374).

6.1.2. GH deficiency and treatment

There is now a substantial body of evidence indicating that GH replacement therapy has a beneficial effect upon many of the parameters outlined above. Body composition improves consistently with growth hormone replacement. Lean mass increases and fat mass decreases significantly, particularly central adiposity with GH treatment (341, 346, 375, 376). The fasting lipid profile improves with reductions in total and LDL cholesterol and an improvement in the total: HDL cholesterol ratio (346, 351, 352, 377, 378).

Growth hormone treatment in hypopituitary adults also impacts upon endothelial function, the inflammatory process and fibrinolytic profile. The markers of inflammation, CRP, IL-6 and TNF-α also fall during GH replacement therapy (379, 380). Measurement of the carotid IMT also demonstrates a significant improvement during GH therapy (364, 365, 381). Although these studies have been of relatively short duration one study compared the outcome of patients after ten years of treatment and demonstrated that the beneficial changes in lipid profile, body composition and carotid IMT were sustained over that period (382).

These changes all reflect beneficial effects on recognized markers of cardiovascular risk. However GH replacement produces changes in some parameters, which may have an adverse effect upon cardiovascular outcome. Although GH replacement therapy results in a reduction of central fat mass, insulin resistance is increased. In one study of 90 patients there was an increase in glycosylated haemoglobin levels from 4.9% ± 0.05 to 5.07% ± 0.06 ($p<0.001$). Plasma glucose levels rose from 4.72mmol/L ± 0.06 to 5.15mmol/L ± 0.07 ($p<0.001$). These changes were evident after six months of treatment and were sustained for two years (383). Lipoprotein (a) is an independent marker of cardiovascular risk, which increases significantly during GH replacement (384-386).

6.1.3. ACTH deficiency and glucocorticoid replacement

Traditionally the daily dose of hydrocortisone was 30mg per day split into two doses (two thirds in the morning and one third in the evening). However, cortisol production rates in normal subjects are considerably less than those defined from

isotope studies in the 1960's-1970's. *Esteban et al.* and *Kelly et al.* have shown that the normal cortisol production rate in young adults is between 5.7mg/m^2/day (approximately 9.9mg/day) and 5.7 $\pm$ 0.3mg/m^2/ day, respectively (145, 146). In recent years, endocrinologists have tried to decrease glucocorticoid replacement doses to levels, which remain safe but do not lead to over treatment. Nevertheless, it is possible that subtle increased glucocorticoid exposure in patients on GC replacement therapy over prolonged periods might contribute to increased morbidity, as observed in patients with Cushing's syndrome (1).

Cortisol day curves reveal that median doses of hydrocortisone of 29.5 + 1.2mg lead to peak cortisol and mean daily cortisol concentrations above the normal range, which in one study lead to a change in therapy in 88% of patients (75% of patients received a dose reduction) (387). *Agha et al.* have shown that patients with 'partial ACTH deficiency' (basal 9.00 cortisol >200nmol/l but a peak cortisol on insulin tolerance test of <500nmol/l) have similar day curves to healthy controls suggesting that these patients may be over-treated by conventional steroid replacement therapy (388). *Fillipson et al.* (389) have described an adverse metabolic profile in a cohort of GH deficient hypopituitary patients on higher doses of glucocorticoid replacement. They found that patients on hydrocortisone replacement had increased total cholesterol, triglycerides, waist circumference and HbA1c compared to the ACTH sufficient patients. Importantly, subjects who had hydrocortisone equivalent doses of less than 20mg/day did not differ in metabolic endpoints compared to the ACTH sufficient patients. However, when a hydrocortisone equivalent doses of more than 20mg/day was administered patients had an adverse metabolic profile (389).

6.1.3.1. Mode of glucocorticoid delivery

Twice or thrice daily doses of glucocorticoids are recommended to mimic the normal circadian rhythm and changes to circulating cortisol but even so, this is rarely achieved. The bioavailability of orally administered hydrocortisone is ~95% (390, 391) and its half-life is 60-90 minutes. A single morning dose of 15mg hydrocortisone leads to supraphysiological serum cortisol concentrations one to two hours post oral administration and a return to subphysiological or undetectable levels 6-8 hours later (390, 392, 393). There is evidence that continuous, prolonged compared to intermittent short exposure to glucocorticoids may have different effects on a number of steroid responsive enzymes (394). Pulsatility may also be also important as it has significant effects on the occupancy of the glucocorticoid receptor (394). Circadian intravenous infusions of hydrocortisone can mimic the normal cortisol rhythm via a programmable pump resulting in beneficial effects in patients with Addison's disease and congenital adrenal hyperplasia (CAH) (395); using these infusions it was also possible to reduce the daily dose of hydrocortisone (396). These infusions are obviously cumbersome and not practical, however, over the last few years there has been a push to design orally active delayed or sustained release formulations of hydrocortisone to reproduce 'physiological replacement' (397). *Johannsson et al*. recently showed that a novel modified release once daily oral hydrocortisone preparation (Duocort) produced a diurnal plasma cortisol profile, which mimicked the physiological serum cortisol profile (398). Similar results are reported with a preparation originating from Sheffield, UK (Chronocort) (399, 400).

6.1.3.2. Morbidity associated with glucocorticoid excess

Patients with glucocorticoid excess (Cushing's syndrome) have significant morbidity and increased mortality (339). Hypertension is present in approximately 80% of patients with endogenous Cushing's syndrome and rises to 95% in patients with ectopic ACTH secretion (1). Hypercortisolaemia has been associated with a hypercoagulable state and several studies have described an increase risk of thromboembolic disorder (suggested by high levels of factor VIII, IX and von Willebrand factor and evidence of enhanced thrombin generation) in patients with Cushing's syndrome. (401).

Hypercortisolism leads to hyperglycaemia and insulin resistance and stimulates hepatic gluconeogenesis and glycogenolysis. In vivo glucocorticoids reduce glucose uptake by reducing GLUT4 translocation and increasing lipolysis (402). Assessment of lipid status in clinical studies of patients with Cushing's disease is not well defined but patients have a low HDL, elevated total cholesterol and LDL cholesterol (403).

There are many phenotypic changes in Cushing's syndrome including redistribution of adipose tissue from peripheral to central parts of the body, with a greater increase in visceral fat (404) and loss of subcutaneous fat from the limbs. There is also a decrease in muscle mass with a predominantly proximal myopathy (Section 1.5). Importantly, even patients who have only mild increases in serum cortisol levels are susceptible to changes in adipose tissue distribution (405). The underlying mechanisms by which elevated levels of cortisol alter adipose tissue distribution are not fully understood. Changes in lipoprotein lipase activity, preadipocyte differentiation and survival and altered cytokine production

have all been implicated (406). In vitro studies have shown that cortisol is associated with stimulation of differentiation of adipose stromal cells to mature adipocytes (407, 408). Glucocorticoids can induce exaggerated adipocyte formation and hypertrophy (108, 409). The action of insulin in conjunction with glucocorticoids promotes preadipocyte differentiation and lipid accumulation (410, 411). Expression and activity of 11 β-HSD1 enzyme has been implicated in the accumulation of visceral adipose tissue both in simple obesity and in Cushing's syndrome (412). There is contradictory evidence between murine models and human studies and depending on fat depot sampled. *Bujalska et al.* first proposed that excessive activity of 11 β-HSD1 enzyme within visceral adipose tissue could lead to increased adipose tissue levels of glucococorticoids and 'Cushing's disease of the omentum' (413). This was also suggested by transgenic models with over-expression of 11 β-HSD1 within adipose tissue resulting in increased accumulation of central fat with increased tissue corticosterone concentrations and an increased adipocyte size (178). However in human fat there are contradictory results with some groups reporting an increase in 11 β-HSD1 activity and expression with obesity (414-416) and others a decrease (417).

In simple obesity, despite the association of cortisol production with obesity there is a weak, negative association of circulating cortisol concentrations and various measures of adiposity including weight, body mass index (BMI), waist-hip ratio and waist circumference in community dwelling men (406, 418).

In obese patients there is an elevated cortisol secretion rate but circulating cortisol levels are typically lower, due to an increased cortisol clearance (418, 419). When free cortisol levels are assessed there is no association with

increasing weight. Cortisol production rate and body surface area are positively correlated with 24 hour plasma free cortisol levels suggesting that activation of the HPA axis and elevated free cortisol levels are associated with increase adiposity (420).

Therefore, when you compare the metabolic and phenotypic characteristics of growth hormone deficiency and glucocorticoid excess there are significant similarities.

6.1.4. GH and 11 β-HSD1

As discussed in previous chapters and in Section 1.4.6, at the tissue level glucocorticoid action is modulated by isozymes of 11 beta-hydroxysteroid dehydrogenase (11β-HSD), type 1 and 2. 11β-HSD1 is modulated by many factors, including GH/ IGF-I, thyroid hormone, insulin, glucocorticoids and sex steroids (2). Thus, in patients with hypopituitarism there may be alterations in tissue specific exposure to glucocorticoids independent of circulating values. This is particularly relevant in patients with GH deficiency.

GH acting via IGF-I inhibits the autocrine generation of cortisol through inhibition of 11β-HSD1 (182). The phenotype of GHD in the context of hypopituitarism may, in part be mediated through increased 11β-HSD1 activity (182) as in these GHD patients the THF+allo-THF/ THE ratio (indicative of increased 11β-HSD1 activity) is increased by 50% from baseline and reduces after commencing GH therapy (even in elderly patients) without alteration in the UFF/UFE ratio, indicative of a resulting decrease in 11β-HSD1 oxoreductase activity (183, 184) without any change in 11β-HSD2 activity. Conversely, patients with acromegaly and high IGF-

I concentrations have decreased 11β-HSD1 activity; a defect that resolves with appropriate treatment of the GH excess (182). These studies are endorsed by *in vivo* studies, which show a decrease in hepatic 11β-HSD1 expression in rats treated with GH (185-187) and *in vitro* experiments have shown that GH has no direct effect on 11β-HSD1 but rather acts via IGF-I (i.e. IGF-I inhibits 11β-HSD1 activity) (182, 188). Clinically patients starting on GH may need a slight increase in glucocorticoid replacement dose or patients who are ACTH replete prior to GH replacement may need retesting once on GH treatment (421). However, in GH deficient patients, cortisol bioavailability is increased in key tissue such as liver, fat and muscle. Therefore, many of the changes reported in GH deficiency could be secondary to alterations in cortisol exposure at a tissue level secondary to modulation of 11β-HSD1. However, to date the impact of GH on 11β-HSD1 has only been examined in a few clinical studies (182-184, 422-424) (many of which involved patients with acromegaly) (182, 422, 424). In these small studies, ranging from 6-23 participants, there were varying incidences of ACTH deficiency with some including no patients on hydrocortisone therapy (182) to all patients receiving on hydrocortisone therapy (183, 184).

6.1.4.1. Measurement of 11 β-HSD1 activity in vivo using urinary gas chromatography/ gas spectrometry

The metabolism of cortisol has been extensively reviewed by *Tomlinson et al.* (2), the major route comprises the interconversion of cortisol (Kendall's compound F) to cortisone (Kendall's compund E) through the activity of 11 β-HSD isozymes or reduction of the C4-5 bond by either 5α-reductase or 5β-reductase to yield 5α-

THF (allo THF) and 5β-THF respectively (2) (Figure 6.1). THF, allo THF and tetrahydrocortisone (THE) are rapidly conjugated with glucuronic acid and excreted in the urine (2). Downstream, cleavage of the THF and THE to the C19 steroids 11 hydro or 11-oxo-androsterone or etiocholanolone occur. Alternatively reduction of the 20-oxo group by 20α or 20β hydroxysteroid dehydrogenases yield α and β cortols and cortolones, respectively, with the subsequent oxidation at the C21 position to form the extremely polar metabolites cortolic and cortolonic acids. Approximately 50% of secreted cortisol appears in the urine as THF, allo THF and THE, 25% appears as cortols/ cortolones, 10% as C19 steroids, 10% cortolic/ cortolonic acids and remaining are free unconjugated steroids (F, E, 6β and 20α/ 20β-metabolites of F and E) (2).

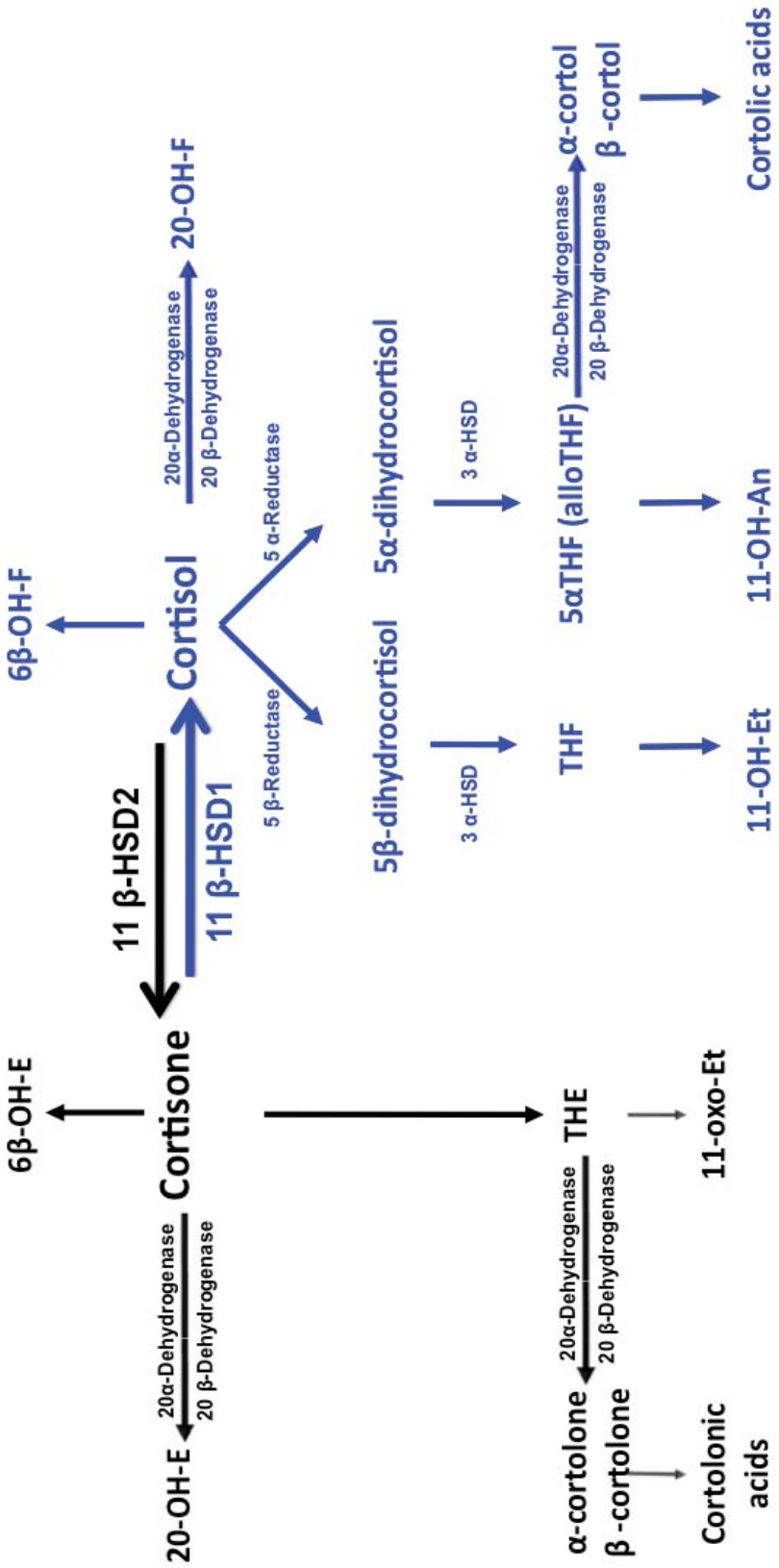

Figure 6.1. *The major pathways involved in cortisol metabolism (E= cortisone, F= cortisol, Et = etiocholanolone, An = androsterone).*

6.2. Hypothesis

Our hypothesis is that 11 β-HSD1 is upregulated in hypopituitarism due to unphysiological glucocorticoid replacement therapy and the ensuing increase in tissue specific cortisol generation contributes to the changes in body composition reported in hypopituitarism.

6.3. Strategy of Research and Aims

To assess the effect of hydrocortisone therapy on 11 β-HSD1 in vivo, the urinary corticosteroid metabolite profile of growth hormone deficient hypopituitary patients (some with ACTH deficiency compared to those with normal ACTH reserve) were assessed with the following aims.

a. To assess differences in total cortisol metabolites, measures of 11 β-HSD1 (THF +alloTHF/THE) and urinary free cortisol levels in hypopituitary patients, with and without ACTH deficiency.

b. To assess the impact of hydrocortisone therapy in hypopituitarism on measures of body composition.

c. To assess if corticosteroid metabolism is correlated with measures of body composition.

6.4. Methods

6.4.1. Gas Chromatography/ Mass spectrometry for corticosteroid metabolites in human and mouse urine

6.4.1.1. Principles

GC/MS urinary steroid analysis was carried out by Beverley Hughes at the Institute for Biomedical Research, Centre for Endocrinology, Diabetes and Metabolism (CEDAM), University of Birmingham. The GC/MS was based on the method described by *Palermo et al.* (311). The methods of sample work-up for GC/MS analysis (conjugate hydrolysis, extraction and derivatization) and their methodologies have been published in detail in several manuscripts (149, 312) and in depth description is beyond the scope of this thesis.

GC/MS was used to analyse the metabolites of steroid hormones and their precursors. In the CEDAM, at the University of Birmingham, approximately 40 steroids are targeted for selected-ion-monitoring analysis, which cover all disorders of steroid synthesis and metabolism. A recent review by *Krone et al.* from this Department has highlighted several key features of urinary steroid metabolite analysis including the major shortcoming of data presentation in clinical GC/MS urine steroid profiling (313). Tabulating only the quantified amounts of steroid metabolites can be confusing and difficult to interpret, therefore improvement in the visual presentation of data has been made within the department (313).

The pathway to steroid hormone production is commonly divided into the synthesis of mineralocorticoid, glucocorticoids and sex steroids (Figure 1.4). We

have added two groups to this classification; 'androgen precursors' includes the Δ5-steroids pregnenolone, 17OHpregenenolone, DHEA and the Δ4-steroids androstenedione and their metabolites as this represents the main pathway to active androgens. The second additional group is 'glucocorticoid precursors', which consists of the Δ4-steroids progesterone, 17OHprogesterone and 21-deoxycortisol and their metabolites (313). Within CEDAM normal ranges have been developed from a large number of healthy controls. The GC/MS profile of an individual patient is plotted for each determined parameter against the normal reference population (Figure 6.2). Such profiles allow for an immediate overview of the complete set of metabolites (313). Most hormonal imbalances caused by enzyme deficiencies or "blocks" cause depletion of a steroid product and build-up of the upstream precursors. Thus, a ratio of metabolites of the substrate to metabolites of the product should indicate if there is such a block. In this thesis ratios of glucocorticoid metabolites are used to determine the relative activity of 11 β-HSD1 and 11 β-HSD2.

6.4.1.2. Methods

Quantitative data on excretion of individual steroids requires accurate 24 hour sampling and 1ml of a 24-hour collection for analysis. For murine studies individual mouse urine was collected on filter paper and processed.

The following isotope labelled internal standards were used; (9,11,12,12-^{2}H) cortisol and (9,12,12-^{2}H) cortisone. The standards were calibrated by high performance liquid chromatography (HPLC) analysis of solubilised, non-labelled standard on known weight. Free steroid was extracted using Sep-pak C18

cartridges (314). Labelled steroid d_4-cortisol (0.18μg), and d_3-cortisone (0.12μg), as well as internal standards (stigmasterol and cholesteryl butyrate), 200μg were then added. The samples were then derived using 100μl of 2% methoxyamine hydrochloride in pyridine and 50μl of trimethylsilylimidzole. Lipidex chromatography was then used to purify the steroid derivative.

GC/MS was carried out using a Hewlett Packard 5970 mass spectometer and 15m fused-silica capillary column, 0.25mmID, 0.25μm film thickness (J&B Scientific, Folsom CA, USA) using 2μl of sample. Steroids were quantified by comparing individual peak area to the peak area of the internal standards, for cortisol fragment 605m/z compared to 609 m/z and for cortisone fragment 531 m/z compared to 534 m/z. The relative peak area was calculated and the metabolite concentration expressed as μg/24hr. A quality control (QC) was analysed with each batch. The intra and inter-assay co-efficient of variance was <10%.

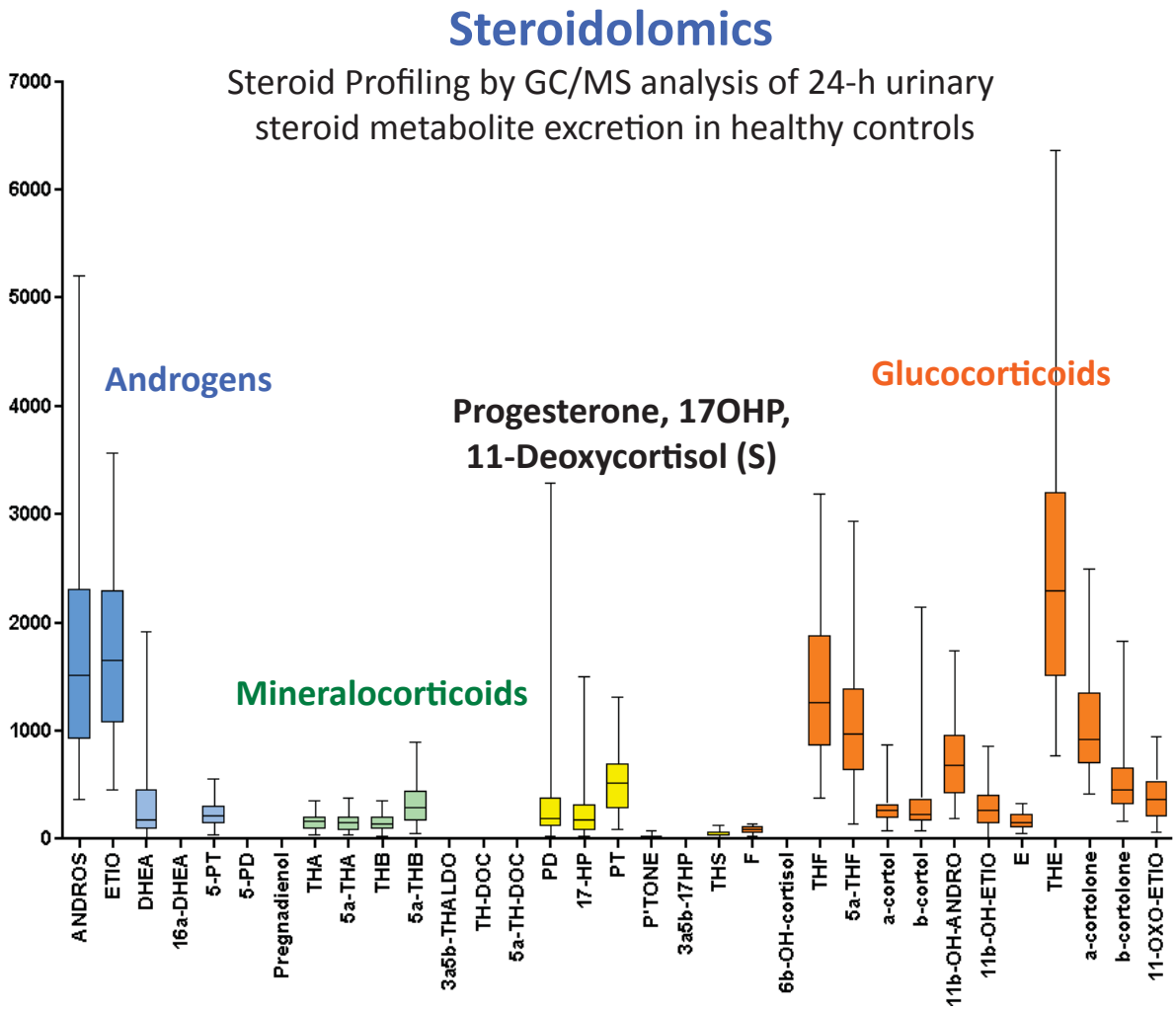

Figure 6.2. *Representative graph of steroid metabolite excretion (μg/ 24 hours) assessed by 24 hour urinary gas chromatography/ mass spectrometry in healthy adults divided into metabolites of androgens, mineralocorticoids and progesterone (17-OHP and 11-deoxycortisol) and glucocorticoids. Box and whisker plots represent mean and 5th and 95th percentile.*

6.4.2. Assays for Clinical study

6.4.2.1. GH assay used in this study

Serum GH was measured using DPC Immulite 1000 immunometric assay calibrated against IS 80/505. This standard (IS 80/505) was assigned a value in International Units, and therefore GH was reported in mIU/L with a conversion factor of 2 for µg/litre. For results < 20 mIU/L the DPC assay gave similar results to the RIA. For results >20 mIU/L the DPC assay gave results between 10-20% lower. The assay was transferred to the Immulite 2500 when DPC was bought by Siemens. This did not result in any significant change in GH values. Serum GH levels were measured by an in house RIA in a central laboratory as previously described (425) (the value in mIU/litre was divided by a conversion factor of 2 to obtain µg/litre). The limit of detection of the assay is 0.5µg/litre and the interassay CV is 5.7% at 2 µg/litre, 4.3% at 3µg/litre, 5.5% at 7.3 µg/litre and 4.47% at 14.7 µg/litre.

A new international standard was produced in 2001 (WHO IS 98/574). This is comprised of recombinant material consisting of a 22kDa growth hormone of >95% purity. Unlike the previous standard, IS 98/574 has been assigned values in both mass and International Units, allowing conversion between mass units and International Units such that 1µg corresponds to 3 milli-International Units. Although our GH assay has remained the same (Siemens Immulite 2500), it has now been calibrated against the new IS 98/574 and since May 12th 2008, results have been reported in µg/L.

6.4.2.1.1 GH Assays – General Description

The measurement of GH has evolved from polyclonal radioimmunoassay (RIA) to modern two-site monoclonal antibodies which are now non-isotopic and have enhanced sensitivity. The old assays were limited by sensitivity, being unable to tell unmeasurable levels from measurable low concentrations (426).

The development of GH assays was closely linked to the invention of the classic immunoassay. When enzyme immunoassays and other non-radioactive immunoassays became available they were also applied to GH measurement (427). As the production of monoclonal antibodies became possible the specificity of GH assays increased as these monoclonal antibodies are directed against a very distinct three dimensional structure on the surface of the antigen and therefore are less likely to recognise isoforms and fragments of the molecule (427). The most frequently used assays today are the classical sandwich-type immunometric assays with secondary antibody labelled by something which can be quantified by labelling with radioactivity (IRMA), enzyme mediated colorimetry (ELISA), time resolved fluorescence (IFMA) or chemiluminescence (ILMA/ ICMA). These sandwich type assays have sensitivities of around 0.2µg/litre and some of them can have sensitivities as low as 0.002µg/litre (427). This is in contrast to older competitive assays, which frequently use polyclonal antibodies (which are the basis of many of our recommendations for diagnosis and long term follow up in acromegaly). Compared to the more recent assays they are less sensitive with lower detection limits between 0.5 and 1 µg/litre for GH. (427)

6.4.2.2. IGF-I assays used in this study

Serum IGF-I was measured using an in-house RIA with acid ethanol extraction performed to remove IGF-binding proteins, as previously described (428). The limit of detection of the assay is 2.0nmol/litre. The interassay CV is 5.4-8.4% between 16-104 nmol/litre. Reference ranges were derived from adults with no known or suspected endocrine disorders. Reference range values were 14-48nmol/litre at 21-30 years (n=71), 13-37 nmol/litre at age 31-45 years (n=123) and 8.9-32nmol/litre (n=75) above 45 years.

6.4.2.2.1 IGF-I assays – General description

Several factors of IGF-I physiology are important to remember when utilising information from IGF-I assays and in assessing IGF-I assay performance including: circadian rhythms, nutrition, age, IGF-BPs, insulin, oestrogen, androgens, thyroxine and cortisol.(429) IGF-I levels increase from birth until puberty (5 fold increase) then decrease with age (3.5 fold decrease from puberty to old age).(429) For these reasons it is important when assessing IGF-I that once compares to age adjusted reference ranges. After the age of 30 it is reasonable to have age related reference ranges according to decades due to the steady rate of decline.

Diabetes and renal disease can lead to significant increases in IGF-BP, therefore if assays are used in which there is IGFBP assay interference the IGF-I value may be artificially high.(430) There is significant day to day sample variability in IGF-I levels, *Milani et al.* reported that serial samples (intervals of 6-12 weeks) from the same patient may show large variability in IGF-I (3-36%).(431)

All of the initial IGF-I assays were conventional radioimmunoassays (RIAs) that used competitive binding between radiolabelled and unlabeled IGF-I in serum and were therefore open to binding protein interference (429). The degree of interference in these original RIA was related to the affinity of the antibody, in higher affinity antibodies the sample could be diluted to overcome effect of binding proteins (432). Because of these problems with binding protein interference a large number of techniques were developed to remove or nullify their effect. These included acid gel filtration chromatography (which is the gold standard as it has high reproducibility but is difficult to perform) and acid/ ethanol precipitation (which is easy to use and highly reproducibility but does not remove all binding proteins). The West Midlands Regional Endocrine Laboratory uses the acid ethanol technique which removes the vast majority of IGF-BP3 and 5 which are bound to acid labile subunit but does not remove smaller binding proteins that do not bind to ALS such as IGF-BP1 and 4 (433, 434). Another potential limitation of this method is that some of the IGF-I is also precipitated by this method and laboratories need to account for this if possible otherwise the IGF-I concentration will be an underestimation. Some units add IGF-II to the elute from acid ethanol extraction to increase the removal of IGF-BP1 and 4, which completely eliminates IGFBP assay interference (435) but this needed an antibody with low affinity for IGF-II but high affinity for IGF-I. Newer techniques have tried to avoid the problem of binding protein interference by using a two antibody capture technique (436) which does not need radiolabelled tracers and successfully eliminates binding protein interference.

6.4.2.3. Diagnosis of ACTH deficiency

The hypothalamic pituitary adrenal axis was deficient if the + 30 minute cortisol response to a 250μg 'short' synacthen testing was <550nmol/litre (437) or less than 500nmol/litre following insulin induced hypoglycaemia during an insulin stress test. Samples were assayed for cortisol using a chemiluminescence immunoassay (Advia Centaur; Bayer Diagnostics, Newbury, UK) with an interassay imprecision of less than 10% for serum cortisol concentrations between 68 and 970 nmol/liter (with interassay coefficients of variation of 10.2% at 76 nmol/liter, 7.7% at 528 nmol/liter, and 7.4% at 882 nmol/liter) (438). This assay is equivalent to the previously described Bayer ACS 180 (437) using the same reagents on a larger automated platform (439).

6.4.2.4. Diagnosis of TSH deficiency

The thyroid axis was deficient if the free T4 concentration was below the local reference range, with an inappropriately low/ normal TSH. Serum free T_4, free triiodothyronine (T_3), and TSH were measured by chemiluminescent immunoassay (Advia Centaur; Bayer Diagnostics, Newbury, England). The laboratory reference range for free T_4 was 0.70 to 1.55 ng/dL (9.0-20.0 pmol/L), with an interassay coefficient of variation of 8.2% to 9.8% over the range of 0.64 to 4.27 ng/dL (8.2-54.9 pmol/L). Serum TSH concentration had a reference range of 0.4-5.5 mU/L, with an interassay coefficient of variation of 4.4% to 10.9% over the range of 0.41 to 24.5 mU/L. The lower limit of reporting for the TSH assay was 0.1 mU/L, with a mean functional sensitivity 0.02 mU/L. Free T_4 and TSH

concentrations were determined in all; in those with serum TSH concentrations below the reference range, serum free T_3 (reference range, 227.3-422.1 pg/dL [3.5-6.5 pmol/L], interassay coefficient of variation of 4.2%-6.9% over the range of 259.7-1039.0 pg/dL [4.0-16.0 pmol/L]) was additionally measured. The reference ranges used for free T_4, TSH, and free T_3 were those recommended by the manufacturer and used in other studies of this cohort and studies from our unit (440, 441).

6.4.2.5. Diagnosis of FSH and LH deficiency

Hypothalamic-pituitary gonadal dysfunction in males was diagnosed in the setting of a low serum testosterone and inappropriately low/ normal gonadotropins. In females hypothalamic-pituitary gonadal dysfunction was diagnosed in premenopausal females if the patient was amenorrheic (with normal prolactin levels) and in post-menopausal females if the FSH was inappropriately low (<35IU/ litre).

6.4.2.6. DEXA and measurement of body composition in clinical study

Whole body Dual Energy x-ray absorptiometry (DEXA) scanning was performed to assess body composition and bone mineral density using a total body scanner (DPX-L, Lunar Corp., Madison, WI, USA). For total fat and lean mass measurements, coefficients of variation were less than 3%. Regional fat mass was defined as previously reported (442). Waist region was defined within a box area between the upper part of D12 and the iliac crest and the thigh region was

defined as a box positioned so that its upper border at the level of the inferior border of the hip region (see Figure 6.3). Further division of waist fat was made to characterise the 'central' or 'omental' fat region. Central fat was deemed to be the area overlying the vertebrae below D12 and either side of the vertebral column. Muscle strength was not assessed in this study, as it was not an outcome at initial study design.

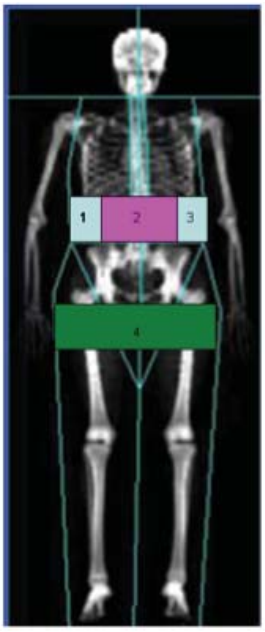

***Figure 6.3**. Method of calculating central abdominal fat to peripheral fat ratio using whole body DEXA scanning, where area 2 = central fat and area 4 = peripheral fat.*

6.4.3. Statistical methods

Statistical analysis was performed using Prism for Windows version 5.0 (GraphPad Software Inc, San Diego, CA, USA) software packages. Continuous data were summarised using means and standard deviations (or standard error of mean) if parametrically distributed or medians and inter-quartile ranges if non-parametrically distributed. Parametric data was compared using a paired t-test

and non-parametric data was analysed using a Mann-Whitney test. Multiple comparisons were assessed using one-way analysis of variance (ANOVA), with Kruskal-Wallis for non-parametric data. Associations between variables were analysed using Pearson correlation for parametric data and Spearman rank correlation for non-parametric data. The level for statistical significance was taken at $p<0.05$.

6.4.4. Ethics

The study was approved by the local research ethics committee and Scientific Advisory Committee of the Wellcome Trust Clinical Research Facility at the Queen Elizabeth Hospital, Birmingham at which the study was performed. All patients were recruited from the Pituitary Clinic at the Queen Elizabeth Hospital, Birmingham and gave informed written consent.

6.5. Results

6.5.1. Patient characteristics

In total, 53 patients consented for the study (19 female). Baseline characteristics are detailed in Table 6.1. All patients had severe GH deficiency (GHD) as diagnosed on either insulin tolerance test or glucagon stimulation test [of note 32/51 (62.8%) had an IGF-I in the normal age related reference range, highlighting the poor sensitivity of IGF-I as a screening test for the diagnosis of GHD]. GHD deficient patients did not receive GH replacement therapy during this study. In the female group 11/19 (52.6%) and male group 22/34 (67.6%) were

ACTH deficient, respectively, but there was no difference in rates of ACTH deficiency between genders (p=0.37). In the ACTH deficient group (n=33), 19 patients received less than or equal to 20mg hydrocortisone per day (8 female) and 14 patients received >20mg per day (2 female). 28 patients received twice daily and 5 patients received thrice-daily hydrocortisone therapy. 19/53 patients had TSH deficiency and were receiving thyroxine therapy with freeT4 concentrations in the normal range. 33/53 patients had hypogonadotropic hypogonadism and were on replacement therapy.

Variable	Total group	Male	Female
AGE	46 (35-58.5)	47.5 (36.7 – 68.2)	44 (23-53)
SBP	135 (118.5-148.5)	134 (118 – 148.8)	135 (116-149)
DBP	77 (71.5 – 86)	77.5 (70 – 86)	75 (72-86)
AGHDA	11.5 (6-15)	9 (4-13)	14 (6-18)
BMI	29 (25 – 33.9)	28.2 (25.4 – 31)	33.8 (25.4 – 38.2) *
WHR	0.93 (0.88 – 0.96)	0.95 (0.92 – 0.97)	0.87 (0.82 – 0.92) ***
Fat %	30.7 (24.2 -39.8)	26.2 (23.7 – 31.3)	42 (33.8 – 47.0) ***
Fat Mass	26.5 (18.9 – 37.25)	22.3 (19.2 – 31.4)	35 (21.6 – 45.8) ***
Fat Free Mass	60.8 (52.0 – 65.5)	63.4 (60 – 68.9)	47.9 (44.3 -53.9) ***

Table 6.1. *Basic demographic, quality of life and body composition data on total group, male and females. * p<0.05, ***p<0.0001, female compared to male. Median and interquartile ranges.*

6.5.2. Steroid metabolite excretion rates in hypopituitary patients with and without ACTH deficiency

Each patient provided a 24-hour urine collection, while taking their routine hydrocortisone dose and other replacement therapies, for assessment of corticosteroid metabolites by gas chromatography/ mass spectrometry and compared to healthy controls (Figure 6.2). Patients were subdivided into patients who had hypopituitarism (and severe GHD) but who were not ACTH deficient (Figure 6.4.a) and patients who had hypopituitarism (and severe GHD) and were ACTH deficient (and receiving hydrocortisone therapy) (Figure 6.4.b).

Metabolites of glucocorticoids were particularly increased in patients receiving hydrocortisone therapy (Figure 6.4.b, blue box) compared to both healthy controls and patients who had hypopituitarism (and severe GHD) but who were not ACTH deficient.

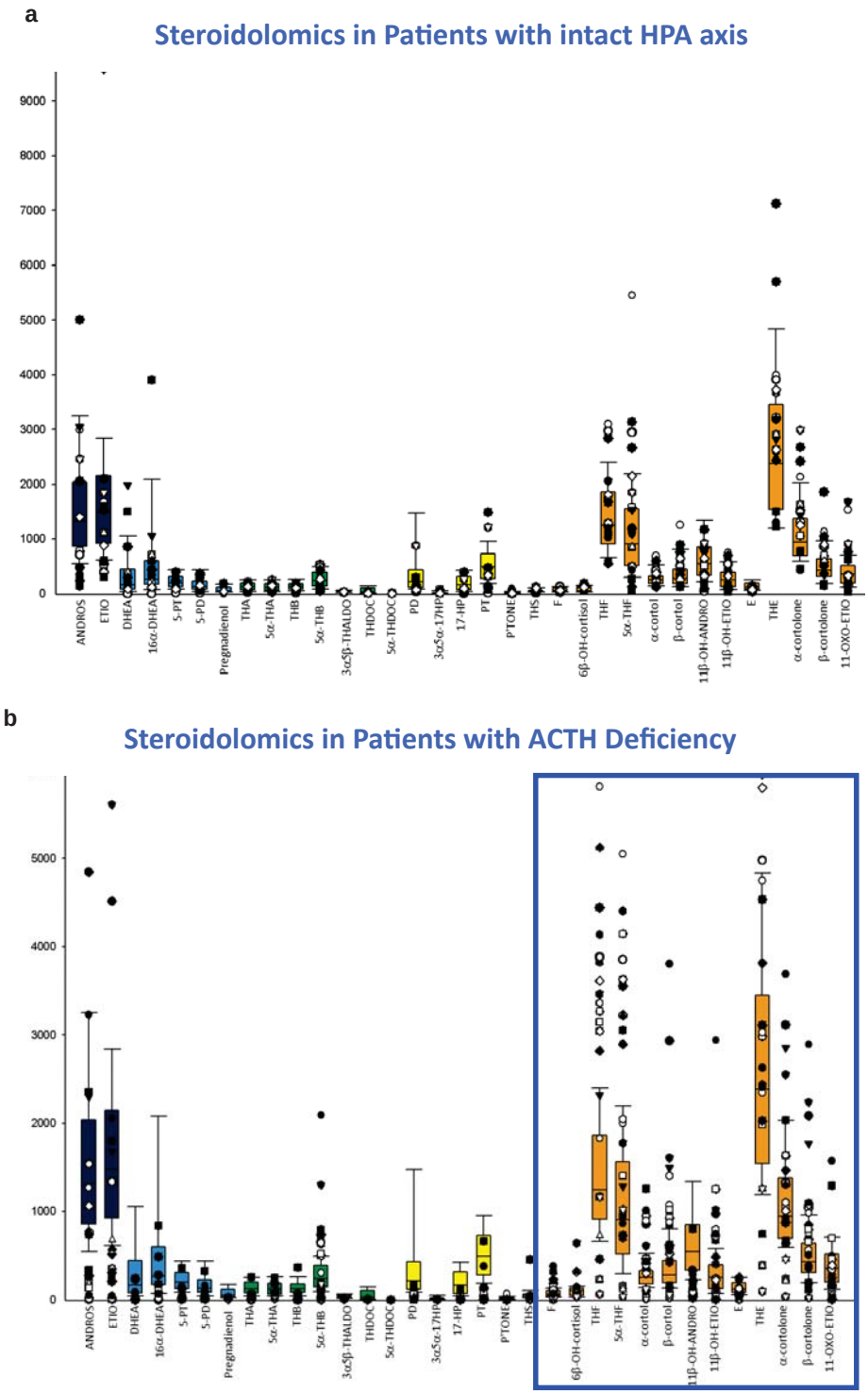

Figure 6.4. *Representative graph of steroid metabolite excretion (μg/ 24 hours) assessed by 24 hour urinary gas chromatography/ mass spectrometry in patients with hypopituitarism (GHD but normal HPA axis) (a) and patients with hypopituitarism who were receiving hydrocortisone therapy for ACTH deficiency (b) divided into metabolites of androgens, mineralocorticoids and progesterone (17-OHP and 11-deoxycortisol) and glucocorticoids. Metabolites of glucocorticoids are particularly increased in patients receiving hydrocortisone therapy (b, blue box). Box and whisker plots represent mean and 5th and 95th percentile of healthy control group. Symbols represent individual patient results.*

6.5.3. Comparison of corticosteroid metabolites

To further clarify the results of Section 6.5.2, we analysed the total cortisol (F) metabolites (Figure 6.5.a) (μg/ 24 hours), THF + allo-THF/THE (a measure of global 11β-HSD1 activity) (Figure 6.5.b) and urinary free cortisol (Figure 6.5.c) between patients with normal ACTH reserve and patients receiving increasing doses of hydrocortisone therapy (hydrocortisone doses less than or equal to 20mg per day or greater than 20 mg per day) assessed by gas chromatography/ mass spectrometry of 24-hour urinary collections. This showed an increase in total cortisol metabolites at higher doses of hydrocortisone (Figure 6.5.a), a higher THF + alloTHF/THE ratio (11 β-HSD1) (Figure 6.5.b) at both doses of hydrocortisone, but no change in urinary free cortisol levels between groups (Figure 6.5.c).

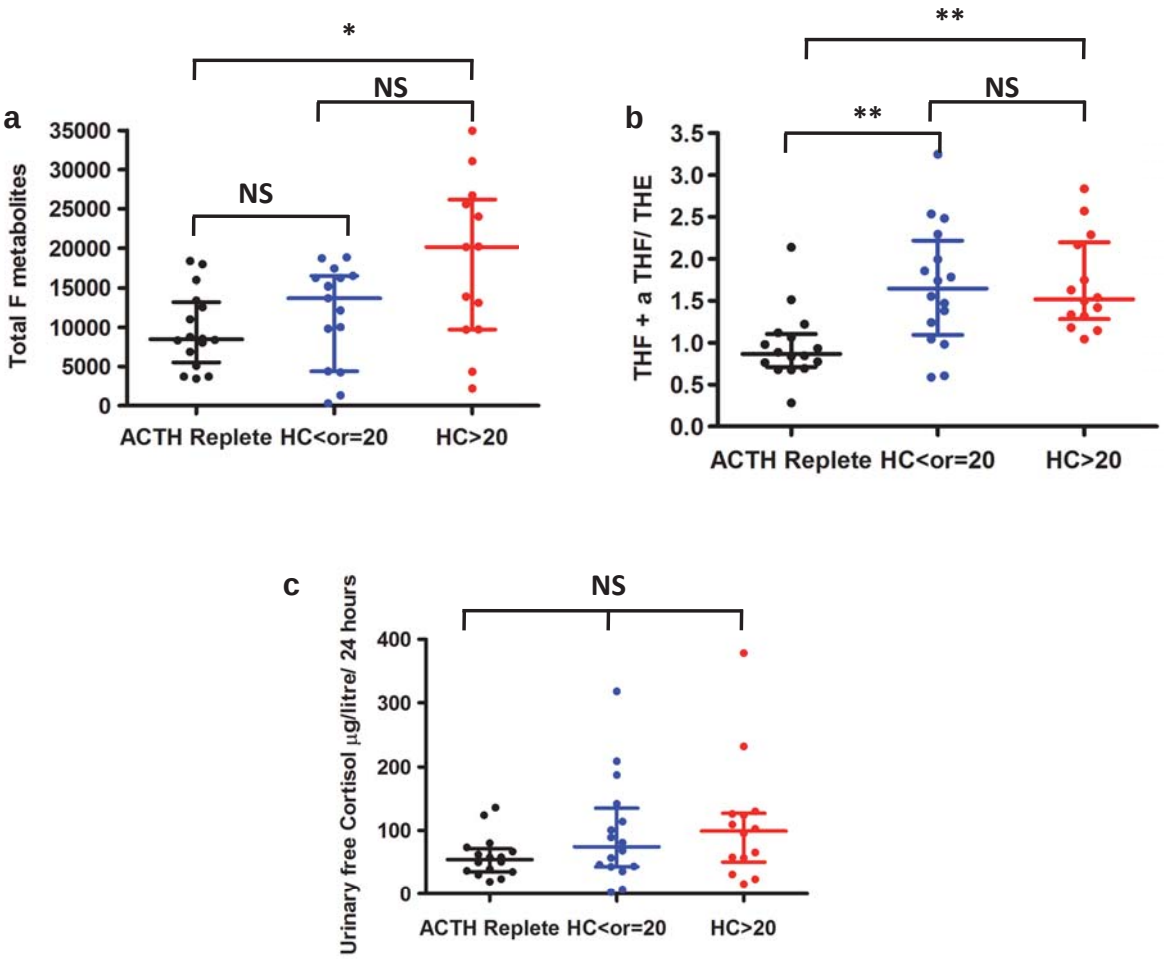

Figure 6.5. *Differences in total cortisol (F) metabolites (a) (µg/ 24 hours), THF + allo-THF/THE (b) and urinary free cortisol (c) between patients with normal ACTH reserve and patients receiving increasing doses of hydrocortisone (HC) therapy (at doses less than or equal to 20mg per day or greater than 20 mg per day) assessed by 24 hour urinary gas chromatography/ mass spectrometry. * p<0.05, ** p<0.001, NS = not significant. Lines represent median and interquartile ranges.*

6.5.4. Effect of hydrocortisone replacement therapy on body composition in hypopituitary patients

The effect of ACTH deficiency and hydrocortisone therapy on body composition assessed by body mass index (BMI) (Figure 6.6.a), fat mass (Figure 6.6.b), and Waist hip ratio (WHR) (Figure 6.6.c). There was no difference between groups for BMI or fat mass (Figure 6.6.a + b). There was an increase in WHR at higher doses of hydrocortisone therapy (Figure 6.6.c).

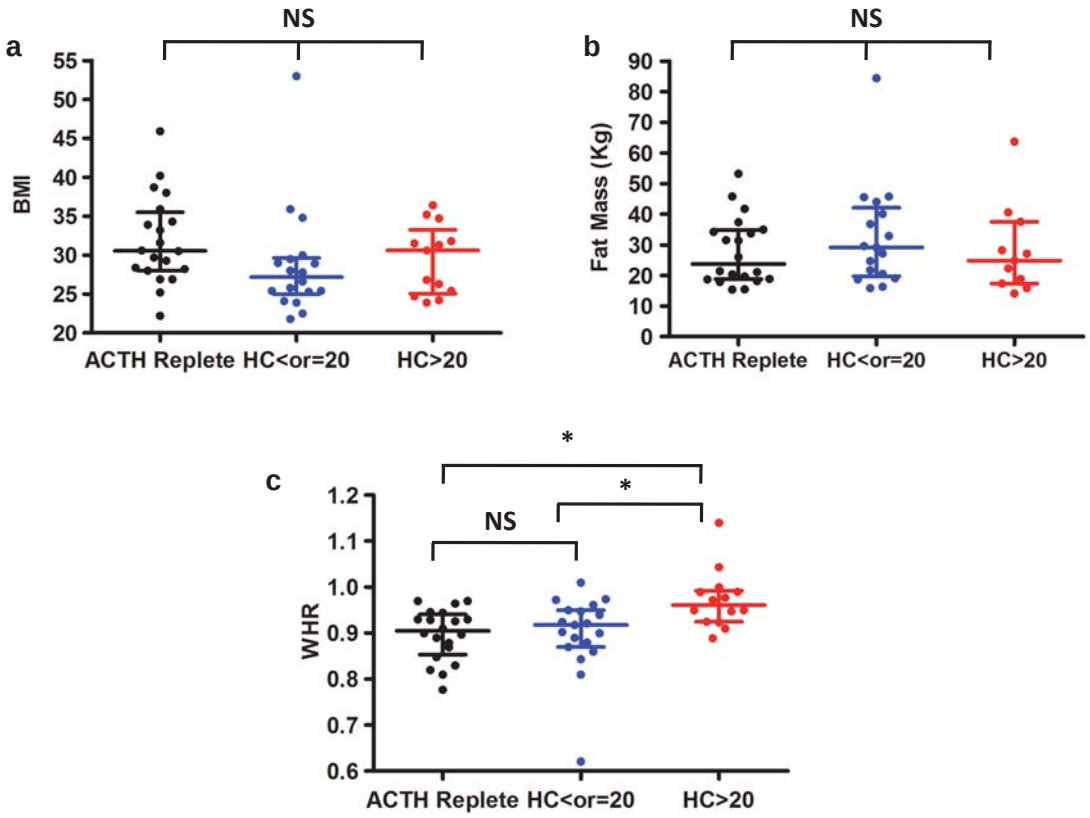

Figure 6.6. *Differences in body mass index (BMI) (a), Fat mass (b) and Waist hip ration (WHR) (c), between patients with normal ACTH reserve and patients receiving increasing doses of hydrocortisone (HC) therapy (at doses less than or equal to 20mg per day or greater than 20 mg per day). * p<0.05, NS = not significant. Lines represent median and interquartile ranges.*

6.5.5. Correlation of 11 β-HSD1 activity and body composition in all hypopituitary patients.

The correlation between 11 β-HSD1 and BMI (Figure 6.7.a), fat mass (Figure 6.7.b), WHR (Figure 6.7.c) and a DEXA derived ratio of central to peripheral fat mass (Figure 6.7.d) was assessed in the entire group of hypopituitary patients. There was a significant negative correlation between BMI and 11 β-HSD1 activity but no correlation for other markers of body composition.

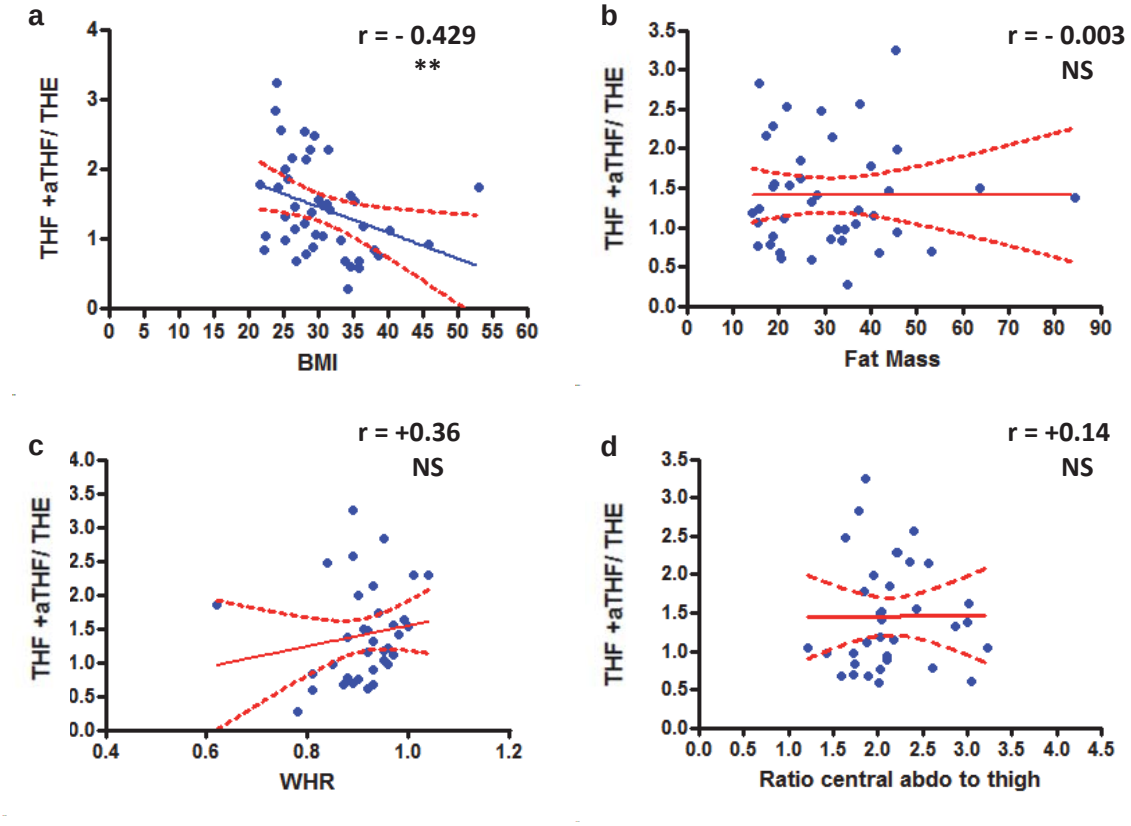

Figure 6.7. *Correlations between total body 11 β-HSD1 activity as assessed by THF + alloTHF/THE ratio in by 24 hour urinary gas chromatography/ mass spectrometry and Body mass index (BMI) (a), fat mass (b), waist hip ratio (c) and ratio of central abdominal fat to thigh fat (d) in all patients. ** p<0.001, NS = not significant, r = correlation coefficient. Full line = linear regression, hatched lines = 95% confidence intervals.*

6.5.6. Correlation between total cortisol metabolites and body composition in all hypopituitary patients

The correlation between Total F metabolites and BMI (Figure 6.8.a), fat mass (Figure 6.8.b), WHR (Figure 6.8.c) and a DEXA derived ratio of central to peripheral fat mass (Figure 6.8.d) was assessed in the entire group of hypopituitary patients. There was a significant positive correlation between the DEXA derived ratio of central to peripheral fat mass and total F metabolites but no correlation for other markers of body composition were statistically significant.

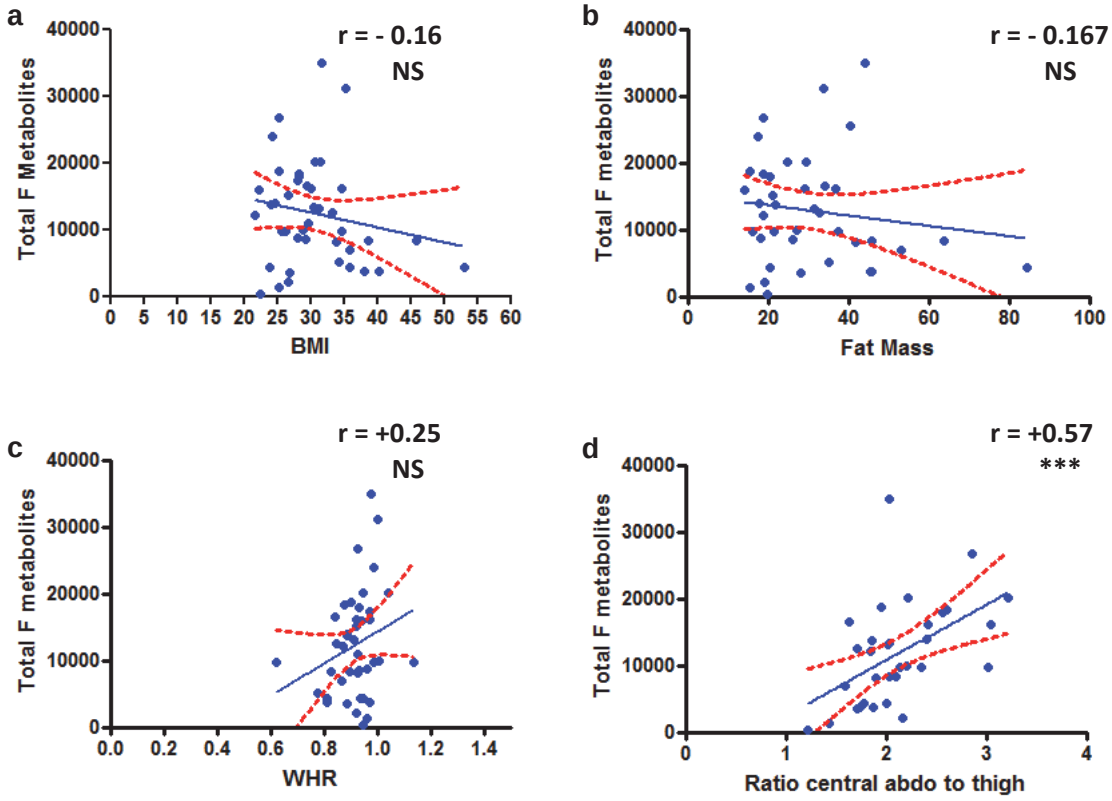

Figure 6.8. *Correlations between total cortisol (F) metabolites as assessed by THF + alloTHF/THE ratio in by 24 hour urinary gas chromatography/ mass spectrometry and Body mass Index (a), fat mass (b), waist hip ratio (c) and ratio of central abdominal fat to thigh fat (d) in all patients. ** p<0.001, NS = not significant, r = correlation coefficient. Full line = linear regression, hatched lines = 95% confidence intervals.*

6.6. Discussion

These results show that hypopituitary patients who receive hydrocortisone therapy have significant alterations in corticosteroid metabolism. There were significant abnormalities in corticosteroid metabolite profiles in ACTH deficient patients (receiving hydrocortisone) when compared to normal controls and hypopituitary patients with normal ACTH reserve. The abnormalities reported were primarily due to an increase in glucocorticoid metabolites (Figure 6.4). There were increases in total cortisol metabolites and THF+allTHF/The ratio (a marker of 11 β-HSD1 activity) in patients on hydrocortisone therapy, and this was dose related. Importantly, however there were no change in urinary free cortisol levels with increasing doses of hydrocortisone, showing that increased doses of hydrocortisone were not simply excreted in the urine as the reached the renal threshold, but rather underwent intracellular metabolism.

Hypopituitarism is associated with increased morbidity and mortality (339) and we have previously shown that in patients with acromegaly, ACTH deficiency is an independent predictor for mortality and daily doses of hydrocortisone of greater than or equal to 25mgs per day were associated with increased mortality, predominantly due to cardiovascular disease (443). In the general population, doses of prednisolone greater than or equal to 7.5mgs/day have also been associated with increased cardiovascular disease (444). As we have shown that *in vitro* 11 β-HSD1 is upregulated by glucocorticoid exposure (Section 4.6), we hypothesised that this may also happen in patients with hypopituitarism who are receiving hydrocortisone therapy and this may have deleterious consequences.

Over the last few years there has been increasing awareness that the replacement doses of hydrocortisone that were classically used were greater than the cortisol production rate in healthy controls (145, 146). This has been highlighted by studies which, by using cortisol day curves, reveal that median doses of hydrocortisone of 29.5 ± 1.2mg lead to peak cortisol and mean daily cortisol concentrations above the normal range, which in one study lead to a change in therapy in 88% of patients (75% of patients received a dose reduction) (387). Studies in patients with partial ACTH deficiency have shown similar day curves to healthy controls suggesting that these patients may be over-treated by conventional steroid replacement therapy (388). *Fillipson et al.* (389) have described an adverse metabolic profile in a cohort of GH deficient (hypopituitary) patients on higher doses of glucocorticoid replacement therapy. They found that patients on hydrocortisone replacement had increased total cholesterol, triglycerides, waist circumference and HbA1c compared to the ACTH sufficient patients. Importantly, subjects who had hydrocortisone equivalent doses of less than 20mg/day did not differ in metabolic endpoints compared to the ACTH sufficient patients. However, when a hydrocortisone equivalent doses of more than 20mg/day was administered patients had an adverse metabolic profile (389). These studies showing the biochemical over-replacement of patients with ACTH deficiency with hydrocortisone are also important at a molecular level as there is evidence that continuous, prolonged compared to intermittent short exposure to glucocorticoids may have different effects on a number of steroid responsive enzymes (394).

As a result of the above evidence, there has been a recent push to design orally active delayed or sustained release formulations of hydrocortisone to reproduce

'physiological replacement' (397). *Johannsson et al*. recently showed that a novel modified release once daily oral hydrocortisone preparation (Duocort) produced a diurnal plasma cortisol profile, which mimicked the physiological serum cortisol profile (398). Similar results are reported with a preparation originating from Sheffield, UK (Chronocort) (399, 400). These results are exciting, however, larger studies are required to fully assess the efficacy and role of these drugs in different cohorts of patients with adrenal insufficiency. Given our results it would be interesting to assess if modified release hydrocortisone would reduce the abnormalities in corticosteroid metabolism reported in our patient cohort.

There was a discrepancy between BMI and WHR and effect of increasing hydrocortisone dose and correlatiosn with THF+alloTHF/THE ratio. We found that the changes in higher hydrocortisone doses and the alterations seen in corticosteroid metabolites are associated with an increased visceral adiposity, as shown by increased WHR in patients on >20mgs of hydrocortisone per day (Figure 6.6.c) and the strong positive correlation between total F metabolites and ratio of central to thigh fat (Figure 6.8.d). Visceral adiposity is known in the general population to be associated with insulin resistance or diabetes mellitus, hypercholesterolaemia and hypertension (342, 343). *Bujalska et al.* first proposed that excessive activity of 11 β-HSD1 enzyme within visceral adipose tissue could lead to increased adipose tissue levels of glucococorticoids and 'Cushing's disease of the omentum' (413). This was also suggested by transgenic models with over-expression of 11 β-HSD1 within adipose tissue resulting in increased accumulation of central fat with increased tissue corticosterone concentrations and an increased adipocyte size (178). The increase in both THF+alloTHF/THE ratios and total cortisol metabolites in our

cohort of patients taking hydrocortisone therapy could lead to significant changes in adipose tissue biology.

Visceral adiposity and decreased lean mass is also reported in patients with GHD and this improves following treatment with GH (341, 346, 375, 376). It is interesting to speculate that many of these changes in body composition (both increased fat mass and decrease muscle mass) reported with GH therapy in patients with hypopituitarism may be due to inhibition of corticosteroid metabolism (in particular 11 β-HSD1) by GH treatment. Importantly, many patients in previous studies of GH replacement were also ACTH deficient and on hydrocortisone therapy. The reduction in 11 β-HSD1, following GH therapy (and the resultant rise in IGF-I) may decrease cortisol exposure to adipose tissue and muscle, thus leading to changes in body composition.

One important limitation of this study is the heterogeneous nature of the cohort of patients with hypopituitarism (gender, body composition, rates of ACTH deficiency and hydrocortisone doses), which is a common feature of many studies of hypopituitarism and GH replacement. Following discussion with statistician colleagues it was decided that multiple regression analysis may not be helpful in separating the effects of gender/ body composition and hydrocortisone replacement, given the small numbers in the study. Instead of relying on multiple regression analysis we are currently performing a study in collaboration with Professor Chris Thompson and Dr Amar Agha at Beaumont Hospital, Dublin of male patients only, with ACTH deficiency, with each patient receiving hydrocortisone therapy at different doses in a cross-over protocol (hydrocortisone 10mg mane and 5mg tarde. hydrocortisone 10mg mane and 10mgs tarde and

hydrocortisone 20mg mane and 10mg tarde). This will allow us to assess the effect of different hydrocortisone exposure rates on cortisol metabolism within individuals. We are also currently performing a follow up double blind placebo controlled study of the effect of GH replacement therapy on corticosteroid metabolites in this patient group.

Chapter 7

Discussion and Future Directions

7.1 Discussion

Glucocorticoids in excess lead to several adverse consequences including insulin resistance, hypertension, osteoporosis, obesity and muscle loss/ weakness (myopathy) (1). Ageing is also associated with similar co-morbidities. In particular, in ageing there is a significant loss in muscle mass and strength or sarcopaenia as described in detail in Section 1.3. Glucocorticoid mediated myopathy and sarcopaenia have several phenotypic, histological and molecular similarities (Section 1.3 and 1.5). There is conflicting data with regard to changes in circulating levels of glucocorticoids in ageing (126, 127). However, in recent years the regulation of glucocorticoids at a tissue level by isozymes of 11 β-HSD has received much interest (2). In particular, 11 β-HSD1 which interconvert's inactive to active GC *in vivo* has been shown to have an important role in adipose tissue, bone, liver and brain, there is however less data regarding 11 β-HSD1 in skeletal muscle (2). There is evidence from our group that 11 β-HSD1 increases in bone and skin with age (5, 6).

We hypothesised that 11 β-HSD1 is an important regulator of skeletal muscle GC exposure and may have a role in GC mediated myopathy. Furthermore, given the similarities between muscle in sarcopaenic subjects and those with GC mediated myopathy and the potential that 11 β-HSD1 is increased with age we hypothesised that 11 β-HSD1 could play a key role in the sarcopaenic process by increasing local GC levels within muscle and leading to alterations in molecular pathways associated with GC mediated myopathy.

We have shown in Chapter 3 that 11 β-HSD1 is expressed and has oxoreductase activity in skeletal muscle. There was also a suggestion of fibre type

predominance in 11 β-HSD1 expression, however, our experiments to date have not fully elucidated this and further work is needed in this area.

11 β-HSD1 is upregulated in the C2C12 murine skeletal muscle cell line by GC exposure. Importantly, 11 β-HSD1 is upregulated by both active (corticosterone, B) and inactive steroids (11-dehydrocorticosterone, A). 11-dehydrocorticosterone requires activation to B by 11 β-HSD1 for biological activity, therefore within C2C12 cells the activation of A to B by 11 β-HSD1 leads to upregulation of 11 β-HSD1. In clinical practice the effect of exposure of skeletal muscle to supraphysiological glucocorticoid concentrations in serum (in endogenous and exogenous Cushing's syndrome) may be further affected by 11 β-HSD1 activity within muscles. Muscle specific activation of the inactive glucocorticoid cortisone which is produced from cortisol by the dehydrogenase activity of 11 β-HSD2 in the kidney (which is known to be significantly elevated in Cushing's syndrome) (317) may lead to a more severe muscle phenotype. The increase in active GC within C2C12 cells is associated with upregulation of key atrophy related genes.

In addition to this upregulation of atrophy genes there is also downregulation of the insulin/ IGF-I-AI3K-Akt-mTOR hypertrophy pathway and in particular GC treatment lead to a decrease in total IRS1 and increase in the inactivating Ser307 phosphorylation of IRS1 which has been shown to negatively regulate insulin signalling through multiple mechanisms including decreased affinity for the insulin receptor and increased degradation. These changes can be reversed through the inhibition of 11 β-HSD1 with the non-specific inhibitor glycyrrhetinic acid.

A key mechanism for muscle repair and regeneration is the proliferation and differentiation of myoblasts into myotubules/ myofibres (8, 11). We have shown

that GCs inhibit myoblast proliferation but, interestingly, inhibition of 11 β-HSD1 leads to increased myoblast proliferation, the exact mechanisms and consequences of this need to be elucidated.

The combination of the above results show that 11 β-HSD1 impacts on both atrophy and hypertrophy pathways in skeletal muscle and also the availability of myoblasts for muscle regeneration/ repair, the net result of these changes being an increase in the severity of GC mediated myopathy (as summarised in Figure 4.11).

We have shown that there is increased 11 β-HSD1 activity and expression in some but not all tissues in old versus young mice. This increase in local GC production is associated with changes in GC mediated myopathy genes. Importantly, however there is a fibre type specific response in these markers. This is important as both GC mediated myopathy and sarcopaenia show a Type IIb fibre Type preponderance with relatively little effect on Type I fibres. To assess the role of 11 β-HSD1 on ageing muscle a global 11 β-HSD1KO mouse was developed. The 11 β-HSD1KO did not show any changes in body weight or muscle strength compared to its WT littermates, however it did show an increase in adrenal weight due to HPA axis activation, which leads to increased circulating GC as a compensatory mechanism, as shown in previous studies (159, 330, 336, 338). At the molecular level, there is evidence in the 11 β-HSD1KO mouse of improvement in atrophy related markers in the tibialis anterior with decreased levels of expression of MAO and a trend to decrease expression of MAFbx. This may be interpreted as the decrease in locally generated cortisol leading to decreased GC mediated myopathy in these usually GC sensitive muscle fibres.

There is also evidence in the soleus muscle of the 11 β-HSD1KO of increased atrophy related genes including MAFbx, MAO and a trend to an increase in caplain. Type I fibres are resistant to GC mediated myopathy and the decrease in locally generated GC in the 11 β-HSD1KO appears to have a detrimental effect. Further work is required to examine fibre type specificity of muscle changes in the 11 β-HSD1KO.

Patients with pituitary hormone deficiency (hypopituitarism) have increased morbidity and mortality (339), however, the exact mechanisms underpinning this have not been fully elucidated. There are a number of possible factors including the effect of the pituitary hormone deficiencies themselves or the hormonal therapy used as replacement. The main deficiencies implicated in this are GH and ACTH deficiency, as are their related treatments, which is covered in detail in Section 6.1.2 and 6.1.3, respectively.

The treatment of ACTH deficiency with hydrocortisone is unphysiological as it does not fully replicate the diurnal rhythm of cortisol secretion and may lead to supraphysiological circulating GC concentrations. Over the last few years there has been increasing awareness that the replacement doses of hydrocortisone that were classically used were greater than the cortisol production rate in healthy controls (145, 146). In ACTH deficiency, median doses of hydrocortisone of 29.5 ± 1.2mg lead to peak cortisol and mean daily cortisol concentrations above the normal range, which in one study lead to a dose reduction in 75% of patients (387). Studies in patients with partial ACTH deficiency have shown similar day curves to healthy controls suggesting that these patients may be over-treated by conventional steroid replacement therapy (388) and there is evidence of adverse

metabolic profile in hypopituitary patients on higher doses of glucocorticoid replacement therapy. (389).

GH acting via IGF-I inhibits the autocrine generation of cortisol through inhibition of 11β-HSD1 (182). The phenotype of GHD in the context of hypopituitarism may, in part be mediated through increased 11β-HSD1 activity (182) as in these GHD patients studies have shown a decrease in 11β-HSD1 oxoreductase activity (183, 184) without any change in 11β-HSD2 activity following GH treatment.

It was our hypothesis is that 11 β-HSD1 is upregulated in hypopituitarism due to unphysiological glucocorticoid replacement therapy and the ensuing increase in tissue specific cortisol generation contributes to the changes in body composition reported in hypopituitarism. There were significant abnormalities in corticosteroid metabolite profiles in ACTH deficient patients (receiving hydrocortisone) when compared to normal controls and hypopituitary patients with normal ACTH reserve. The abnormalities reported were primarily due to an increase in glucocorticoid metabolites (Figure 6.4). There were increases in total cortisol metabolites and THF+allTHF/The ratio (a marker of 11 β-HSD1 activity) in patients on hydrocortisone therapy, and this was dose related. Importantly, however there were no change in urinary free cortisol levels with increasing doses of hydrocortisone, showing that increased doses of hydrocortisone were not simply excreted in the urine as they reached the renal threshold, but rather underwent intracellular metabolism.

We found that the changes in higher hydrocortisone doses and the alterations seen in corticosteroid metabolites are associated with an increased visceral adiposity, as shown by increased WHR in patients on >20mgs of hydrocortisone

per day (Figure 6.6.c) and the strong positive correlation between total F metabolites and ratio of central to thigh fat (Figure 6.8.d). Visceral adiposity is known in the general population to be associated with insulin resistance or diabetes mellitus, hypercholesterolaemia and hypertension (342, 343). Bujalska et al. first proposed that excessive activity of 11 β-HSD1 enzyme within visceral adipose tissue could lead to increased adipose tissue levels of glucococorticoids and 'Cushing's disease of the omentum' (413). The increase in both THF+alloTHF/THE ratios and total cortisol metabolites in our cohort of patients taking hydrocortisone therapy could lead to significant changes in adipose tissue biology.

7.2. Future Directions

The results in this thesis increase our knowledge of the role of 11 β-HSD1 in skeletal muscle and its potential roles in glucocorticoid mediated myopathy, sarcopaenia and the cortisol metabolism in patients receiving cortisol replacement therapy, however, there are many areas to be clarified further.

7.2.1. Lab based studies currently underway within the unit

1. Elucidation of molecular markers of changes in proliferation associated with glucocorticoid excess and inhibition of 11 β-HSD1.

2. Development of a muscle specific 11 β-HSD1KO mouse to study the effect of tissue specific decrease in glucocorticoid exposure without the compensatory hypothalamic pituitary adrenal axis activation seen in the global 11 β-HSD1KO mouse.

3. Rodent model to assess the impact of 11 β-HSD1 pharmacological inhibition on glucocorticoid induced myopathy in mice treated with high dose glucocorticoids.

4. Microarray analysis of soleus and tibialis anterior of old WT vs. 11 β-HSD1KO to assess fibre specific changes further.

7.2.2. Clinical studies currently underway within the unit

1. We have recently received funding from the European Research Council to further investigate the role of carry out a clinical study assessing the role of 11 β-HSD1 in ageing. This will involve a clinical study assessing 11 β-HSD1 activity and expression with increasing age and correlate this with markers of muscle strength and mass.

2. To investigate the effect of hydrocortisone replacement on corticosteroid metabolites we are currently performing a study in collaboration with Professor Chris Thompson and Dr Amar Agha at Beaumont Hospital, Dublin which will involve a cross over study of male patients only, with ACTH deficiency with each patient receiving hydrocortisone therapy at different doses (hydrocortisone 10mgs mane and 5mgs tarde. hydrocortisone 10mgs mane and 10mgs tarde and hydrocortisone 20mgs mane and 10mgs tarde). This will allow us assess the effect of different hydrocortisone exposure rates on corticosterone metabolism within individuals.

3. To assess further the effect of GH treatment on 11 β-HSD1 and corticosteroid metabolites (in patients with and without co-existing ACTH deficiency) we are also currently performing a follow up double blind placebo controlled study of the effect of GH replacement therapy on corticosteroid metabolites.

7.3 Conclusions

11 β-HSD1 is biologically active in skeletal muscle and may play a key role in the development of glucocorticoid-mediated myopathy and age related sarcopaenia. The development of 11 β-HSD1 inhibitors, which are being developed mainly for treatment of the metabolic syndrome, may have a role to play in age related sarcopaenia. Patients treated with unphysiological hydrocortisone replacement therapy have significant alterations in cortisol metabolites, which is associated with an adverse body composition.

Further studies are required to assess in more detail the role of 11 β-HSD1 in GC mediated myopathy (in particular the fibre specificity), the impact of 11 β-HSD1 on sarcopaenia in muscle specific KO models and inhibitor studies and the impact of the new modified release hydrocortisone on cortisol metabolism.

References

1. Newell-Price J, Bertagna X, Grossman AB, Nieman LK. Cushing's syndrome. Lancet. 2006;367(9522):1605-17.
2. Tomlinson JW, Walker EA, Bujalska IJ, Draper N, Lavery GG, Cooper MS, et al. 11beta-hydroxysteroid dehydrogenase type 1: a tissue-specific regulator of glucocorticoid response. EndocrRev. 2004;25(5):831-66.
3. Kado DM, Browner WS, Palermo L, Nevitt MC, Genant HK, Cummings SR. Vertebral fractures and mortality in older women: a prospective study. Study of Osteoporotic Fractures Research Group. Arch Intern Med. 1999;159(11):1215-20.
4. Kamel HK. Sarcopenia and aging. NutrRev. 2003;61(5 Pt 1):157-67.
5. Cooper MS, Rabbitt EH, Goddard PE, Bartlett WA, Hewison M, Stewart PM. Osteoblastic 11beta-hydroxysteroid dehydrogenase type 1 activity increases with age and glucocorticoid exposure. JBone MinerRes. 2002;17(6):979-86.
6. Tiganescu A, Walker EA, Hardy RS, Mayes AE, Stewart PM. Localization, age- and site-dependent expression, and regulation of 11beta-hydroxysteroid dehydrogenase type 1 in skin. J Invest Dermatol. 2011 Jan;131(1):30-6.
7. Yau JL, McNair KM, Noble J, Brownstein D, Hibberd C, Morton N, et al. Enhanced hippocampal long-term potentiation and spatial learning in aged 11beta-hydroxysteroid dehydrogenase type 1 knock-out mice. J Neurosci. 2007 Sep 26;27(39):10487-96.
8. Lluis F, Perdiguero E, Nebreda AR, Munoz-Canoves P. Regulation of skeletal muscle gene expression by p38 MAP kinases. Trends Cell Biol. 2006 Jan;16(1):36-44.
9. Lassar AB, Davis RL, Wright WE, Kadesch T, Murre C, Voronova A, et al. Functional activity of myogenic HLH proteins requires hetero-oligomerization with E12/E47-like proteins in vivo. Cell. 1991 Jul 26;66(2):305-15.
10. Puri PL, Wu Z, Zhang P, Wood LD, Bhakta KS, Han J, et al. Induction of terminal differentiation by constitutive activation of p38 MAP kinase in human rhabdomyosarcoma cells. Genes Dev. 2000 Mar 1;14(5):574-84.
11. Moss FP, Leblond CP. Satellite cells as the source of nuclei in muscles of growing rats. Anat Rec. 1971 Aug;170(4):421-35.
12. Geeves MA, Holmes KC. Structural mechanism of muscle contraction. Annu Rev Biochem. 1999;68:687-728.
13. Morgan SA. The impact of glucocorticoids upon the insulin sensitivity of skeletal muscle [PhD]. Birmingham: University of Birmingham; 2010.
14. Spangenburg EE, Booth FW. Molecular regulation of individual skeletal muscle fibre types. Acta Physiol Scand. [1158 pii]. 2003;178(4):413-24.
15. Pereira Sant'Ana JA, Ennion S, Sargeant AJ, Moorman AF, Goldspink G. Comparison of the molecular, antigenic and ATPase determinants of fast myosin heavy chains in rat and human: a single-fibre study. Pflugers Arch. 1997;435(1):151-63.
16. Pette D, Staron RS. Myosin isoforms, muscle fiber types, and transitions. MicroscResTech. [10.1002/1097-0029(20000915)50:6<500::AID-JEMT7>3.0.CO;2-7 pii ;10.1002/1097-0029(20000915)50:6<500::AID-JEMT7>3.0.CO;2-7 doi]. 2000;50(6):500-9.
17. Lords THo. Ageing Scientific Aspects2005.
18. Baumgartner RN, Koehler KM, Gallagher D, Romero L, Heymsfield SB, Ross RR, et al. Epidemiology of sarcopenia among the elderly in New Mexico. Am J Epidemiol. 1998;147(8):755-63.
19. Melton LJ, III, Khosla S, Riggs BL. Epidemiology of sarcopenia. Mayo Clin Proc. 2000;75 Suppl:S10-S2.

20. Iannuzzi-Sucich M, Prestwood KM, Kenny AM. Prevalence of sarcopenia and predictors of skeletal muscle mass in healthy, older men and women. J GerontolA Biol Sci Med Sci. 2002;57(12):M772-M7.
21. Bendall MJ, Bassey EJ, Pearson MB. Factors affecting walking speed of elderly people. Age Ageing. 1989;18(5):327-32.
22. Fiatarone MA, O'Neill EF, Ryan ND, Clements KM, Solares GR, Nelson ME, et al. Exercise training and nutritional supplementation for physical frailty in very elderly people. N Engl J Med. 1994;330(25):1769-75.
23. Kenney WL, Buskirk ER. Functional consequences of sarcopenia: effects on thermoregulation. J GerontolA Biol Sci Med Sci. 1995;50 Spec No:78-85.
24. Vellas B, Baumgartner RN, Wayne SJ, Conceicao J, Lafont C, Albarede JL, et al. Relationship between malnutrition and falls in the elderly. Nutrition. 1992;8(2):105-8.
25. Lords THo. Ageing Scientific Aspects2005.
26. Allen TH, Anderson EC, Langham WH. Total body potassium and gross body composition in relation to age. J Gerontol. 1960;15:348-57.
27. Young A, Stokes M, Crowe M. Size and strength of the quadriceps muscles of old and young women. Eur J Clin Invest. 1984;14(4):282-7.
28. Young A, Stokes M, Crowe M. The size and strength of the quadriceps muscles of old and young men. Clin Physiol. 1985;5(2):145-54.
29. Lexell J, Taylor CC, Sjostrom M. What is the cause of the ageing atrophy? Total number, size and proportion of different fiber types studied in whole vastus lateralis muscle from 15- to 83-year-old men. J NeurolSci. 1988;84(2-3):275-94.
30. Lindboe CF, Torvik A. The effects of ageing, cachexia and neoplasms on striated muscle. Quantitative histological and histochemical observations on an autopsy material. Acta Neuropathol. 1982;57(2-3):85-92.
31. Scelsi R, Marchetti C, Poggi P. Histochemical and ultrastructural aspects of m. vastus lateralis in sedentary old people (age 65--89 years). Acta Neuropathol. 1980;51(2):99-105.
32. Rice CL, Cunningham DA, Paterson DH, Lefcoe MS. Arm and leg composition determined by computed tomography in young and elderly men. Clin Physiol. 1989;9(3):207-20.
33. Goodpaster BH, Carlson CL, Visser M, Kelley DE, Scherzinger A, Harris TB, et al. Attenuation of skeletal muscle and strength in the elderly: The Health ABC Study. J ApplPhysiol. 2001;90(6):2157-65.
34. Ryan AS, Nicklas BJ. Age-related changes in fat deposition in mid-thigh muscle in women: relationships with metabolic cardiovascular disease risk factors. Int J Obes Relat Metab Disord. 1999;23(2):126-32.
35. Song MY, Ruts E, Kim J, Janumala I, Heymsfield S, Gallagher D. Sarcopenia and increased adipose tissue infiltration of muscle in elderly African American women. Am J Clin Nutr. 2004;79(5):874-80.
36. Visser M, Kritchevsky SB, Goodpaster BH, Newman AB, Nevitt M, Stamm E, et al. Leg muscle mass and composition in relation to lower extremity performance in men and women aged 70 to 79: the health, aging and body composition study. J Am GeriatrSoc. [jgs50217 pii]. 2002;50(5):897-904.
37. Jakobsson F, Borg K, Edstrom L. Fibre-type composition, structure and cytoskeletal protein location of fibres in anterior tibial muscle. Comparison between young adults and physically active aged humans. Acta Neuropathol. 1990;80(5):459-68.
38. McCully KK, Fielding RA, Evans WJ, Leigh JS, Jr., Posner JD. Relationships between in vivo and in vitro measurements of metabolism in young and old human calf muscles. J ApplPhysiol. 1993;75(2):813-9.

39. Orlander J, Kiessling KH, Larsson L, Karlsson J, Aniansson A. Skeletal muscle metabolism and ultrastructure in relation to age in sedentary men. Acta Physiol Scand. 1978;104(3):249-61.
40. Proctor DN, Balagopal P, Nair KS. Age-related sarcopenia in humans is associated with reduced synthetic rates of specific muscle proteins. J Nutr. 1998;128(2 Suppl):351S-5S.
41. Basu R, Basu A, Nair KS. Muscle changes in aging. J NutrHealth Aging. 2002;6(5):336-41.
42. Payette H, Roubenoff R, Jacques PF, Dinarello CA, Wilson PW, Abad LW, et al. Insulin-like growth factor-1 and interleukin 6 predict sarcopenia in very old community-living men and women: the Framingham Heart Study. J Am GeriatrSoc. [51407 pii]. 2003;51(9):1237-43.
43. Roubenoff R, Parise H, Payette HA, Abad LW, D'Agostino R, Jacques PF, et al. Cytokines, insulin-like growth factor 1, sarcopenia, and mortality in very old community-dwelling men and women: the Framingham Heart Study. Am J Med. [S0002934303004789 pii]. 2003;115(6):429-35.
44. Harman D. Aging: a theory based on free radical and radiation chemistry. J Gerontol. 1956;11(3):298-300.
45. Vandenburgh H, Chromiak J, Shansky J, Del TM, Lemaire J. Space travel directly induces skeletal muscle atrophy. FASEB J. 1999;13(9):1031-8.
46. Corpas E, Harman SM, Blackman MR. Human growth hormone and human aging. Endocr Rev. 1993;14(1):20-39.
47. Phillips T, Leeuwenburgh C. Muscle fiber specific apoptosis and TNF-alpha signaling in sarcopenia are attenuated by life-long calorie restriction. FASEB J. [04-2870fje pii ;10.1096/fj.04-2870fje doi]. 2005;19(6):668-70.
48. Morley JE. Anorexia, sarcopenia, and aging. Nutrition. [S0899-9007(01)00574-3 pii]. 2001;17(7-8):660-3.
49. Mitch WE, Goldberg AL. Mechanisms of muscle wasting. The role of the ubiquitin-proteasome pathway. N Engl J Med. 1996;335(25):1897-905.
50. McCormick KM, Thomas DP. Exercise-induced satellite cell activation in senescent soleus muscle. J ApplPhysiol. 1992;72(3):888-93.
51. Cortopassi GA, Shibata D, Soong NW, Arnheim N. A pattern of accumulation of a somatic deletion of mitochondrial DNA in aging human tissues. ProcNatlAcadSci USA. 1992;89(16):7370-4.
52. Meneilly GS, Elliot T, Bryer-Ash M, Floras JS. Insulin-mediated increase in blood flow is impaired in the elderly. J Clin Endocrinol Metab. 1995;80(6):1899-903.
53. Guillet C, Boirie Y. Insulin resistance: a contributing factor to age-related muscle mass loss? Diabetes Metab. [MDOI-DM-12-2005-31-HS2-1262-3636-101019-200509652 pii]. 2005;31 Spec No 2:5S20-5S6.
54. Guillet C, Prod'homme M, Balage M, Gachon P, Giraudet C, Morin L, et al. Impaired anabolic response of muscle protein synthesis is associated with S6K1 dysregulation in elderly humans. FASEB J. [10.1096/fj.03-1341fje doi ;03-1341fje pii]. 2004;18(13):1586-7.
55. Rasmussen BB, Fujita S, Wolfe RR, Mittendorfer B, Roy M, Rowe VL, et al. Insulin resistance of muscle protein metabolism in aging. FASEB J. [05-4607fje pii ;10.1096/fj.05-4607fje doi]. 2006;20(6):768-9.
56. Lexell J. Human aging, muscle mass, and fiber type composition. J GerontolA Biol Sci Med Sci. 1995;50 Spec No:11-6.

57. Ryall JG, Schertzer JD, Lynch GS. Cellular and molecular mechanisms underlying age-related skeletal muscle wasting and weakness. Biogerontology. [10.1007/s10522-008-9131-0 doi]. 2008;9(4):213-28.
58. Renault V, Thornell LE, Eriksson PO, Butler-Browne G, Mouly V. Regenerative potential of human skeletal muscle during aging. Aging Cell. 2002 Dec;1(2):132-9.
59. Snow MH. The effects of aging on satellite cells in skeletal muscles of mice and rats. Cell Tissue Res. 1977 Dec 19;185(3):399-408.
60. Brack AS, Conboy MJ, Roy S, Lee M, Kuo CJ, Keller C, et al. Increased Wnt signaling during aging alters muscle stem cell fate and increases fibrosis. Science. 2007 Aug 10;317(5839):807-10.
61. Roth SM, Martel GF, Ivey FM, Lemmer JT, Metter EJ, Hurley BF, et al. Skeletal muscle satellite cell populations in healthy young and older men and women. Anat Rec. 2000 Dec 1;260(4):351-8.
62. Dreyer HC, Blanco CE, Sattler FR, Schroeder ET, Wiswell RA. Satellite cell numbers in young and older men 24 hours after eccentric exercise. Muscle Nerve. 2006 Feb;33(2):242-53.
63. Verdijk LB, Koopman R, Schaart G, Meijer K, Savelberg HH, van Loon LJ. Satellite cell content is specifically reduced in type II skeletal muscle fibers in the elderly. Am J Physiol Endocrinol Metab. 2007 Jan;292(1):E151-7.
64. Musaro A, Cusella De Angelis MG, Germani A, Ciccarelli C, Molinaro M, Zani BM. Enhanced expression of myogenic regulatory genes in aging skeletal muscle. Exp Cell Res. 1995 Nov;221(1):241-8.
65. Kostrominova TY, Macpherson PC, Carlson BM, Goldman D. Regulation of myogenin protein expression in denervated muscles from young and old rats. Am J Physiol Regul Integr Comp Physiol. 2000 Jul;279(1):R179-88.
66. Alway SE, Degens H, Krishnamurthy G, Smith CA. Potential role for Id myogenic repressors in apoptosis and attenuation of hypertrophy in muscles of aged rats. Am J Physiol Cell Physiol. 2002 Jul;283(1):C66-76.
67. Dedkov EI, Kostrominova TY, Borisov AB, Carlson BM. MyoD and myogenin protein expression in skeletal muscles of senile rats. Cell Tissue Res. 2003 Mar;311(3):401-16.
68. Thomas M, Langley B, Berry C, Sharma M, Kirk S, Bass J, et al. Myostatin, a negative regulator of muscle growth, functions by inhibiting myoblast proliferation. JBiolChem. [10.1074/jbc.M004356200 doi ;M004356200 pii]. 2000;275(51):40235-43.
69. Dulic V, Stein GH, Far DF, Reed SI. Nuclear accumulation of p21Cip1 at the onset of mitosis: a role at the G2/M-phase transition. MolCell Biol. 1998;18(1):546-57.
70. Joulia-Ekaza D, Cabello G. The myostatin gene: physiology and pharmacological relevance. CurrOpinPharmacol. [S1471-4892(07)00050-1 pii ;10.1016/j.coph.2006.11.011 doi]. 2007;7(3):310-5.
71. Allen DL, Unterman TG. Regulation of myostatin expression and myoblast differentiation by FoxO and SMAD transcription factors. AmJPhysiol Cell Physiol. [00542.2005 pii ;10.1152/ajpcell.00542.2005 doi]. 2007;292(1):C188-C99.
72. Joulia D, Bernardi H, Garandel V, Rabenoelina F, Vernus B, Cabello G. Mechanisms involved in the inhibition of myoblast proliferation and differentiation by myostatin. ExpCell Res. [S0014482703000740 pii]. 2003;286(2):263-75.
73. Kawada S, Tachi C, Ishii N. Content and localization of myostatin in mouse skeletal muscles during aging, mechanical unloading and reloading. J Muscle Res Cell Motil. 2001;22(8):627-33.

74. Baumann AP, Ibebunjo C, Grasser WA, Paralkar VM. Myostatin expression in age and denervation-induced skeletal muscle atrophy. J Musculoskelet Neuronal Interact. 2003 Mar;3(1):8-16.
75. Welle S, Bhatt K, Shah B, Thornton C. Insulin-like growth factor-1 and myostatin mRNA expression in muscle: comparison between 62-77 and 21-31 yr old men. Exp Gerontol. 2002 Jun;37(6):833-9.
76. Raue U, Slivka D, Jemiolo B, Hollon C, Trappe S. Myogenic gene expression at rest and after a bout of resistance exercise in young (18-30 yr) and old (80-89 yr) women. J Appl Physiol. 2006 Jul;101(1):53-9.
77. Sato T, Akatsuka H, Kito K, Tokoro Y, Tauchi H, Kato K. Age changes in size and number of muscle fibers in human minor pectoral muscle. MechAgeing Dev. [0047-6374(84)90156-8 pii]. 1984;28(1):99-109.
78. Volpi E, Mittendorfer B, Rasmussen BB, Wolfe RR. The response of muscle protein anabolism to combined hyperaminoacidemia and glucose-induced hyperinsulinemia is impaired in the elderly. J Clin Endocrinol Metab. 2000;85(12):4481-90.
79. Frost RA, Nystrom GJ, Jefferson LS, Lang CH. Hormone, cytokine, and nutritional regulation of sepsis-induced increases in atrogin-1 and MuRF1 in skeletal muscle. AmJPhysiol EndocrinolMetab. [00359.2006 pii ;10.1152/ajpendo.00359.2006 doi]. 2007;292(2):E501-E12.
80. Tiao G, Fagan J, Roegner V, Lieberman M, Wang JJ, Fischer JE, et al. Energy-ubiquitin-dependent muscle proteolysis during sepsis in rats is regulated by glucocorticoids. JClinInvest. [10.1172/JCI118421 doi]. 1996;97(2):339-48.
81. Sacheck JM, Hyatt JP, Raffaello A, Jagoe RT, Roy RR, Edgerton VR, et al. Rapid disuse and denervation atrophy involve transcriptional changes similar to those of muscle wasting during systemic diseases. FASEB J. [fj.06-6604com pii ;10.1096/fj.06-6604com doi]. 2007;21(1):140-55.
82. Glass DJ. Signalling pathways that mediate skeletal muscle hypertrophy and atrophy. NatCell Biol. [10.1038/ncb0203-87 doi ;ncb0203-87 pii]. 2003;5(2):87-90.
83. Solomon V, Goldberg AL. Importance of the ATP-ubiquitin-proteasome pathway in the degradation of soluble and myofibrillar proteins in rabbit muscle extracts. JBiolChem. 1996;271(43):26690-7.
84. Sandri M, Sandri C, Gilbert A, Skurk C, Calabria E, Picard A, et al. Foxo transcription factors induce the atrophy-related ubiquitin ligase atrogin-1 and cause skeletal muscle atrophy. Cell. [S0092867404004003 pii]. 2004;117(3):399-412.
85. Rena G, Guo S, Cichy SC, Unterman TG, Cohen P. Phosphorylation of the transcription factor forkhead family member FKHR by protein kinase B. JBiolChem. 1999;274(24):17179-83.
86. Stitt TN, Drujan D, Clarke BA, Panaro F, Timofeyva Y, Kline WO, et al. The IGF-1/PI3K/Akt pathway prevents expression of muscle atrophy-induced ubiquitin ligases by inhibiting FOXO transcription factors. MolCell. [S1097276504002114 pii]. 2004;14(3):395-403.
87. Iranmanesh A, Lizarralde G, Veldhuis JD. Age and relative adiposity are specific negative determinants of the frequency and amplitude of growth hormone (GH) secretory bursts and the half-life of endogenous GH in healthy men. J Clin Endocrinol Metab. 1991;73(5):1081-8.
88. Welle S, Brooks AI, Delehanty JM, Needler N, Thornton CA. Gene expression profile of aging in human muscle. Physiol Genomics. [10.1152/physiolgenomics.00049.2003 doi ;00049.2003 pii]. 2003;14(2):149-59.

89. Whitman SA, Wacker MJ, Richmond SR, Godard MP. Contributions of the ubiquitin-proteasome pathway and apoptosis to human skeletal muscle wasting with age. Pflugers Arch. [10.1007/s00424-005-1473-8 doi]. 2005;450(6):437-46.
90. Clavel S, Coldefy AS, Kurkdjian E, Salles J, Margaritis I, Derijard B. Atrophy-related ubiquitin ligases, atrogin-1 and MuRF1 are up-regulated in aged rat Tibialis Anterior muscle. MechAgeing Dev. [S0047-6374(06)00170-9 pii ;10.1016/j.mad.2006.07.005 doi]. 2006;127(10):794-801.
91. Edstrom E, Altun M, Hagglund M, Ulfhake B. Atrogin-1/MAFbx and MuRF1 are downregulated in aging-related loss of skeletal muscle. J GerontolA Biol Sci Med Sci. [61/7/663 pii]. 2006;61(7):663-74.
92. Deruisseau KC, Kavazis AN, Powers SK. Selective downregulation of ubiquitin conjugation cascade mRNA occurs in the senescent rat soleus muscle. Exp Gerontol. [S0531-5565(05)00080-X pii ;10.1016/j.exger.2005.04.005 doi]. 2005;40(6):526-31.
93. Ralliere C, Tauveron I, Taillandier D, Guy L, Boiteux JP, Giraud B, et al. Glucocorticoids do not regulate the expression of proteolytic genes in skeletal muscle from Cushing's syndrome patients. JClinEndocrinolMetab. 1997;82(9):3161-4.
94. Lexell J, Downham D, Sjostrom M. Distribution of different fibre types in human skeletal muscles. Fibre type arrangement in m. vastus lateralis from three groups of healthy men between 15 and 83 years. J NeurolSci. 1986;72(2-3):211-22.
95. Andersen JL. Muscle fibre type adaptation in the elderly human muscle. ScandJMedSciSports. [0299 pii]. 2003;13(1):40-7.
96. Zhou MY, Klitgaard H, Saltin B, Roy RR, Edgerton VR, Gollnick PD. Myosin heavy chain isoforms of human muscle after short-term spaceflight. J ApplPhysiol. 1995;78(5):1740-4.
97. Klitgaard H, Zhou M, Schiaffino S, Betto R, Salviati G, Saltin B. Ageing alters the myosin heavy chain composition of single fibres from human skeletal muscle. Acta Physiol Scand. 1990;140(1):55-62.
98. Essen-Gustavsson B, Borges O. Histochemical and metabolic characteristics of human skeletal muscle in relation to age. Acta Physiol Scand. 1986;126(1):107-14.
99. Larsson L, Sjodin B, Karlsson J. Histochemical and biochemical changes in human skeletal muscle with age in sedentary males, age 22--65 years. Acta Physiol Scand. 1978;103(1):31-9.
100. Andersen JL, Terzis G, Kryger A. Increase in the degree of coexpression of myosin heavy chain isoforms in skeletal muscle fibers of the very old. Muscle Nerve. [10.1002/(SICI)1097-4598(199904)22:4<449::AID-MUS4>3.0.CO;2-2 pii]. 1999;22(4):449-54.
101. Danon MJ, Schliselfeld LH. Study of skeletal muscle glycogenolysis and glycolysis in chronic steroid myopathy, non-steroid histochemical type-2 fiber atrophy, and denervation. ClinBiochem. [S0009-9120(06)00282-7 pii ;10.1016/j.clinbiochem.2006.09.002 doi]. 2007;40(1-2):46-51.
102. Horber FF, Scheidegger JR, Grunig BE, Frey FJ. Evidence that prednisone-induced myopathy is reversed by physical training. JClinEndocrinolMetab. 1985;61(1):83-8.
103. Khaleeli AA, Betteridge DJ, Edwards RH, Round JM, Ross EJ. Effect of treatment of Cushing's syndrome on skeletal muscle structure and function. ClinEndocrinol(Oxf). 1983;19(4):547-56.
104. Khaleeli AA, Edwards RH, Gohil K, McPhail G, Rennie MJ, Round J, et al. Corticosteroid myopathy: a clinical and pathological study. ClinEndocrinol(Oxf). 1983;18(2):155-66.

105. Marolda M, Palma V, Camporeale FS, Carandente M, Cioffi M, Orsini AV, et al. Steroid myopathy: clinical and immunohistochemical study of a case. ItalJNeurolSci. 1991;12(4):409-13.
106. Moukas M, Vassiliou MP, Amygdalou A, Mandragos C, Takis F, Behrakis PK. Muscular mass assessed by ultrasonography after administration of low-dose corticosteroids and muscle relaxants in critically ill hemiplegic patients. ClinNutr. [S0261561401905321 pii]. 2002;21(4):297-302.
107. Pleasure DE, Walsh GO, Engel WK. Atrophy of skeletal muscle in patients with Cushing's syndrome. ArchNeurol. 1970;22(2):118-25.
108. Rebuffe-Scrive M, Krotkiewski M, Elfverson J, Bjorntorp P. Muscle and adipose tissue morphology and metabolism in Cushing's syndrome. JClinEndocrinolMetab. 1988;67(6):1122-8.
109. Baumgartner RN, Waters DL, Gallagher D, Morley JE, Garry PJ. Predictors of skeletal muscle mass in elderly men and women. MechAgeing Dev. [S0047-6374(98)00130-4 pii]. 1999;107(2):123-36.
110. Morley JE, Kaiser F, Raum WJ, Perry HM, III, Flood JF, Jensen J, et al. Potentially predictive and manipulable blood serum correlates of aging in the healthy human male: progressive decreases in bioavailable testosterone, dehydroepiandrosterone sulfate, and the ratio of insulin-like growth factor 1 to growth hormone. ProcNatlAcadSci USA. 1997;94(14):7537-42.
111. Sih R, Morley JE, Kaiser FE, Perry HM, III, Patrick P, Ross C. Testosterone replacement in older hypogonadal men: a 12-month randomized controlled trial. J Clin Endocrinol Metab. 1997;82(6):1661-7.
112. Snyder PJ, Peachey H, Hannoush P, Berlin JA, Loh L, Lenrow DA, et al. Effect of testosterone treatment on body composition and muscle strength in men over 65 years of age. J Clin Endocrinol Metab. 1999;84(8):2647-53.
113. Tenover JS. Effects of testosterone supplementation in the aging male. J Clin Endocrinol Metab. 1992;75(4):1092-8.
114. Kelijman M. Age-related alterations of the growth hormone/insulin-like-growth-factor I axis. J Am GeriatrSoc. 1991;39(3):295-307.
115. Ashton WS, Degnan BM, Daniel A, Francis GL. Testosterone increases insulin-like growth factor-1 and insulin-like growth factor-binding protein. Ann Clin Lab Sci. 1995;25(5):381-8.
116. Flynn MA, Weaver-Osterholtz D, Sharpe-Timms KL, Allen S, Krause G. Dehydroepiandrosterone replacement in aging humans. J Clin Endocrinol Metab. 1999;84(5):1527-33.
117. Veldhuis JD, Liem AY, South S, Weltman A, Weltman J, Clemmons DA, et al. Differential impact of age, sex steroid hormones, and obesity on basal versus pulsatile growth hormone secretion in men as assessed in an ultrasensitive chemiluminescence assay. J Clin Endocrinol Metab. 1995;80(11):3209-22.
118. Popovic V, Leal A, Micic D, Koppeschaar HP, Torres E, Paramo C, et al. GH-releasing hormone and GH-releasing peptide-6 for diagnostic testing in GH-deficient adults. Lancet. [S0140-6736(00)02755-0 pii ;10.1016/S0140-6736(00)02755-0 doi]. 2000;356(9236):1137-42.
119. Landin-Wilhelmsen K, Wilhelmsen L, Lappas G, Rosen T, Lindstedt G, Lundberg PA, et al. Serum insulin-like growth factor I in a random population sample of men and women: relation to age, sex, smoking habits, coffee consumption and physical activity, blood pressure and concentrations of plasma lipids, fibrinogen, parathyroid hormone and osteocalcin. Clin Endocrinol (Oxf). 1994;41(3):351-7.

120. Blackman MR, Sorkin JD, Munzer T, Bellantoni MF, Busby-Whitehead J, Stevens TE, et al. Growth hormone and sex steroid administration in healthy aged women and men: a randomized controlled trial. JAMA. [joc21207 pii]. 2002;288(18):2282-92.
121. Lissett CA, Shalet SM. Effects of growth hormone on bone and muscle. Growth Horm IGF Res. 2000;10 Suppl B:S95-101.
122. Papadakis MA, Grady D, Black D, Tierney MJ, Gooding GA, Schambelan M, et al. Growth hormone replacement in healthy older men improves body composition but not functional ability. Ann Intern Med. 1996;124(8):708-16.
123. Rudman D, Feller AG, Nagraj HS, Gergans GA, Lalitha PY, Goldberg AF, et al. Effects of human growth hormone in men over 60 years old. N Engl J Med. 1990;323(1):1-6.
124. Renganathan M, Messi ML, Delbono O. Overexpression of IGF-1 exclusively in skeletal muscle prevents age-related decline in the number of dihydropyridine receptors. J Biol Chem. 1998;273(44):28845-51.
125. Sherlock M, Toogood AA. Aging and the growth hormone/insulin like growth factor-I axis. Pituitary. 2007;10(2):189-203.
126. Seeman TE, Robbins RJ. Aging and hypothalamic-pituitary-adrenal response to challenge in humans. Endocr Rev. 1994;15(2):233-60.
127. Van CE, Leproult R, Kupfer DJ. Effects of gender and age on the levels and circadian rhythmicity of plasma cortisol. J Clin Endocrinol Metab. 1996;81(7):2468-73.
128. Sapolsky RM, Krey LC, McEwen BS. The neuroendocrinology of stress and aging: the glucocorticoid cascade hypothesis. Endocr Rev. 1986;7(3):284-301.
129. Djaldetti M, Gafter U, Fishman P. Ultrastructural observations in myopathy complicating Cushing's disease. AmJMedSci. 1977;273(3):273-7.
130. Arlt W, Stewart PM. Adrenal corticosteroid biosynthesis, metabolism, and action. EndocrinolMetab ClinNorth Am. [S0889-8529(05)00003-4 pii ;10.1016/j.ecl.2005.01.002 doi]. 2005;34(2):293-313, viii.
131. Beato M, Sanchez-Pacheco A. Interaction of steroid hormone receptors with the transcription initiation complex. EndocrRev. 1996;17(6):587-609.
132. Lu NZ, Cidlowski JA. The origin and functions of multiple human glucocorticoid receptor isoforms. AnnNYAcadSci. [10.1196/annals.1321.008 doi ;1024/1/102 pii]. 2004;1024:102-23.
133. McKenna NJ, Lanz RB, O'Malley BW. Nuclear receptor coregulators: cellular and molecular biology. EndocrRev. 1999;20(3):321-44.
134. Cidlowski JA, Cidlowski NB. Regulation of glucocorticoid receptors by glucocorticoids in cultured HeLa S3 cells. Endocrinology. 1981;109(6):1975-82.
135. Danielsen M, Stallcup MR. Down-regulation of glucocorticoid receptors in mouse lymphoma cell variants. MolCell Biol. 1984;4(3):449-53.
136. Dong Y, Poellinger L, Gustafsson JA, Okret S. Regulation of glucocorticoid receptor expression: evidence for transcriptional and posttranslational mechanisms. MolEndocrinol. 1988;2(12):1256-64.
137. McIntyre WR, Samuels HH. Triamcinolone acetonide regulates glucocorticoid-receptor levels by decreasing the half-life of the activated nuclear-receptor form. JBiolChem. 1985;260(1):418-27.
138. Svec F, Rudis M. Glucocorticoids regulate the glucocorticoid receptor in the AtT-20 cell. JBiolChem. 1981;256(12):5984-7.
139. Wang X, DeFranco DB. Alternative effects of the ubiquitin-proteasome pathway on glucocorticoid receptor down-regulation and transactivation are mediated by CHIP, an E3 ligase. MolEndocrinol. [me.2004-0383 pii ;10.1210/me.2004-0383 doi]. 2005;19(6):1474-82.

140. Kim YS, Kim J, Kim Y, Lee YH, Kim JH, Lee SJ, et al. The role of calpains in ligand-induced degradation of the glucocorticoid receptor. BiochemBiophysResCommun. [S0006-291X(08)01363-6 pii ;10.1016/j.bbrc.2008.07.040 doi]. 2008;374(2):373-7.
141. Ma K, Mallidis C, Bhasin S, Mahabadi V, Artaza J, Gonzalez-Cadavid N, et al. Glucocorticoid-induced skeletal muscle atrophy is associated with upregulation of myostatin gene expression. AmJPhysiol EndocrinolMetab. [10.1152/ajpendo.00487.2002 doi ;00487.2002 pii]. 2003;285(2):E363-E71.
142. Zhao W, Qin W, Pan J, Wu Y, Bauman WA, Cardozo C. Dependence of dexamethasone-induced Akt/FOXO1 signaling, upregulation of MAFbx, and protein catabolism upon the glucocorticoid receptor. BiochemBiophysResCommun. [S0006-291X(08)02337-1 pii ;10.1016/j.bbrc.2008.11.123 doi]. 2009;378(3):668-72.
143. Waddell DS, Baehr LM, van den Brandt J, Johnsen SA, Reichardt HM, Furlow JD, et al. The glucocorticoid receptor and FOXO1 synergistically activate the skeletal muscle atrophy-associated MuRF1 gene. AmJPhysiol EndocrinolMetab. [00646.2007 pii ;10.1152/ajpendo.00646.2007 doi]. 2008;295(4):E785-E97.
144. Gwynne JT, Strauss JF, III. The role of lipoproteins in steroidogenesis and cholesterol metabolism in steroidogenic glands. EndocrRev. 1982;3(3):299-329.
145. Esteban NV, Loughlin T, Yergey AL, Zawadzki JK, Booth JD, Winterer JC, et al. Daily cortisol production rate in man determined by stable isotope dilution/mass spectrometry. JClinEndocrinolMetab. 1991;72(1):39-45.
146. Kerrigan JR, Veldhuis JD, Leyo SA, Iranmanesh A, Rogol AD. Estimation of daily cortisol production and clearance rates in normal pubertal males by deconvolution analysis. JClinEndocrinolMetab. 1993;76(6):1505-10.
147. McEwen BS, De Kloet ER, Rostene W. Adrenal steroid receptors and actions in the nervous system. Physiol Rev. 1986 Oct;66(4):1121-88.
148. Hammond GL. Molecular properties of corticosteroid binding globulin and the sex-steroid binding proteins. EndocrRev. 1990;11(1):65-79.
149. Shackleton CH. Genetic disorders of steroid metabolism diagnosed my mass spectrometry. In: Blau N, Duren M, Gibson KM, editors. Laboratory guide to the methods in biochemical genetics. Berlin Heidelberg: Springer; 2008. p. 549-605.
150. White PC, Mune T, Agarwal AK. 11 beta-Hydroxysteroid dehydrogenase and the syndrome of apparent mineralocorticoid excess. Endocr Rev. 1997 Feb;18(1):135-56.
151. Jang C, Obeyesekere VR, Dilley RJ, Alford FP, Inder WJ. 11Beta hydroxysteroid dehydrogenase type 1 is expressed and is biologically active in human skeletal muscle. ClinEndocrinol(Oxf). [CEN2669 pii ;10.1111/j.1365-2265.2006.02669.x doi]. 2006;65(6):800-5.
152. Abdallah BM, Beck-Nielsen H, Gaster M. Increased expression of 11beta-hydroxysteroid dehydrogenase type 1 in type 2 diabetic myotubes. EurJClinInvest. [ECI1552 pii ;10.1111/j.1365-2362.2005.01552.x doi]. 2005;35(10):627-34.
153. Whorwood CB, Donovan SJ, Wood PJ, Phillips DI. Regulation of glucocorticoid receptor alpha and beta isoforms and type I 11beta-hydroxysteroid dehydrogenase expression in human skeletal muscle cells: a key role in the pathogenesis of insulin resistance? JClinEndocrinolMetab. 2001;86(5):2296-308.
154. Lavery GG, Walker EA, Turan N, Rogoff D, Ryder JW, Shelton JM, et al. Deletion of hexose-6-phosphate dehydrogenase activates the unfolded protein response pathway and induces skeletal myopathy. JBiolChem. [M710067200 pii ;10.1074/jbc.M710067200 doi]. 2008;283(13):8453-61.
155. Lavery GG, Walker EA, Draper N, Jeyasuria P, Marcos J, Shackleton CH, et al. Hexose-6-phosphate dehydrogenase knock-out mice lack 11 beta-hydroxysteroid

dehydrogenase type 1-mediated glucocorticoid generation. JBiolChem. [M512635200 pii ;10.1074/jbc.M512635200 doi]. 2006;281(10):6546-51.
156. Jang C, Obeyesekere VR, Alford FP, Inder WJ. Skeletal muscle 11beta hydroxysteroid dehydrogenase type 1 activity is upregulated following elective abdominal surgery. Eur J Endocrinol. [EJE-08-0619 pii ;10.1530/EJE-08-0619 doi]. 2009;160(2):249-55.
157. Aubry EM, Odermatt A. Retinoic acid reduces glucocorticoid sensitivity in C2C12 myotubes by decreasing 11beta-hydroxysteroid dehydrogenase type 1 and glucocorticoid receptor activities. Endocrinology. 2009 Jun;150(6):2700-8.
158. Whorwood CB, Donovan SJ, Flanagan D, Phillips DI, Byrne CD. Increased glucocorticoid receptor expression in human skeletal muscle cells may contribute to the pathogenesis of the metabolic syndrome. Diabetes. 2002 Apr;51(4):1066-75.
159. Kotelevtsev Y, Holmes MC, Burchell A, Houston PM, Schmoll D, Jamieson P, et al. 11beta-hydroxysteroid dehydrogenase type 1 knockout mice show attenuated glucocorticoid-inducible responses and resist hyperglycemia on obesity or stress. ProcNatlAcadSciUSA. 1997;94(26):14924-9.
160. Maser E, Oppermann UC. Role of type-1 11beta-hydroxysteroid dehydrogenase in detoxification processes. Eur J Biochem. 1997 Oct 15;249(2):365-9.
161. Sreerama L, Sladek NE. Identification of the class-3 aldehyde dehydrogenases present in human MCF-7/0 breast adenocarcinoma cells and normal human breast tissue. Biochem Pharmacol. 1994 Aug 3;48(3):617-20.
162. Winzer K, Van Noorden CJ, Kohler A. Sex-specific biotransformation and detoxification after xenobiotic exposure of primary cultured hepatocytes of European flounder (Platichthys flesus L.). Aquat Toxicol. 2002 Sep 10;59(1-2):17-33.
163. Frey FJ. Kinetics and dynamics of prednisolone. Endocr Rev. 1987 Nov;8(4):453-73.
164. Murphy BE. Specificity of human 11 beta-hydroxysteroid dehydrogenase. J Steroid Biochem. 1981 Aug;14(8):807-9.
165. Ferrari P, Smith RE, Funder JW, Krozowski ZS. Substrate and inhibitor specificity of the cloned human 11 beta-hydroxysteroid dehydrogenase type 2 isoform. Am J Physiol. 1996 May;270(5 Pt 1):E900-4.
166. Diederich S, Eigendorff E, Burkhardt P, Quinkler M, Bumke-Vogt C, Rochel M, et al. 11beta-hydroxysteroid dehydrogenase types 1 and 2: an important pharmacokinetic determinant for the activity of synthetic mineralo- and glucocorticoids. J Clin Endocrinol Metab. 2002 Dec;87(12):5695-701.
167. Lakshmi V, Monder C. Purification and characterization of the corticosteroid 11 beta-dehydrogenase component of the rat liver 11 beta-hydroxysteroid dehydrogenase complex. Endocrinology. 1988;123(5):2390-8.
168. Condon J, Ricketts ML, Whorwood CB, Stewart PM. Ontogeny and sexual dimorphic expression of mouse type 2 11beta-hydroxysteroid dehydrogenase. MolCell Endocrinol. [S0303-7207(97)04000-8 pii]. 1997;127(2):121-8.
169. Davani B, Khan A, Hult M, Martensson E, Okret S, Efendic S, et al. Type 1 11beta -hydroxysteroid dehydrogenase mediates glucocorticoid activation and insulin release in pancreatic islets. JBiolChem. [10.1074/jbc.C000600200 doi ;C000600200 pii]. 2000;275(45):34841-4.
170. Maser E, Volker B, Friebertshauser J. 11 Beta-hydroxysteroid dehydrogenase type 1 from human liver: dimerization and enzyme cooperativity support its postulated role as glucocorticoid reductase. Biochemistry. [bi015803t pii]. 2002;41(7):2459-65.

171. McKnight SL, Lane MD, Gluecksohn-Waelsch S. Is CCAAT/enhancer-binding protein a central regulator of energy metabolism? Genes Dev. 1989 Dec;3(12B):2021-4.
172. Ramos RA, Nishio Y, Maiyar AC, Simon KE, Ridder CC, Ge Y, et al. Glucocorticoid-stimulated CCAAT/enhancer-binding protein alpha expression is required for steroid-induced G1 cell cycle arrest of minimal-deviation rat hepatoma cells. Mol Cell Biol. 1996 Oct;16(10):5288-301.
173. Seckl JR, Walker BR. Minireview: 11beta-hydroxysteroid dehydrogenase type 1- a tissue-specific amplifier of glucocorticoid action. Endocrinology. 2001 Apr;142(4):1371-6.
174. Sandeep TC, Yau JL, MacLullich AM, Noble J, Deary IJ, Walker BR, et al. 11Beta-hydroxysteroid dehydrogenase inhibition improves cognitive function in healthy elderly men and type 2 diabetics. ProcNatlAcadSciUSA. [10.1073/pnas.0306996101 doi ;0306996101 pii]. 2004;101(17):6734-9.
175. Lindsay RS, Wake DJ, Nair S, Bunt J, Livingstone DE, Permana PA, et al. Subcutaneous adipose 11 beta-hydroxysteroid dehydrogenase type 1 activity and messenger ribonucleic acid levels are associated with adiposity and insulinemia in Pima Indians and Caucasians. JClinEndocrinolMetab. 2003;88(6):2738-44.
176. Kannisto K, Pietilainen KH, Ehrenborg E, Rissanen A, Kaprio J, Hamsten A, et al. Overexpression of 11beta-hydroxysteroid dehydrogenase-1 in adipose tissue is associated with acquired obesity and features of insulin resistance: studies in young adult monozygotic twins. JClinEndocrinolMetab. [10.1210/jc.2004-0153 doi ;89/9/4414 pii]. 2004;89(9):4414-21.
177. Morton NM, Holmes MC, Fievet C, Staels B, Tailleux A, Mullins JJ, et al. Improved lipid and lipoprotein profile, hepatic insulin sensitivity, and glucose tolerance in 11beta-hydroxysteroid dehydrogenase type 1 null mice. JBiolChem. [10.1074/jbc.M103676200 doi ;M103676200 pii]. 2001;276(44):41293-300.
178. Masuzaki H, Paterson J, Shinyama H, Morton NM, Mullins JJ, Seckl JR, et al. A transgenic model of visceral obesity and the metabolic syndrome. Science. [10.1126/science.1066285 doi ;294/5549/2166 pii]. 2001;294(5549):2166-70.
179. Rask E, Olsson T, Soderberg S, Andrew R, Livingstone DE, Johnson O, et al. Tissue-specific dysregulation of cortisol metabolism in human obesity. JClinEndocrinolMetab. 2001;86(3):1418-21.
180. Weinstein RS, Wan C, Liu Q, Wang Y, Almeida M, O'Brien CA, et al. Endogenous glucocorticoids decrease skeletal angiogenesis, vascularity, hydration, and strength in aged mice. Aging Cell. 2010 Apr;9(2):147-61.
181. Cooper MS, Walker EA, Bland R, Fraser WD, Hewison M, Stewart PM. Expression and functional consequences of 11beta-hydroxysteroid dehydrogenase activity in human bone. Bone. [S8756-3282(00)00344-6 pii]. 2000;27(3):375-81.
182. Moore JS, Monson JP, Kaltsas G, Putignano P, Wood PJ, Sheppard MC, et al. Modulation of 11beta-hydroxysteroid dehydrogenase isozymes by growth hormone and insulin-like growth factor: in vivo and in vitro studies. JClinEndocrinolMetab. 1999;84(11):4172-7.
183. Gelding SV, Taylor NF, Wood PJ, Noonan K, Weaver JU, Wood DF, et al. The effect of growth hormone replacement therapy on cortisol-cortisone interconversion in hypopituitary adults: evidence for growth hormone modulation of extrarenal 11 beta-hydroxysteroid dehydrogenase activity. Clin Endocrinol (Oxf). 1998;48(2):153-62.
184. Toogood AA, Taylor NF, Shalet SM, Monson JP. Modulation of cortisol metabolism by low-dose growth hormone replacement in elderly hypopituitary patients. J Clin Endocrinol Metab. 2000;85(4):1727-30.

185. Liu YJ, Nakagawa Y, Nasuda K, Saegusa H, Igarashi Y. Effect of growth hormone, insulin and dexamethasone on 11 beta-hydroxysteroid dehydrogenase activity on a primary culture of rat hepatocytes. Life Sci. [0024320596002883 pii]. 1996;59(3):227-34.
186. Liu YJ, Nakagawa Y, Toya K, Ozeki T. Sex-specific effects of growth hormone on hepatic 11beta-hydroxysteroid dehydrogenase activity and gene expression in hypothyroid rats. Life Sci. [S0024320597003895 pii]. 1997;61(3):325-34.
187. Low SC, Chapman KE, Edwards CR, Wells T, Robinson IC, Seckl JR. Sexual dimorphism of hepatic 11 beta-hydroxysteroid dehydrogenase in the rat: the role of growth hormone patterns. J Endocrinol. 1994;143(3):541-8.
188. Voice MW, Seckl JR, Edwards CR, Chapman KE. 11 beta-hydroxysteroid dehydrogenase type 1 expression in 2S FAZA hepatoma cells is hormonally regulated: a model system for the study of hepatic glucocorticoid metabolism. Biochem J. 1996;317 (Pt 2):621-5.
189. Muller R, Kugelberg E. Myopathy in Cushing's syndrome. JNeurolNeurosurgPsychiatry. 1959;22:314-9.
190. Pirlich M, Biering H, Gerl H, Ventz M, Schmidt B, Ertl S, et al. Loss of body cell mass in Cushing's syndrome: effect of treatment. JClinEndocrinolMetab. 2002;87(3):1078-84.
191. Vignos PJ, Jr., Greene R. Oxidative respiration of skeletal muscle in experimental corticosteroid myopathy. JLab ClinMed. [0022-2143(73)90324-7 pii]. 1973;81(3):365-78.
192. Lane RJ, Mastaglia FL. Drug-induced myopathies in man. Lancet. 1978;2(8089):562-6.
193. Mills GH, Kyroussis D, Jenkins P, Hamnegard CH, Polkey MI, Wass J, et al. Respiratory muscle strength in Cushing's syndrome. AmJRespirCrit Care Med. 1999;160(5 Pt 1):1762-5.
194. Chromiak JA, Vandenburgh HH. Glucocorticoid-induced skeletal muscle atrophy in vitro is attenuated by mechanical stimulation. AmJPhysiol. 1992;262(6 Pt 1):C1471-C7.
195. Menconi M, Gonnella P, Petkova V, Lecker S, Hasselgren PO. Dexamethasone and corticosterone induce similar, but not identical, muscle wasting responses in cultured L6 and C2C12 myotubes. JCell Biochem. [10.1002/jcb.21833 doi]. 2008;105(2):353-64.
196. Sacheck JM, Ohtsuka A, McLary SC, Goldberg AL. IGF-I stimulates muscle growth by suppressing protein breakdown and expression of atrophy-related ubiquitin ligases, atrogin-1 and MuRF1. AmJPhysiol EndocrinolMetab. [10.1152/ajpendo.00073.2004 doi ;00073.2004 pii]. 2004;287(4):E591-E601.
197. Sultan KR, Henkel B, Terlou M, Haagsman HP. Quantification of hormone-induced atrophy of large myotubes from C2C12 and L6 cells: atrophy-inducible and atrophy-resistant C2C12 myotubes. AmJPhysiol Cell Physiol. [00163.2005 pii ;10.1152/ajpcell.00163.2005 doi]. 2006;290(2):C650-C9.
198. Tobimatsu K, Noguchi T, Hosooka T, Sakai M, Inagaki K, Matsuki Y, et al. Overexpression of the transcriptional coregulator Cited2 protects against glucocorticoid-induced atrophy of C2C12 myotubes. BiochemBiophysResCommun. [S0006-291X(08)02217-1 pii ;10.1016/j.bbrc.2008.11.062 doi]. 2009;378(3):399-403.
199. Uozumi Y, Ito T, Takahashi K, Matsuda T, Mohri T, Kimura Y, et al. Myogenic induction of taurine transporter prevents dexamethasone-induced muscle atrophy. AdvExpMedBiol. 2006;583:265-70.

200. Capaccio JA, Kurowski TT, Czerwinski SM, Chatterton RT, Jr., Hickson RC. Testosterone fails to prevent skeletal muscle atrophy from glucocorticoids. JApplPhysiol. 1987;63(1):328-34.
201. Gilson H, Schakman O, Combaret L, Lause P, Grobet L, Attaix D, et al. Myostatin gene deletion prevents glucocorticoid-induced muscle atrophy. Endocrinology. [en.2006-0539 pii ;10.1210/en.2006-0539 doi]. 2007;148(1):452-60.
202. Hickson RC, Galassi TM, Capaccio JA, Chatterton RT, Jr. Limited resistance of hypertrophied skeletal muscle to glucocorticoids. JSteroid Biochem. 1986;24(6):1179-83.
203. Kaasik P, Umnova M, Pehme A, Alev K, Aru M, Selart A, et al. Ageing and dexamethasone associated sarcopenia: peculiarities of regeneration. JSteroid BiochemMolBiol. [S0960-0760(07)00103-3 pii ;10.1016/j.jsbmb.2006.11.024 doi]. 2007;105(1-5):85-90.
204. Kelly FJ, Goldspink DF. The differing responses of four muscle types to dexamethasone treatment in the rat. BiochemJ. 1982;208(1):147-51.
205. Menezes LG, Sobreira C, Neder L, Rodrigues-Junior AL, Martinez JA. Creatine supplementation attenuates corticosteroid-induced muscle wasting and impairment of exercise performance in rats. JApplPhysiol. [01188.2005 pii ;10.1152/japplphysiol.01188.2005 doi]. 2007;102(2):698-703.
206. Rouleau G, Karpati G, Carpenter S, Soza M, Prescott S, Holland P. Glucocorticoid excess induces preferential depletion of myosin in denervated skeletal muscle fibers. Muscle Nerve. [10.1002/mus.880100509 doi]. 1987;10(5):428-38.
207. Salehian B, Mahabadi V, Bilas J, Taylor WE, Ma K. The effect of glutamine on prevention of glucocorticoid-induced skeletal muscle atrophy is associated with myostatin suppression. Metabolism. [S0026-0495(06)00176-4 pii ;10.1016/j.metabol.2006.05.009 doi]. 2006;55(9):1239-47.
208. Schakman O, Kalista S, Bertrand L, Lause P, Verniers J, Ketelslegers JM, et al. Role of Akt/GSK-3beta/beta-catenin transduction pathway in the muscle anti-atrophy action of insulin-like growth factor-I in glucocorticoid-treated rats. Endocrinology. [en.2008-0439 pii ;10.1210/en.2008-0439 doi]. 2008;149(8):3900-8.
209. Uchikawa K, Takahashi H, Hase K, Masakado Y, Liu M. Strenuous exercise-induced alterations of muscle fiber cross-sectional area and fiber-type distribution in steroid myopathy rats. AmJPhysMedRehabil. [10.1097/PHM.0b013e31815869d0 doi]. 2008;87(2):126-33.
210. Zhao W, Pan J, Zhao Z, Wu Y, Bauman WA, Cardozo CP. Testosterone protects against dexamethasone-induced muscle atrophy, protein degradation and MAFbx upregulation. JSteroid BiochemMolBiol. [S0960-0760(08)00077-0 pii ;10.1016/j.jsbmb.2008.03.024 doi]. 2008;110(1-2):125-9.
211. DuBois DC, Almon RR. Glucocorticoid sites in skeletal muscle: adrenalectomy, maturation, fiber type, and sex. AmJPhysiol. 1984;247(1 Pt 1):E118-E25.
212. Hickson RC, Kurowski TT, Andrews GH, Capaccio JA, Chatterton RT, Jr. Glucocorticoid cytosol binding in exercise-induced sparing of muscle atrophy. JApplPhysiol. 1986;60(4):1413-9.
213. Short KR, Bigelow ML, Nair KS. Short-term prednisone use antagonizes insulin's anabolic effect on muscle protein and glucose metabolism in young healthy people. AmJPhysiol EndocrinolMetab. [00345.2009 pii ;10.1152/ajpendo.00345.2009 doi]. 2009;297(6):E1260-E8.
214. Bowes SB, Benn JJ, Scobie IN, Umpleby AM, Lowy C, Sonksen PH. Leucine metabolism in patients with Cushing's syndrome before and after successful treatment. ClinEndocrinol(Oxf). 1993;39(5):591-8.

215. Dardevet D, Sornet C, Taillandier D, Savary I, Attaix D, Grizard J. Sensitivity and protein turnover response to glucocorticoids are different in skeletal muscle from adult and old rats. Lack of regulation of the ubiquitin-proteasome proteolytic pathway in aging. JClinInvest. [10.1172/JCI118264 doi]. 1995;96(5):2113-9.
216. Rieu I, Sornet C, Grizard J, Dardevet D. Glucocorticoid excess induces a prolonged leucine resistance on muscle protein synthesis in old rats. ExpGerontol. [S0531556504001913 pii ;10.1016/j.exger.2004.06.005 doi]. 2004;39(9):1315-21.
217. Guerriero V, Jr., Florini JR. Dexamethasone effects on myoblast proliferation and differentiation. Endocrinology. 1980 Apr;106(4):1198-202.
218. Sklar RM, Hudson A, Brown RH, Jr. Glucocorticoids increase myoblast proliferation rates by inhibiting death of cycling cells. In Vitro Cell Dev Biol. 1991 Jun;27A(6):433-4.
219. Montano MM, Lim RW. Glucocorticoid effects on the skeletal muscle differentiation program: analysis of clonal proliferation, morphological differentiation and the expression of muscle-specific and regulatory genes. Endocr Res. 1997 Feb-May;23(1-2):37-57.
220. te Pas MF, de Jong PR, Verburg FJ. Glucocorticoid inhibition of C2C12 proliferation rate and differentiation capacity in relation to mRNA levels of the MRF gene family. MolBiolRep. 2000;27(2):87-98.
221. Carlson CJ, Booth FW, Gordon SE. Skeletal muscle myostatin mRNA expression is fiber-type specific and increases during hindlimb unloading. AmJPhysiol. 1999;277(2 Pt 2):R601-R6.
222. Wegner J, Albrecht E, Fiedler I, Teuscher F, Papstein HJ, Ender K. Growth- and breed-related changes of muscle fiber characteristics in cattle. JAnim Sci. 2000;78(6):1485-96.
223. Gonzalez-Cadavid NF, Taylor WE, Yarasheski K, Sinha-Hikim I, Ma K, Ezzat S, et al. Organization of the human myostatin gene and expression in healthy men and HIV-infected men with muscle wasting. ProcNatlAcadSciUSA. 1998;95(25):14938-43.
224. Reisz-Porszasz S, Bhasin S, Artaza JN, Shen R, Sinha-Hikim I, Hogue A, et al. Lower skeletal muscle mass in male transgenic mice with muscle-specific overexpression of myostatin. AmJPhysiol EndocrinolMetab. [10.1152/ajpendo.00107.2003 doi ;00107.2003 pii]. 2003;285(4):E876-E88.
225. McPherron AC, Lawler AM, Lee SJ. Regulation of skeletal muscle mass in mice by a new TGF-beta superfamily member. Nature. [10.1038/387083a0 doi]. 1997;387(6628):83-90.
226. Whittemore LA, Song K, Li X, Aghajanian J, Davies M, Girgenrath S, et al. Inhibition of myostatin in adult mice increases skeletal muscle mass and strength. BiochemBiophysResCommun. [S0006291X02029534 pii]. 2003;300(4):965-71.
227. Zhu X, Hadhazy M, Wehling M, Tidball JG, McNally EM. Dominant negative myostatin produces hypertrophy without hyperplasia in muscle. FEBS Lett. [S0014-5793(00)01570-2 pii]. 2000;474(1):71-5.
228. Yang J, Ratovitski T, Brady JP, Solomon MB, Wells KD, Wall RJ. Expression of myostatin pro domain results in muscular transgenic mice. MolReprodDev. [10.1002/mrd.1097 pii ;10.1002/mrd.1097 doi]. 2001;60(3):351-61.
229. Schuelke M, Wagner KR, Stolz LE, Hubner C, Riebel T, Komen W, et al. Myostatin mutation associated with gross muscle hypertrophy in a child. NEnglJMed. [10.1056/NEJMoa040933 doi ;350/26/2682 pii]. 2004;350(26):2682-8.
230. Artaza JN, Bhasin S, Mallidis C, Taylor W, Ma K, Gonzalez-Cadavid NF. Endogenous expression and localization of myostatin and its relation to myosin heavy

chain distribution in C2C12 skeletal muscle cells. JCell Physiol. [10.1002/jcp.10044 pii ;10.1002/jcp.10044 doi]. 2002;190(2):170-9.
231. Baar K, Nader G, Bodine S. Resistance exercise, muscle loading/unloading and the control of muscle mass. Essays Biochem. [bse0420061 pii ;10.1042/bse0420061 doi]. 2006;42:61-74.
232. Li BG, Hasselgren PO, Fang CH. Insulin-like growth factor-I inhibits dexamethasone-induced proteolysis in cultured L6 myotubes through PI3K/Akt/GSK-3beta and PI3K/Akt/mTOR-dependent mechanisms. IntJBiochemCell Biol. [S1357-2725(05)00129-9 pii ;10.1016/j.biocel.2005.04.008 doi]. 2005;37(10):2207-16.
233. Fang CH, Li BG, James JH, King JK, Evenson AR, Warden GD, et al. Protein breakdown in muscle from burned rats is blocked by insulin-like growth factor i and glycogen synthase kinase-3beta inhibitors. Endocrinology. [en.2004-0869 pii ;10.1210/en.2004-0869 doi]. 2005;146(7):3141-9.
234. Fang CH, Li BG, Wray CJ, Hasselgren PO. Insulin-like growth factor-I inhibits lysosomal and proteasome-dependent proteolysis in skeletal muscle after burn injury. JBurn Care Rehabil. [10.1097/01.BCR.0000028580.55168.5B doi]. 2002;23(5):318-25.
235. Kandarian SC, Jackman RW. Intracellular signaling during skeletal muscle atrophy. Muscle Nerve. [10.1002/mus.20442 doi]. 2006;33(2):155-65.
236. Wing SS, Goldberg AL. Glucocorticoids activate the ATP-ubiquitin-dependent proteolytic system in skeletal muscle during fasting. AmJPhysiol. 1993;264(4 Pt 1):E668-E76.
237. Wing SS, Haas AL, Goldberg AL. Increase in ubiquitin-protein conjugates concomitant with the increase in proteolysis in rat skeletal muscle during starvation and atrophy denervation. BiochemJ. 1995;307 (Pt 3):639-45.
238. Zhao W, Wu Y, Zhao J, Guo S, Bauman WA, Cardozo CP. Structure and function of the upstream promotor of the human Mafbx gene: the proximal upstream promotor modulates tissue-specificity. JCell Biochem. [10.1002/jcb.20468 doi]. 2005;96(1):209-19.
239. Southgate RJ, Neill B, Prelovsek O, El-Osta A, Kamei Y, Miura S, et al. FOXO1 regulates the expression of 4E-BP1 and inhibits mTOR signaling in mammalian skeletal muscle. JBiolChem. [M702039200 pii ;10.1074/jbc.M702039200 doi]. 2007;282(29):21176-86.
240. Bodine SC, Stitt TN, Gonzalez M, Kline WO, Stover GL, Bauerlein R, et al. Akt/mTOR pathway is a crucial regulator of skeletal muscle hypertrophy and can prevent muscle atrophy in vivo. NatCell Biol. [10.1038/ncb1101-1014 doi ;ncb1101-1014 pii]. 2001;3(11):1014-9.
241. Furuyama T, Kitayama K, Yamashita H, Mori N. Forkhead transcription factor FOXO1 (FKHR)-dependent induction of PDK4 gene expression in skeletal muscle during energy deprivation. BiochemJ. [10.1042/BJ20030022 doi ;BJ20030022 pii]. 2003;375(Pt 2):365-71.
242. Imae M, Fu Z, Yoshida A, Noguchi T, Kato H. Nutritional and hormonal factors control the gene expression of FoxOs, the mammalian homologues of DAF-16. JMolEndocrinol. 2003;30(2):253-62.
243. Constantin D, Constantin-Teodosiu D, Layfield R, Tsintzas K, Bennett AJ, Greenhaff PL. PPARdelta agonism induces a change in fuel metabolism and activation of an atrophy programme, but does not impair mitochondrial function in rat skeletal muscle. JPhysiol. [jphysiol.2007.135459 pii ;10.1113/jphysiol.2007.135459 doi]. 2007;583(Pt 1):381-90.

244. Inoki K, Ouyang H, Zhu T, Lindvall C, Wang Y, Zhang X, et al. TSC2 integrates Wnt and energy signals via a coordinated phosphorylation by AMPK and GSK3 to regulate cell growth. Cell. [S0092-8674(06)01016-6 pii ;10.1016/j.cell.2006.06.055 doi]. 2006;126(5):955-68.
245. Nobukuni T, Kozma SC, Thomas G. hvps34, an ancient player, enters a growing game: mTOR Complex1/S6K1 signaling. CurrOpinCell Biol. [S0955-0674(07)00031-2 pii ;10.1016/j.ceb.2007.02.019 doi]. 2007;19(2):135-41.
246. Goldspink G. Mechanical signals, IGF-I gene splicing, and muscle adaptation. Physiology(Bethesda). [20/4/232 pii ;10.1152/physiol.00004.2005 doi]. 2005;20:232-8.
247. Hornberger TA, Sukhija KB, Chien S. Regulation of mTOR by mechanically induced signaling events in skeletal muscle. Cell Cycle. [2921 pii]. 2006;5(13):1391-6.
248. Rommel C, Bodine SC, Clarke BA, Rossman R, Nunez L, Stitt TN, et al. Mediation of IGF-1-induced skeletal myotube hypertrophy by PI(3)K/Akt/mTOR and PI(3)K/Akt/GSK3 pathways. NatCell Biol. [10.1038/ncb1101-1009 doi ;ncb1101-1009 pii]. 2001;3(11):1009-13.
249. Proud CG. Regulation of protein synthesis by insulin. BiochemSocTrans. [BST20060213 pii ;10.1042/BST20060213 doi]. 2006;34(Pt 2):213-6.
250. Hanada M, Feng J, Hemmings BA. Structure, regulation and function of PKB/AKT--a major therapeutic target. Biochim Biophys Acta. 2004 Mar 11;1697(1-2):3-16.
251. Sano H, Kane S, Sano E, Miinea CP, Asara JM, Lane WS, et al. Insulin-stimulated phosphorylation of a Rab GTPase-activating protein regulates GLUT4 translocation. J Biol Chem. 2003 Apr 25;278(17):14599-602.
252. Watson RT, Kanzaki M, Pessin JE. Regulated membrane trafficking of the insulin-responsive glucose transporter 4 in adipocytes. Endocr Rev. 2004 Apr;25(2):177-204.
253. Aguirre V, Uchida T, Yenush L, Davis R, White MF. The c-Jun NH(2)-terminal kinase promotes insulin resistance during association with insulin receptor substrate-1 and phosphorylation of Ser(307). J Biol Chem. 2000 Mar 24;275(12):9047-54.
254. Aguirre V, Werner ED, Giraud J, Lee YH, Shoelson SE, White MF. Phosphorylation of Ser307 in insulin receptor substrate-1 blocks interactions with the insulin receptor and inhibits insulin action. J Biol Chem. 2002 Jan 11;277(2):1531-7.
255. Giorgino F, Almahfouz A, Goodyear LJ, Smith RJ. Glucocorticoid regulation of insulin receptor and substrate IRS-1 tyrosine phosphorylation in rat skeletal muscle in vivo. JClinInvest. [10.1172/JCI116424 doi]. 1993;91(5):2020-30.
256. Rojas FA, Hirata AE, Saad MJ. Regulation of insulin receptor substrate-2 tyrosine phosphorylation in animal models of insulin resistance. Endocrine. 2003 Jul;21(2):115-22.
257. Ruzzin J, Wagman AS, Jensen J. Glucocorticoid-induced insulin resistance in skeletal muscles: defects in insulin signalling and the effects of a selective glycogen synthase kinase-3 inhibitor. Diabetologia. 2005 Oct;48(10):2119-30.
258. Saad MJ, Folli F, Kahn JA, Kahn CR. Modulation of insulin receptor, insulin receptor substrate-1, and phosphatidylinositol 3-kinase in liver and muscle of dexamethasone-treated rats. J Clin Invest. 1993 Oct;92(4):2065-72.
259. Barbour LA, Mizanoor RS, Gurevich I, Leitner JW, Fischer SJ, Roper MD, et al. Increased P85alpha is a potent negative regulator of skeletal muscle insulin signaling and induces in vivo insulin resistance associated with growth hormone excess. JBiolChem. [M506967200 pii ;10.1074/jbc.M506967200 doi]. 2005;280(45):37489-94.
260. Giorgino F, Pedrini MT, Matera L, Smith RJ. Specific increase in p85alpha expression in response to dexamethasone is associated with inhibition of insulin-like

growth factor-I stimulated phosphatidylinositol 3-kinase activity in cultured muscle cells. JBiolChem. 1997;272(11):7455-63.
261. Leis H, Page A, Ramirez A, Bravo A, Segrelles C, Paramio J, et al. Glucocorticoid Receptor Counteracts Tumorigenic Activity of Akt in Skin through Interference with the Phosphatidylinositol 3-Kinase Signaling Pathway. MolEndocrinol. [10.1210/me.2003-0350 doi ;me.2003-0350 pii]. 2004;18(2):303-11.
262. Kelly FJ, McGrath JA, Goldspink DF, Cullen MJ. A morphological/biochemical study on the actions of corticosteroids on rat skeletal muscle. Muscle Nerve. [10.1002/mus.880090102 doi]. 1986;9(1):1-10.
263. Wernerman J, Botta D, Hammarqvist F, Thunell S, von der DA, Vinnars E. Stress hormones given to healthy volunteers alter the concentration and configuration of ribosomes in skeletal muscle, reflecting changes in protein synthesis. ClinSci(Lond). 1989;77(6):611-6.
264. Aumailley M, Gayraud B. Structure and biological activity of the extracellular matrix. JMolMed. 1998;76(3-4):253-65.
265. Kovanen V, Suominen H, Heikkinen E. Collagen of slow twitch and fast twitch muscle fibres in different types of rat skeletal muscle. EurJApplPhysiol OccupPhysiol. 1984;52(2):235-42.
266. Ahtikoski AM, Riso EM, Koskinen SO, Risteli J, Takala TE. Regulation of type IV collagen gene expression and degradation in fast and slow muscles during dexamethasone treatment and exercise. Pflugers Arch. [10.1007/s00424-003-1226-5 doi]. 2004;448(1):123-30.
267. Cai D, Frantz JD, Tawa NE, Jr., Melendez PA, Oh BC, Lidov HG, et al. IKKbeta/NF-kappaB activation causes severe muscle wasting in mice. Cell. [S0092867404009006 pii ;10.1016/j.cell.2004.09.027 doi]. 2004;119(2):285-98.
268. Rivero JL, Talmadge RJ, Edgerton VR. Interrelationships of myofibrillar ATPase activity and metabolic properties of myosin heavy chain-based fibre types in rat skeletal muscle. HistochemCell Biol. 1999;111(4):277-87.
269. Seene T, Kaasik P, Pehme A, Alev K, Riso EM. The effect of glucocorticoids on the myosin heavy chain isoforms' turnover in skeletal muscle. JSteroid BiochemMolBiol. [S0960076003003820 pii]. 2003;86(2):201-6.
270. Max SR, Silbergeld EK. Skeletal muscle glucocorticoid receptor and glutamine synthetase activity in the wasting syndrome in rats treated with 2,3,7,8-tetrachlorodibenzo-p-dioxin. ToxicolApplPharmacol. 1987;87(3):523-7.
271. Marliss EB, Aoki TT, Pozefsky T, Most AS, Cahill GF, Jr. Muscle and splanchnic glutmine and glutamate metabolism in postabsorptive andstarved man. JClinInvest. [10.1172/JCI106552 doi]. 1971;50(4):814-7.
272. Falduto MT, Young AP, Hickson RC. Exercise inhibits glucocorticoid-induced glutamine synthetase expression in red skeletal muscles. AmJPhysiol. 1992;262(1 Pt 1):C214-C20.
273. Magiakou MA, Mastorakos G, Gomez MT, Rose SR, Chrousos GP. Suppressed spontaneous and stimulated growth hormone secretion in patients with Cushing's disease before and after surgical cure. JClinEndocrinolMetab. 1994;78(1):131-7.
274. Giustina A, Veldhuis JD. Pathophysiology of the neuroregulation of growth hormone secretion in experimental animals and the human. EndocrRev. 1998;19(6):717-97.
275. Horber FF, Haymond MW. Human growth hormone prevents the protein catabolic side effects of prednisone in humans. JClinInvest. [10.1172/JCI114694 doi]. 1990;86(1):265-72.

276. Schakman O, Gilson H, de CV, Lause P, Verniers J, Havaux X, et al. Insulin-like growth factor-I gene transfer by electroporation prevents skeletal muscle atrophy in glucocorticoid-treated rats. Endocrinology. [en.2004-1594 pii ;10.1210/en.2004-1594 doi]. 2005;146(4):1789-97.
277. Li BG, Hasselgren PO, Fang CH, Warden GD. Insulin-like growth factor-I blocks dexamethasone-induced protein degradation in cultured myotubes by inhibiting multiple proteolytic pathways: 2002 ABA paper. JBurn Care Rehabil. [10.1097/01.BCR.0000105100.44745.36 doi]. 2004;25(1):112-8.
278. Chrysis D, Underwood LE. Regulation of components of the ubiquitin system by insulin-like growth factor I and growth hormone in skeletal muscle of rats made catabolic with dexamethasone. Endocrinology. 1999;140(12):5635-41.
279. Czerwinski SM, Kurowski TG, O'Neill TM, Hickson RC. Initiating regular exercise protects against muscle atrophy from glucocorticoids. JApplPhysiol. 1987;63(4):1504-10.
280. Falduto MT, Czerwinski SM, Hickson RC. Glucocorticoid-induced muscle atrophy prevention by exercise in fast-twitch fibers. JApplPhysiol. 1990;69(3):1058-62.
281. Falduto MT, Young AP, Hickson RC. Exercise interrupts ongoing glucocorticoid-induced muscle atrophy and glutamine synthetase induction. AmJPhysiol. 1992;263(6 Pt 1):E1157-E63.
282. Hickson RC, Davis JR. Partial prevention of glucocorticoid-induced muscle atrophy by endurance training. AmJPhysiol. 1981;241(3):E226-E32.
283. Hickson RC, Kurowski TT, Capaccio JA, Chatterton RT, Jr. Androgen cytosol binding in exercise-induced sparing of muscle atrophy. AmJPhysiol. 1984;247(5 Pt 1):E597-E603.
284. Marone JR, Falduto MT, Essig DA, Hickson RC. Effects of glucocorticoids and endurance training on cytochrome oxidase expression in skeletal muscle. JApplPhysiol. 1994;77(4):1685-90.
285. Czerwinski SM, Zak R, Kurowski TT, Falduto MT, Hickson RC. Myosin heavy chain turnover and glucocorticoid deterrence by exercise in muscle. JApplPhysiol. 1989;67(6):2311-5.
286. Falduto MT, Hickson RC, Young AP. Antagonism by glucocorticoids and exercise on expression of glutamine synthetase in skeletal muscle. FASEB J. 1989;3(14):2623-8.
287. Falduto MT, Young AP, Smyrniotis G, Hickson RC. Reduction of glutamine synthetase mRNA in hypertrophied skeletal muscle. AmJPhysiol. 1992;262(6 Pt 2):R1131-R6.
288. Braith RW, Magyari PM, Pierce GL, Edwards DG, Hill JA, White LJ, et al. Effect of resistance exercise on skeletal muscle myopathy in heart transplant recipients. AmJCardiol. [S0002-9149(05)00293-6 pii ;10.1016/j.amjcard.2005.01.048 doi]. 2005;95(10):1192-8.
289. Braith RW, Welsch MA, Mills RM, Jr., Keller JW, Pollock ML. Resistance exercise prevents glucocorticoid-induced myopathy in heart transplant recipients. MedSciSports Exerc. 1998;30(4):483-9.
290. Yaffe D, Saxel O. Serial passaging and differentiation of myogenic cells isolated from dystrophic mouse muscle. Nature. 1977;270(5639):725-7.
291. Blau HM, Pavlath GK, Hardeman EC, Chiu CP, Silberstein L, Webster SG, et al. Plasticity of the differentiated state. Science. 1985;230(4727):758-66.
292. Chomczynski P, Sacchi N. Single-step method of RNA isolation by acid guanidinium thiocyanate-phenol-chloroform extraction. AnalBiochem. 1987;162(1):156-9.

293. Ramos-Vara JA. Technical aspects of immunohistochemistry. Vet Pathol. 2005 Jul;42(4):405-26.
294. Ricketts ML, Verhaeg JM, Bujalska I, Howie AJ, Rainey WE, Stewart PM. Immunohistochemical localization of type 1 11beta-hydroxysteroid dehydrogenase in human tissues. JClinEndocrinolMetab. 1998;83(4):1325-35.
295. Shaw CS, Sherlock M, Stewart PM, Wagenmakers AJ. Adipophilin distribution and colocalization with lipid droplets in skeletal muscle. Histochem Cell Biol. 2009 May;131(5):575-81.
296. Towbin H, Staehelin T, Gordon J. Electrophoretic transfer of proteins from polyacrylamide gels to nitrocellulose sheets: procedure and some applications. Proc Natl Acad Sci U S A. 1979 Sep;76(9):4350-4.
297. Milasincic DJ, Calera MR, Farmer SR, Pilch PF. Stimulation of C2C12 myoblast growth by basic fibroblast growth factor and insulin-like growth factor 1 can occur via mitogen-activated protein kinase-dependent and -independent pathways. Mol Cell Biol. 1996 Nov;16(11):5964-73.
298. Bujalska IJ, Gathercole LL, Tomlinson JW, Darimont C, Ermolieff J, Fanjul AN, et al. A novel selective 11beta-hydroxysteroid dehydrogenase type 1 inhibitor prevents human adipogenesis. JEndocrinol. [197/2/297 pii ;10.1677/JOE-08-0050 doi]. 2008;197(2):297-307.
299. Krahenbuhl S, Hasler F, Krapf R. Analysis and pharmacokinetics of glycyrrhizic acid and glycyrrhetinic acid in humans and experimental animals. Steroids. 1994 Feb;59(2):121-6.
300. Whorwood CB, Sheppard MC, Stewart PM. Licorice inhibits 11 beta-hydroxysteroid dehydrogenase messenger ribonucleic acid levels and potentiates glucocorticoid hormone action. Endocrinology. 1993;132(6):2287-92.
301. Albiston AL, Obeyesekere VR, Smith RE, Krozowski ZS. Cloning and tissue distribution of the human 11 beta-hydroxysteroid dehydrogenase type 2 enzyme. Mol Cell Endocrinol. 1994 Nov;105(2):R11-7.
302. Stewart PM, Murry BA, Mason JI. Human kidney 11 beta-hydroxysteroid dehydrogenase is a high affinity nicotinamide adenine dinucleotide-dependent enzyme and differs from the cloned type I isoform. JClinEndocrinolMetab. 1994;79(2):480-4.
303. Cadepond F, Ulmann A, Baulieu EE. RU486 (mifepristone): mechanisms of action and clinical uses. Annu Rev Med. 1997;48:129-56.
304. Mahajan DK, London SN. Mifepristone (RU486): a review. Fertil Steril. 1997 Dec;68(6):967-76.
305. Chan S, Seto JT, Houweling PJ, Yang N, North KN, Head SI. Properties of extensor digitorum longus muscle and skinned fibers from adult and aged male and female Actn3 knockout mice. Muscle Nerve. 2011 Jan;43(1):37-48.
306. Romero-Suarez S, Shen J, Brotto L, Hall T, Mo C, Valdivia HH, et al. Muscle-specific inositide phosphatase (MIP/MTMR14) is reduced with age and its loss accelerates skeletal muscle aging process by altering calcium homeostasis. Aging (Albany NY). 2010 Aug;2(8):504-13.
307. Bockhold KJ, Rosenblatt JD, Partridge TA. Aging normal and dystrophic mouse muscle: analysis of myogenicity in cultures of living single fibers. Muscle Nerve. 1998 Feb;21(2):173-83.
308. Brooks SV, Faulkner JA. The magnitude of the initial injury induced by stretches of maximally activated muscle fibres of mice and rats increases in old age. J Physiol. 1996 Dec 1;497 (Pt 2):573-80.

309. Lewandoski M, Wassarman KM, Martin GR. Zp3-cre, a transgenic mouse line for the activation or inactivation of loxP-flanked target genes specifically in the female germ line. Curr Biol. 1997 Feb 1;7(2):148-51.
310. Semjonous NM, Sherlock M, Jeyasuria P, Parker KL, Walker EA, Stewart PM, et al. Hexose-6-phosphate dehydrogenase contributes to skeletal muscle homeostasis independent of 11beta-hydroxysteroid dehydrogenase type 1. Endocrinology. 2011 Jan;152(1):93-102.
311. Palermo M, Shackleton CH, Mantero F, Stewart PM. Urinary free cortisone and the assessment of 11 beta-hydroxysteroid dehydrogenase activity in man. ClinEndocrinol(Oxf). 1996;45(5):605-11.
312. Shackleton CHL, Marcos PGM. Steroid profiling: Diagnosis of disorders affecting steroid synthesis and metabolism. In: Gross M, Caprioli R, editors. The Encyclopedia of Mass Spectrometry. Amsterdam: Elsevier; 2006. p. 789-813.
313. Krone N, Hughes BA, Lavery GG, Stewart PM, Arlt W, Shackleton CH. Gas chromatography/mass spectrometry (GC/MS) remains a pre-eminent discovery tool in clinical steroid investigations even in the era of fast liquid chromatography tandem mass spectrometry (LC/MS/MS). J Steroid Biochem Mol Biol. 2010 Aug;121(3-5):496-504.
314. Shackleton CH, Whitney JO. Use of Sep-pak cartridges for urinary steroid extraction: evaluation of the method for use prior to gas chromatographic analysis. Clin Chim Acta. 1980 Nov 6;107(3):231-43.
315. Monder C, Stewart PM, Lakshmi V, Valentino R, Burt D, Edwards CR. Licorice inhibits corticosteroid 11 beta-dehydrogenase of rat kidney and liver: in vivo and in vitro studies. Endocrinology. 1989;125(2):1046-53.
316. Nishimura M, Mikura M, Hirasaka K, Okumura Y, Nikawa T, Kawano Y, et al. Effects of dimethyl sulphoxide and dexamethasone on mRNA expression of myogenesis- and muscle proteolytic system-related genes in mouse myoblastic C2C12 cells. J Biochem. 2008 Dec;144(6):717-24.
317. Stewart PM, Walker BR, Holder G, O'Halloran D, Shackleton CH. 11 beta-Hydroxysteroid dehydrogenase activity in Cushing's syndrome: explaining the mineralocorticoid excess state of the ectopic adrenocorticotropin syndrome. JClinEndocrinolMetab. 1995;80(12):3617-20.
318. Orzechowski A, Jank M, Gajkowska B, Sadkowski T, Godlewskia MM. A novel antioxidant-inhibited dexamethasone-mediated and caspase-3-independent muscle cell death. Ann N Y Acad Sci. 2003 Dec;1010:205-8.
319. Dirks-Naylor AJ, Griffiths CL. Glucocorticoid-induced apoptosis and cellular mechanisms of myopathy. J Steroid Biochem Mol Biol. 2009 Oct;117(1-3):1-7.
320. Lee MC, Wee GR, Kim JH. Apoptosis of skeletal muscle on steroid-induced myopathy in rats. J Nutr. 2005 Jul;135(7):1806S-8S.
321. Schakman O, Gilson H, Thissen JP. Mechanisms of glucocorticoid-induced myopathy. J Endocrinol. 2008 Apr;197(1):1-10.
322. Morgan SA, Sherlock M, Gathercole LL, Lavery GG, Lenaghan C, Bujalska IJ, et al. 11beta-hydroxysteroid dehydrogenase type 1 regulates glucocorticoid-induced insulin resistance in skeletal muscle. Diabetes. [db09-0525 pii ;10.2337/db09-0525 doi]. 2009;58(11):2506-15.
323. Rogoff D, Black K, McMillan DR, White PC. Contribution of hexose-6-phosphate dehydrogenase to NADPH content and redox environment in the endoplasmic reticulum. Redox Rep. 2010;15(2):64-70.
324. Bhat BG, Hosea N, Fanjul A, Herrera J, Chapman J, Thalacker F, et al. Demonstration of proof of mechanism and pharmacokinetics and pharmacodynamic relationship with 4'-cyano-biphenyl-4-sulfonic acid (6-amino-pyridin-2-yl)-amide (PF-

915275), an inhibitor of 11 -hydroxysteroid dehydrogenase type 1, in cynomolgus monkeys. JPharmacolExpTher. [jpet.107.128280 pii ;10.1124/jpet.107.128280 doi]. 2008;324(1):299-305.
325. Alberts P, Nilsson C, Selen G, Engblom LO, Edling NH, Norling S, et al. Selective inhibition of 11 beta-hydroxysteroid dehydrogenase type 1 improves hepatic insulin sensitivity in hyperglycemic mice strains. Endocrinology. 2003 Nov;144(11):4755-62.
326. Lords THo. Ageing Scientific Aspects. 2005. p. Point 4.27.
327. Lords THo. Ageing Scientific Aspects. 2005. p. Point 2.4.
328. Shackleton CH, Hughes BA, Lavery GG, Walker EA, Stewart PM. The corticosteroid metabolic profile of the mouse. Steroids. [S0039-128X(08)00114-1 pii ;10.1016/j.steroids.2008.04.004 doi]. 2008;73(11):1066-76.
329. Wang YX, Zhang CL, Yu RT, Cho HK, Nelson MC, Bayuga-Ocampo CR, et al. Regulation of muscle fiber type and running endurance by PPARdelta. PLoS Biol. 2004 Oct;2(10):e294.
330. Harris HJ, Kotelevtsev Y, Mullins JJ, Seckl JR, Holmes MC. Intracellular regeneration of glucocorticoids by 11beta-hydroxysteroid dehydrogenase (11beta-HSD)-1 plays a key role in regulation of the hypothalamic-pituitary-adrenal axis: analysis of 11beta-HSD-1-deficient mice. Endocrinology. 2001 Jan;142(1):114-20.
331. Gaugler M, Brown A, Merrell E, Disanto-Rose M, Rathmacher JA, Reynolds THt. PKB signaling and atrogene expression in skeletal muscle of aged mice. J Appl Physiol. 2011 Jul;111(1):192-9.
332. Morton NM, Paterson JM, Masuzaki H, Holmes MC, Staels B, Fievet C, et al. Novel adipose tissue-mediated resistance to diet-induced visceral obesity in 11 beta-hydroxysteroid dehydrogenase type 1-deficient mice. Diabetes. 2004 Apr;53(4):931-8.
333. Langfort J, Ploug T, Ihlemann J, Enevoldsen LH, Stallknecht B, Saldo M, et al. Hormone-sensitive lipase (HSL) expression and regulation in skeletal muscle. Adv Exp Med Biol. 1998;441:219-28.
334. Lawson AJ, Walker EA, Lavery GG, Bujalska IJ, Hughes B, Arlt W, et al. Cortisone-reductase deficiency associated with heterozygous mutations in 11beta-hydroxysteroid dehydrogenase type 1. Proc Natl Acad Sci U S A. 2011 Mar 8;108(10):4111-6.
335. Lavery GG, Walker EA, Tiganescu A, Ride JP, Shackleton CH, Tomlinson JW, et al. Steroid biomarkers and genetic studies reveal inactivating mutations in hexose-6-phosphate dehydrogenase in patients with cortisone reductase deficiency. JClinEndocrinolMetab. [jc.2008-0743 pii ;10.1210/jc.2008-0743 doi]. 2008;93(10):3827-32.
336. Holmes MC, Kotelevtsev Y, Mullins JJ, Seckl JR. Phenotypic analysis of mice bearing targeted deletions of 11beta-hydroxysteroid dehydrogenases 1 and 2 genes. Mol Cell Endocrinol. 2001 Jan 22;171(1-2):15-20.
337. Carter RN, Paterson JM, Tworowska U, Stenvers DJ, Mullins JJ, Seckl JR, et al. Hypothalamic-pituitary-adrenal axis abnormalities in response to deletion of 11beta-HSD1 is strain-dependent. J Neuroendocrinol. 2009 Nov;21(11):879-87.
338. Paterson JM, Holmes MC, Kenyon CJ, Carter R, Mullins JJ, Seckl JR. Liver-selective transgene rescue of hypothalamic-pituitary-adrenal axis dysfunction in 11beta-hydroxysteroid dehydrogenase type 1-deficient mice. Endocrinology. 2007 Mar;148(3):961-6.
339. Sherlock M, Ayuk J, Tomlinson JW, Toogood AA, Aragon-Alonso A, Sheppard MC, et al. Mortality in Patients with Pituitary Disease. Endocr Rev. [er.2009-0033 pii ;10.1210/er.2009-0033 doi]. 2010.

340. Beshyah SA, Freemantle C, Thomas E, Rutherford O, Page B, Murphy M, et al. Abnormal body composition and reduced bone mass in growth hormone deficient hypopituitary adults. ClinEndocrinol(Oxf). 1995;42(2):179-89.
341. Lonn L, Kvist H, Grangard U, Bengtsson BA, Sjostrom L. CT-determined body composition changes with recombinant human growth hormone treatment to adults with growth hormone deficiency. Basic Life Sci. 1993;60:229-31.
342. Haffner SM, Stern MP, Hazuda HP, Rosenthal M, Knapp JA, Malina RM. Role of obesity and fat distribution in non-insulin-dependent diabetes mellitus in Mexican Americans and non-Hispanic whites. Diabetes Care. 1986;9(2):153-61.
343. Kissebah AH, Vydelingum N, Murray R, Evans DJ, Hartz AJ, Kalkhoff RK, et al. Relation of body fat distribution to metabolic complications of obesity. J Clin Endocrinol Metab. 1982;54(2):254-60.
344. Johansson JO, Fowelin J, Landin K, Lager I, Bengtsson BA. Growth hormone-deficient adults are insulin-resistant. Metabolism. 1995;44(9):1126-9.
345. Abdu TA, Neary R, Elhadd TA, Akber M, Clayton RN. Coronary risk in growth hormone deficient hypopituitary adults: increased predicted risk is due largely to lipid profile abnormalities. ClinEndocrinol(Oxf). 2001;55(2):209-16.
346. Abs R, Feldt-Rasmussen U, Mattsson AF, Monson JP, Bengtsson BA, Goth MI, et al. Determinants of cardiovascular risk in 2589 hypopituitary GH-deficient adults - a KIMS database analysis. EurJEndocrinol. 2006;155(1):79-90.
347. Kearney T, Navas de GC, Chrisoulidou A, Gray R, Bannister P, Venkatesan S, et al. Hypopituitarsim is associated with triglyceride enrichment of very low-density lipoprotein. JClinEndocrinolMetab. 2001;86(8):3900-6.
348. Leonsson M, Hulthe J, Oscarsson J, Johannsson G, Wendelhag I, Wikstrand J, et al. Intima-media thickness in cardiovascularly asymptomatic hypopituitary adults with growth hormone deficiency: relation to body mass index, gender, and other cardiovascular risk factors. Clin Endocrinol (Oxf). 2002;57(6):751-9.
349. O'Neal D, Hew FL, Sikaris K, Ward G, Alford F, Best JD. Low density lipoprotein particle size in hypopituitary adults receiving conventional hormone replacement therapy. J Clin Endocrinol Metab. 1996;81(7):2448-54.
350. Beshyah SA, Johnston DG. Cardiovascular disease and risk factors in adults with hypopituitarism. ClinEndocrinol(Oxf). 1999;50(1):1-15.
351. Cuneo RC, Salomon F, Watts GF, Hesp R, Sonksen PH. Growth hormone treatment improves serum lipids and lipoproteins in adults with growth hormone deficiency. Metabolism. 1993;42(12):1519-23.
352. de BH, Blok GJ, Voerman HJ, Phillips M, Schouten JA. Serum lipid levels in growth hormone-deficient men. Metabolism. 1994;43(2):199-203.
353. Rosen T, Eden S, Larson G, Wilhelmsen L, Bengtsson BA. Cardiovascular risk factors in adult patients with growth hormone deficiency. Acta Endocrinol(Copenh). 1993;129(3):195-200.
354. Sanmarti A, Lucas A, Hawkins F, Webb SM, Ulied A. Observational study in adult hypopituitary patients with untreated growth hormone deficiency (ODA study). Socio-economic impact and health status. Collaborative ODA (Observational GH Deficiency in Adults) Group. EurJEndocrinol. 1999;141(5):481-9.
355. Vahl N, Jorgensen JO, Hansen TB, Klausen IB, Jurik AG, Hagen C, et al. The favourable effects of growth hormone (GH) substitution on hypercholesterolaemia in GH-deficient adults are not associated with concomitant reductions in adiposity. A 12 month placebo-controlled study. IntJObesRelat Metab Disord. 1998;22(6):529-36.
356. Amato G, Carella C, Fazio S, La MG, Cittadini A, Sabatini D, et al. Body composition, bone metabolism, and heart structure and function in growth hormone (GH)-

deficient adults before and after GH replacement therapy at low doses. JClinEndocrinolMetab. 1993;77(6):1671-6.
357. Markussis V, Beshyah SA, Fisher C, Sharp P, Nicolaides AN, Johnston DG. Detection of premature atherosclerosis by high-resolution ultrasonography in symptom-free hypopituitary adults. Lancet. 1992;340(8829):1188-92.
358. Merimee TJ. A follow-up study of vascular disease in growth-hormone-deficient dwarfs with diabetes. N Engl J Med. 1978;298(22):1217-22.
359. Dunne FP, Elliot P, Gammage MD, Stallard T, Ryan T, Sheppard MC, et al. Cardiovascular function and glucocorticoid replacement in patients with hypopituitarism. ClinEndocrinol(Oxf). 1995;43(5):623-9.
360. Longobardi S, Cuocolo A, Merola B, Di Rella F, Colao A, Nicolai E, et al. Left ventricular function in young adults with childhood and adulthood onset growth hormone deficiency. Clin Endocrinol (Oxf). 1998;48(2):137-43.
361. Merola B, Cittadini A, Colao A, Longobardi S, Fazio S, Sabatini D, et al. Cardiac structural and functional abnormalities in adult patients with growth hormone deficiency. J Clin Endocrinol Metab. 1993;77(6):1658-61.
362. Thuesen L, Jorgensen JO, Muller JR, Kristensen BO, Skakkebaek NE, Vahl N, et al. Short and long-term cardiovascular effects of growth hormone therapy in growth hormone deficient adults. ClinEndocrinol(Oxf). 1994;41(5):615-20.
363. O'Leary DH, Polak JF, Kronmal RA, Manolio TA, Burke GL, Wolfson SK, Jr. Carotid-artery intima and media thickness as a risk factor for myocardial infarction and stroke in older adults. Cardiovascular Health Study Collaborative Research Group. N Engl J Med. 1999;340(1):14-22.
364. Irving RJ, Carson MN, Webb DJ, Walker BR. Peripheral vascular structure and function in men with contrasting GH levels. JClinEndocrinolMetab. 2002;87(7):3309-14.
365. Pfeifer M, Verhovec R, Zizek B, Prezelj J, Poredos P, Clayton RN. Growth hormone (GH) treatment reverses early atherosclerotic changes in GH-deficient adults. JClinEndocrinolMetab. 1999;84(2):453-7.
366. Ross R. Atherosclerosis--an inflammatory disease. NEnglJMed. 1999;340(2):115-26.
367. Andreassen M, Vestergaard H, Kristensen LO. Concentrations of the acute phase reactants high-sensitive C-reactive protein and YKL-40 and of interleukin-6 before and after treatment in patients with acromegaly and growth hormone deficiency. ClinEndocrinol(Oxf). 2007;67(6):909-16.
368. Gomez JM, Sahun M, Vila R, Domenech P, Catalina P, Soler J, et al. Peripheral fibrinolytic markers, soluble adhesion molecules, inflammatory cytokines and endothelial function in hypopituitary adults with growth hormone deficiency. ClinEndocrinol(Oxf). 2006;64(6):632-9.
369. Leonsson M, Hulthe J, Johannsson G, Wiklund O, Wikstrand J, Bengtsson BA, et al. Increased Interleukin-6 levels in pituitary-deficient patients are independently related to their carotid intima-media thickness. Clin Endocrinol (Oxf). 2003;59(2):242-50.
370. Vaughan DE. Plasminogen activator inhibitor-1: a common denominator in cardiovascular disease. JInvestigMed. 1998;46(8):370-6.
371. Devin JK, Blevins LS, Jr., Verity DK, Chen Q, Bloodworth JR, Jr., Covington J, et al. Markedly impaired fibrinolytic balance contributes to cardiovascular risk in adults with growth hormone deficiency. JClinEndocrinolMetab. 2007;92(9):3633-9.
372. Johansson JO, Landin K, Johannsson G, Tengborn L, Bengtsson BA. Long-term treatment with growth hormone decreases plasminogen activator inhibitor-1 and

tissue plasminogen activator in growth hormone-deficient adults. ThrombHaemost. 1996;76(3):422-8.
373. Johansson JO, Landin K, Tengborn L, Rosen T, Bengtsson BA. High fibrinogen and plasminogen activator inhibitor activity in growth hormone-deficient adults. ArteriosclerThromb. 1994;14(3):434-7.
374. Kvasnicka J, Marek J, Kvasnicka T, Weiss V, Markova M, Stepan J, et al. Increase of adhesion molecules, fibrinogen, type-1 plasminogen activator inhibitor and orosomucoid in growth hormone (GH) deficient adults and their modulation by recombinant human GH replacement. Clin Endocrinol (Oxf). 2000;52(5):543-8.
375. Bengtsson BA, Abs R, Bennmarker H, Monson JP, Feldt-Rasmussen U, Hernberg-Stahl E, et al. The effects of treatment and the individual responsiveness to growth hormone (GH) replacement therapy in 665 GH-deficient adults. KIMS Study Group and the KIMS International Board. JClinEndocrinolMetab. 1999;84(11):3929-35.
376. Salomon F, Cuneo RC, Hesp R, Sonksen PH. The effects of treatment with recombinant human growth hormone on body composition and metabolism in adults with growth hormone deficiency. NEnglJMed. 1989;321(26):1797-803.
377. Boguszewski CL, Meister LH, Zaninelli DC, Radominski RB. One year of GH replacement therapy with a fixed low-dose regimen improves body composition, bone mineral density and lipid profile of GH-deficient adults. EurJEndocrinol. 2005;152(1):67-75.
378. Colao A, Di SC, Cuocolo A, Spinelli L, Tedesco N, Pivonello R, et al. Improved cardiovascular risk factors and cardiac performance after 12 months of growth hormone (GH) replacement in young adult patients with GH deficiency. JClinEndocrinolMetab. 2001;86(5):1874-81.
379. Serri O, St-Jacques P, Sartippour M, Renier G. Alterations of monocyte function in patients with growth hormone (GH) deficiency: effect of substitutive GH therapy. JClinEndocrinolMetab. 1999;84(1):58-63.
380. Sesmilo G, Biller BM, Llevadot J, Hayden D, Hanson G, Rifai N, et al. Effects of growth hormone administration on inflammatory and other cardiovascular risk markers in men with growth hormone deficiency. A randomized, controlled clinical trial. AnnInternMed. 2000;133(2):111-22.
381. Borson-Chazot F, Serusclat A, Kalfallah Y, Ducottet X, Sassolas G, Bernard S, et al. Decrease in carotid intima-media thickness after one year growth hormone (GH) treatment in adults with GH deficiency. JClinEndocrinolMetab. 1999;84(4):1329-33.
382. Gibney J, Wallace JD, Spinks T, Schnorr L, Ranicar A, Cuneo RC, et al. The effects of 10 years of recombinant human growth hormone (GH) in adult GH-deficient patients. JClinEndocrinolMetab. 1999;84(8):2596-602.
383. Florakis D, Hung V, Kaltsas G, Coyte D, Jenkins PJ, Chew SL, et al. Sustained reduction in circulating cholesterol in adult hypopituitary patients given low dose titrated growth hormone replacement therapy: a two year study. ClinEndocrinol(Oxf). 2000;53(4):453-9.
384. Eden S, Wiklund O, Oscarsson J, Rosen T, Bengtsson BA. Growth hormone treatment of growth hormone-deficient adults results in a marked increase in Lp(a) and HDL cholesterol concentrations. ArteriosclerThromb. 1993;13(2):296-301.
385. O'Halloran DJ, Wieringa G, Tsatsoulis A, Shalet SM. Increased serum lipoprotein(a) concentrations after growth hormone (GH) treatment in patients with isolated GH deficiency. Ann Clin Biochem. 1996;33 (Pt 4):330-4.
386. Wieringa G, Shalet SM. Changes in lipoprotein (a) levels measured by six kit methods during growth hormone treatment of growth hormone deficient adults. Growth HormIGFRes. 2000;10(4):231.

387. Peacey SR, Guo CY, Robinson AM, Price A, Giles MA, Eastell R, et al. Glucocorticoid replacement therapy: are patients over treated and does it matter? ClinEndocrinol(Oxf). 1997;46(3):255-61.
388. Agha A, Liew A, Finucane F, Baker L, O'Kelly P, Tormey W, et al. Conventional glucocorticoid replacement overtreats adult hypopituitary patients with partial ACTH deficiency. ClinEndocrinol(Oxf). 2004;60(6):688-93.
389. Filipsson H, Monson JP, Koltowska-Haggstrom M, Mattsson A, Johannsson G. The impact of glucocorticoid replacement regimens on metabolic outcome and comorbidity in hypopituitary patients. JClinEndocrinolMetab. 2006;91(10):3954-61.
390. Charmandari E, Johnston A, Brook CG, Hindmarsh PC. Bioavailability of oral hydrocortisone in patients with congenital adrenal hyperplasia due to 21-hydroxylase deficiency. JEndocrinol. 2001;169(1):65-70.
391. Derendorf H, Mollmann H, Barth J, Mollmann C, Tunn S, Krieg M. Pharmacokinetics and oral bioavailability of hydrocortisone. JClinPharmacol. 1991;31(5):473-6.
392. DeVile CJ, Stanhope R. Hydrocortisone replacement therapy in children and adolescents with hypopituitarism. ClinEndocrinol(Oxf). 1997;47(1):37-41.
393. Howlett TA. An assessment of optimal hydrocortisone replacement therapy. ClinEndocrinol(Oxf). 1997;46(3):263-8.
394. Crown A, Lightman S. Why is the management of glucocorticoid deficiency still controversial: a review of the literature. ClinEndocrinol(Oxf). 2005;63(5):483-92.
395. Merza Z, Rostami-Hodjegan A, Memmott A, Doane A, Ibbotson V, Newell-Price J, et al. Circadian hydrocortisone infusions in patients with adrenal insufficiency and congenital adrenal hyperplasia. ClinEndocrinol(Oxf). 2006;65(1):45-50.
396. Lovas K, Husebye ES. Continuous subcutaneous hydrocortisone infusion in Addison's disease. Eur J Endocrinol. 2007;157(1):109-12.
397. Debono M, Ross RJ, Newell-Price J. Inadequacies of glucocorticoid replacement and improvements by physiological circadian therapy. EurJEndocrinol. 2009;160(5):719-29.
398. Johannsson G, Bergthorsdottir R, Nilsson AG, Lennernas H, Hedner T, Skrtic S. Improving glucocorticoid replacement therapy using a novel modified-release hydrocortisone tablet: a pharmacokinetic study. EurJEndocrinol. 2009;161(1):119-30.
399. Debono M, Ghobadi C, Rostami-Hodjegan A, Huatan H, Campbell MJ, Newell-Price J, et al. Modified-release hydrocortisone to provide circadian cortisol profiles. JClinEndocrinolMetab. 2009;94(5):1548-54.
400. Verma S, Vanryzin C, Sinaii N, Kim MS, Nieman LK, Ravindran S, et al. A pharmacokinetic and pharmacodynamic study of delayed- and extended-release hydrocortisone (Chronocort) versus conventional hydrocortisone (Cortef) in the treatment of congenital adrenal hyperplasia. ClinEndocrinol(Oxf). 2009.
401. van ZB, Nur E, Squizzato A, Dekkers OM, Twickler MT, Fliers E, et al. Hypercoagulable state in Cushing's syndrome: a systematic review. JClinEndocrinolMetab. 2009.
402. Arnaldi G, Mancini T, Polenta B, Boscaro M. Cardiovascular risk in Cushing's syndrome. Pituitary. 2004;7(4):253-6.
403. Colao A, Pivonello R, Spiezia S, Faggiano A, Ferone D, Filippella M, et al. Persistence of increased cardiovascular risk in patients with Cushing's disease after five years of successful cure. JClinEndocrinolMetab. 1999;84(8):2664-72.
404. Mayo-Smith W, Hayes CW, Biller BM, Klibanski A, Rosenthal H, Rosenthal DI. Body fat distribution measured with CT: correlations in healthy subjects, patients with

anorexia nervosa, and patients with Cushing syndrome. Radiology. 1989 Feb;170(2):515-8.
405. Garrapa GG, Pantanetti P, Arnaldi G, Mantero F, Faloia E. Body composition and metabolic features in women with adrenal incidentaloma or Cushing's syndrome. J Clin Endocrinol Metab. 2001 Nov;86(11):5301-6.
406. Fernandez-Rodriguez E, Stewart PM, Cooper MS. The pituitary-adrenal axis and body composition. Pituitary. 2009;12(2):105-15.
407. Ahdjoudj S, Lasmoles F, Oyajobi BO, Lomri A, Delannoy P, Marie PJ. Reciprocal control of osteoblast/chondroblast and osteoblast/adipocyte differentiation of multipotential clonal human marrow stromal F/STRO-1(+) cells. J Cell Biochem. 2001;81(1):23-38.
408. Bujalska IJ, Kumar S, Hewison M, Stewart PM. Differentiation of adipose stromal cells: the roles of glucocorticoids and 11beta-hydroxysteroid dehydrogenase. Endocrinology. 1999;140(7):3188-96.
409. MacDougald OA, Lane MD. Transcriptional regulation of gene expression during adipocyte differentiation. Annu Rev Biochem. 1995;64:345-73.
410. Mancini T, Doga M, Mazziotti G, Giustina A. Cushing's syndrome and bone. Pituitary. 2004;7(4):249-52.
411. Ottosson M, Lonnroth P, Bjorntorp P, Eden S. Effects of cortisol and growth hormone on lipolysis in human adipose tissue. J Clin Endocrinol Metab. 2000 Feb;85(2):799-803.
412. Stewart PM, Tomlinson JW. Cortisol, 11 beta-hydroxysteroid dehydrogenase type 1 and central obesity. Trends EndocrinolMetab. [S1043276002005660 pii]. 2002;13(3):94-6.
413. Bujalska IJ, Kumar S, Stewart PM. Does central obesity reflect "Cushing's disease of the omentum"? Lancet. [S0140-6736(96)11222-8 pii ;10.1016/S0140-6736(96)11222-8 doi]. 1997;349(9060):1210-3.
414. Rask E, Walker BR, Soderberg S, Livingstone DE, Eliasson M, Johnson O, et al. Tissue-specific changes in peripheral cortisol metabolism in obese women: increased adipose 11beta-hydroxysteroid dehydrogenase type 1 activity. J Clin Endocrinol Metab. 2002 Jul;87(7):3330-6.
415. Engeli S, Bohnke J, Feldpausch M, Gorzelniak K, Heintze U, Janke J, et al. Regulation of 11beta-HSD genes in human adipose tissue: influence of central obesity and weight loss. Obes Res. 2004 Jan;12(1):9-17.
416. Sandeep TC, Andrew R, Homer NZ, Andrews RC, Smith K, Walker BR. Increased in vivo regeneration of cortisol in adipose tissue in human obesity and effects of the 11beta-hydroxysteroid dehydrogenase type 1 inhibitor carbenoxolone. Diabetes. 2005 Mar;54(3):872-9.
417. Tomlinson JW, Moore JS, Clark PM, Holder G, Shakespeare L, Stewart PM. Weight loss increases 11beta-hydroxysteroid dehydrogenase type 1 expression in human adipose tissue. JClinEndocrinolMetab. [10.1210/jc.2003-031376 doi ;89/6/2711 pii]. 2004;89(6):2711-6.
418. Travison TG, O'Donnell AB, Araujo AB, Matsumoto AM, McKinlay JB. Cortisol levels and measures of body composition in middle-aged and older men. Clin Endocrinol (Oxf). 2007 Jul;67(1):71-7.
419. Jessop DS, Dallman MF, Fleming D, Lightman SL. Resistance to glucocorticoid feedback in obesity. J Clin Endocrinol Metab. 2001 Sep;86(9):4109-14.
420. Purnell JQ, Brandon DD, Isabelle LM, Loriaux DL, Samuels MH. Association of 24-hour cortisol production rates, cortisol-binding globulin, and plasma-free cortisol

levels with body composition, leptin levels, and aging in adult men and women. J Clin Endocrinol Metab. 2004 Jan;89(1):281-7.
421. Giavoli C, Libe R, Corbetta S, Ferrante E, Lania A, Arosio M, et al. Effect of recombinant human growth hormone (GH) replacement on the hypothalamic-pituitary-adrenal axis in adult GH-deficient patients. JClinEndocrinolMetab. 2004;89(11):5397-401.
422. Frajese GV, Taylor NF, Jenkins PJ, Besser GM, Monson JP. Modulation of cortisol metabolism during treatment of acromegaly is independent of body composition and insulin sensitivity. Horm Res. 2004;61(5):246-51.
423. Paulsen SK, Pedersen SB, Jorgensen JO, Fisker S, Christiansen JS, Flyvbjerg A, et al. Growth hormone (GH) substitution in GH-deficient patients inhibits 11beta-hydroxysteroid dehydrogenase type 1 messenger ribonucleic acid expression in adipose tissue. J Clin Endocrinol Metab. 2006 Mar;91(3):1093-8.
424. Trainer PJ, Drake WM, Perry LA, Taylor NF, Besser GM, Monson JP. Modulation of cortisol metabolism by the growth hormone receptor antagonist pegvisomant in patients with acromegaly. J Clin Endocrinol Metab. 2001 Jul;86(7):2989-92.
425. Davis JR, Sheppard MC, Shakespear RA, Lynch SS, Clayton RN. Does growth hormone releasing factor desensitize the somatotroph? Interpretation of responses of growth hormone during and after 10-hour infusion of GRF 1-29 amide in man. ClinEndocrinol(Oxf). 1986;24(2):135-40.
426. Sata A, Ho KK. Growth hormone measurements in the diagnosis and monitoring of acromegaly. Pituitary. [10.1007/s11102-007-0034-x doi]. 2007;10(2):165-72.
427. Bidlingmaier M, Strasburger CJ. Growth hormone assays: current methodologies and their limitations. Pituitary. [10.1007/s11102-007-0030-1 doi]. 2007;10(2):115-9.
428. Dauncey MJ, Shakespear RA, Rudd BT, Ingram DL. Variations in somatomedin-C/insulin-like growth factor-I associated with environmental temperature and nutrition. HormMetab Res. 1990;22(5):261-4.
429. Clemmons DR. IGF-I assays: current assay methodologies and their limitations. Pituitary. [10.1007/s11102-007-0032-z doi]. 2007;10(2):121-8.
430. Underwood LE, Thissen JP, Lemozy S, Ketelslegers JM, Clemmons DR. Hormonal and nutritional regulation of IGF-I and its binding proteins. Horm Res. 1994;42(4-5):145-51.
431. Milani D, Carmichael JD, Welkowitz J, Ferris S, Reitz RE, Danoff A, et al. Variability and reliability of single serum IGF-I measurements: impact on determining predictability of risk ratios in disease development. J Clin Endocrinol Metab. 2004;89(5):2271-4.
432. Furlanetto RW, Underwood LE, Van Wyk JJ, D'Ercole AJ. Estimation of somatomedin-C levels in normals and patients with pituitary disease by radioimmunoassay. J Clin Invest. [10.1172/JCI108816 doi]. 1977;60(3):648-57.
433. Mesiano S, Young IR, Browne CA, Thorburn GD. Failure of acid-ethanol treatment to prevent interference by binding proteins in radioligand assays for the insulin-like growth factors. J Endocrinol. 1988;119(3):453-60.
434. Mohan S, Baylink DJ. Development of a simple valid method for the complete removal of insulin-like growth factor (IGF)-binding proteins from IGFs in human serum and other biological fluids: comparison with acid-ethanol treatment and C18 Sep-Pak separation. J Clin Endocrinol Metab. 1995;80(2):637-47.

435. Blum WF, Ranke MB, Kietzmann K, Gauggel E, Zeisel HJ, Bierich JR. A specific radioimmunoassay for the growth hormone (GH)-dependent somatomedin-binding protein: its use for diagnosis of GH deficiency. JClinEndocrinolMetab. 1990;70(5):1292-8.
436. Schuller AG, Lindenbergh-Kortleve DJ, de Boer WI, Zwarthoff EC, Drop SL. Localization of the epitope of a monoclonal antibody against human insulin-like growth factor binding protein-1, functionally interfering with insulin-like growth factor binding. Growth Regul. 1993;3(1):32-4.
437. Clark PM, Neylon I, Raggatt PR, Sheppard MC, Stewart PM. Defining the normal cortisol response to the short Synacthen test: implications for the investigation of hypothalamic-pituitary disorders. Clin Endocrinol (Oxf). 1998;49(3):287-92.
438. Tomlinson JW, Moore JS, Clark PM, Holder G, Shakespeare L, Stewart PM. Weight loss increases 11beta-hydroxysteroid dehydrogenase type 1 expression in human adipose tissue. J Clin Endocrinol Metab. [10.1210/jc.2003-031376 doi ;89/6/2711 pii]. 2004;89(6):2711-6.
439. Agha A, Tomlinson JW, Clark PM, Holder G, Stewart PM. The long-term predictive accuracy of the short synacthen (corticotropin) stimulation test for assessment of the hypothalamic-pituitary-adrenal axis. J Clin Endocrinol Metab. [jc.2005-1131 pii ;10.1210/jc.2005-1131 doi]. 2006;91(1):43-7.
440. Boelaert K, Horacek J, Holder RL, Watkinson JC, Sheppard MC, Franklyn JA. Serum thyrotropin concentration as a novel predictor of malignancy in thyroid nodules investigated by fine-needle aspiration. J Clin Endocrinol Metab. [jc.2006-0527 pii ;10.1210/jc.2006-0527 doi]. 2006;91(11):4295-301.
441. Wilson S, Parle JV, Roberts LM, Roalfe AK, Hobbs FD, Clark P, et al. Prevalence of subclinical thyroid dysfunction and its relation to socioeconomic deprivation in the elderly: a community-based cross-sectional survey. J Clin Endocrinol Metab. [jc.2006-1557 pii ;10.1210/jc.2006-1557 doi]. 2006;91(12):4809-16.
442. Stewart PM, Boulton A, Kumar S, Clark PM, Shackleton CH. Cortisol metabolism in human obesity: impaired cortisone-->cortisol conversion in subjects with central adiposity. JClinEndocrinolMetab. 1999;84(3):1022-7.
443. Sherlock M, Reulen RC, Alonso AA, Ayuk J, Clayton RN, Sheppard MC, et al. ACTH deficiency, higher doses of hydrocortisone replacement, and radiotherapy are independent predictors of mortality in patients with acromegaly. JClinEndocrinolMetab. [jc.2009-1097 pii ;10.1210/jc.2009-1097 doi]. 2009;94(11):4216-23.
444. Wei L, MacDonald TM, Walker BR. Taking glucocorticoids by prescription is associated with subsequent cardiovascular disease. AnnInternMed. 2004;141(10):764-70.

Publications

ORIGINAL ARTICLE

11β-Hydroxysteroid Dehydrogenase Type 1 Regulates Glucocorticoid-Induced Insulin Resistance in Skeletal Muscle

Stuart A. Morgan,[1] Mark Sherlock,[1] Laura L. Gathercole,[1] Gareth G. Lavery,[1] Carol Lenaghan,[2] Iwona J. Bujalska,[1] David Laber,[2] Alice Yu,[2] Gemma Convey,[2] Rachel Mayers,[2] Krisztina Hegyi,[3] Jaswinder K. Sethi,[3] Paul M. Stewart,[1] David M. Smith,[2] and Jeremy W. Tomlinson[1]

OBJECTIVE—Glucocorticoid excess is characterized by increased adiposity, skeletal myopathy, and insulin resistance, but the precise molecular mechanisms are unknown. Within skeletal muscle, 11β-hydroxysteroid dehydrogenase type 1 (11β-HSD1) converts cortisone (11-dehydrocorticosterone in rodents) to active cortisol (corticosterone in rodents). We aimed to determine the mechanisms underpinning glucocorticoid-induced insulin resistance in skeletal muscle and indentify how 11β-HSD1 inhibitors improve insulin sensitivity.

RESEARCH DESIGN AND METHODS—Rodent and human cell cultures, whole-tissue explants, and animal models were used to determine the impact of glucocorticoids and selective 11β-HSD1 inhibition upon insulin signaling and action.

RESULTS—Dexamethasone decreased insulin-stimulated glucose uptake, decreased IRS1 mRNA and protein expression, and increased inactivating $pSer^{307}$ insulin receptor substrate (IRS)-1. 11β-HSD1 activity and expression were observed in human and rodent myotubes and muscle explants. Activity was predominantly oxo-reductase, generating active glucocorticoid. A1 (selective 11β-HSD1 inhibitor) abolished enzyme activity and blocked the increase in $pSer^{307}$ IRS1 and reduction in total IRS1 protein after treatment with 11DHC but not corticosterone. In C57Bl6/J mice, the selective 11β-HSD1 inhibitor, A2, decreased fasting blood glucose levels and improved insulin sensitivity. In KK mice treated with A2, skeletal muscle $pSer^{307}$ IRS1 decreased and $pThr^{308}$ Akt/PKB increased. In addition, A2 decreased both lipogenic and lipolytic gene expression.

CONCLUSIONS—Prereceptor facilitation of glucocorticoid action via 11β-HSD1 increases $pSer^{307}$ IRS1 and may be crucial in mediating insulin resistance in skeletal muscle. Selective 11β-HSD1 inhibition decreases $pSer^{307}$ IRS1, increases $pThr^{308}$ Akt/PKB, and decreases lipogenic and lipolytic gene expression that may represent an important mechanism underpinning their insulin-sensitizing action. ***Diabetes*** **58:2506–2515, 2009**

From the [1]Centre for Endocrinology, Diabetes and Metabolism, Institute of Biomedical Research, School of Clinical & Experimental Medicine, University of Birmingham, Birmingham, U.K.; the [2]AstraZeneca Diabetes & Obesity Drug Discovery, Mereside, Alderley Park, Macclesfield, Cheshire, U.K.; and the [3]Department of Clinical Biochemistry, University of Cambridge Metabolic Research Laboratories, Institute of Metabolic Science, Addenbrooke's Hospital, Cambridge, U.K.

Corresponding author: Jeremy W. Tomlinson, j.w.tomlinson@bham.ac.uk.

Received 9 April 2009 and accepted 16 July 2009. Published ahead of print at http://diabetes.diabetesjournals.org on 12 August 2009. DOI: 10.2337/db09-0525.

The pathophysiological effects of glucocorticoids are well described and impact upon almost all organ systems within the body. This is highlighted in patients with glucocorticoids excess, Cushing's syndrome characterized by central obesity, hypertension, proximal myopathy, insulin resistance, and in some cases overt type 2 diabetes. In addition, up to 2.5% of the population are taking prescribed glucocorticoids (1), and their side effects represent a considerable clinical burden for both patient and clinician.

Glucocorticoids induce whole-body insulin resistance (2); however, the precise molecular mechanisms that underpin this observation have not been defined in detail. In simple obesity and insulin resistance, circulating cortisol levels are not elevated (3), but in key insulin target tissues including liver, fat, and muscle, glucocorticoid availability to bind and activate the glucocorticoid receptor is controlled by 11β-hydroxysteroid dehydrogenase type 1 (11β-HSD1). 11β-HSD1 is an endo-lumenal enzyme that interconverts inactive (cortisone in humans and 11-dehydrocorticosterone [11DHC] in rodents) and active glucocorticoids (cortisol in humans and corticosterone [CORT] in rodents) (4). Critically, the directionality of 11β-HSD1 activity is cofactor (NADPH) dependent that is supplied by a tightly associated endo-lumenal enzyme, hexose-6-phopshate dehydrogenase (H6PDH). Decreases in H6PDH expression and activity decrease 11β-HSD1 oxo-reductase and increase dehydrogenase activity (5). Despite this bidirectional potential, the predominant direction of activity in liver, adipose, and muscle is oxo-reductase generating active glucocorticoid (cortisol and CORT), therefore, amplifying local glucocorticoid action.

Binding of insulin to its cell surface receptor leads to a conformational change and tyrosine autophosphorylation. Consequently, the insulin receptor substrate (IRS) family of adaptor proteins are recruited to the intracellular domain of the receptor and are phosphorylated at multiple tyrosine residues by the receptor tyrosine kinase to permit the docking of phosphatidylinositol-3-kinase (PI3K) and subsequent generation of $PI(3,4,5)P_3$. Generation of this second messenger acts to recruit the Akt/PKB family of serine/threonine kinases to the plasma membrane where they are then activated (6). Further downstream, activated Akt1/protein kinase B (PKB) phosphorylates a rab-GAP (GTPase) protein, AS160, which is a crucial regulator of the translocation of GLUT4 GLUT storage vesicles to the plasma membrane (7). It is this mechanism that permits

insulin-stimulated glucose entry into target tissues including skeletal muscle (8).

The molecular mechanisms underpinning insulin resistance are complex and variable. Serine/threonine phosphorylation of IRS1 (in particular Ser^{307} phosphorylation) has been shown to negatively regulate insulin signaling through multiple mechanisms including decreased affinity for the insulin receptor and increased degradation (9,10).

The interaction of glucocorticoids and the insulin signaling cascade has only been examined in a small number of studies that have offered variable explanations for the induction of insulin resistance (11–14). Importantly, the role of serine phosphorylation and the impact of prereceptor glucocorticoid metabolism have not been explored. The 11β-HSD1 knockout mouse is relatively insulin sensitive (15), and specific inhibitors of 11β-HSD1 improve lipid profiles, glucose tolerance, and insulin sensitivity and have considerable potential as therapeutic agents (16–18). However, the molecular mechanisms that underpin these observations remain to be defined.

Therefore, we have characterized the impact of glucocorticoids upon the insulin-signaling cascade and analyzed the expression, activity, and functional impact of 11β-HSD1 in vitro and using in vivo mouse models.

RESEARCH DESIGN AND METHODS

Cell culture. Mouse skeletal muscle cell line, C2C12 myoblasts (ECACC, U.K.), were grown in DMEM (PAA, U.K.) supplemented with 10% FBS (37°C, 5% CO_2). Cells were grown to 60–70% confluence before differentiation (initiated by replacing growth media with DMEM with 5% horse serum). After 8 days, myoblasts had fused to form multinucleated myotubes. Before treatment, cells were washed out with serum-free media for 4 h. For experiments examining Ser^{24} phosphorylation, C2C12 cells stably overexpressing myc-rIRS1 were generated and used as described previously for 3T3-L1 adipocytes (19).

Primary human myoblasts were obtained from PromoCell (Heidelberg, Germany). Myoblasts were cultured to confluence, as per the manufacturer's guidelines using the supplied media. Once confluent, media was changed to a chemically defined media (PromoCell, Germany) including 2% horse serum and cells differentiated into myotubes for 11 days. After differentiation, cells were incubated with serum-free media for 4 h before treatment.

Unless otherwise stated, for all cell culture experiments investigating insulin-signaling cascade protein phosphorylation, media was spiked with human insulin (0.1 μg/ml, Sigma, U.K.) for the final 15 min of the treatment period to achieve insulin stimulation. In experiments using the glucocorticoid receptor antagonist, RU38486, cells were pretreated with RU38486 (10 μmol/l) for 10 min before adding Dexamethasone (Dex). Treatments and reagents were supplied by Sigma, Poole, U.K. unless otherwise stated. Selective 11β-HSD1 inhibitors (A1 and A2, >95% and >99% purity, respectively) were provided through material transfer agreements with AstraZeneca (Macclesfield, U.K.). Inhibitor properties are presented within the results section.

RNA extraction, reverse transcription PCR, and real-time PCR. Total RNA was extracted from cell lysates using the Tri-Reagent system and from whole-tissue explants using RNeasy Fibrous Tissue Mini Kit (Qiagen). Integrity, concentration, and reverse transcription were performed as we have previously described (20). Specific mRNA levels were determined using an ABI 7500 sequence detection system (Perkin-Elmer Applied Biosystems, Warrington, U.K.). Reactions were performed in 20 μl volumes on 96-well plates in reaction buffer containing 2 × TaqMan Universal PCR Master mix (Applied Biosystems, Foster City, CA). Probes and primers for all genes were supplied by applied biosystems 'assay on demand' (Applied Biosystems). All reactions were normalized against 18S rRNA as an internal housekeeping gene.

Data were obtained as ct values (ct = cycle number at which logarithmic PCR plots cross a calculated threshold line) and used to determine Δct values with Δct = (ct of the target gene) – (ct of the housekeeping gene). Data are expressed as arbitrary units using the following transformation (expression = $10^5 \times [2^{-\Delta ct}]$ arbitrary units [AUs]). When used, fold changes were calculated using the following equation: [fold increase = $2^{-\text{difference in } \Delta ct}$].

Genecard analysis. Taqman 348-well custom arrays were purchased from Applied Biosystems containing 45 custom genes and 3 housekeeping genes. Five hundred nanograms of cDNA were mixed with Taqman universal PCR master mix (Applied Biosystems), and the array was run on an ABI 7900HT Fast Real-Time PCR System (Applied Biosystems). Data were obtained as ct values and fold changes calculated. Results were validated with standard Taqman RT-PCR.

Protein extraction and immunoblotting. Cells were scraped into 100 μl RIPA buffer (50 mmol/l Tris pH 7.4, 1% NP40, 0.25% sodium deoxycholate, 150 mmol/l NaCl, 1 mmol/l EDTA), 1 mmol/l phenylmethylsulfonyl fluoride, and protease inhibitor cocktail (Roche, Lewes, U.K.), incubated at −80°C (10 min) on ice (30 min), and centrifuged at 4°C (10 min, 14,000 rpm). The supernatant was transferred to a fresh tube and total protein concentration determined by a commercially available assay (Bio-Rad Laboratories, Hercules, CA).

Twenty micrograms of protein was resolved on an SDS-PAGE gel (acrylamide percentage varied according to protein size). Proteins were transferred onto nitrocellulose membrane, Hybond ECL (GE Healthcare, Chalfont St. Giles, U.K.). Primary (anti-IRS1, anti-$pSer^{307}$ IRS1, anti-IRS2, and anti-AS160 from Upstate, Dundee, U.K.; anti-PKB/akt, anti-$pSer^{473}$ PKB/akt [recognizing isoforms 1 and 2], and anti-Thr^{308} Akt/PKB from R&D Systems, Abingdon, U.K.; and anti-$pTyr^{608}$ IRS1 from Biosource, Nivelles, Belgium) and secondary antibodies (Dako, Glostrop, U.K.) were used at a dilution of 1/5,000. Membranes were reprobed for β-actin and primary and secondary antibodies used at a dilution of 1/5,000 (Abcam plc, Cambridge, U.K.). Bands were visualized using ECL detection kit (GE Healthcare, Chalfont St. Giles, U.K.) and quantified with Genesnap by Syngene (Cambridge, U.K.).

Glucose transport assay. Glucose uptake activity was analyzed by measuring the uptake of 2-deoxy-D-[^{3}H] glucose as described previously (21). After treatment, cells were washed three times with Krebs-Ringer-Hepes (KRP) buffer and incubated with 0.9 ml KRP buffer at 37°C for 20 min. Insulin (0.5 μg/ml) was then added, and the cells were incubated at 37°C for 20 min. Glucose uptake was initiated by the addition of 0.1 ml KRP buffer and 37MBq/l 2-deoxy-D-[^{3}H] glucose (GE Healthcare) and 7 mmol/l glucose as final concentrations. After 60 min, glucose uptake was terminated by washing the cells three times with cold PBS. Cells were lysed and radioactivity retained by the cell lysates determined by scintillation counting.

11β-HSD1 assay. Briefly, intact cells were incubated with 100 nmol/l 11DHC and tritiated tracer for 2–24 h dependent upon assay system. In studies using selective 11β-HSD1 inhibitors, cells were incubated for 24 h with inhibitor before 11β-HSD1 assay being performed. Steroids were then extracted using dichloromethane, separated using a mobile phase consisting of ethanol and chloroform (8:92) by thin layer chromatography, and scanned using a Bioscan 3000 image analyzer (Lablogic, U.K.). Protein levels were assayed using a commercially available kit (Bio-Rad, Richmond, CA).

Mouse protocols. The selective 11β-HSD1 inhibitor A2 was used in two separate mouse protocols. All experimental procedures were conducted in accordance with the Animal Scientific Procedures Act 1986, Animal Welfare Act 2006, and local guidelines. First, male C57Bl6/J mice (6 weeks of age) were maintained for 20 weeks on a diet comprising 48 kcal% fat/10 kcal% fructose (Research Diets RD06072801, New Brunswick, NJ). Mice were housed with a standard light cycle (06:00 h on/18:00 h off), and A2 was administered (20 mg/kg b.i.d) by oral gavage for 28 days and compared against vehicle-control and pair-fed, vehicle-treated animals (n = 9–10). Food intake was assessed over the 28-day period, and on day 24 after 12-h fast, an oral glucose tolerance test (OGTT, 2 g/kg) was performed. Conscious tail-prick samples were analyzed for glucose using the Accu-Chek Aviva system (Roche) and for insulin using Ultra Sensitive Mouse Insulin ELISA kits (Crystal Chem #90800, Downers Grove, IL).

Separately, the impact of A2 upon skeletal muscle gene and protein expression in an additional hyperglycemic model were determined (male KK/Ta Jcl mice aged 7 weeks; CLEA Japan, Tokyo, Japan). Animals had free access to water and irradiated RM3 (E) diet composed of 11.5 kcal% fat, 27 kcal% protein, and 62 kcal% carbohydrate (Special Diets Services, Witham, U.K.). Compound A2 (20 mg/kg) or vehicle (10 ml/kg) was administered by oral gavage at 08:00 and 20:00 h for 4 consecutive days. After the administration of the third dose of A2, mice were anesthetized by inhalation of 2–3% v/v isoflurane (vaporized by oxygen at 1.6 l/min flow rate) and a 5 mg slow-release cortisone pellet (~8 mg · kg^{-1} · day^{-1} in a 29 g mouse) implanted subcutaneously in the lateral aspect of the neck (Innovative Research of America, Sarasota, FL). On day 4, 1–2 h after the seventh oral dose of A2, a rising-dose carbon dioxide concentration was used to humanely kill mice in the fed state and femoral quadriceps muscles were removed and snap frozen in liquid nitrogen.

Statistical analysis. Where data were normally distributed, unpaired Student's t tests were used to compare single treatments to control. If normality tests failed, then nonparametric tests were used. One-way ANOVA on ranks was used to compare multiple treatments, doses, or times (SigmaStat 3.1; Systat Software, Point Richmond, CA). Statistical analysis on real-time PCR data was performed on mean Δct values.

TABLE 1
mRNA expression of key components of the insulin-signaling cascade and glucocorticoid metabolism in C2C12 rodent skeletal myocytes measured using real-time PCR after treatment with Dex (1 μmol/l, 24 h) with or without the glucocorticoid receptor antagonist, RU38486 (10 μmol/l)

Gene	Control	Dexamethasone (1 μmol/l, 24 h)	Dexamethasone (1 μmol/l, 24 h) + RU38486 (10 μmol/l, 24 h)
InsR	4.4 ± 0.4	6.1 ± 0.5†	5.4 ± 0.5
IRS1	8.7 ± 0.7	4.5 ± 0.4*	7.5 ± 0.7§
AKT1	45.2 ± 5.4	39.4 ± 2.8	45.1 ± 3.4
AKT2	1.5 ± 0.3	2.3 ± 0.1*	1.9 ± 0.3
PI3K(p85)	1.4 ± 0.2	2.2 ± 0.2*	2.2 ± 0.1
GLUT4	2.3 ± 0.3	13.1 ± 1.5‡	3.7 ± 0.4‖
11βHSD1	32.9 ± 2.9	27.6 ± 2.7	35.6 ± 3.6
H6PDH	0.10 ± 0.0149	1.30 ± 0.07‡	0.18 ± 0.02¶
AS160	0.12 ± 0.02	0.23 ± 0.02*	0.12 ± 0.01§

Data are the mean values from $n = 5$ experiments and expressed as AUs ± SE (*$P < 0.05$, †$P < 0.01$, and ‡$P < 0.001$ vs. control; §$P < 0.05$, ‖$P < 0.01$, and ¶$P < 0.001$ vs. Dex).

RESULTS

Glucocorticoid impact upon the insulin-signaling cascade. In agreement with published data, treatment with the synthetic glucocorticoid Dex (1 μmol/l, 24 h) decreased insulin-stimulated glucose uptake (2.1 ± 0.3 vs. 1.7 ± 0.2 dpm × 10^5, $P < 0.05$, $n = 4$) consistent with the induction of insulin resistance in differentiated rodent C2C12 skeletal myocytes.

Using real-time PCR, Dex (1 μmol/l, 24 h) decreased mRNA expression of IRS1 (8.7 ± 0.7 vs. 4.5 ± 0.4 AU, $P < 0.05$, $n = 5$), an effect that was blocked by the glucocorticoid antagonist RU-38486 (Table 1). In contrast, IR, Akt/PKB2, PI3K, AS160, and GLUT4 expression all increased after Dex treatment. RU38486 reversed only the effects of Dex upon GLUT4 and AS160 expression. Although Dex treatment did not alter 11β-HSD1 expression, H6PDH expression increased (0.10 ± 0.01 vs. 1.30 ± 0.07 AU, $P < 0.001$) and was reversed by coincubation with RU38486 (0.18 ± 0.02 AU, $P < 0.001$ vs. Dex). Absolute mRNA expression data after Dex treatment with and without the glucocorticoid receptor antagonist RU38486 are presented in Table 1.

At the protein level, treatment with Dex decreased IRS1 total protein expression (0.4-fold, $P < 0.05$) that was recovered by coincubation with RU38486 (Fig. 1*A* and *B*). Insulin-stimulated, activating Tyr^{608} phosphorylation of IRS1 was unchanged with Dex treatment (Fig. 1*A* and *B*). However, we observed enhanced inactivating Ser^{307} phosphorylation (3.3-fold, $P < 0.05$) after Dex treatment that was prevented by RU-38486 (Fig. 1*A* and *B*). Total IRS2 protein expression was increased by Dex (1.7-fold, $P < 0.001$) (Fig. 1*A* and *C*). Further downstream, Akt/PKB protein expression did not change with Dex treatment, but activating Ser^{473} phosphorylation decreased (0.5-fold, $P < 0.05$) (Fig. 1*A* and *D*). Dex treatment increased AS160 expression 1.5-fold ($P < 0.05$), which was blocked by coincubation with RU38486 (Fig. 1*A* and *E*).

Diacylglycerol (DAG)-dependent protein kinase C (PKC) isoforms have been implicated in the phosphorylation of IRS1 at Ser^{24}, and this has been linked to the pathogenesis of insulin resistance (19). We examined the effect of Dex using C2C12 cells stably overexpressing IRS1. Although Dex increased Ser^{307} phosphorylation in this model, there was no detectable impact upon Ser^{24} phosphorylation or ectopic IRS1-myc protein levels (Fig. 1*F*).

To determine whether our observations with synthetic glucocorticoids were applicable in a physiological context, further experiments were performed using endogenous rodent glucocorticoids (11DHC and CORT). Consistent with our observations using Dex, CORT caused a dose- and time-dependent decrease in IRS1 total protein expression (dose: 1.0 [control] vs. 0.59-fold [100 nmol/l], $P < 0.01$, 0.47-fold [250 nmol/l], $P < 0.05$, 0.44-fold [500 nmol/l], $P < 0.01$, 0.38-fold [1,000 nmol/l], $P < 0.01$; time: 1.0 [control] vs. 0.19 ± 0.04 [48 h], $P < 0.05$) (Fig. 2*A* and *B*). This was accompanied by a dose- (1.0 [control] vs. 2.80-fold [250 nmol/l], $P < 0.01$, 3.99-fold [500 nmol/l], $P < 0.01$, 4.37-fold [1,000 nmol/l], $P < 0.001$) (Fig. 2*A*) and time- (1.0 [control] vs. 3.0 ± 0.08 [48 h], $P < 0.05$) (Fig. 2*B*) dependent increase in Ser^{307} phosphorylation.

11β-HSD1 in rodent and human skeletal muscle. 11β-HSD1 mRNA was highly expressed in C2C12 cells. Expression was also detected in whole-tissue explants of mouse quadriceps muscle, although levels were lower than those seen in liver and adipose tissue (Table 2). In all systems (C2C12 cells, human primary cultures, and whole-tissue explants from mice), functional, bidirectional 11β-HSD1 activity was demonstrated with predominant oxo-reductase activity (Fig. 3*A* and *B*). In mouse quadriceps explants, oxo-reductase activity was significantly decreased after coincubation with the nonselective 11β-HSD inhibitor, glycyrrhetinic acid (2 μmol/l, 2 h) (114.0 ± 5.7 vs. 44.6 ± 11.1 pmol · g^{-1} · h^{-1}, $P < 0.05$) (Fig. 3*A* and *B*). A1 and A2 are selective 11β-HSD1 inhibitors provided through an investigator-led collaboration with AstraZeneca. A1 has a half-maximal inhibitory concentration (IC_{50}) for human recombinant 11β-HSD1 of 0.3 nmol/l and for rat 637 nmol/l, mouse 33 nmol/l, and human 11β-HSD2 >15 μmol/l. A2 has an IC_{50} for human recombinant 11β-HSD1 of 7 nmol/l and for rat 94 nmol/l, mouse 26 nmol/l, and human 11β-HSD2 >15 μmol/l. Treatment with A1 (1 μmol/l, 24 h), significantly decreased oxo-reductase activity in mouse quadriceps whole-tissue explants, differentiated C2C12 cells, and primary cultures of differentiated human skeletal myocytes (Fig. 3*C*).

Functional impact of 11β-HSD1 inhibition

Rodent and human cell lines and primary cultures. Paralleling our observations with Dex and CORT, 11DHC (250 nmol/l, 24 h) decreased IRS1 total protein expression (0.5-fold, $P < 0.05$) and increased $pSer^{307}$ IRS1 (2.0-fold, $P < 0.05$) in C2C12 cells. Coincubation with the nonselective 11β-HSD inhibitor glycyrrhetinic acid (2.5 μmol/l, 24 h) reversed 11DHC-induced $pSer^{307}$ IRS1 to levels seen in control untreated cells (1.1-fold, $P = 0.56$ vs. control) (Fig. 4*A*). Glycyrrhetinic acid treatment alone was without effect (data not shown). Similarly, observations with the selective 11β-HSD1 inhibitor A1 (2.5 μmol/l, 24 h) mirrored those with glycyrrhetinic acid, completely blocking the effects of 11DHC to decrease total IRS1 expression and increase $pSer^{307}$ IRS1 (Fig. 4*B*). Extending these findings, in primary cultures of human skeletal muscle, cortisone (250 nmol/l, 24 h) decreased insulin-stimulated $pThr^{308}$ Akt/PKB without altering total Akt/PKB protein expression. These observations were completely abolished following coincubation with A1 (Fig. 4*C*).

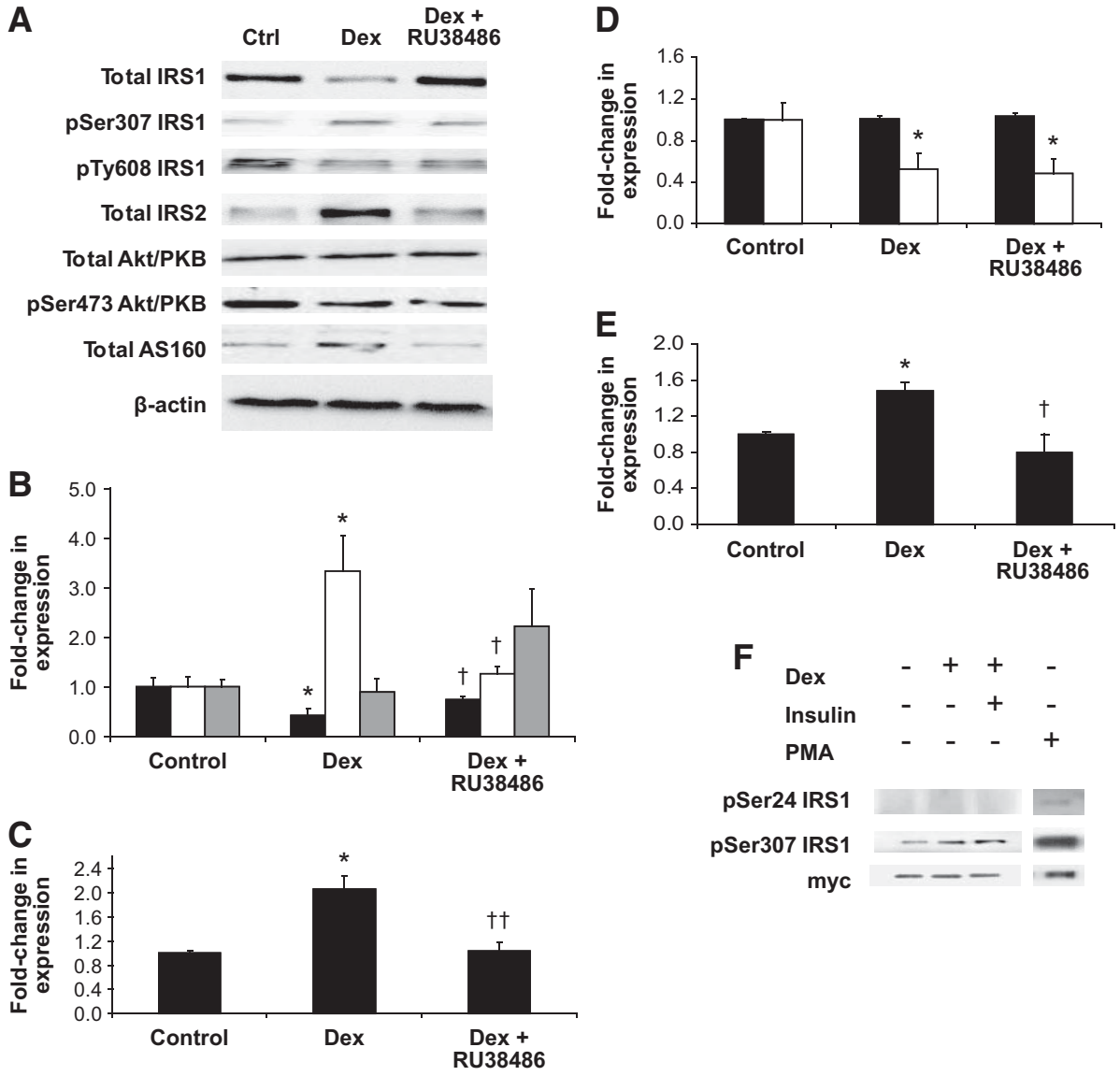

FIG. 1. Dex treatment (1 μmol/l, 24 h) in C2C12 rodent skeletal myocytes decreases IRS1 total protein expression, increases pSer^{307} IRS1, but does not change pTyr^{608} IRS1. These observations are reversed by coincubation with the glucocorticoid antagonist RU38486. IRS2 expression increased after Dex treatment. Although Akt/PKB expression does not change, activating pSer^{473} Akt/PKB decreases but is not recovered by coincubation with RU38486. Total AS160 protein expression increased after Dex pretreatment and was reversed with RU38486. Representative Western blots are shown in panel 1*A* with quantitation relative to β-actin as internal loading control shown in subsequent panels (IRS1 [total IRS1: black bars, pSer^{307} IRS1: white bars, pTyr^{608} IRS1: gray bars] [*B*], IRS2 [*C*], akt/PKB [total Akt/PKB: black bars, pSer^{473} Akt/PKB: white bars] [*D*], and AS160 [*E*]) (*$P < 0.05$ vs. control, †$P < 0.05$, ††$P < 0.01$ vs. Dex). In C2C12 cells stably overexpressing IRS1, Dex increases Ser^{307} but does not induce Ser^{24} phosphorylation (*F*). Ctrl, control. PMA, phorbol myristate acetate.

Mouse in vivo studies

Food intake, glucose tolerance, and insulin sensitivity. Food intake decreased within the first 48 h in the A2-treated animals in comparison with vehicle-treated controls. However, by day 4 and for the remainder of the 28-day protocol, food intake did not differ between the groups (day 4: 15.4 ± 0.7 vs. 16.5 ± 0.7 kcal/day [A2 vs. control], $P = 0.08$). At day 28, fasting blood glucose and insulin levels were lower in the A2-treated animals compared with both vehicle-treated and pair-fed controls (glucose: 6.8 ± 0.3 vs. 7.4 ± 0.35 vs. 7.7 ± 0.3 mmol/l, $P < 0.05$; insulin: 0.60 ± 0.10 vs. 0.82 ± 0.14 vs. 0.91 ± 0.11 ng/ml, $P < 0.05$, A2 vs. vehicle vs. pair-fed vehicle). Similarly, homeostasis model assessment values were lower (4.2 ± 0.9 vs. 6.0 ± 0.98 vs. 7.1 ± 0.9 [A2 vs. vehicle vs. pair-fed vehicle], $P < 0.05$) as was insulin secretion (area under curve, AUC) across an OGTT (2.29 ± 0.23 vs. 2.95 ± 0.37 vs. 2.94 ± 0.21 ng · ml^{-1} · h^{-1} [A2 vs. vehicle vs. pair-fed vehicle], $P < 0.05$). Glucose levels across the OGTT (AUC) did not change significantly (22.4 ± 0.46 vs. 24.2 ± 0.42 vs. 22.9 ± 0.45 mmol · l^{-1} · h^{-1} [A2 vs. vehicle vs. pair-fed vehicle], P = not significant).

Gene and protein expression in skeletal muscle from KK mice. Cortisone pellet–implanted KK mice treated with A2 for 4 consecutive days had increased total IRS1 protein expression, decreased Ser^{307} phosphorylation, and increased Thr^{308} phosphorylation of Akt/PKB in whole-tissue quadriceps explants. Tyr^{608} phosphorylation did not change (Fig. 5*A*). Genecard analysis of quadriceps mRNA expression following A2 treatment is shown in Table 3. Positive findings were endorsed with real-time PCR (Fig. 5*B*). 11β-HSD1 expression decreased (0.48-fold) (Table 3,

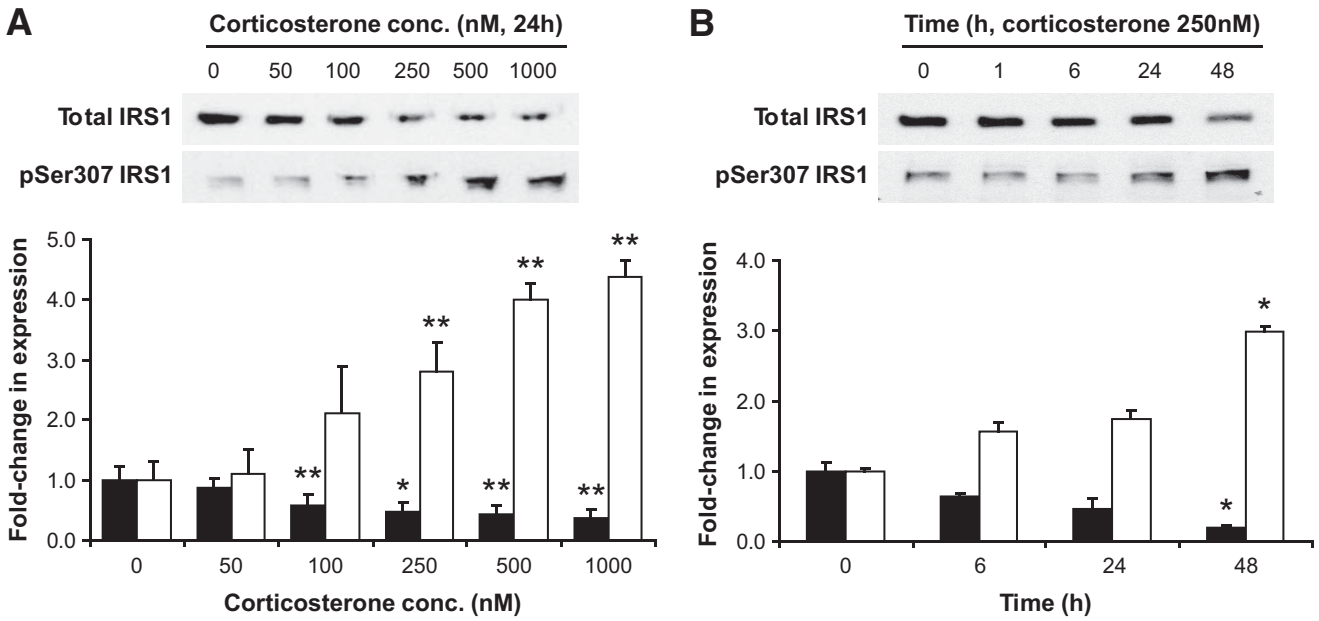

FIG. 2. The endogenous rodent glucocorticoid, CORT, induces a dose- (*A*) and time- (*B*) dependent decrease in total IRS1 protein expression (black bars) and increase in pSer^{307} IRS1 (white bars). Data presented are the means of $n = 4–6$ experiments with representative Western blots inserted above (*$P < 0.05$, **$P < 0.01$ vs. control).

Fig. 5*B*) without effect on glucocorticoid receptor or H6PDH expression. In agreement with our protein expression data, IRS1 mRNA expression increased after selective 11β-HSD1 inhibition (Fig. 5*B*). The regulatory subunit of PI3K p85 decreased 0.25-fold after treatment with A2 with no change in catalytic subunit (p110) expression (Table 3, Fig. 5*B*). PI3K activity was not measured as part of this study. A2 treatment decreased expression of key target genes involved in lipogenesis (ACC1 0.3-fold, DGAT 0.4-fold), lipolysis (HSL 0.3-fold, ATGL 0.39-fold) and lipid oxidation (ACC2 0.6-fold) (Table 3, Fig. 5*B*). In addition, PDK4 increased 1.7-fold (Fig. 5*B*).

DISCUSSION

In this study, we have characterized in detail the impact of both synthetic and endogenous glucocorticoids upon insulin signaling in the rodent skeletal muscle cell line, C2C12. In addition, we have characterized expression and activity of 11β-HSD1 in both rodent and human skeletal muscle, ascribed a functional significance to its activity in terms of insulin sensitization, and have begun to explore the mechanisms by which this occurs.

Glucocorticoids impair insulin signaling at multiple levels, importantly decreasing total IRS1 protein expression and increasing Ser^{307} phosphorylation. IRS-1 serine phosphorylation at this site has been reported to decrease the affinity of IRS1 for the insulin receptor and increased IRS1 degradation (9,10), and this may account for the decrease in total protein expression that we observed. It is also sufficient to account for the glucocorticoid-induced decrease of insulin-stimulated glucose uptake. The pivotal role of IRS1 in skeletal muscle insulin signaling is highlighted by IRS1 knockout mice (22–24) that develop marked insulin resistance. Serine phosphorylation of IRS1 at numerous residues has been implicated in the development of insulin resistance (19,25–27). Specifically, Ser^{307} phosphorylation is a negative regulator of IRS1 function. Inflammatory cytokines including tumor necrosis factor-α and C-reactive protein increase Ser^{307} phosphorylation (28,29), and insulin itself has been described to have similar effects (30,31). Although several kinases have been implicated in serine phosphorylation of IRS1 (32), PKCθ is believed to have a critical role, notably after free fatty acid (FFA) exposure (33,34). PKCθ knockout animals resist lipid-induced skeletal muscle insulin resistance (35), and rodent models with muscle-specific targeted serine-to-alanine substitutions at residues within IRS1 including Ser^{307} resist fat-induced insulin resistance (36). Glucocorticoid induction of lipolysis and consequent FFA generation (37) as well as increased FFA uptake will activate PKCθ, and this may well be an important contributor to the insulin resistance induced by glucocorticoid. This is endorsed by our gene expression analysis of lipogenic/lipolytyic genes in rodent muscle after 4-day treatment with the selective 11β-HSD1 inhibitor A2 (see discussion below). In addition, the lack of Ser^{24} phosphorylation may also add weight to this hypothesis. PKCθ does not contribute to phorbol-12-myristate-13-acetate–induced

TABLE 2
Comparative mRNA expression of 11β-HSD1, glucocorticoid receptor, and H6PDH in mouse skeletal muscle and C2C12 myotubes

Gene	C2C12	Quadriceps	Liver	Adipose
11β-HSD1	32.9 ± 2.9	0.29 ± 0.03	18.40 ± 1.96	1.26 ± 0.14
H6PDH	0.10 ± 0.015	0.1 ± 0.006	0.12 ± 0.005	0.11 ± 0.0009
Glucocorticoid receptor	0.56 ± 0.022	5.67 ± 0.29	3.33 ± 0.36	3.9 ± 0.68

Data are expressed as AUs (AU means ± SE, $n = 3–5$ experiments). Expression in rodent liver and adipose tissue are provided as a quantitative reference.

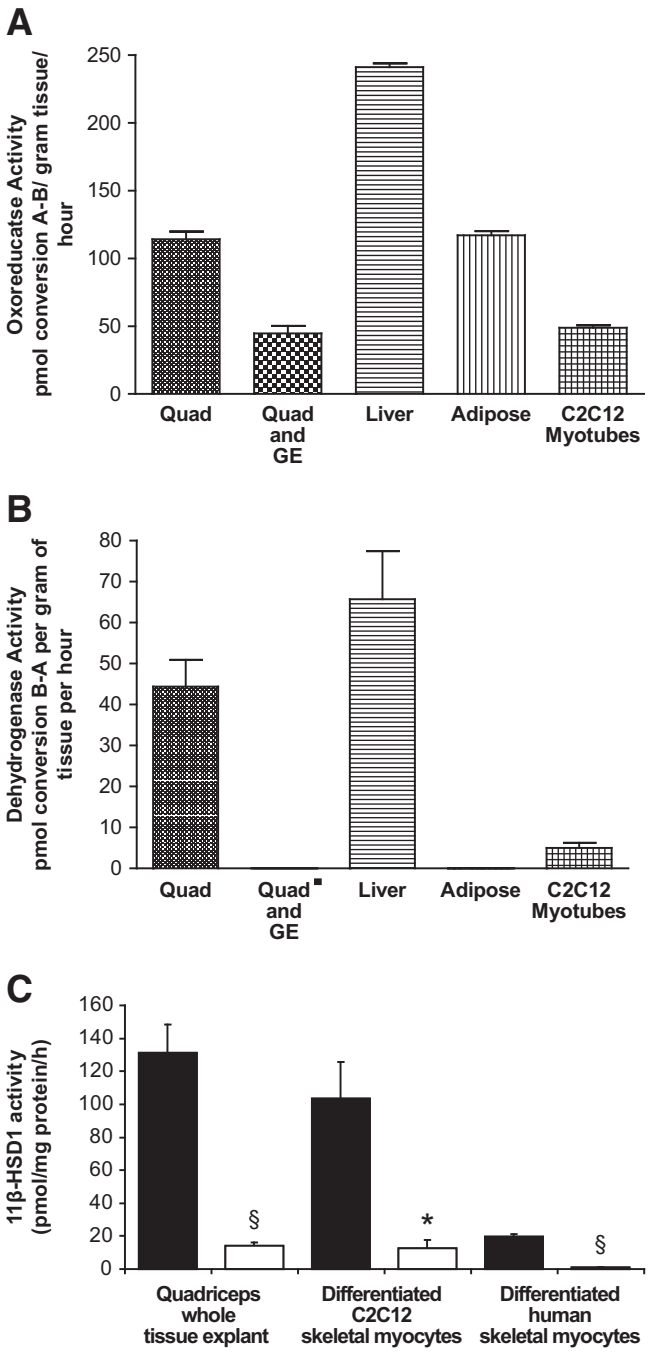

FIG. 3. Functional 11β-HSD1 enzyme oxo-reductase (*A*) and dehydrogenase (*B*) activity is present in explants of mouse quadriceps muscle with levels comparable with that seen in adipose tissue and liver. 11β-HSD1 activity is also observed in differentiated C2C12 rodent skeletal myocytes (data presented as picomole per milligram of protein per hour for C2C12 cells). Although dehydrogenase activity is present, the predominant activity is oxo-reductase generating active glucocorticoid. Coincubation of skeletal muscle explants with the nonselective 11β-HSD inhibitor, glycyrrhetinic acid, significantly decreases activity (data shown are the means ± SE of $n = 3$–6 experiments, *$P < 0.05$). In addition, the selective 11β-HSD1 inhibitor, A1 (1 μmol/l, 24 h), decreases oxo-reductase activity in rodent whole-tissue quadriceps explants, differentiated C2C12 skeletal myocytes, and primary cultures of human skeletal myocytes (*C*) (data shown are the means ± SE of $n = 3$–6 experiments, *$P < 0.05$, §$P < 0.005$) (control = black bars, A1 = white bars). GE, glycyrrhetinic acid.

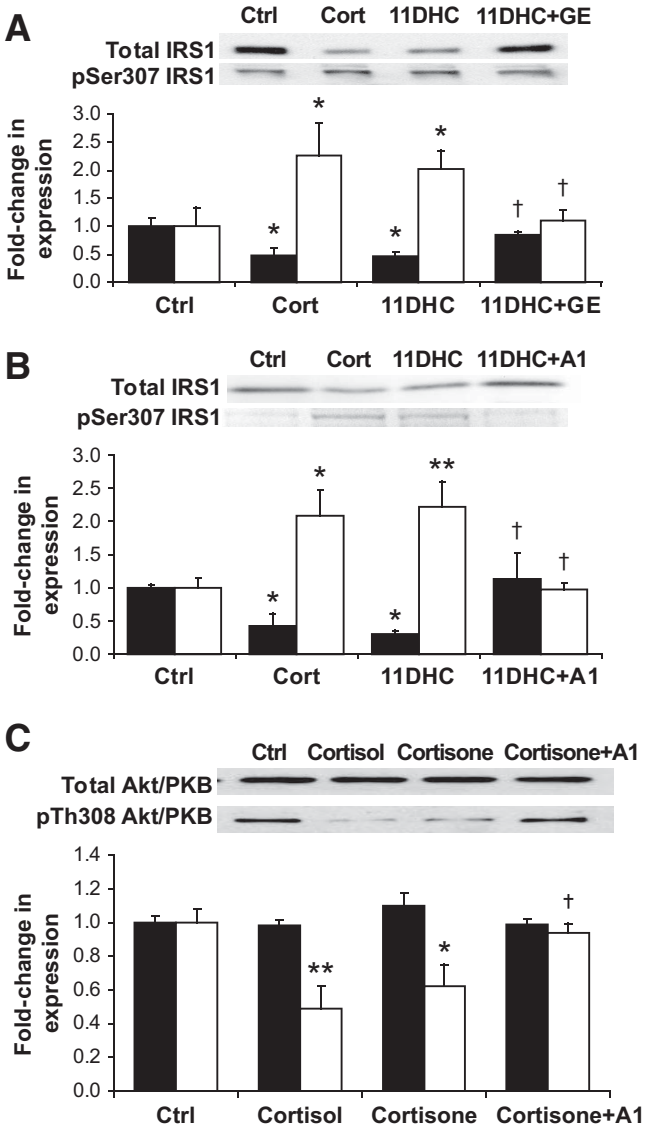

FIG. 4. Both CORT and 11DHC decrease IRS1 expression (black bars) and increase pSer^{307} IRS1 (white bars). The activity of 11DHC is dependent upon its activation to CORT by 11β-HSD1. Inhibition of 11β-HSD1 using glycyrrhetinic acid (*A*) or the selective 11β-HSD1 inhibitor, A1 (*B*), reverses the effect of 11DHC upon IRS1 expression and phosphorylation. Similarly, in primary cultures of human myotubes, A1 blocks the cortisone-induced decrease in pThr^{308} Akt/PKB (white bars) after insulin stimulation without changing total Akt/PKB expression (black bars) (*C*). Data presented are the mean of $n = 4$ experiments with representative Western blots inserted (*$P < 0.05$, **$P < 0.01$ vs. control, †$P < 0.05$ vs. 11DHC or cortisone). Ctrl, control.

Ser^{24} phosphorylation but instead is dependent upon PKCα activation (19).

Other studies have also highlighted the pivotal role of IRS1 in glucocorticoid-associated insulin resistance, although serine phosphorylation has not been examined. The results of these studies do show a degree of variability and some but not all have shown decreased activating tyrosine phosphorylation of IRS1 (11–13). Others have reported changes in insulin receptor expression and activation, PI3K activity and expression, and IRS2 expression and phosphorylation (12,38,39). The explanation for these inconsistencies is not entirely clear but may reflect differences between animal and cell models and specific investigative protocols.

Downstream of IRS1, we observed decreased activating pSer^{473} Akt/PKB and pThr^{308} Akt/PKB, and we propose that this may be a direct consequence of reduced insulin signaling capacity through enhanced IRS1 inactivation. In addition, we observed an increase in AS160 protein ex-

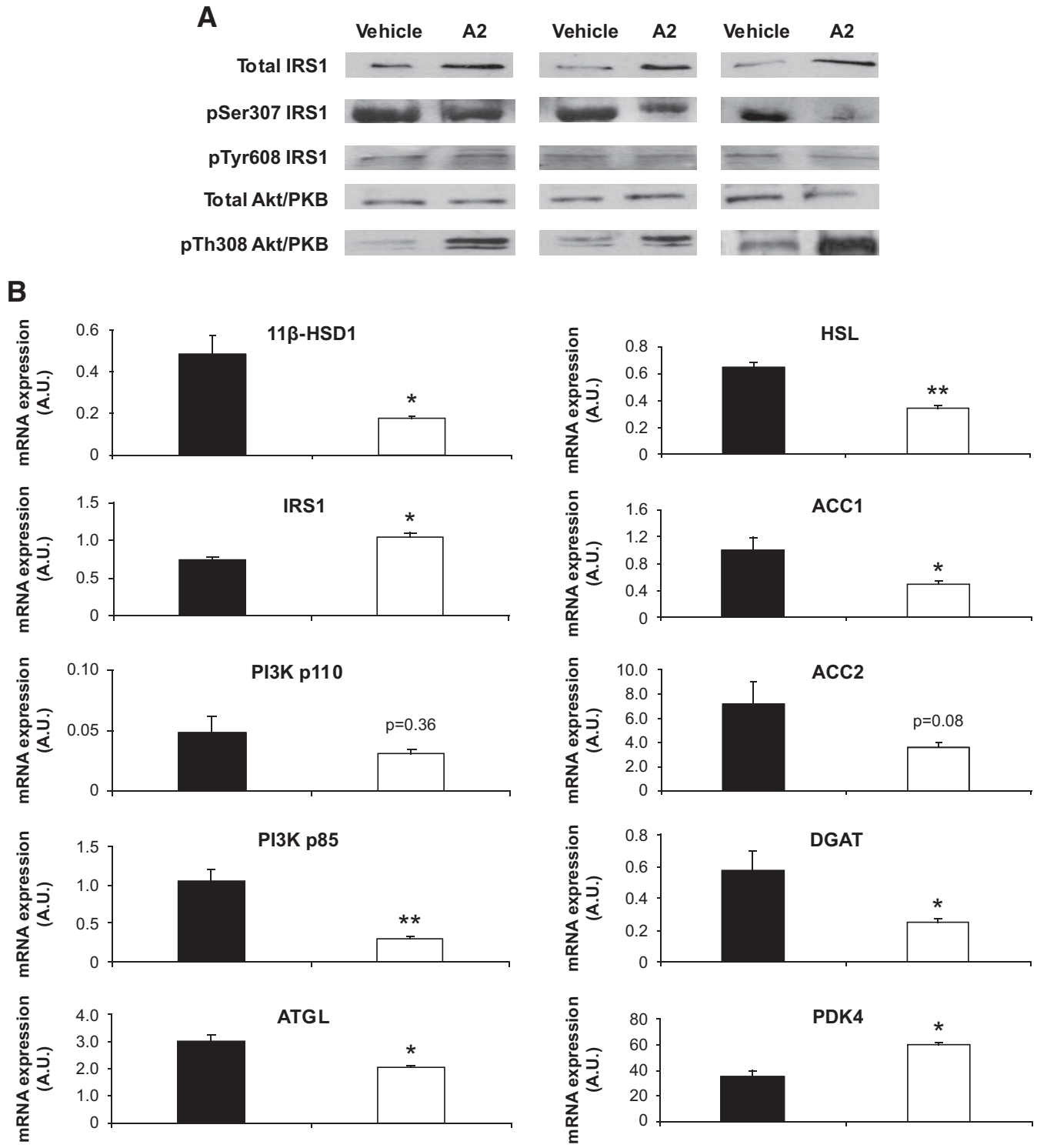

FIG. 5. In cortisone pellet–implanted KK mice, the selective 11β-HSD1 inhibitor, A2, increases IRS1 total protein expression, decreases inactivating pSer^{307} IRS1, and further downstream enhances insulin-stimulated pThr^{308} Akt/PKB in quadriceps muscle explants. Representative Western blots are shown (A2 vs. vehicle) (*A*). Real-time PCR analysis endorsing observation from the Genecard analysis presented in Table 3. Gene expression from whole-tissue quadriceps explants obtained from cortisone pellet–implanted KK mice treated for 4 days with the selective 11β-HSD1 inhibitor, A2 (white bars), or vehicle (black bars) (*$P < 0.05$, **$P < 0.01$) ($n = 3$ per group) (*B*).

pression. AS160 is a recently identified protein with Rab-guanosine triphosphate (GTP)ase activity. Under basal conditions, it is resident within GLUT4-containing vesicles and limits the GTP availability that is necessary for vesicle translocation to the cell membrane to permit glucose entry. Upon phosphorylation by activated Akt/PKB, AS160 dissociates from the vesicle, allowing GTP to bind to Rab proteins and vesicle translocation to the cell membrane to occur (7). While regulation of AS160 phosphorylation at differing sites by growth factors including IGF-1 and EGF has been described (40), glucocorticoid regulation has not been explored. Our data show that glucocorticoids increase both AS160 protein and mRNA expression in a glucocorticoid receptor–dependent mechanism. These ob-

TABLE 3
Quadriceps skeletal muscle Genecard analysis of 45 preselected gene targets implicated in the pathogenesis of glucocorticoid-induced insulin resistance

	Gene of interest	Cortisone + vehicle (means Δct ± SE)	Cortisone + A2 (means Δct ± SE)	Fold change in gene expression after M1 treatment
	Insr	15.9 ± 0.2	16.5 ± 0.2	0.65
	Irs1	16.9 ± 0.1	16.6 ± 0.1	1.27
	Irs2	17.2 ± 0.2	16.3 ± 0.8	1.93
	Pik3r1 (p85α)	14.9 ± 0.2	16.9 ± 0.4	**0.25**
	Pik3cb (p110β)	19.4 ± 0.3	19.8 ± 0.1	0.79
	Pdk1	15.9 ± 0.2	16.9 ± 0.1	**0.49**
	Akt1	16.3 ± 0.1	17.1 ± 0.2	0.59
	Akt2	17.7 ± 0.3	18.2 ± 0.3	0.74
	Prkcz (PKCζ)	19.2 ± 0.3	20.6 ± 0.6	**0.37**
	Prkci (PKCλ)	19.6 ± 0.1	20.2 ± 0.1	0.62
	Tbc1d1	15.7 ± 0.3	16.5 ± 0.1	0.58
	Tbc1d4 (AS160)	17.2 ± 0.3	18.1 ± 0.3	0.53
	Rab10	11.7 ± 0.3	12.3 ± 0.1	0.68
	Slc2a1 (GLUT-1)	16.8 ± 0.2	17.0 ± 0.1	0.91
	Slc2a4 (GLUT-4)	14.1 ± 0.1	14.1 ± 0.1	1.03
	Ptpn1 (PTP-1b)	17.8 ± 0.1	18.8 ± 0.1	0.52
	Ptpn11 (SHP2)	16.1 ± 0.2	16.4 ± 0.1	0.77
	Pten	15.8 ± 0.1	16.6 ± 0.1	0.60
	Ppp2r1a (PP2A)	14.9 ± 0.2	15.2 ± 0.1	0.81
	Socs1	21.5 ± 0.4	21.2 ± 0.4	1.20
	Socs3	19.4 ± 0.2	19.4 ± 0.1	0.98
	Frap1 (mTOR)	16.5 ± 0.2	17.3 ± 0.3	0.55
	Foxo1	16.9 ± 0.2	17.4 ± 0.1	0.75
	Foxo3a	15.9 ± 0.1	16.7 ± 0.5	0.58
	Prkaa2 (AMPK)	14.8 ± 0.1	15.0 ± 0.3	0.91
Insulin signalling cascade	Ppargc1a (PGC-1α)	16.9 ± 0.2	17.1 ± 0.1	0.93
	H6pd	15.6 ± 0.1	16.2 ± 0.3	0.66
Glucocorticoid	Hsd11b1 (11β-HSD1)	17.5 ± 0.6	18.5 ± 0.8	**0.48**
metabolism and action	Nr3c1 (GRα)	15.8 ± 0.1	16.3 ± 0.2	0.72
	Acaca (ACC1)	15.1 ± 1.0	16.7 ± 0.2	**0.33**
	Acacb (ACC2)	13.6 ± 0.3	14.4 ± 0.2	0.60
	Lpl	12.6 ± 0.2	13.2 ± 0.1	0.68
	Lipe (HSL)	16.4 ± 0.6	18.1 ± 0.1	**0.30**
	Pnpla2 (ATGL)	13.7 ± 0.5	15.1 ± 0.1	**0.39**
	Dgkd (DGKδ)	21.3 ± 0.5	21.4 ± 0.1	0.97
Lipid metabolism	Pparg (PPARγ)	21.2 ± 0.5	22.4 ± 0.3	**0.43**
	Sptlc1 (SPT1)	17.8 ± 0.1	18.6 ± 0.0	0.59
	Ugcg (glucosylceramide synthase)	18.8 ± 0.1	19.5 ± 0.1	0.61
	Asah1 (acid ceramidase)	19.0 ± 0.1	19.3 ± 0.1	0.82
	Lass1	16.9 ± 0.1	17.3 ± 0.1	0.77
Ceramide metabolism	Lass6	20.5 ± 0.4	21.1 ± 0.0	0.68
	Prkca (PKC-α)	16.6 ± 0.2	16.6 ± 0.1	0.94
	Prkcb1 (PKC-β)	22.7 ± 0.3	22.8 ± 0.3	0.96
	Prkcc PKC-γ)	22.6 ± 0.1	23.1 ± 0.7	0.69
Other genes	Ppara (PPARα)	18.7 ± 0.3	19.0 ± 0.1	0.85
	Ppib (cyclophilin B)	18.1 ± 0.2	18.4 ± 0.1	0.79
Internal controls	Hprt1	16.5 ± 0.2	17.1 ± 0.0	0.69

Cortisone pellet–implanted KK mice were treated with a selective 11β-HSD1 inhibitor, A2, or vehicle for 4 days before animals were killed (n = 3 per group, for detailed protocol see RESEARCH DESIGNS AND METHODS). Data presented as means Δct ± SE for both groups of animals relative to 18 s as an internal housekeeping gene, higher Δct values corresponding with lower gene expression. Fold changes in gene expression were calculated as described in RESEARCH DESIGNS AND METHODS. Specific target genes and all changes >2-fold increase or 0.5-fold decrease vs. vehicle (highlighted in bold) were endorsed with real-time PCR (see Fig. 5).

servations are interesting and point toward a separate mechanism of regulation rather than simply a downstream consequence of decreased IRS1 activation.

Although the net effect of glucocorticoid was to induce insulin resistance, we did observe an increase in IRS2 mRNA and protein expression. In addition IR, PI3K (p85 subunit), and GLUT4 mRNA expression increased, although protein expression was not examined in this study nor was PI3K-specific activity. It is possible that this represents a compensatory mechanism to preserve insulin sensitivity in an attempt to compensate for the inhibition of signaling through IRS1. However, overall the effect of

glucocorticoid exposure is to limit insulin-stimulated glucose uptake.

In addition to the effect of exogenous glucocorticoids, we have shown that prereceptor metabolism of endogenous glucocorticoid by 11β-HSD1 is a crucial regulator of insulin sensitivity in skeletal muscle. 11β-HSD1 is expressed and biologically active in human skeletal muscle (41). Overexpression of 11β-HSD1 has been described in rodent skeletal muscle in models of diabetes (42) and myotubes isolated from patients with insulin resistance and type 2 diabetes (43,44). However, this is not a consistent finding (45), and its precise contribution to metabolic and muscle phenotype is still to be clarified. Selective 11β-HSD1 inhibitors are currently in development; in rodents and primates they limit local glucocorticoid availability and improve glucose tolerance, lipid profiles, and insulin sensitivity (16,46). Very recently, studies using in vitro differentiated primary in human myoblasts have shown that 11β-HSD1 inhibition (pharmacological or siRNA) can limit cortisone- but not cortisol-induced changes in glucose uptake, glycogen synthesis, and palmitate oxidation. However, in this model, an insulin-sensitizing action could not be demonstrated (47). In our study, we have clearly shown expression and activity of 11β-HSD1 in human and rodent skeletal muscle that is blocked by selective and nonselective 11β-HSD1 inhibitors. This is functionally important and not only restores IRS1 protein levels to control values but also decreases pSer^{307} IRS1, enhances Akt/PKB activation, and may represent an important insulin-sensitizing mechanism of selective 11β-HSD1 inhibitors. These observations appear consistent in both our in vitro and rodent in vivo models. A2 has an insulin-sensitizing action as evidenced by decreased fasting glucose and insulin levels, decreased homeostasis model assessment scores, and reduced insulin secretion across an OGTT. Unfortunately, clamp studies were not performed as part of this protocol but have been reported elsewhere with other selective 11β-HSD1 inhibitors (16). In addition to the actions described above, A2 administration to mice in vivo decreased lipogenic gene expression (ACC1, FAS, and DGAT) and increased FFA utilization (decreased ACC2 leading to a decrease in the malonyl CoA-mediated inhibition of β-oxidation) in agreement with published observations (48). Furthermore, decreased HSL and ATGL will afford decreases in FFA and DAG generation. Interestingly, we also observed a 1.7-fold increase in PDK4 expression with A2 treatment in vivo. PDK4 is a negative regulator of the pyruvate dehydrogenase complex, limiting acetyl CoA generation. Rodents with deletion of PDK4 have increased glucose oxidation (49), and in cell culture systems, glucocorticoids increase PDK4 expression (47). The discrepancies with our data, where A2 increased PDK4 expression, almost certainly reflect the complexities of whole-animal versus cell culture models (we too have observed decreased PDK4 expression after Dex treatment in C2C12 myotubes [data not shown]). Importantly, the increase in PDK4 with selective 11β-HSD1 inhibitors may further serve to drive lipid oxidation at the expense of glucose oxidation. The net effect of all these observations will be to decrease intramyocellular lipid accumulation as well as local FFA and DAG generation. Consequently, PKCθ activation will be decreased, and this may be responsible for the reduction in Ser^{307} phosphorylation after selective 11β-HSD1 inhibition. However, this hypothesis remains to be proven and needs to be addressed in future studies.

In conclusion, Ser^{307} phosphorylation of IRS1 is a novel mechanism of glucocorticoid-induced insulin resistance. The prereceptor modulation of glucocorticoid availability is an important regulator of glucocorticoid action in skeletal muscle. Selective 11β-HSD1 inhibitors enhance insulin action, and we propose that this may predominantly be through modulation of lipid metabolism within skeletal muscle. Clinical data utilizing 11β-HSD1 inhibitors are beginning to emerge in obese patients and those with type 2 diabetes (50); it is likely that their efficacy in muscle will provide an additional pharmacological benefit in the treatment of type 2 diabetes and insulin resistance.

ACKNOWLEDGMENTS

Funding for this study has been provided by the Wellcome Trust, U.K. (program grant to P.M.S. and Clinician Scientist Fellowship to J.W.T.), a case award studentship from the Biotechnology and Biological Sciences Research Council in conjunction with AstraZeneca (to S.A.M.), the Medical Research Council (Clinical Research Training Fellowship to M.S.), and Diabetes U.K. (project grant to J.S.).

C.L., D.L., A.Y., G.C., and D.M.S. are employed by AstraZeneca, U.K., which manufactures pharmaceuticals related to the treatment of diabetes and its complications. In addition, those indicated are also stockholders in AstraZeneca. No other potential conflicts of interest relevant to this article were reported.

REFERENCES

1. Van Staa TP, Leufkens HG, Abenhaim L, Begaud B, Zhang B, Cooper C. Use of oral corticosteroids in the United Kingdom. Q J Med 2000;93:105–111
2. Larsson H, Ahren B. Short-term dexamethasone treatment increases plasma leptin independently of changes in insulin sensitivity in healthy women. J Clin Endocrinol Metab 1996;81:4428–4432
3. Fraser R, Ingram MC, Anderson NH, Morrison C, Davies E, Connell JM. Cortisol effects on body mass, blood pressure, and cholesterol in the general population. Hypertension 1999;33:1364–1368
4. Tomlinson JW, Walker EA, Bujalska IJ, Draper N, Lavery GG, Cooper MS, Hewison M, Stewart PM. 11β-hydroxysteroid dehydrogenase type 1: a tissue-specific regulator of glucocorticoid response. Endocr Rev 2004;25:831–866
5. Lavery GG, Walker EA, Draper N, Jeyasuria P, Marcos J, Shackleton CH, Parker KL, White PC, Stewart PM. Hexose-6-phosphate dehydrogenase knockout mice lack 11β-hydroxysteroid dehydrogenase type 1-mediated glucocorticoid generation. J Biol Chem 2006;281:6546–6551
6. Hanada M, Feng J, Hemmings BA. Structure, regulation and function of PKB/AKT: major therapeutic target. Biochim Biophys Acta 2004;1697:3–16
7. Sano H, Kane S, Sano E, Miinea CP, Asara JM, Lane WS, Garner CW, Lienhard GE. Insulin-stimulated phosphorylation of a Rab GT. Pase-activating protein regulates GLUT4 translocation. J Biol Chem 2003;278:14599–14602
8. Watson RT, Kanzaki M, Pessin JE. Regulated membrane trafficking of the insulin-responsive glucose transporter 4 in adipocytes. Endocr Rev 2004;25:177–204
9. Aguirre V, Uchida T, Yenush L, Davis R, White MF. The c-Jun NH(2)-terminal kinase promotes insulin resistance during association with insulin receptor substrate-1 and phosphorylation of Ser(307). J Biol Chem 2000;275:9047–9054
10. Aguirre V, Werner ED, Giraud J, Lee YH, Shoelson SE, White MF. Phosphorylation of Ser307 in insulin receptor substrate-1 blocks interactions with the insulin receptor and inhibits insulin action. J Biol Chem 2002;277:1531–1537
11. Giorgino F, Almahfouz A, Goodyear LJ, Smith RJ. Glucocorticoid regulation of insulin receptor and substrate IRS-1 tyrosine phosphorylation in rat skeletal muscle in vivo. J Clin Invest 1993;91:2020–2030
12. Rojas FA, Hirata AE, Saad MJ. Regulation of insulin receptor substrate-2 tyrosine phosphorylation in animal models of insulin resistance. Endocrine 2003;21:115–122
13. Saad MJ, Folli F, Kahn JA, Kahn CR. Modulation of insulin receptor, insulin

receptor substrate-1, and phosphatidylinositol 3-kinase in liver and muscle of dexamethasone-treated rats. J Clin Invest 1993;92:2065–2072
14. Ruzzin J, Wagman AS, Jensen J. Glucocorticoid-induced insulin resistance in skeletal muscles: defects in insulin signalling and the effects of a selective glycogen syntheses kinase-3 inhibitor. Diabetologia 2005;48: 2119–2130
15. Morton NM, Holmes MC, Fievet C, Staels B, Tailleux A, Mullins JJ, Seckl JR. Improved lipid and lipoprotein profile, hepatic insulin sensitivity, and glucose tolerance in 11β-hydroxysteroid dehydrogenase type 1 null mice. J Biol Chem 2001;276:41293–41300
16. Alberts P, Nilsson C, Selen G, Engblom LO, Edling NH, Norling S, Klingstrom G, Larsson C, Forsgren M, Ashkzari M, Nilsson CE, Fiedler M, Bergqvist E, Eva BB, Abrahmsen LB. Selective inhibition of 11{β}-hydroxysteroid dehydrogenase type 1 improves hepatic insulin sensitivity in hyperglycemic mice strains. Endocrinology 2003;144:4755–4762
17. Berthiaume M, Laplante M, Festuccia W, Gelinas Y, Poulin S, Lalonde J, Joanisse DR, Thieringer R, Deshaies Y. Depot-specific modulation of rat intraabdominal adipose tissue lipid metabolism by pharmacological inhibition of 11β-hydroxysteroid dehydrogenase type 1. Endocrinology 2007; 148:2391–2397
18. Hermanowski-Vosatka A, Balkovec JM, Cheng K, Chen HY, Hernandez M, Koo GC, Le Grand CB, Li Z, Metzger JM, Mundt SS, Noonan H, Nunes CN, Olson SH, Pikounis B, Ren N, Robertson N, Schaeffer JM, Shah K, Springer MS, Strack AM, Strowski M, Wu K, Wu T, Xiao J, Zhang BB, Wright SD, Thieringer R. 11β-HSD1 inhibition ameliorates metabolic syndrome and prevents progression of atherosclerosis in mice. J Exp Med 2005;202:517–527
19. Nawaratne R, Gray A, Jorgensen CH, Downes CP, Siddle K, Sethi JK. Regulation of insulin receptor substrate 1 pleckstrin homology domain by protein kinase C: role of serine 24 phosphorylation. Mol Endocrinol 2006;20:1838–1852
20. Tomlinson JW, Finney J, Gay C, Hughes BA, Hughes SV, Stewart PM. Impaired glucose tolerance and insulin resistance are associated with increased adipose 11β-hydroxysteroid dehydrogenase type 1 expression and elevated hepatic 5α-reductase activity. Diabetes 2008;57:2652–2660
21. Liu F, Kim J, Li Y, Liu X, Li J, Chen X. An extract of Lagerstroemia speciosa L. has insulin-like glucose uptake-stimulatory and adipocyte differentiation-inhibitory activities in 3T3–L1 cells. J Nutr 2001;131:2242–2247
22. Araki E, Lipes MA, Patti ME, Bruning JC, Haag B III, Johnson RS, Kahn CR. Alternative pathway of insulin signalling in mice with targeted disruption of the IRS-1 gene. Nature 1994;372:186–190
23. Kido Y, Burks DJ, Withers D, Bruning JC, Kahn CR, White MF, Accili D. Tissue-specific insulin resistance in mice with mutations in the insulin receptor, IRS-1, and IRS-2. J Clin Invest 2000;105:199–205
24. Previs SF, Withers DJ, Ren JM, White MF, Shulman GI. Contrasting effects of IRS-1 versus IRS-2 gene disruption on carbohydrate and lipid metabolism in vivo. J Biol Chem 2000;275:38990–38994
25. Mussig K, Fiedler H, Staiger H, Weigert C, Lehmann R, Schleicher ED, Haring HU. Insulin-induced stimulation of JNK and the PI 3-kinase/mTOR pathway leads to phosphorylation of serine 318 of IRS-1 in C2C12 myotubes. Biochem Biophys Res Commun 2005;335:819–825
26. Werner ED, Lee J, Hansen L, Yuan M, Shoelson SE. Insulin resistance due to phosphorylation of insulin receptor substrate-1 at serine 302. J Biol Chem 2004;279:35298–35305
27. Waraich RS, Weigert C, Kalbacher H, Hennige AM, Lutz SZ, Haring HU, Schleicher ED, Voelter W, Lehmann R. Phosphorylation of Ser357 of rat insulin receptor substrate-1 mediates adverse effects of protein kinase C-delta on insulin action in skeletal muscle cells. J Biol Chem 2008;283: 11226–11233
28. D'Alessandris C, Lauro R, Presta I, Sesti G. C-reactive protein induces phosphorylation of insulin receptor substrate-1 on Ser307 and Ser 612 in L6 myocytes, thereby impairing the insulin signalling pathway that promotes glucose transport. Diabetologia 2007;50:840–849
29. de AC, Teruel T, Hernandez R, Lorenzo M. Tumor necrosis factor-α produces insulin resistance in skeletal muscle by activation of inhibitor κB kinase in a p38 MAPK-dependent manner. J Biol Chem 2004;279:17070–17078
30. Gual P, Gremeaux T, Gonzalez T, Le Marchand-Brustel Y, Tanti JF. MAP kinases and mTOR mediate insulin-induced phosphorylation of insulin receptor substrate-1 on serine residues 307, 612 and 632. Diabetologia 2003;46:1532–1542
31. Danielsson A, Nystrom FH, Stralfors P. Phosphorylation of IRS1 at serine 307 and serine 312 in response to insulin in human adipocytes. Biochem Biophys Res Commun 2006;342:1183–1187
32. Draznin B. Molecular mechanisms of insulin resistance: serine phosphorylation of insulin receptor substrate-1 and increased expression of p85α: the two sides of a coin. Diabetes 2006;55:2392–2397
33. Yu C, Chen Y, Cline GW, Zhang D, Zong H, Wang Y, Bergeron R, Kim JK, Cushman SW, Cooney GJ, Atcheson B, White MF, Kraegen EW, Shulman GI. Mechanism by which fatty acids inhibit insulin activation of insulin receptor substrate-1 (IRS-1)-associated phosphatidylinositol 3-kinase activity in muscle. J Biol Chem 2002;277:50230–50236
34. Gao Z, Zhang X, Zuberi A, Hwang D, Quon MJ, Lefevre M, Ye J. Inhibition of insulin sensitivity by free fatty acids requires activation of multiple serine kinases in 3T3–L1 adipocytes. Mol Endocrinol 2004;18:2024–2034
35. Kim JK, Fillmore JJ, Sunshine MJ, Albrecht B, Higashimori T, Kim DW, Liu ZX, Soos TJ, Cline GW, O'Brien WR, Littman DR, Shulman GI. PKC-θ knockout mice are protected from fat-induced insulin resistance. J Clin Invest 2004;114:823–827
36. Morino K, Neschen S, Bilz S, Sono S, Tsirigotis D, Reznick RM, Moore I, Nagai Y, Samuel V, Sebastian D, White M, Philbrick W, Shulman GI. Muscle-specific IRS-1 Ser→Ala transgenic mice are protected from fat-induced insulin resistance in skeletal muscle. Diabetes 2008;57:2644–2651
37. Djurhuus CB, Gravholt CH, Nielsen S, Mengel A, Christiansen JS, Schmitz OE, Moller N. Effects of cortisol on lipolysis and regional interstitial glycerol levels in humans. Am J Physiol Endocrinol Metab 2002;283:E172–E177
38. Giorgino F, Pedrini MT, Matera L, Smith RJ. Specific increase in p85α expression in response to dexamethasone is associated with inhibition of insulin-like growth factor-I stimulated phosphatidylinositol 3-kinase activity in cultured muscle cells. J Biol Chem 1997;272:7455–7463
39. Giorgino F, Smith RJ. Dexamethasone enhances insulin-like growth factor-I effects on skeletal muscle cell proliferation. Role of specific intracellular signaling pathways. J Clin Invest 1995;96:1473–1483
40. Geraghty KM, Chen S, Harthill JE, Ibrahim AF, Toth R, Morrice NA, Vandermoere F, Moorhead GB, Hardie DG, MacKintosh C. Regulation of multisite phosphorylation and 14–3-3 binding of AS160 in response to IGF-1, EGF, PMA and AICAR. Biochem J 2007;407:231–241
41. Jang C, Obeyesekere VR, Dilley RJ, Alford FP, Inder WJ. 11Beta hydroxysteroid dehydrogenase type 1 is expressed and is biologically active in human skeletal muscle. Clin Endocrinol (Oxf) 2006;65:800–805
42. Zhang M, Lv XY, Li J, Xu ZG, Chen L. Alteration of 11β-hydroxysteroid dehydrogenase type 1 in skeletal muscle in a rat model of type 2 diabetes. Mol Cell Biochem 2009;324:147–155
43. Abdallah BM, Beck-Nielsen H, Gaster M. Increased expression of 11β-hydroxysteroid dehydrogenase type 1 in type 2 diabetic myotubes. Eur J Clin Invest 2005;35:627–634
44. Whorwood CB, Donovan SJ, Flanagan D, Phillips DI, Byrne CD. Increased glucocorticoid receptor expression in human skeletal muscle cells may contribute to the pathogenesis of the metabolic syndrome. Diabetes 2002;51:1066–1075
45. Jang C, Obeyesekere VR, Dilley RJ, Krozowski Z, Inder WJ, Alford FP. Altered activity of 11β-hydroxysteroid dehydrogenase types 1 and 2 in skeletal muscle confers metabolic protection in subjects with type 2 diabetes. J Clin Endocrinol Metab 2007;92:3314–3320
46. Bhat BG, Hosea N, Fanjul A, Herrera J, Chapman J, Thalacker F, Stewart PM, Rejto P. Demonstration of proof of mechanism and pharmacokinetics and pharmacodynamic relationship with PF-915275, an inhibitor of 11{β}HSD1, in cynomolgus monkeys. J Pharmacol Exp Ther 2007;324:299–305
47. Salehzadeh F, Al-Khalili L, Kulkarni SS, Wang M, Lonnqvist F, Krook A. Glucocorticoid-mediated effects on metabolism are reversed by targeting 11β hydroxysteroid dehydrogenase type 1 in human skeletal muscle. Diabete Metab Res Rev 2009;25:250–258
48. Berthiaume M, Laplante M, Festuccia WT, Cianflone K, Turcotte LP, Joanisse DR, Olivecrona G, Thieringer R, Deshaies Y. 11β-HSD1 inhibition improves triglyceridemia through reduced liver VLDL secretion and partitions lipids toward oxidative tissues. Am J Physiol Endocrinol Metab 2007;293:E1045–E1052
49. Jeoung NH, Harris RA. Pyruvate dehydrogenase kinase-4 deficiency lowers blood glucose and improves glucose tolerance in diet-induced obese mice. Am J Physiol Endocrinol Metab 2008;295:E46–E54
50. Hawkins M, Hunter D, Kishore P, Schwartz S, Hompesch M, Hollis G, Levy R, Williams B, Huber R. INCB013739, a Selective Inhibitor of 11β-Hydroxysteroid Dehydrogenase Type 1 (11βHSD1), Improves Insulin Sensitivity and Lower Plasma Cholesterol Over 28 Days in Patients with Type 2 Diabetes Mellitus (Abstract). 68th Scientific Sessions of the American Diabetes Association, 6–10 June 2008, Moscone Convention Center, San Francisco, California